METABOLIC CUES AND REGULATORY PROTEINS THAT GOVERN *LEGIONELLA PNEUMOPHILA* DIFFERENTIATION AND VIRULENCE

by

Rachel L. Edwards

A dissertation submitted in partial fulfillment
of the requirements for the degree of
Doctor of Philosophy
(Cellular and Molecular Biology)
in The University of Michigan
2008

Doctoral Committee:

      Associate Professor Michele S. Swanson, Chair
      Professor Michael J. Imperiale
      Associate Professor Alice Telesnitsky
      Assistant Professor Matthew R. Chapman
      Assistant Professor Eric S. Krukonis

DEDICATION

For Jim

ACKNOWLEDGEMENTS

TABLE OF CONTENTS

LIST OF FIGURES

LIST OF TABLES

LIST OF APPENDICES

CHAPTER ONE

INTRODUCTION

Summary of thesis

In both natural and man-made water systems, the gram-negative bacterium *Legionella pneumophila* likely resides within complex biofilm communities. However, when various freshwater protozoa ingest *L. pneumophila*, the microbes can efficiently establish an intracellular niche protected from digestion. Moreover, if humans inhale bacteria-laden aerosols, *L. pneumophila* can survive and replicate within alveolar macrophages to cause the severe pneumonia, Legionnaires' disease. To persist within these diverse niches, *L. pneumophila* alternates between at least two distinct phenotypic phases: a non-infectious, replicative form required for intracellular growth and an infectious, transmissive form that enhances survival in the extracellular milieu. In this thesis, I identify metabolites that cue *L. pneumophila* differentiation and analyze several proteins that enable the bacterium to initiate its phenotypic switch as appropriate for the local environment.

My work extends our knowledge of the regulatory elements that govern *L. pneumophila* differentiation. In particular, previous studies established that the LetA/LetS two-component system regulates host transmission through the activity of the global regulator CsrA, and the stringent response pathway coordinates transcription through the production of the signaling molecule ppGpp (Fettes *et al.*, 2001; Hammer and Swanson, 1999; Hammer *et al.*, 2002; Lynch *et al.*, 2003; Molofsky and Swanson, 2003; Zusman *et al.*, 2002). In Chapter Two, I provide evidence that the design of the LetA/LetS two-component system enables *L. pneumophila* to customize its

1

transcriptional and phenotypic profiles. Moreover, I present data that suggests that the model of the flexible LetA/LetS regulon may be applicable to many two-component systems, which may equip microbes with a mechanism to fine-tune their traits. In Chapter Three, I identify a new metabolic cue that triggers *L. pneumophila* differentiation. Specifically, I find (1) excess short chain fatty acids inhibit growth and induce all transmission phenotypes, (2) the response of *L. pneumophila* to the short chain fatty acids is dependent on the LetA/LetS system and the stringent response enzyme SpoT, and (3) excess short chain fatty acids perturb fatty acid biosynthesis, which is likely sensed via an interaction between SpoT and a critical component of the fatty acid biosynthetic pathway, acyl carrier protein. In Chapter Four, I determine the transcriptional profiles of replicative and transmissive phase *L. pneumophila* by microarray analysis. Also, using genotypic and phenotypic approaches, I demonstrate that nicotinic acid is an additional trigger of *L. pneumophila* differentiation. In Chapter Five, I summarize the key findings of my work and discuss both the implications and the unsolved questions regarding *L. pneumophila* virulence regulation, metabolism and pathogenesis.

Life cycle of *L. pneumophila*

When planktonic, transmissive *L. pneumophila* are engulfed by phagocytic cells, the bacteria avoid lysosomal degradation and instead establish a vacuole isolated from the endocytic network (Fig. 1.1). To gauge nutrient conditions within its host cell, *L. pneumophila* employs the Pht family of transporters (Sauer *et al.*, 2005). If vacuolar conditions are favorable, the post-transcriptional regulator CsrA, and perhaps the sRNA chaperone Hfq, suppresses transmissive traits and promotes intracellular replication (Fettes *et al.*, 2001; McNealy *et al.*, 2005; Molofsky and Swanson, 2003). When nutrients are depleted, bacterial replication halts and the enzymes RelA and SpoT produce ppGpp (Hammer and Swanson, 1999; Zusman *et al.*, 2002). The accumulation

of ppGpp in the bacterial cytosol stimulates the LetA/LetS two-component system to relieve CsrA repression of transmissive traits (Hammer and Swanson, 1999; Hammer *et al.*, 2002; Molofsky and Swanson, 2003). Together, the LetA/LetS system, the enhancer protein LetE, and the alternative sigma factors RpoS, RpoN and FliA induce traits thought to promote efficient host transmission and survival in the environment, including: evasion of phagosome-lysosome fusion, motility, cytotoxicity, sodium sensitivity and resistance to environmental stresses (Bachman and Swanson, 2001, 2004a, b; Hammer *et al.*, 2002; Jacobi *et al.*, 2004; Lynch *et al.*, 2003). Under defined conditions, *L. pneumophila* may further develop into the highly resilient and infectious cell type, the mature intracellular form (Faulkner and Garduno, 2002; Garduno *et al.*, 2002). Eventually, the exhausted host cell lyses, and progeny are released into the environment. While *L. pneumophila* that fail to find a new phagocyte probably establish complex biofilms, planktonic bacteria that encounter another suitable host can initiate the intracellular life cycle once more.

Broth model of differentiation

Broth cultures of *L. pneumophila* grown to either the exponential or stationary phase exhibit traits similar to replicative and transmissive bacteria, respectively, that are observed in co-cultures with phagocytic cells (Fig. 1.1). While many of the different stages and regulatory elements of the *L. pneumophila* life cycle were originally discerned by observing synchronous broth cultures, subsequent analysis in eukaryotic cells has supported many of these findings. Likewise, comparison of the transcription profiles of *L. pneumophila* cultured in broth and in *Acanthamoeba castellanii* has revealed that 84% of replicative phase genes and 77% of transmissive phase genes are up-regulated both *in vitro* and *in vivo*, thereby confirming the utility of broth culture studies (Bruggemann *et al.*, 2006). Several lines of evidence suggest that the replicative and transmissive phases observed in both broth and eukaryotic cell cultures are reciprocal. For example, when

3

stationary phase *L. pneumophila* are cultured within eukaryotic cells, they suppress their transmissive traits of cytotoxicity, sodium sensitivity, and motility, and instead replicate profusely (Alli *et al.*, 2000; Byrne and Swanson, 1998). Following the replicative period, transmissive traits are induced, and the host cell lyses (Alli *et al.*, 2000; Byrne and Swanson, 1998). Similarly, FlaA, Mip, DotH and DotO proteins, which are known to enhance invasion of eukaryotic cells, are expressed during the entry and exit periods, but not during replication (Hammer and Swanson, 1999; Watarai *et al.*, 2001a; Wieland *et al.*, 2005). In contrast, the promoter of CsrA, a repressor of transmission traits, is only active during the replicative period, not during invasion or host cell lysis (Molofsky and Swanson, 2003).

While pure bacterial cultures are advantageous for many molecular and biochemical techniques, several characteristics of *L. pneumophila* have only been observed *in vivo*, emphasizing the simplicity and limitations of the broth model. For instance, the replication vacuole in A/J mouse macrophages acidifies and *L. pneumophila* remain acid tolerant, whereas exponentially growing broth cultures are acid sensitive (Sturgill-Koszycki and Swanson, 2000). Additionally, bacteria harvested from *A. castellanii* are more infectious than agar-grown bacteria, suggesting that the intracellular environment of amoebae can affect virulence traits (Cirillo *et al.*, 1999). Moreover, after extended culture in HeLa cells, *L. pneumophila* differentiates to the cyst-like MIF, a cell type also observed in amoebae and clinical samples, but not in broth or macrophage cultures (Garduno *et al.*, 2002; Greub and Raoult, 2003). The substantial differences observed between broth and phagocytic cell cultures highlight the impact of experimental design and lend caution to making inferences based on any single laboratory model.

Amino acid availability governs differentiation

Although the exact nutrient composition of the *L. pneumophila* replication vacuole is unknown, several lines of evidence indicate that amino acids are critical, and

differences in these concentrations can affect the differentiation state of the microbe. Foremost, broth studies indicate that *L. pneumophila* depends on amino acids for its sole source of carbon and energy (Tesh *et al.*, 1983). Additionally, the uptake of amino acids by its host cell via the human transporter protein SLC1A5 (hATB$^{0,+}$) is required for *L. pneumophila* to replicate in macrophages (Wieland *et al.*, 2005). Furthermore, *L. pneumophila* uses amino acid transporters to determine the nutrient availability of the environment and trigger its differentiation as deemed appropriate (discussed below) (Sauer *et al.*, 2005). Finally, when amino acids are depleted, *L. pneumophila* utilizes the stringent response to induce a panel of traits that enable escape from its spent host, survival in the environment, and the capacity to invade another suitable host (discussed below) (Hammer and Swanson, 1999). The regulatory linkage of nutrient availability to differentiation is essential for *L. pneumophila* pathogenesis, as it determines the phenotypic profile of the microbe.

Pht family of transporters

To sense amino acid availability and determine if differentiation to a replicative state is advantageous, transmissive *L. pneumophila* use a family of phagosomal transporters (Phts) (Sauer *et al.*, 2005). In particular, a *L. pneumophila* mutant of the *phtA* gene was shown to have a pronounced defect in intracellular growth in murine bone marrow-derived macrophages, and it failed to differentiate to the replicative state (Sauer *et al.*, 2005). However, the ability of the *phtA* mutant to infect macrophages and establish a protected ER-derived vacuole was not compromised (Sauer *et al.*, 2005). Using sequence analysis, PhtA was predicted to be a transmembrane protein that traverses the membrane twelve times and belong to the Major Facilitator Superfamily of transporters (Pao *et al.*, 1998; Sauer *et al.*, 2005). Indeed, the growth defect of the *phtA* mutant in both minimal media and macrophages can be bypassed by supplementing

media with free threonine or threonine dipeptides (Sauer *et al.*, 2005). Taken together with the aforementioned data, it is proposed that *L. pneumophila* uses the PhtA transporter as a mechanism to couple nutrient acquisition to differentiation (Fig. 1.3) (Sauer *et al.*, 2005).

Examination of the *L. pneumophila* genome reveals that strains Philadelphia 1 and Lens have 11 *phtA* homologues, while the Paris strain has nine (Cazalet *et al.*, 2004; Sauer *et al.*, 2005). Though several of these loci are likely gene duplications, it is conceivable that *L. pneumophila* encodes *pht* homologues dedicated to transporting each of the six essential amino acids, either arginine, cysteine, methionine, serine, threonine or valine (Ristroph *et al.*, 1981). In support of this model, a *phtJ* (previously *milA*) mutant has a growth defect in macrophages and alveolar epithelial cells (Harb and Abu Kwaik, 2000), which can be suppressed by valine supplementation (Sauer and Swanson, unpublished). Other intracellular environmental pathogens may also exploit transporters to evaluate nutrient availability before undergoing differentiation, since *pht* homologues have been identified in *Coxiella burnetti* and *Francisella tularensis*, two closely related pathogens that also efficiently parasitize both macrophages and amoebae (Oyston *et al.*, 2004). Thus, the Pht family of transporters may equip vacuolar pathogens to assess the nutrient composition in their protective vacuole before committing to differentiation.

Stringent response

Microbes trigger a global change in their cellular metabolism known as the stringent response when confronted with nutritional and metabolic stresses, such as the limitation of amino acids, carbon, iron, nitrogen, phosphorous and fatty acids (Magnusson *et al.*, 2005). Numerous physiological processes are coordinately altered, including growth inhibition, down-regulation of nucleic acid and protein synthesis, enhancement of protein degradation, and up-regulation of amino acid synthesis and transport. The stringent response is triggered when uncharged tRNAs accumulate in the

A-site of the 50S ribosome. Using ATP as a phosphate donor, the ribosome-associated enzyme RelA is activated to synthesize the alarmone, ppGpp (guanosine 3', 5'-bispyrophsophate), and its precursor, pppGpp (guanosine 3'-diphosphate, 5'-triphosphate) by phosphorylating GDP and GTP, respectively. The ppGpp effector molecule then binds directly to the β and β' subunits of the RNA polymerase (RNAP) core enzyme. As a result, the transcription of some classes of genes is up-regulated, while the expression of other sets of genes is inhibited (Magnusson *et al.*, 2005; Srivatsan and Wang, 2008).

There is considerable evidence that ppGpp acts as a global regulator to modulate a variety of bacterial cellular and physiological processes. Furthermore, numerous intracellular and extracellular pathogens appear to exploit the stringent response pathway to activate virulence genes and persist in the hostile environment of their host; these include *Mycobacterium tuberculosis*, *Listeria monocytogenes*, *Pseudomonas aeruginosa*, *Streptococcus pyogenes, Staphylococcus aureus, Borrelia burgdorferi* and *Salmonella typhimurium* (Godfrey *et al.*, 2002; Magnusson *et al.*, 2005). By monitoring environmental conditions and invoking the stringent response, pathogens can elicit swift changes in gene expression to adapt to the metabolic stresses encountered in their host, thereby promoting self-preservation.

In broth culture, *L. pneumophila* accumulate ppGpp upon entry into stationary phase, when amino acids are depleted, or when *relA* is induced (Hammer and Swanson, 1999). As a result, the microbe converts from a replicative to transmissive state, as characterized by the expression of virulence traits (Hammer and Swanson, 1999). *L. pneumophila relA* mutants are unable to produce detectable levels of ppGpp and are defective for the transmission traits of pigmentation and motility (Zusman *et al.*, 2002). However, *relA* is dispensable for intracellular growth in both human macrophages and amoebae, suggesting *relA* activity contributes exclusively to the transmissive phase, not replication (Zusman *et al.*, 2002). By analogy to other bacteria that use a stringent response, it is proposed that ppGpp acts as an alarmone to induce the coordinate

expression of traits that equip *L. pneumophila* to escape its spent host and persist in the environment until it encounters another phagocyte.

In broth cultures, the *L. pneumophila* RelA enzyme appears to be the major ppGpp synthetase because only minimal levels of the alarmone are detected in *relA* mutants (Zusman *et al.*, 2002). However, many prokaryotes contain a second enzyme, SpoT, which, depending on environmental conditions, exhibits either ppGpp synthatase or hydrolase activity (Chatterji and Kumar Ojha, 2001). When growth conditions are favorable, SpoT diminishes ppGpp levels in the cytosol through its hydrolase activity (Chatterji and Kumar Ojha, 2001). But under certain nutrient limitations, such as nitrogen, phosphorous and fatty acid starvation, SpoT can synthesize ppGpp to elicit the stringent response (Magnusson *et al.*, 2005). Sequence analysis indicates the *L. pneumophila* genome contains a homologue 52% identical to the *Escherichia coli spoT* gene that appears to be essential for viability, as attempts to delete the locus were unsuccessful (Zusman *et al.*, 2002). Recent work in *E. coli* indicates that SpoT interacts with the functional form of acyl carrier protein to respond to fatty acid starvation (Battesti and Bouveret, 2006). Therefore, we postulated that *L. pneumophila* might similarly employ SpoT to sense fatty acid concentrations. Indeed, our data suggest that perturbations in the fatty acid biosynthetic pathway cue *L. pneumophila* differentiation through an interaction between SpoT and acyl carrier protein (Chapter 3 and Appendix A). We predict that this provides the bacterium with a mechanism to sense local conditions and make decisions regarding its fate.

Evidence that other factors trigger differentiation

Although the RelA-induced stringent response pathway is the most well characterized mechanism by which *L. pneumophila* controls differentiation, several lines of evidence indicate that other signals are likely to be involved. By phenotypic analysis, *relA* mutants appear less defective for transmissive traits than other known regulators of

8

differentiation, suggesting additional factors act in concert with RelA (Hammer and Swanson, 1999; Zusman *et al.*, 2002). Also, *letA* mutants (discussed below) do express traits that are normally impaired when certain growth conditions are altered, such as aeration, temperature or media composition (Fernandez-Moreia and Swanson, unpublished). Furthermore, broth cultures of *letA* and *letS* mutants are defective in their ability to infect mouse macrophages, but surviving bacteria can initiate secondary and tertiary infections as efficiently as wild-type (Hammer *et al.*, 2002). Additionally, *L. pneumophila letA* mutants are more infectious when harvested from cultures of murine bone marrow-derived macrophages (Byrne and Swanson, unpublished). Taken together, these data indicate that additional regulators can bypass RelA and the LetA/LetS two-component system by receiving signals and initiating differentiation. Whether the signals stem from the unique environment of the *L. pneumophila* vacuole or are only induced when bacterial density within the vacuole reaches a certain threshold remains to be determined.

Acetyl-phosphate

In addition to ppGpp, acetyl-phosphate can act as a global signal for many cellular processes, including chemotaxis, nitrogen and phosphate assimilation, biofilm development and the expression of virulence traits (Wolfe, 2005). Acetyl-phosphate is a high energy phosphate compound that can be synthesized by two separate reactions: (1) from acetyl-CoA and P_i by phosphotransacetylase, encoded by the *pta* gene, or (2) from ATP and acetate, in a reaction catalyzed by acetyl kinase, the product of *ackA* (McCleary *et al.*, 1993; Wolfe, 2005). Response regulators of two-component systems can use acetyl-phosphate to catalyze their own phosphorylation (Wolfe, 2005). Accordingly, the *Bordetella pertussis* response regulator, BvgA, can be phosphorylated in the absence of its cognate histidine kinase using acetyl-phosphate as a donor (Boucher *et al.*, 1994). Likewise, either acetyl phosphate or the histidine kinase BarA can activate the *S.*

typhimurium response regulator SirA to induce the expression of invasion genes (Lawhon *et al.*, 2002). The *L. pneumophila* genome contains homologues of both *pta* and *ackA* of *E. coli* (Gal-Mor and Segal, 2003a), suggesting that acetyl-phosphate may phosphorylate one of the two-component systems to induce gene expression.

Transcriptional control of differentiation via sigma factors

To regulate gene expression, one mechanism commonly employed by bacteria is to modify RNAP activity by altering its sigma factor. In *E. coli,* RNAP consists of a core enzyme and one of seven potential sigma factors that direct the RNAP to a distinct cohort of promoters (Nystrom, 2004). For growth-related activities and proliferation, *E. coli* require the housekeeping sigma factor, σ^{70}, encoded by *rpoD* (Nystrom, 2004). However, during conditions of growth arrest, starvation, stress or maintenance, the bacteria replace σ^{70} with alternate sigma factors, thereby recruiting RNAP to the promoters of a cohort of genes that will confer survival under the deleterious conditions (Nystrom, 2004). Analysis of the *L. pneumophila* genome has identified six alternative sigma factors: RpoD (σ^{D}/σ^{70}), RpoE, RpoH, RpoN (σ^{54}), RpoS (σ^{S}/σ^{38}) and FliA (σ^{28}), as well as the sigma factor-dependent enhancer, FleQ, and the anti-sigma factors, FlgM and anti-sigma factor B (Cazalet *et al.*, 2004; Chien *et al.*, 2004). Several of the *L. pneumophila* sigma factors have been implicated by genetic analysis to regulate subsets of transmission traits (Bachman and Swanson, 2001; Molofsky *et al.*, 2005).

Recent biochemical and genetic data obtained with *E. coli* indicate that the effector molecule of the stringent response, ppGpp, controls sigma factor competition for the RNAP core enzyme (Nystrom, 2004). In particular, ppGpp regulates the ability of different alternative sigma factors to bind RNAP, and ppGpp also controls the production and activity of many sigma factors (Magnusson *et al.*, 2005). Therefore, under nutrient limiting conditions, the stringent response governs sigma factor competition and other

aspects of gene transcription, thus altering the expression profile and enhancing the fitness of the microbe.

RpoS

The stationary phase sigma factor, RpoS, is required for *L. pneumophila* sodium sensitivity, maximal expression of flagellin, and lysosomal evasion, but it is dispensable for the other known transmissive phase phenotypes (Bachman and Swanson, 2001; Hales and Shuman, 1999). In accordance with the theory of sigma factor competition, over-expression of *rpoS* decreases *csrA*, *letE*, *fliA* and *flaA* transcripts, and inhibits the *fliA*-dependent transmission traits of motility, infectivity and cytotoxicity (Bachman and Swanson, 2004b). Also, multiple copies of *rpoS* inhibit intracellular replication in *A. castellanii* (Hales and Shuman, 1999). Although the global regulation of gene expression by sigma factors in *L. pneumophila* has not been confirmed biochemically, these data support the model that, during stringency, ppGpp alters the competition among sigma factors for RNAP, thus allowing recruitment of RNAP to the appropriate set of transmission genes (Bachman and Swanson, 2004b; Hales and Shuman, 1999).

RpoN and FleQ

Since the assembly of the bacterial flagellum is an energetically taxing process, microbes encode a complex regulatory cascade to ensure that the timing and synthesis of both structural and accessory proteins of the flagellar regulon are tightly controlled. In *L. pneumophila*, the alternative sigma factor RpoN and the coactivator FleQ are at the top of this transcriptional hierarchy; hence, *rpoN* and *fleQ* mutants lack a flagellum and produce very little flagellin protein (Jacobi *et al.*, 2004). Additionally, both RpoN and FleQ positively regulate transcription of several genes within the second tier of the regulation cascade, including *fliM*, *fleN* and *fleSR* (Jacobi *et al.*, 2004). In contrast, RpoN and FleQ are dispensable for *fliA* and *flaA* transcription, suggesting that additional factors may

govern genes within the transcriptional cascade of the *L. pneumophila* flagellar regulon (Jacobi *et al.*, 2004).

FliA

To induce *flaA* transcription, assemble a monopolar flagellum, and become motile, *L. pneumophila* require a second sigma factor, FliA (Heuner *et al.*, 1997; Heuner *et al.*, 2002). Besides controlling genes of the flagellar regulon, FliA governs a set of motility-independent traits thought to promote host transmission and persistence. In particular, *L. pneumophila* require FliA to produce a melanin-like pigment, alter its surface properties, avoid lysosomes, and replicate within *Dictyostelium discoideum* (Hammer *et al.*, 2002; Heuner *et al.*, 2002; Molofsky *et al.*, 2005). By coordinating motility with other essential virulence traits, *L. pneumophila* can fine-tune its expression profile to enhance its versatility when confronted by a multitude of host defenses and environmental stresses.

Post-transcriptional control of differentiation

LetA/LetS two-component system

Two-component systems are widely used by prokaryotic organisms to adapt to environmental fluctuations. Typically, these signal transduction systems consist of a membrane–bound sensor protein that monitors the environment and a cytoplasmic response regulator that binds target DNA sequences (Appleby *et al.*, 1996; Bijlsma and Groisman, 2003). Upon stimulation, the sensor autophosphorylates a conserved histidine residue using the γ-phosphoryl group of ATP as a donor (Appleby *et al.*, 1996; Bijlsma and Groisman, 2003). The phosphate is then transferred to an aspartic acid in the response regulator, allowing for activation or repression of target genes (Appleby *et al.*, 1996; Bijlsma and Groisman, 2003). The specific signal for autophosphorylation may be

abiotic or biotic, and be produced by the environment, the host cell, or generated by the bacteria themselves via quorum sensing (Heeb and Haas, 2001). However, for many microbial two-component systems, the corresponding signal remains elusive.

The LetA/LetS (*Legionella* transmission activator and sensor, respectively) system of *L. pneumophila* was originally identified by screening for mutants defective for flagellin expression (Hammer *et al.*, 2002). Further analysis demonstrated that, as cells exit exponential phase, LetA/LetS induces an array of traits likely to promote transmission, including the ability to infect both macrophages and *A. castellanii*, avoid phagosome-lysosome fusion, sodium sensitivity, stress resistance, motility, pigmentation and macrophage cytotoxicity (Bachman and Swanson, 2004a; Hammer *et al.*, 2002; Lynch *et al.*, 2003). Accordingly, *letA* and *letS* mutants do not express transmissive traits, and instead constitutively display phenotypes similar to wild-type replicative bacteria (Hammer *et al.*, 2002; Lynch *et al.*, 2003). Bacteria that lack LetA fail to respond to ppGpp (Hammer *et al.*, 2002), but whether LetS is activated directly by the alarmone or by another signaling molecule that stimulates its autophosphorylation is unknown. By analogy to other two-component systems, LetS is the proposed membrane-associated sensor kinase and LetA the cognate response regulator.

LetA/LetS belongs to a family of signal-transducing proteins that includes BvgA/BvgS of *Bordetella*, GacA/GacS of *Acinetobacter baumannii*, PigQ/PigW of *Serratia marcescens*, VarA/VarS of *Vibrio cholerae*, SirA/BarA of *Salmonella*, GacA/GacS of *Pseudomonas* and the UvrY/BarA, EvgA/EvgS and TorR/TorS systems of *E. coli* (Heeb and Haas, 2001; Lapouge *et al.*, 2008; Perraud *et al.*, 1999). The BvgA/BvgS system, which established the paradigm for this family of signaling molecules, deviates from classic two-component systems by employing a four-step phosphorelay in which His-Asp-His-Asp residues are sequentially phosphorylated (Uhl and Miller, 1996a). BvgS is a tripartite, transmembrane sensor whose periplasmic domain is linked by a membrane-spanning region to three cytoplasmic signaling

domains: a transmitter, receiver and histidine phosphotransfer domain (Cotter and

DiRita, 2000). In response to an unknown signal, BvgS autophosphorylates a histidine in

the transmitter, and then sequentially transfers the phosphoryl group to aspartic acid and

histidine residues first in the receiver and then in the histidine phosphotransfer domain,

respectively (Cotter and DiRita, 2000). BvgA is the response regulator that, when

transphosphorylated by BvgS, gains affinity for Bvg-activated promoters (Cotter and

DiRita, 2000).

It has been suggested that the multi-step design of this family of two-component

systems enables the bacteria to express a spectrum of phenotypes in response to different

environmental conditions. In support of this model, *Bordetella* alternate between several

distinct phenotypic phases, and it is the BvgA/BvgS system that regulates the phases by

temporally controlling the expression of different classes of genes (Cotter and Miller,

1997). Due to the similarities in domain architecture of the BvgA/BvgS and LetA/LetS

systems, we predicted that *L. pneumophila* may use the four-step phosphorelay to fine-

tune its panel of transmission traits. Indeed, in Chapter 3 I demonstrate that the complex

design of the LetA/LetS system enables *L. pneumophila* to customize its transcriptional

and phenotypic profiles, thereby enhancing its versatility and fitness.

All transmission traits activated by LetA/LetS and repressed by CsrA (discussed

below) are also affected by a mutation in *letE,* suggesting that LetE either enhances

LetA/LetS function or inhibits CsrA activity (Bachman and Swanson, 2004a). LetE

apparently functions as a small protein, rather than a regulatory RNA, but the mechanism

by which LetE augments transmission traits has not been elucidated (Bachman and

Swanson, 2004a). Homologues of *letE* have not been identified in other microbial

genomes, and sequence analysis has provided little insight to its biochemical activity.

Thus, additional research is necessary to determine how this protein functions and,

furthermore, how LetE interacts with other regulators to coordinate *L. pneumophila*

differentiation (Bachman and Swanson, 2004a).

Carbon storage regulatory (Csr) system

In a variety of microbes, the global regulatory system CsrA/CsrB functions post-transcriptionally to control stationary phase gene expression. Numerous cellular processes are regulated by this highly conserved system, including the inhibition of biofilm formation, gluconeogenesis, glycogen biosynthesis and catabolism, as well as the activation of glycolysis, acetate metabolism, flagellum biosynthesis and motility (Suzuki *et al.*, 2002). CsrA is a small effector protein that binds near the ribosomal binding site, and, depending on the target mRNA, either stabilizes the transcript or promotes transcript decay (Romeo, 1998). CsrB is an untranslated RNA that contains imperfect repeats located in the predicted loop regions of the RNA molecule (Romeo, 1998). In *E. coli*, CsrB forms a globular complex with approximately 18 CsrA molecules, likely facilitated through binding the repeat elements (Romeo, 1998). As a result, CsrB antagonizes the activity of CsrA by sequestering the molecule away from its target mRNAs, thus reducing the concentration of free CsrA (Romeo, 1998).

A homologue of the *E. coli csrA* gene was identified in *L. pneumophila* and shown to be essential for replication in broth culture, macrophages and *A. castellanii* (Fettes *et al.*, 2001; Forsbach-Birk *et al.*, 2004; Molofsky and Swanson, 2003). Genetic data indicate that, in *L. pneumophila,* every transmission trait induced by the LetA/LetS two-component system is repressed by CsrA (Fettes *et al.*, 2001; Molofsky and Swanson, 2003). In addition, the loss of CsrA activity bypasses all transmission trait defects displayed by a *letA* mutant, suggesting LetA functions to alleviate CsrA repression (Molofsky and Swanson, 2003). The model predicts that when nutrients are depleted, the stringent response produces ppGpp, and LetA/LetS is activated. The two-component system then transcribes the regulatory RNAs, which titrates CsrA away from its mRNA targets, allowing transmissive phase traits to be induced (Fig. 1.2).

Although only one mRNA target of CsrA has been identified in *L. pneumophila* (C. Buchrieser, personal communication), the CsrA-repressed transmission traits of

cytotoxicity, lysosome evasion and motility all depend on the efficient transcription of the flagellar sigma factor, FliA (Fettes *et al.*, 2001; Hammer *et al.*, 2002; Molofsky and Swanson, 2003). Furthermore, over-expression of *csrA* leads to a reduction in *fliA* and *flaA* transcript levels (Fettes *et al.*, 2001). By analogy to other prokaryotic Csr regulatory systems, it is predicted that *L. pneumophila* CsrA inhibits the stability or translation of *fliA* mRNA, thus affecting transcription of *flaA* and the expression of motility and transmission phenotypes (Romeo, 1998). While data suggest that several copies of *csrA* are present in *L. pneumophila*, the significance of multiple *csrA* homologues is unclear (Brassinga *et al.*, 2003). Recently, two *L. pneumophila* small regulatory RNAs were identified bioinformatically, designated as RsmY and RsmZ (Kulkarni *et al.*, 2006), which were then found to be functionally analogous to CsrB of *E. coli* (Kulkarni *et al.*, 2006). Furthermore, the transcription of *rsmY* and *rsmZ* is dependent on LetA, which binds to a conserved motif located upstream of the RNAs (Sahr *et. al.*, unpublished[1]). Additional research will provide insight into how the *L. pneumophila* Csr system regulates its mRNA targets to enhance the fitness of *L. pneumophila* and control its differentiation.

Hfq and small RNAs (sRNAs)

In addition to the Csr regulatory system, prokaryotes can employ other noncoding RNAs to modulate gene expression (Gottesman, 2004; Majdalani *et al.*, 2005). These sRNAs require the Hfq chaperone protein, and, through complementary base pairing with mRNAs, can modify either the translation or stability of their mRNA targets (Gottesman, 2004; Majdalani *et al.*, 2005). Data indicate that Hfq contributes to virulence in a number of bacterial pathogens, presumably by altering the interaction of sRNAs with *rpoS*, thus affecting *rpoS* translation (McNealy *et al.*, 2005).

---

[1] Sahr, T., Brüggemann, H., Jules, M., Albert-Weissenberger, C., Cazalet, C. and Buchrieser, C. Two non-coding RNAs govern virulence regulation and transmission in *Legionella pneumophila*. In preparation.

Recently, a *hfq* homologue was identified in *L. pneumophila*, and the gene appears to be temporally regulated by both RpoS and LetA (McNealy *et al.*, 2005). In the replicative phase, RpoS induces the expression of *hfq* (McNealy *et al.*, 2005). Exponential phase transcripts, such as *csrA* and *fur* (ferric uptake regulator), are then stabilized by Hfq and most likely by sRNAs (McNealy *et al.*, 2005). Upon entering stationary phase, ppGpp accumulates and the LetA/LetS two-component system is induced (Hammer and Swanson, 1999; Hammer *et al.*, 2002). As a result, LetA activates transmissive phase traits, while directly or indirectly repressing *hfq* transcription (McNealy *et al.*, 2005). Although sRNAs other than RsmY and RsmZ have not been found in *L. pneumophila*, they could be identified using Hfq as a tool, and, subsequently, their role in post-transcriptional regulation of differentiation examined.

Regulation of the Dot/Icm type IV secretion system

To escape the endocytic pathway and establish a replicative vacuole, *L. pneumophila* depends on a group of 26 genes designated *dot/icm* (defect in organelle trafficking/intracellular multiplication) (Sexton and Vogel, 2002). This family of genes has homology to bacterial conjugation systems and mediates the transfer of mobilizable plasmids between bacterial strains (Sexton and Vogel, 2002). In addition, the type IV secretion system encoded by the *dot/icm* genes translocates effector molecules into host cells (Sexton and Vogel, 2002). At present, information regarding factors that regulate the timing and expression of genes required for assembling the secretion apparatus and its secreted effectors is limited. A series of nine *icm::lacZ* translational fusions were constructed, and examination of their temporal expression indicated that, in broth culture, several *icm* genes show a modest increase in their expression level upon entering stationary phase, including: *icmF*, *icmM*, *icmP*, *icmR* and *icmT* (Gal-Mor *et al.*, 2002). Subsequent studies demonstrated that LetA moderately regulates the expression of *icmP*, *icmR* and *icmT*, while RelA and RpoS have only minor effects on *dot/icm* expression

17

(Gal-Mor and Segal, 2003b; Zusman *et al.*, 2002). In contrast, *letA* mutants show a substantial decrease in *dotA* transcription, indicating that LetA may regulate a subset of *dot/icm* genes (Lynch *et al.*, 2003).

While each of the previously described studies have implicated indirect regulators of *dot/icm* genes, the only evidence for direct regulation is by the response regulator CpxR (Gal-Mor and Segal, 2003a). CpxR and its cognate sensor kinase CpxA constitute a classic two-component system whose autophosphorylation is stimulated by stress signals (Gal-Mor and Segal, 2003a). Data indicate that CpxR directly regulates *icmR* gene expression, and, while likely indirect, can also moderately induce the *icmV-dotA* and *icmW-icmX* operons. Nevertheless, CpxR is dispensable for intracellular growth in both human-derived macrophages and *A. castellanii*, suggesting that *dot/icm* genes must be positively regulated by other factors to enable *L. pneumophila* to establish a replicative vacuole (Gal-Mor and Segal, 2003a).

Genomic methods of studying differentiation

When confronted with environmental fluctuations, *L. pneumophila* must coordinately regulate its gene expression profile to enhance its fitness and adaptability. Since a large number of genes are dedicated to controlling differentiation, and a diverse repertoire of genes are expressed during the different phenotypic states, modern techniques have been applied to allow a comprehensive analysis of *L. pneumophila* biology. Recently, the complete genome sequences of *L. pneumophila* strains Lens, Paris and Philadelphia 1 were published, and many genes predicted to promote microbial adaptation were identified, including six sigma factors, 13 histidine kinases, 14 response regulators and 23 members of the GGDEF-EAL family of regulators (Cazalet *et al.*, 2004; Chien *et al.*, 2004). A comparison of the genome sequences of Lens, Paris and Philadelphia 1 revealed a remarkable plasticity and diversity of *L. pneumophila*, two characteristics thought to enhance the versatility of the microbe. In addition, genome-

18

wide promoter trap strategies have been utilized to discern *L. pneumophila* genes that are specifically expressed during intracellular replication; this class of factors includes redox proteins, a response regulator and sensor kinase, several heavy metal transporters, and a gene homologous to the Pht family of transporters, *smlA* (Rankin *et al.*, 2002). Furthermore, proteomic analysis of *L. pneumophila* has been used to successfully identify 130 expressed proteins, including: flagellin, legiolysin, and components and substrates of the Dot/Icm type IV secretion system (IcmX, RalF, SdeA and SidC) (Lebeau *et al.*, 2005). In the future, research that is directed toward the global analysis of the *L. pneumophila* genome and proteome may identify regulatory factors that promote survival under disparate environmental conditions, as well as components essential to its pathogenesis.

Figure 1.1.
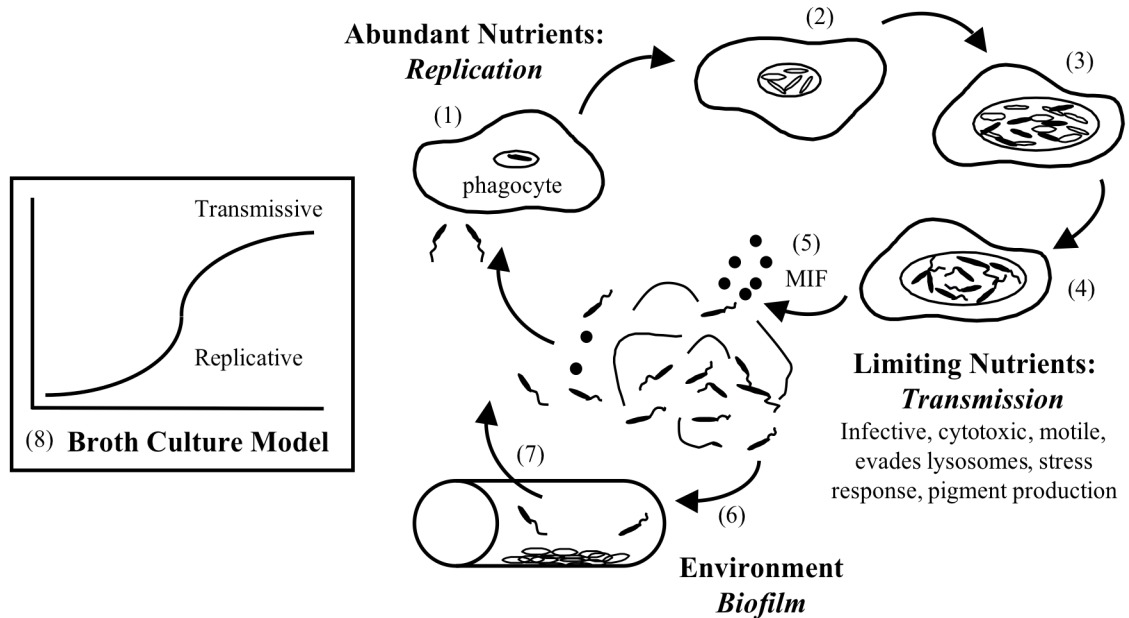
Figure 1.1. Life cycle of *L. pneumophila.*

(1) Transmissive *L. pneumophila* engulfed by phagocytic cells reside in vacuoles and avoid lysosomal degradation. (2) Under favorable conditions, transmissive bacteria begin to replicate. (3) When nutrients are depleted, replicating bacteria stop dividing and begin to express transmission traits. (4) Microbes may develop into a more resilient and infectious mature intracellular form (MIF). (5) The host cell is lysed and transmissive microbes are released into the environment. (6) *L. pneumophila* that do not encounter a new host cell probably establish biofilms in water systems and ponds. (7) When microbes encounter a host cell, the cycle begins anew. (8) *L. pneumophila* cultured in broth to either exponential or stationary phase exhibit many of the traits of the replicative and transmissive forms, respectively. *Modified from Molofsky AB and Swanson MS (2004) Mol Microbiol 53(1):29-40.*

Figure 1.2.
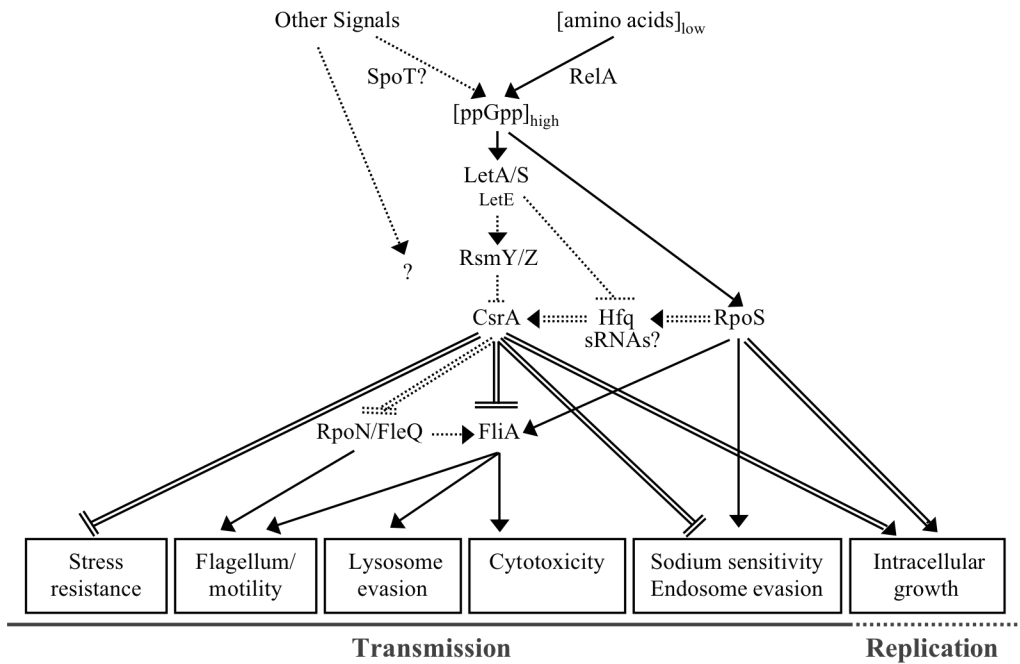
Figure 1.2. A model for regulation of *L. pneumophila* differentiation.
Arrows indicate activation and bars indicate inhibition. Replicative phase regulatory interactions are represented by solid double lines, while transmission phase regulatory pathways are indicated by a single solid line. Speculative interactions are designated by dotted lines.

Figure 1.3.
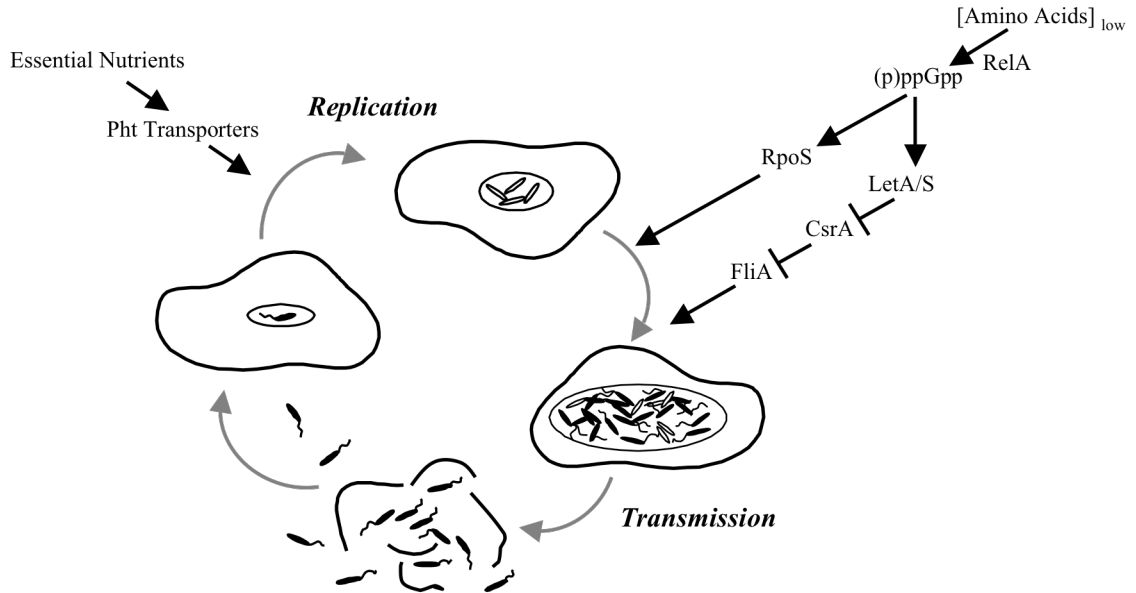
Figure 1.3. Pht transporters couple nutrient acquisition to microbial differentiation. Transport of amino acids and other essential metabolites by Pht proteins trigger intracellular transmissive *L. pneumophila* to differentiate to the replicative form. Nutrient acquisition via Pht proteins is also essential for *L. pneumophila* to replicate in macrophages. When replicative bacteria fail to acquire essential amino acids, *L. pneumophila* induce expression of transmission traits.

CHAPTER TWO

THE MULTI-STEP DESIGN OF THE LETA/LETS TWO-COMPONENT SYSTEM ENABLES *LEGIONELLA PNEUMOPHILA* TO CUSTOMIZE ITS ARRAY OF VIRULENCE TRAITS

Summary

When confronted with environmental stresses, *Legionella pneumophila* converts from a non-infectious, replicative form to an infectious form required for host transmission. This process is mediated by the LetA/LetS two-component system, which belongs to a family of signal-transducing proteins that employ a four-step phosphorelay to regulate gene expression. We determined that histidine 307 in LetS is the primary histidine required to activate LetA and that other residues in LetS cannot substitute for LetA/LetS function. Additionally, a threonine substitution at position 311 of LetS generated a *L. pneumophila* mutant with an intermediate phenotype. When compared with WT and *letS* null bacteria, *letS*^{T311M} mutants were intermediate for the transmission traits of infectivity, cytotoxicity and lysosome evasion. In contrast, *letS*^{T311M} mutants resemble either WT or *letS* null bacteria for the other transmissive phase phenotypes. After observing that only 30-50% of *letS*^{T311M} mutants were motile, we demonstrated by flow cytometry that every cell in the population eventually activates the flagellin promoter to a similar level, but the expression is delayed when compared to WT. Moreover, transcriptional profile analysis of *letS*^{T311M} mutants indicated that gene expression of not only the flagellar regulon but also numerous other loci was delayed when compared to WT. We postulate that, compared to the WT LetS sensor protein, the LetS^{T311M} mutant relays phosphate either slowly or less efficiently, thereby leading to

sluggish gene expression and a unique phenotypic profile. Accordingly, we propose that the multi-step design of this family of two-component systems allows microbes to modulate their phenotypic profiles as deemed appropriate for the local environment.

Introduction

In aquatic reservoirs, the gram-negative bacterium *Legionella pneumophila* most likely resides within biofilm communities (Fields *et al.*, 2002). However, when *L. pneumophila* are ingested by various species of amoebae or ciliated protozoa, they avoid digestion and instead establish a protective intracellular niche (Fields *et al.*, 2002). Consequently, if humans inhale aerosols contaminated with *L. pneumophila*, the bacteria can exploit alveolar macrophages (Horwitz and Silverstein, 1980) to cause an acute pneumonia, Legionnaires' disease (McDade *et al.*, 1977). Due to the disparate conditions under which *L. pneumophila* persists, the pathogen must employ strategies that enable swift adaptations to environmental fluctuations.

One mechanism by which *L. pneumophila* acclimate to their surroundings is by altering their cellular physiology in a process known as differentiation (Molofsky and Swanson, 2004). When either protozoa or professional phagocytes engulf transmissive phase *L. pneumophila*, the microbes avoid lysosomal degradation and instead establish vacuoles isolated from the endosomal network, a process mediated by a type IV secretion system (Berger and Isberg, 1993; Roy *et al.*, 1998; Segal *et al.*, 1998; Vogel, 1998) and the shedding of vesicles rich in lipopolysaccharide (Fernandez-Moreira *et al.*, 2006). If conditions in the vacuole are favorable, *L. pneumophila* represses its transmissive traits and instead undergoes robust replication (Fettes *et al.*, 2001; Molofsky and Swanson, 2003). Once amino acid supplies and other nutrients are exhausted, bacterial replication halts, and the progeny induce traits that promote escape from their spent host, survival in the extracellular milieu, and the ability to infect subsequent phagocytic cells (Hammer

and Swanson, 1999; Molofsky and Swanson, 2003; Sauer *et al.*, 2005; Zusman *et al.*, 2002).

From studies of synchronous broth cultures, many of the regulatory elements that govern the reciprocal phases displayed by *L. pneumophila* during its life cycle have been discerned. During the exponential (E) phase of growth, the post-transcriptional regulator CsrA and the sRNA chaperone Hfq suppress transmissive traits and promote replication (Fettes *et al.*, 2001; McNealy *et al.*, 2005; Molofsky and Swanson, 2003). However, once E phase *L. pneumophila* experience nutrient deprivation, cell division stops, and the enzymes RelA and SpoT produce the alarmone ppGpp (Hammer and Swanson, 1999; Zusman *et al.*, 2002). Activation of the stringent response pathway leads to an accumulation of ppGpp in the bacterial cytosol (Hammer and Swanson, 1999; Zusman *et al.*, 2002). As a result, the LetA/LetS two-component system (*Legionella* transmission activator and sensor, respectively) transcribes two small regulatory RNAs, RsmY and RsmZ, which then bind to CsrA to relieve its repression on the transmission traits (Hammer and Swanson, 1999; Hammer *et al.*, 2002; Molofsky and Swanson, 2003). Together with alternative sigma factors and other regulatory proteins, the LetA/LetS system induces traits that enable efficient host transmission and survival in the environment including: sodium sensitivity, infectivity, cytotoxicity, motility, lysosome evasion and pigment production (Edwards and Swanson, 2006; Steinert *et al.*, 2007).

For most two-component systems, the physiological stimulus that activates the signal transduction pathway has remained elusive. Nevertheless, for the two-component systems where the environmental cues or conditions are known, it appears that multiple inputs can induce the phosphorelay (Calva and Oropeza, 2006). In *L. pneumophila*, the precise signal that triggers LetS autophosphorylation has yet to be identified. However, similar to other two-component systems, we predict that various stimuli may induce the phosphorelay, and likewise *L. pneumophila* differentiation.

Originally identified by screening for mutants defective for flagellin production, the LetA/LetS two-component system was subsequently shown to regulate all known transmissive phase phenotypes (Hammer *et al.*, 2002). Although conventional two-component systems require a two-step phosphorelay to induce a response, the *L. pneumophila* LetA/LetS system belongs to a family of signal-transducing proteins whose tripartite sensor kinase regulates their response pathways. The model for this unorthodox family of signaling molecules is the *Bordetella* BvgA/BvgS system, which employs a four-step relay involving consecutive phosphorylation of His-Asp-His-Asp residues (Uhl and Miller, 1996b, c). BvgS is the sensor protein whose large periplasmic domain is also linked by a membrane-spanning region to three cytoplasmic signaling domains (Cotter and DiRita, 2000). BvgA is the cytoplasmically located activator kinase that, upon phosphorylation, gains an affinity for Bvg-regulated promoters (Cotter and DiRita, 2000; Cotter and Jones, 2003). Upon receiving an appropriate signal, BvgS autophosphorylates on a conserved histidine residue and then sequentially transfers the phosphoryl group along the relay, culminating with BvgA activation (Uhl and Miller, 1994). It has been proposed that the complexity of the BvgA/BvgS signaling mechanism enables *Bordetella* to express a spectrum of traits according to local conditions (Cotter and Miller, 1997; Cummings *et al.*, 2006; Stockbauer *et al.*, 2001). In support of this model, *Bordetella* alternates among at least three distinct phenotypic phases in response to various external stimuli (Cotter and Miller, 1997; Lacey, 1960). Work by Cotter and Miller has deduced that the multi-step design of the BvgA/BvgS system enables *Bordetella* to regulate the amount of phosphorylated BvgA (BvgA~P) present in the cell. The level of BvgA~P, together with the binding affinities for BvgA that are present in Bvg-regulated promoters, enables *Bordetella* to control the temporal expression of different classes of genes, and likewise, its different phenotypic states (Cotter and Jones, 2003).

Unlike the well-studied *Bordetella* system, other members within this family of tripartite two-component systems have not been analyzed to discern whether they also

employ similar regulatory processes to enhance their spectrum of traits. Sequence analysis indicates that the three predicted signaling domains of LetS are highly homologous to the analogous regions of *B. bronchiseptica* BvgS; the domain architecture is also comparable. Therefore, we postulated that, similar to the *Bordetella* signal transduction system, LetA/LetS equips *L. pneumophila* to customize its genotypic and phenotypic expression profiles. To test this hypothesis, we constructed single amino acid substitutions in LetS and analyzed the mutants via transcriptional and phenotypic methods. Our data suggest that, although their down-stream circuitries differ, the *L. pneumophila* LetA/LetS two-component system resembles *Bordetella* BvgA/BvgS by functioning as a rheostat to fine-tune its virulence traits, thereby augmenting versatility and fitness.

Experimental procedures

Bacterial strains and culture conditions. *L. pneumophila* Lp02 (*thyA hsdR rpsL*; MB110), a virulent thymine auxotroph derived from the Philadelphia 1 clinical isolate, was the parental strain for all constructed mutants (Berger and Isberg, 1993). MB355 contains the pflaG plasmid, which encodes a transcriptional fusion of the *flaA* promoter to green fluorescent protein (Hammer and Swanson, 1999). MB417 contains *letS-36*, a mariner insertion allele in *lpg1912* that confers kanamycin resistance and carries the pflaG plasmid for fluorescence quantification (Hammer *et al.*, 2002). To construct a *letS* insertion mutant that lacks pflaG, the *letS* locus containing the transposon insertion was amplified from MB417 and transferred to Lp02 by natural competence, resulting in strain MB416 (Hammer *et al.*, 2002). Bacteria were cultured at 37°C in 5 ml aliquots of *N*- (2-acetamido)-2-aminoethanesulfonic acid (ACES; Sigma)-buffered yeast extract (AYE) broth and supplemented with 100 μg/ml thymidine when necessary. Post-exponential (PE) cultures were defined as having an optical density at 600 nm (OD_{600}) of 3.4 to 4.5;

within each experiment, similar culture densities were used to analyze strain phenotypes. To enumerate colony-forming units (CFU), *L. pneumophila* were plated on ACES-buffered charcoal-yeast extract agar supplemented with 100 µg/ml thymidine (CYET) and incubated at 37°C. For constructing amino acid substitutions in *letS*, the semi-defined media CAA was prepared as described (Mintz *et al.*, 1988) and thymidine added to 100 µg/ml (CAAT media). For solid CAAT media, agar was added to 15 mg/ml, starch to 5 mg/ml, and trimethoprim to 100 µg/ml.

Macrophage culture. Bone marrow-derived macrophages were isolated from femurs of A/J mice (Jackson Laboratory) and cultured in RPMI-1640 containing 10% heat-inactivated fetal bovine serum (RPMI/FBS; Gibco BRL) as described previously (Swanson and Isberg, 1995). After a 7-day incubation in L-cell supernatant-conditioned media, macrophages were plated at 2.5×10^5/well in 24-well plates for infectivity and degradation assays and to 5×10^4/well in 96-well plates for cytotoxicity assays.

Construction of chromosomal substitutions. The 3.1-kb *letS* locus was amplified from Lp02 genomic DNA using primers LetS F and LetS R (Table 2.2), the PCR fragment purified and ligated into pGEM-T (Promega), and the resulting plasmid designated as pletS (pMB596). Nucleotide substitutions were introduced into the *letS* ORF in pletS using the QuikChange XL site-directed mutagenesis kit (Stratagene). A glutamate was substituted for the histidine at amino acid 307 by changing CAT to CAA with primers LetS Mut His F and LetS Mut His R (Table 2.2), resulting in the plasmid pletS^{H307Q} (pMB610). To substitute methionine for the threonine at residue 311 of *letS*, ACC was changed to ATG using primers LetS Mutagenesis F and LetS Mutagenesis R (Table 2.2), resulting in pletS^{T311M} (pMB597). Synthesis of plasmid DNA, template digestion and transformations into XL10-gold were performed according to the manufacturer.

28

Mutagenesis was verified by sequencing the *letS* locus using the primer LetS Mut Seq F (Table 2.2).

The gene encoding thymidylate synthetase was excised from pMB540 and subcloned into the *Eco*RI site of pletS (MB598). The interrupted gene was amplified by PCR using primers LetS F and LetS R (Table 2.2), transferred to Lp02 by natural competence as described (Stone and Abu Kwaik, 1999), and selected for growth in the absence of thymidine (MB599). The point mutants were amplified from their respective plasmids, pletS^{H307Q} or pletS^{T311M}, using primers LetS F and LetS R (Table 2.2), the PCR fragments purified (Qiaquick PCR purification kit; Qiagen), and the PCR products transferred to a patch of MB599 on CYET media. Following a 2-day incubation at 30°C, the cells were resuspended in 1 ml CAA and plated onto solid CAAT media with or without trimethoprim. Recombinants were selected for growth on media containing trimethoprim and confirmed both by their thymidine requirement and by sequencing the *letS* locus with the LetS Mut Seq F primer (Table 2.2).

Sequence and protein analysis. The membrane-spanning regions of LetS were predicted using Kyte-Doolittle hydropathy plots (Kyte and Doolittle, 1982). To predict the protein domains that are present in LetA and LetS, amino acid sequences were analyzed using the Conserved Domain Database (Marchler-Bauer *et al.*, 2005). For alignments of the two-component sensor kinases, amino acid sequences from *L. pneumophila* LetS; *B. bronchiseptica* BvgS; *E. coli* ArcB, BarA, EvgS and TorS; *Pseudomonas aeruginosa* GacS; and *Salmonella typhimurium* BarA were aligned using T-Coffee (Notredame *et al.*, 2000). To determine the percent identity and similarity between *L. pneumophila* LetS and *B. bronchiseptica* BvgS amino acid sequences, the GeneStream align program was used (Pearson *et al.*, 1997).

Infectivity. To ascertain the degree to which *L. pneumophila* bind, enter, and survive inside macrophages, PE bacteria were co-cultured with macrophages at a 1:1 ratio in duplicate (Byrne and Swanson, 1998). The cells were centrifuged at 400 × g for 10 min at 4°C and then incubated an additional 2 h at 37°C (Molofsky *et al.*, 2005). To remove extracellular bacteria, the infected monolayers were washed three times with fresh RPMI/FBS. Macrophages were mechanically lysed in 1 ml of PBS, the lysate plated onto CYET, and the intracellular bacteria enumerated. Infectivity was expressed as (cell-associated CFU at 2 h/CFU added at 0 h) × 100 (Bachman and Swanson, 2004b; Byrne and Swanson, 1998).

Cytotoxicity. To measure contact-dependent cytotoxicity of *L. pneumophila* for macrophages, PE phase bacteria suspended in RPMI/FBS were added to macrophages at various multiplicities of infection (MOIs) in triplicate. After centrifugation at 400 × g for 10 min at 4°C (Molofsky *et al.*, 2005), cells were incubated for 1 h at 37°C. To assess macrophage viability, the infected monolayers were incubated for 6-12 h with RPMI/FBS that contained 10% alamarBlue™ (Trek Diagnostic Systems), and then reduction of the colorimetric dye was measured spectrophoretically and calculated as described (Byrne and Swanson, 1998; Hammer and Swanson, 1999; Molofsky *et al.*, 2005).

Lysosomal degradation. The percent of microbes that were intact following a 2-h incubation in macrophages was determined by fluorescence microscopy. Briefly, cells plated onto coverslips in a 24-well plate were infected with PE *L. pneumophila* at an MOI ~1. Following centrifugation at 400 × g for 10 min at 4°C, the cells were incubated at 37°C for 2 h. After removing uninternalized bacteria by washing with RPMI/FBS, the macrophages were fixed, permeabilized and stained for *L. pneumophila* as described, and duplicate coverslips were scored for intact rods versus degraded particles (Bachman and Swanson, 2001; Molofsky and Swanson, 2003; Swanson and Isberg, 1996).

Sodium sensitivity. Sodium sensitivity was determined by plating 10-fold serial dilutions of PE broth cultures in PBS onto CYET agar containing or lacking 100 mM NaCl (Molofsky and Swanson, 2003). Following a 6-day incubation at 37°C, CFUs were enumerated, and the percent of sodium sensitive bacteria calculated as described (Byrne and Swanson, 1998).

Pigmentation. To quantify pigment accumulation, 1 ml samples were obtained from broth cultures maintained in the PE phase for 5 days at 37°C. The aliquots were centrifuged at $16,000 \times g$ for 10 min and supernatants measured at OD_{550nm} (Molofsky and Swanson, 2003; Wiater *et al.*, 1994).

Flow cytometry. To monitor the promoter activity for an entire *letS*[T311M] population of cells, MB597 was transformed with pflaG, which contains the promoter for the flagellin gene, *flaA*, fused to a GFP reporter (Hammer and Swanson, 1999). The resulting strain, MB605, was cultured in AYE media and monitored for induction of the *flaA* promoter over time. At the designated optical densities, samples were centrifuged at $5,900 \times g$, washed in PBS to remove impurities and the cells normalized to 5×10^5 in PBS. Total GFP fluorescence was analyzed using a BD FACSAria™ cell sorter. PE MB355 and MB417 were used as positive and negative controls, respectively.

Statistical analyses for phenotypic assays. To calculate *p*-values for infectivity, lysosomal degradation, sodium sensitivity and pigmentation assays, one-way analysis of variance (ANOVA) was used for at least 3 independent samples.

RNA isolation, RNA labeling and microarray hybridization. WT and *letS*[T311M] mutants were cultured on an orbital shaker at 37°C to either $OD_{600} = 2$ or $OD_{600} = 3$ in 500 ml

31

AYE containing 100 µg/ml thymidine. Upon reaching the appropriate optical density, 10

ml aliquots were centrifuged at 6,000 × g for 2 min. at 4ºC. The culture supernatants

were discarded, and the pellets were flash frozen and stored at -80ºC. Total RNA was

extracted using TRIzol (Invitrogen) as described previously (Milohanic *et al.*, 2003). The

RNA was reverse-transcribed and labeled with Cy3 or Cy5 according to the

manufacture's instructions (Amersham Biosciences). The microarrays were designed to

contain gene-specific 70mer oligonucleotides based on all predicted genes within the

genome of *L. pneumophila* strain Paris (CR628336) and its plasmid (CR628338) as

described previously (Bruggemann *et al.*, 2006). Hybridizations were performed

following the manufacturers' recommendations (Corning) using 250 pmol of Cy3 and

Cy5 labeled cDNA. Slides were scanned on a GenePix 4000A scanner (Axon

Instruments) and the laser power and PMT were adjusted to balance the two channels.

The resulting files were analyzed using Genepix Pro 5.0 software. Spots were excluded

from analysis if they contained high background fluorescence, slide abnormalities or

weak intensity. To obtain statistical data for the gene expression profiles, all microarrays

were performed in duplicate with a dye swap.

Data and statistical analysis for microarrays. Data normalization and differential

analysis were conducted using the R software (http://www.R-project.org). No

background subtraction was performed, but a careful graphical examination of all the

slides was performed to ensure a homogeneous, low-level background in both channels.

A loess normalization (Yang *et al.*, 2002) was performed on a slide-by-slide basis

(BioConductor package marray;

http://bioconductor.org/packages/2.2/bioc/html/marray.html). Differential analysis was

carried out separately for each comparison between the two time points, using the VM

method (Delmar *et al.*, 2005), together with the Benjamini and Yekutieli p-value

adjustment method (Reiner *et al.*, 2003). If not stated otherwise, only differently

expressed genes with 1.6-fold-changes were taken into consideration. Empty and flagged spots were excluded from the data set, and only genes without missing values for the comparison of interest were analyzed.

Results

Architecture of the LetA/LetS signal transduction system

The *L. pneumophila* LetA/LetS two-component system belongs to a family of signaling molecules that use a multi-step phosphorelay to activate or repress their target genes. LetS is a 103 kDa sensor kinase that is likely localized to the membrane by two transmembrane regions (Kyte and Doolittle, 1982). In addition, LetS is predicted to have three cytoplasmic signaling domains, namely a transmitter, receiver and histidine phosphotransfer domain (Marchler-Bauer *et al.*, 2005). The cognate response regulator, LetA, is a 43 kDa protein that contains a receiver domain and a helix-turn-helix motif (Marchler-Bauer *et al.*, 2005). By analogy to proteins of similar structure, it is predicted that, in response to a signal input, LetS autophosphorylates on a histidine residue and then sequentially transfers the phosphoryl group to an aspartic acid in the receiver domain, to a second histidine in the histidine phosphotransfer domain, and finally to an aspartic acid located in the receiver domain of LetA. Sequence analysis indicates that, overall, LetS is only 18% identical to BvgS at the amino acid level (Pearson *et al.*, 1997). However, within each H box region, which contains the primary phosphorylation site, LetS is 78% identical and 89% similar to BvgS (Pearson *et al.*, 1997). Due to the similarities displayed between LetS and BvgS in this critical portion of each protein, we predicted that *L. pneumophila* also uses a four-step phosphorelay to customize its traits when challenged by local stresses and fluctuations.

33

The H-box regions of many sensor kinases are highly conserved

Since LetS belongs to a family of tripartite two-component systems, we postulated that other sensor kinases within this unorthodox class of signaling molecules might have comparable domain architecture, and likewise, might employ similar regulatory mechanisms. Amino acid sequences from *L. pneumophila* LetS, *B. bronchiseptica* BvgS, *Escherichia coli* ArcB, BarA, EvgS and TorS, *Pseudomonas aeruginosa* GacS, and *Salmonella typhimurium* BarA were aligned using T-Coffee (Notredame *et al.*, 2000). Indeed, the H-box regions of all the sensor proteins analyzed are remarkably similar. Moreover, the primary histidine residue, which is the proposed site for autophosphorylation, is conserved (Fig. 2.1B). Importantly, the threonine residue, which, when substituted with methionine enables *Bordetella* to display an intermediate class of genes and phenotypes (Cotter and Miller, 1997), is also conserved among all family members analyzed (Fig. 2.1B). Therefore, we sought to test whether the rheostat model of the *Bordetella* BvgA/BvgS system is also applicable to other members of this family of signal transducing proteins.

Histidine 307 of LetS is critical for LetA/LetS activity

In response to a stimulus, the sensor protein of a microbial two-component system autophosphorylates on a conserved histidine residue using ATP as a phosphate donor. In *Bordetella*, a histidine-to-glutamine substitution at amino acid 729 of BvgS abolishes its autophosphorylation as well as BvgA activation (Uhl and Miller, 1994). Sequence alignments between the *L. pneumophila* and *Bordetella* sensor kinases predict that histidine 307 of LetS is the initial site of phosphorylation (Fig. 2.1A). To test this model,

we substituted a glutamine residue for histidine 307 of LetS. The unmarked, chromosomal point mutant, designated as *letS*[H307Q], was verified by amplifying and sequencing the *letS* locus. Subsequently, *letS*[H307Q] was analyzed for its expression of PE phenotypes using WT *L. pneumophila* and a *letS* transposon insertion mutant (allele *letS-36*) as positive and negative controls, respectively.

Phenotypic analysis of *letS*[H307Q] mutants indicated that, after a 2 h incubation with macrophages, less than 5% of the *L. pneumophila* inoculum remains cell-associated (Fig. 2.2A). In addition, histidine 307 of LetS is essential for both flagellin- and contact-dependent cell death of macrophages (Molofsky *et al.*, 2005). Likewise, phase-contrast microscopy indicated that *letS*[H307Q] mutants are completely defective for motility (data not shown). Using immunofluorescence microscopy to analyze the morphology of intracellular bacteria following a 2 h incubation within macrophages, we determined that, similar to the *letS* insertion mutant, only 40% of *letS*[H307Q] mutants resist lysosomal degradation (Fig. 2.2C). Furthermore, histidine 307 of LetS is necessary for salt sensitivity, a phenotype that reflects activity of the type IV secretion system (Byrne and Swanson, 1998; Sadosky *et al.*, 1993; Vogel *et al.*, 1996), as well as for the production of a soluble melanin-like pigment that accumulates in the PE phase (Warren and Miller, 1979; Wiater *et al.*, 1994; Wintermeyer *et al.*, 1994). Taken together, these data are consistent with the model that histidine 307 is the autophosphorylation site of LetS that is critical for LetA/LetS activity, and other residues in LetS cannot substitute to activate LetA.

An amino acid substitution at position 311 of LetS unveils a hierarchy among PE phenotypes

The *Bordetella* BvgA/BvgS paradigm suggests that the design of the two-component system equips the bacteria with a rheostat to customize their expression profile. In support of this model, seminal work from Cotter and Miller demonstrated that a single amino acid substitution at residue 733 of BvgS created a mutant that displayed intermediate phenotypes (Cotter and Miller, 1997). To test this model, a methionine was substituted for the corresponding threonine at position 311 in the cytoplasmic transmitter domain of LetS, four residues from the proposed autophosphorylation site. After sequence verification, the *letS^T311M* mutant was analyzed for each PE phenotype. The *letS^T311M* mutants were identical to WT *L. pneumophila* in the PE phase with regard to their sodium sensitivity, as no apparent defect was detected (Fig. 2.3A). However, *letS^T311M* mutants resembled *letS* null bacteria in that neither mutant accumulated appreciable levels of the soluble pigment (Fig. 2.3B). Moreover, when *letS^T311M* mutants were compared to WT and *letS* null bacteria, the point mutant was intermediate for several PE traits. For example, *letS^T311M* mutants were intermediate for entry and survival in macrophages (Fig. 2.4A) and for contact-dependent cytotoxicity (Fig. 2.4B). Likewise, only approximately 25-40% of *letS^T311M* mutants were motile, as indicated by microscopic analysis (data not shown). By analyzing the number of bacteria that escape lysosomal degradation, we also deduced that the *letS^T311M* mutant was intermediate when compared to WT and *letS* null bacteria (Fig. 2.4C). Therefore, these phenotypic data support the model that the design of the LetA/LetS system enables the bacteria to display a spectrum of traits. Moreover, a hierarchy exists with regard to the expression of the *L. pneumophila* PE phenotypes.

Promoter analysis demonstrates that the letS^{T311M} mutant has a kinetic delay

The PE phenotypes of infectivity, cytotoxicity and lysosome evasion all depend on motility (Molofsky *et al.*, 2005). Since the *letS^{T311M}* mutant was intermediate for each of these traits, we predicted that either all cells expressed the flagellin promoter at a weaker level than WT or a mixed population of *letS^{T311M}* cells was present. To distinguish between these two models, we monitored promoter expression by transforming WT and the *letS^{T311M}* mutant with a reporter construct that contained a transcriptional fusion of the flagellin promoter *flaA* fused to *gfp*. Flow cytometry indicated that at, an OD$_{600}$ = 1, the majority of cells in WT cultures had low levels of *flaA* expression (Fig. 2.5A). At the transition between the E and PE phases (OD$_{600}$ ~ 3), two populations of cells were present in WT samples: One had low *flaA* promoter activity and another showed robust induction of the flagellin promoter (Fig. 2.5A). Once WT *L. pneumophila* reached the PE phase (OD$_{600}$ = 3.4), every cell in the population induced *flaA* to high levels (Fig. 2.5A). It was striking that the *letS^{T311M}* mutant displayed a similar profile of *flaA* promoter activity when compared to WT *L. pneumophila*, albeit delayed (Fig. 2.5B). For example, cells in the *letS^{T311M}* mutant population did not induce high levels of the flagellin promoter until OD$_{600}$ = 4.2, a density significantly higher than the OD$_{600}$ = 3.1 for WT *flaA* expression (compare Fig. 2.5 A and B). Thus, every cell in the *letS^{T311M}* mutant population is able to activate the *flaA* promoter to WT levels, but the cells have a kinetic defect.

Transcriptome analysis indicates that the letS^{T311M} mutant has a delayed transcriptional profile

To deduce whether the *letS^{T311M}* mutant has a transcriptional delay beyond the flagellin promoter, the mutant was compared via microarrays to WT *L. pneumophila* at different stages of growth. At an OD$_{600}$ = 2, 58 genes were significantly repressed in the *letS^{T311M}* mutant when compared to WT (Table 2.3). Several categories of genes were

represented, including genes that are required for flagellum biosynthesis (*flgDEFGHIJKL/lpg1218-26* and *fliHG/lpg1758-9*; Table 2.4). Corresponding to the class II genes of the flagellar cascade, these genes are typically induced in WT *L. pneumophila* at the late E and early PE phases (Bruggemann *et al.*, 2006). In addition, several regulatory genes were repressed, such as the two small regulatory RNAs *rsmY* and *rsmZ* and the response regulator *lqsR/lpg2732* (Tables 2.3 and 2.4). Previous microarray experiments revealed that *lqsR* regulates the expression of genes involved in virulence, motility and cell division, consistent with a role for LqsR in the transition from the E to the PE phase. However, the expression of *lqsR* was also shown to be dependent on RpoS and to a lesser extent, LetA (Tiaden *et al.*, 2007). Therefore, we cannot exclude the possibility that the *letS*^{T311M} mutation has an indirect effect on *lqsR* gene expression. Transcriptional analysis also showed that genes encoding poly-hydroxybutyrate synthesis (*phaB1-3/lpg1059-61*) were poorly expressed by the mutant strain (Tables 2.3 and 2.4).

Similarly, at an OD$_{600}$ = 3, which corresponded to the early PE phase, 92 genes were significantly reduced in the *letS*^{T311M} mutant as compared to WT *L. pneumophila* (Tables 2.3 and 2.4). Fifty of these genes encode unknown functions, and most lack similarity with any other protein or domain stored in the publicly available databases (Table 2.3). Among the known genes, expression of several Dot/Icm type IV secretion substrates and homologs were reduced at OD$_{600}$ = 3 in the *letS*^{T311M} mutant (*sdeA/lpg2157*, *sidF/lpg2584*, *sidG/lpg1355*; Tables 2.3 and 2.4), as was the newly identified cytotoxic glycosyltransferase (Belyi *et al.*, 2008). The expression of several regulatory proteins was also clearly affected by the *letS*^{T311M} mutation. For example, the PE-specific sigma factor *rpoE/lpg1577* (Bruggemann *et al.*, 2006) was reduced 4-fold in the *letS*^{T311M} mutant when compared to WT bacteria. Also, mRNAs for two proteins that contain GGDEF and EAL domains, *rre41/lpg0029* and *lpg2132*, as well as several members of putative two-component systems (*lpg2145*, *stuC/lpg2146* and *arcB/lpg2181*) were significantly diminished in the *letS*^{T311M} mutant (Table 2.4).

One especially informative class of genes was the flagellar regulon. Expression of *flaA* (*lpg1340*) was decreased four-fold in the *letS*[T311M] mutant when compared to WT. It is important to note that *flaA*, which encodes flagellin, is located at the bottom of the flagellar hierarchy and is commonly referred to as a class IV gene in the flagellar biosynthesis cascade (Steinert *et al.*, 2007). Moreover, expression of the upstream flagellar class II genes was diminished in the *letS*[T311M] mutant at $OD_{600} = 2$, but was no longer depressed at this later time point (Tables 2.3 and 2.4). Therefore, both our transcriptional profiling and flow cytometry data indicate that the *letS*[T311M] mutant is delayed in induction of the flagellar regulon.

When the *letS*[T311M] mutant was compared to WT at $OD_{600} = 2$, the expression of only 10 genes was significantly elevated (Table 2.5). These included: *udk/lpg1853*, which codes for a uridine kinase, *secD/lpg2001* and *secF/lpg2000*, which are both predicted to encode membrane proteins involved in protein export, and the carbon storage regulator *csrA/lpg1593*. Based on the differences in gene induction observed between the *letS*[T311M] mutant and WT *L. pneumophila* at $OD_{600} = 2$, we infer that this cohort of genes represent a *letS*[T311M] intermediate transcriptional profile. Furthermore, at an $OD_{600} = 3$, several genes were more highly expressed by the *letS*[T311M] mutant when compared to WT *L. pneumophila*. For example, the hemin binding protein *hbp/lpg0024*, the glutamine synthetase *glnA/lpg1364*, and the cell division protein *lpg0915* were induced 2-3 fold over WT levels (Table 2.5). Thus, *letS*[T311M] bacteria display an intermediate transcriptional profile during the early PE phase.

Discussion

The *L. pneumophila* LetA/LetS two-component system belongs to a family of signaling molecules that employs a four-step phosphorelay to activate or repress their target genes. The archetype for this family of two-component systems, the *Bordetella* BvgA/BvgS system, predicted that the multi-step design enables the bacteria to display

several genotypic and phenotypic phases. This is in stark contrast to the classical type of two-component systems, which are thought to function as on/off switches to regulate their cohort of genes. To investigate whether the BvgA/BvgS paradigm applies to other tripartite family members, we analyzed LetA/LetS system of *L. pneumophila*. By sequence analysis we demonstrated that the H-box regions of the sensor kinases are highly conserved among all family members (Fig. 2.1). Moreover, both the primary histidine residues and the threonine residues located four amino acids downstream of the autophosphorylation sites are also conserved (Fig. 2.1). Using as a tool the *letS*^{T311M} mutant, which was predicted to employ a sluggish phosphorelay, both our genotypic and phenotypic analysis indicate that the tripartite design of LetS enables *Legionella* to customize its traits to combat the stresses and challenges in its local environment. Based on the sequence homology within this family of two-component systems, we predict that the multi-step design is widely used by microbes to confer versatility and enhance overall fitness.

Our data revealed a hierarchy among LetA/LetS-regulated genes and phenotypes (Fig. 2.3A). For example, the *letS*^{T311M} mutant was similar to WT *L. pneumophila* with respect to salt sensitivity. This phenotype depends on the expression of the Dot/Icm type IV secretion system and is thought to reflect a large pore formed by the apparatus that allows sodium ions to enter the bacterial cell (Byrne and Swanson, 1998; Sadosky *et al.*, 1993; Vogel *et al.*, 1996). In support of this model, *dot*/*icm* genes were not significantly induced or repressed in the *letS*^{T311M} mutant when compared to WT bacteria, thus corroborating our phenotypic data (Fig. 2.3A and data not shown).

Unlike sodium-sensitivity, for several other *L. pneumophila* PE phenotypes, the *letS*^{T311M} mutant pattern fell between that of WT and *letS* null bacteria. In particular, the point mutant was intermediate for its entry and survival in macrophages, cytotoxicity, and avoidance of the lysosomal compartment (Fig. 2.4). Moreover, microscopic examination of the *letS*^{T311M} mutant at various points during the *L. pneumophila* growth phase

indicated that less than half of the population of the point mutant was motile at any given time (data not shown). Previous studies indicated that infectivity, cytotoxicity and lysosomal degradation are all largely dependent upon motility (Molofsky *et al.*, 2005). Thus, the intermediate phenotype displayed by the point mutant in each of these assays underscores the interdependency of this set of traits (Fig. 2.4 and data not shown).

To assemble the flagellum, *L. pneumophila* requires a four-tiered regulatory cascade, in which the expression and timing of each component must be tightly controlled (Steinert *et al.*, 2007). The behavior of the *letS*^{T311M} mutant illustrates that the precise coordination of the flagellar regulon is essential for constructing a functional apparatus. Even though only a subset of the *letS*^{T311M} mutant population become motile (data not shown), every cell in the *letS*^{T311M} population eventually induces the promoter for flagellin to WT levels, as judged by flow cytometry data (Fig. 2.5). Furthermore, microarray data determined that, at an $OD_{600} = 2$, mRNAs for the flagellar class II genes (*flgDEFGHIJKL/lpg1218-26* and *fliHG/lpg1758-9*) were diminished in the *letS*^{T311M} mutant as compared to WT *L. pneumophila* (Tables 2.3 and 2.4). At a later growth phase ($OD_{600} = 3$), this defect disappeared; instead, expression of the flagellar class IV gene *flaA* was reduced in the *letS*^{T311M} mutant (Tables 2.3 and 2.4). Accordingly, we infer that the motility defect of the *letS*^{T311M} mutant is the result of its kinetic defect that disrupts coordination of the flagellar regulatory cascade.

In *Bordetella,* the ability of the BvgA/BvgS system to regulate different classes of genes depends on the rate of the phosphorelay, the amount of BvgA~P, and the binding affinities for BvgA protein for the promoter regions of Bvg-regulated genes (Cotter and Jones, 2003). Accordingly, high rates of phosphate flow through the relay lead to high levels of BvgA~P, which can bind to promoter regions that contain either high or low affinity BvgA binding sites (Cotter and Jones, 2003). Conversely, lower rates of phospho-transfer leads to less BvgA~P in the cell (Cotter and Jones, 2003). As a result, BvgA only binds to and activates genes that have high affinity binding sites (Cotter and

Jones, 2003). It is predicted that the intermediate phase displayed in the *Bordetella* *bvgS^{T733M}* mutant reflects a decrease in the intracellular concentration of BvgA~P (Jones *et al.*, 2005; Williams *et al.*, 2005).

While we have not ruled out the formal possibility that the transcriptional and phenotypic defects observed in the *L. pneumophila letS^{T311M}* mutant reflect protein stability, we favor a model in which the *letS^{T311M}* mutant transduces the signal more slowly or less efficiently through the relay. In this scenario, the amount of phosphorylated LetA (LetA~P) in the cell is significantly less than that of WT *L. pneumophila*, thereby altering the timing of the expression of LetA/LetS-regulated traits. Based on our data, we predict that when *L. pneumophila* is replicating, the two-component system is either not active or somehow represses a subset of LetA/LetS-regulated genes. During this phase of the life cycle, genes that are required for replication are induced; these include genes for DNA replication and protein synthesis, and also the global repressor of PE phenotypes *csrA* (Fettes *et al.*, 2001; Molofsky and Swanson, 2003). Perhaps lower levels of LetA~P are sufficient to activate genes of the Dot/Icm type IV secretion system, and likewise, induce sodium sensitivity, since for these traits the *letS^{T311M}* mutant was transcriptionally and phenotypically similar to WT *L. pneumophila* (Fig. 2.3, 2.6 and data not shown). We deduce that more LetA~P is needed to induce the flagellar cascade, since the *letS^{T311M}* mutant was delayed in transcription of the flagellar genes (Fig. 2.5 and 2.6; Tables 2.3 and 2.4) and also intermediate for each of the motility-dependent phenotypes (Fig. 2.4 and 2.6). Finally, high levels of LetA~P are likely required for pigmentation, because the *letS^{T311M}* mutant never accumulated detectable levels of the soluble pigment (Fig. 2.3 and 2.6). Likewise, we infer that higher levels of LetA~P are needed to transcribe *lpg0012*, *lpg1174* and *lpg1895*, since the mRNA of each was significantly diminished in the *letS^{T311M}* mutant when compared to WT bacteria at both $OD_{600} = 2$ and $OD_{600} = 3$ (Table 2.3 and Fig. 2.6). Taken together, our transcriptional and phenotypic data supports the rheostat model of regulation,

whereby microbes use a multi-step two-component system to fine-tune their expression of gene hierarchies.

Although the *Bordetella* BvgA/BvgS system has been an informative paradigm for this family of signaling molecules, significant differences in the architecture of the *Bordetella* and *Legionella* regulatory cascades exist. For example, the *Bordetella* two-component system controls many classes of genes through differences in the binding affinities of BvgA~P to variations in the consensus sequences of the Bvg-regulated promoter regions. However, no conserved LetA-dependent DNA-binding motifs could be identified upstream of any of the LetA/LetS-regulated genes (Sahr *et. al.*, unpublished**)**. Instead, bioinformatics and biochemical data suggest that LetA may only bind to and induce two small RNAs, RsmY and RsmZ (Kulkarni *et al.*, 2006). These results imply that the model of LetA/LetS regulation must deviate from the *Bordetella* system. Moreover, the regulatory cascade that induces the PE phase *L. pneumophila* genes and phenotypes also requires the Csr system (Fettes *et al.*, 2001; Molofsky and Swanson, 2003).

To incorporate these additional features into our model, we predict that, when LetS receives a stimulus, it autophosphorylates and transfers the phosphoryl group along the relay, culminating with LetA phosphorylation. Once activated, LetA then binds to its two DNA targets, RsmY and RsmZ (Fig. 2.7). After their transcription, the small RNAs are then free to titrate CsrA from its respective cohort of mRNAs, thereby enabling RNA polymerase to bind to and translate the transcripts (Fig. 2.7). According to this model, we infer that the *letS*^{T311M} mutant would have less intracellular LetA~P, and likewise less RsmY and RsmZ transcribed. Analogous to the *Bordetella* system, perhaps CsrA has different affinities for particular mRNAs. If so, the amount of RsmY and RsmZ would then affect the order in which mRNAs are relieved from CsrA repression. Perhaps by having the LetA/LetS and Csr systems in tandem, *L. pneumophila* can adapt to stresses more quickly, since mRNA transcripts for critical transmission traits would already have

been generated. Although *Bordetella* lacks the Csr system, many other members within this family of two-component systems do contain this additional level of regulation, including *A. baumannii*, *E. coli*, *S. typhimurium*, *S. marcescens*, *P. aeruginosa* and *V. cholerae* (Lapouge *et al.*, 2008; Lucchetti-Miganeh *et al.*, 2008). Thus, the *L. pneumophila* LetA/LetS system can serve as a valuable alternative model for this large family of signaling molecules.

Table 2.1. Bacterial strains and plasmids

Strain or Plasmid	Relevant genotype/phenotype	Reference or Source
Strains		
E. coli		
DH5α	F⁻ *endA1 hsdR17* (r⁻ m⁺) *supE44 thi-l recA1 gryA* (Nal¹) *relA1* Δ (*lacZYA-argF*⁻)$_{U169}$ φ80d*lacZ*Δ*M15* λ*pir*RK6	Laboratory Collection
XL10-Gold	Tet^R Δ(*mcrA*)*183* Δ(*mcrCB-hsdSMR-mrr*)*173 endA1 supE44 thi-1 recA1 gyrA96 relA1 lac* Hte [F′ *proAB lacI*^{q}*Z*Δ*M15* Tn*10*(Tet^R) Amy Cam^R]	Stratagene
MB596	DH5α pletS	This work
MB597	DH5α pletS^{T311M}	This work
MB598	DH5α pletS::*thyA*	This work
MB610	DH5α pletS^{H307Q}	This work
MB540	DH5α pBluescript KS⁺ with *thyA*	Laboratory Collection
L. pneumophila		
MB110	wild type; *thyA hsdR rpsL*	(Berger and Isberg, 1993)
MB355	pflaG	(Hammer and Swanson, 1999)
MB416	*letS-36*::*kan*	(Hammer *et al.*, 2002)
MB417	*letS*::*kan* pflaG	(Hammer *et al.*, 2002)
MB599	*letS*::*thyA*	This work
MB600	*letS*^{T311M}	This work
MB605	*letS*^{T311M} pflaG	This work
MB611	*letS*^{H307Q}	This work
Plasmids		
pGEM-T	Multiple cloning site within coding region of β-lactamase α fragment linearized with single-T overhangs; 3 kb; Amp^R	Promega
pflaG	150 bp *flaA* promoter fragment fused to GFP, encodes thymidylate synthetase; 10.5 kb; Amp^R	(Hammer and Swanson, 1999)
pletS	pGEM-T containing 3.1 kb *letS* fragment PCR amplified from Lp02 chromosome and ligated into T overhangs; 6.1 kb; Amp^R	This work
pletS^{T311M}	pletS with a ACC to ATG change; 6.1 kb; Amp^R	This work
pletS^{H307Q}	pletS with a CAT to CAA change; 6.1 kb; Amp^R	This work
pletS::*thyA*	pletS with 1.8 kb *thyA* fragment inserted into *Eco*RI site at base 436 of *letS*; 7.9 kb; Amp^R	This work

Table 2.2. Primers for amplification and mutagenesis of *letS*

Primer	Sequence
LetS F	5´-AAT AAT GCA GTC CTT ACC C-3´
LetS R	5´-TGG ATG ACA CCA CAA GC- 3´
LetS Mutagenesis F[*]	5´-CAT GAG TCA TGA AAT TCG TA<u>T G</u>CC AAT GAA TGG CGT GAT TGG-3´
LetS Mutagenesis R[*]	5´-CCA ATC ACG CCA TTC ATT GG<u>C A</u>TA CGA ATT TCA TGA CTC ATG-3´
LetS Mut Seq F	5´-CGA TTG CGT CGA AGT ATG-3´
LetS Mut. His F[*]	5´-TTA TTG CCA ACA TGA GTC A<u>A</u>G AAA TTC GTA CCC CAA TGA ATG GC-3´
LetS Mut. His R[*]	5´-GCC ATT CAT TGG GGT ACG AAT TTC <u>T</u>TG ACT CAT GTT GGC AAT AA-3´

[*]Underlined nucleotides indicate site change

Figure 2.1.

A

B

```
                                           H    T
LetS-Lp  266  --IELSLEKKKTEEKSRQKSEFIANMSHEIRTPMNGVIGFTNVLLESKLDPL-QL-DYVK
BvgS-Bb  642  LLRELHDAKESADAANRAKTTFLATMSHEIRTPMNAIIGMLELALLRPADQEPDR-QSIQ
ArcB-Ec  252  --TERKRYQDALERASRDKTTFISTISHELRTPLNGIVGLSRILLDTELTAE-QE-KYLK
BarA-Ec  275  QNVELDLAKKRAQEAARIKSEFLANMSHELRTPLNGVIGFTRLTLKTELTPT-QR-DHLN
EvgS-Ec  641  LINALEVEKNKAIKATVAKSQFLATMSHEIRTPISSIMGFLELLSGSGLSKE-QRVEAIS
TorS-Ec  426  LVIEHRQARAEAEKASQAKSAFLAAMSHEIRTPLYGILGTAQLLADNPALNA-QR-DDLR
GacS-Pa  266  QNIELDLARKEALEASRIKSEFLANMSHEIRTPLNGILGFTNLLQKSELSPR-QQ-DYLT
BarA-St  275  QNVELDLAKKRAQEAARIKSEFLANMSHELRTPLNGVIGFTRLTLKTELNPT-QR-DHLN
                  :         *: *:: :***:***: .::*   .:         :  . :
```

H Box

Figure 2.1. The *Legionella pneumophila* LetA/LetS two-component system.
(A) Domain architecture of the LetA/LetS two-component system. LetS, a 103 kDa sensor protein, is likely tethered to the inner membrane by two transmembrane (TM) domains at its N terminus. The periplasmic (P) domain is connected to three cytoplasmic signaling domains, a transmitter (T), receiver (R) and histidine phosphotransfer domain (HPD), via a linker (L) region. LetA is a 43 kDa activator kinase that contains a receiver (R) domain and a helix-turn-helix motif (HTH). It is predicted that upon receiving a signal, LetS autophosphorylates on a conserved histidine residue and then the phosphate is sequentially transferred to aspartic acid and histidine residues in LetS and finally to an aspartic acid in LetA. A histidine-to-glutamine substitution at amino acid 307 of LetS abolishes LetS activity, while a threonine-to-methionine substitution at position 311 creates a strain locked in an intermediate phase. (B) Sequence alignment of the *L. pneumophila* LetS H-box region with related tripartite sensor kinases. Amino acid alignments were produced using T-Coffee. Dashes represent gaps introduced to optimize sequence alignments. * indicates identical residues while : and . represent conserved and semi-conserved amino acids, respectively. The H-box region is underlined, and the primary histidine and conserved threonine residues are displayed above the alignment. Abbreviations: Lp *Legionella pneumophila*; Bb *Bordetella bronchiseptica*; Ec *Escherichia coli*; Pa *Pseudomonas aeruginosa*; St *Salmonella typhimurium*.

Figure 2.2. Histidine 307 of LetS is required for the expression of PE phenotypes.
(A) Histidine 307 is required for *L. pneumophila* to bind, enter and survive within macrophages. PE bacteria were co-cultured with macrophages at an MOI=1, and the percent of bacteria remaining after 2 h was calculated. (B) The autophosphorylation site of LetS is essential for contact-dependent cytotoxicity. Macrophages were co-cultured PE phase WT (circles), *letS* (squares) and *letS^{H307Q}* (triangles) bacteria over a range of MOIs, and the number of viable macrophages assessed by the reduction of the colorimetric dye alamarBlue™. Shown is a representative graph from three independent experiments preformed in triplicate. (C) A histidine-to-glutamine substitution at position 307 of LetS abolishes the ability of *L. pneumophila* to resist lysosomal degradation. Macrophages were infected with PE bacteria at an MOI = 1, and the percent of intact bacteria following a 2-h incubation was determined by fluorescence microscopy. (D) Sodium resistance persists if the autophosphorylation site of LetS is disrupted. PE cultures were plated on media with or without 100 mM NaCl, and the percent of sodium sensitive bacteria determined. (E) Substitution of a glutamine residue at position 307 of LetS inhibits pigment production. WT, *letS* and *letS^{H307Q}* bacteria were incubated for 5 days and the soluble pigment quantified from culture supernatants. For bar graphs in panels A, C, D and E the means ± SD from duplicate samples in three independent experiments are displayed. Asterisks indicate statistically significant differences (P<0.01) when compared to WT PE bacteria.

Figure 2.2.

Figure 2.3.

A

B
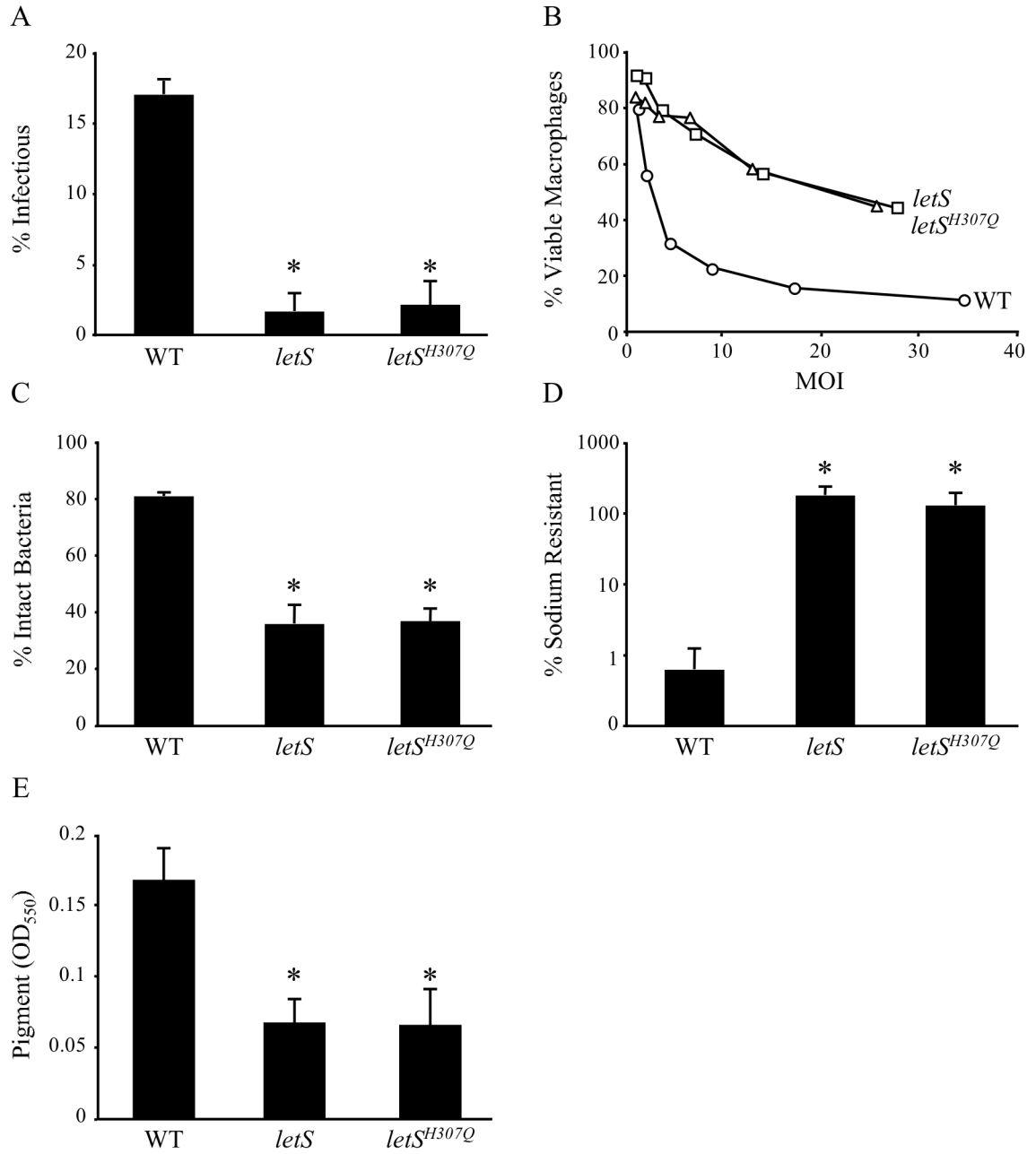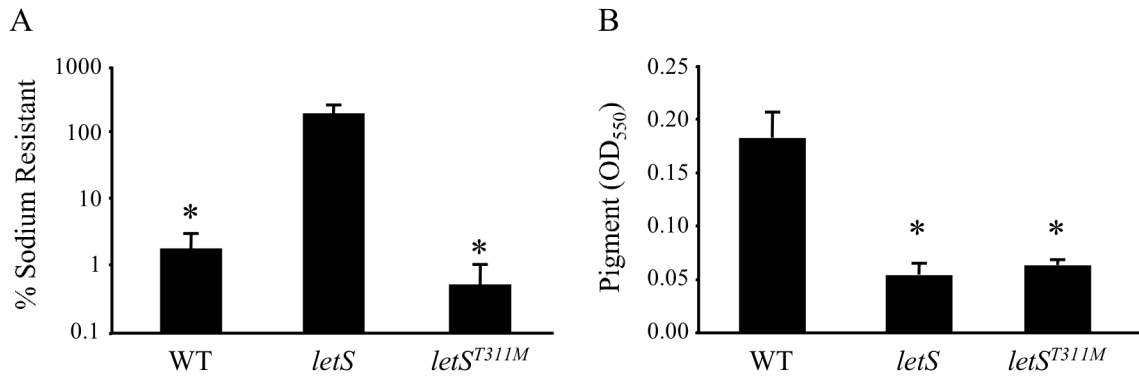
Figure 2.3. A strain containing a threonine-to-methionine substitution four residues from the proposed autophosphorylation site of LetS exhibits either WT or *letS* null phenotypes.
(A) Substitution of a methionine residue at position 311 of LetS does not affect sodium resistance. The percentage of sodium resistant CFU was quantified by plating PE bacteria on CYET containing or lacking 100 mM NaCl. The means ± SD from duplicate samples in three independent experiments are displayed and the asterisks represent significant differences ($P<0.01$) in comparison to *letS* PE cultures. (B) Threonine 311 of LetS is essential for the production of a melanin-like pigment. WT, *letS* and *letS^{T311M}* cells were cultured for 5 days and pigment measured from supernatants at OD_{550}. Shown are the means from three independent experiments. Error bars indicate SD and asterisks denote statistically significant differences ($P<0.01$) when compared WT bacteria.

Figure 2.4.
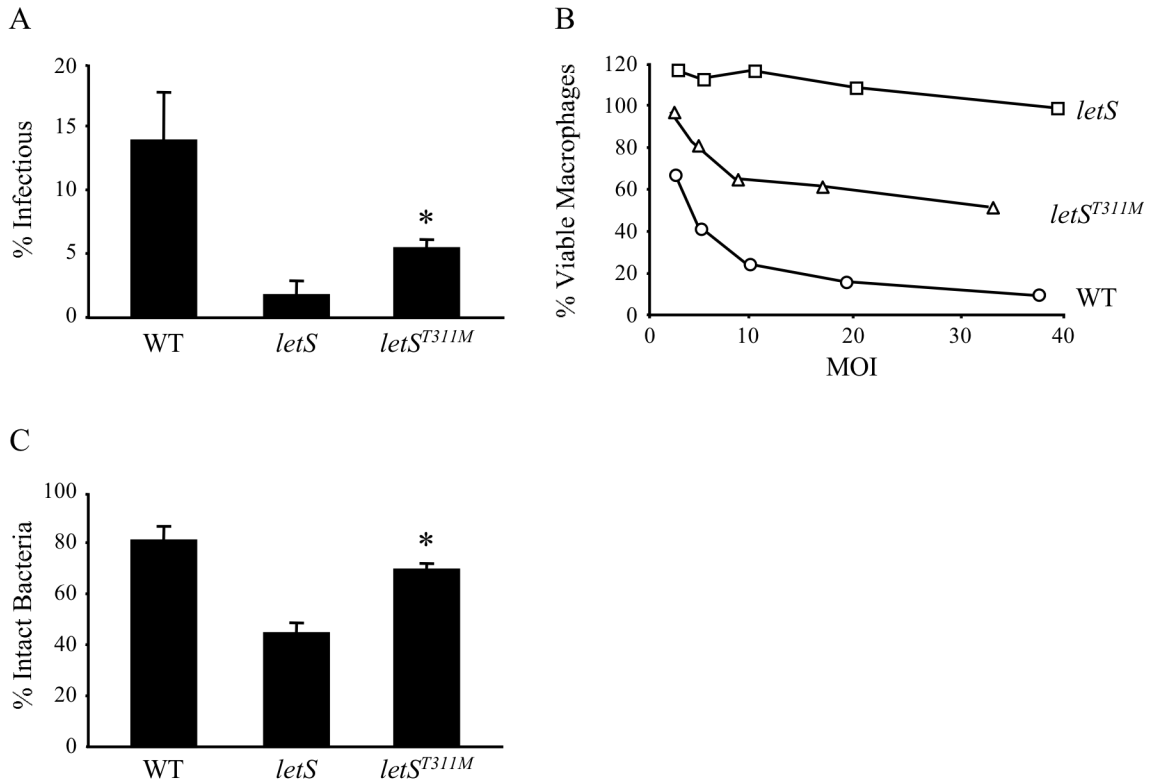
Figure 2.4. A strain containing a threonine-to-methionine substitution at position 311 of LetS displays intermediate phenotypes for several PE traits.
(A) *letS*[T311M] mutants are intermediate in their ability to bind, enter and survive within macrophages. PE microbes were co-cultured with macrophages at an MOI = 1. Following a 2-h incubation, macrophages were lysed and the number of bacteria remaining calculated. The means ± SD from duplicate samples in three independent experiments are displayed. Asterisk indicates statistically significant differences (P<0.01) when compared to WT microbes and (P<0.05) when compared to *letS* null bacteria. (B) A threonine-to-methionine change at amino acid 311 of LetS creates a strain that is intermediately cytotoxic. Macrophages were infected with PE WT (circles), *letS* (squares) and *letS*[T311M] (triangles) microbes at the MOIs shown and macrophage viability measured by the reduction of the dye, alamarBlue™. A representative graph from three independent experiments performed in triplicate is displayed. (C) *letS*[T311M] mutants are intermediate for lysosomal degradation when compared with WT and *letS* null bacteria. Macrophages were infected with PE cultures at an MOI = 1 and the percent of intact bacteria following a 2-h incubation quantified by fluorescence microscopy. Shown are the means from three independent experiments performed in duplicate. Error bars represent SD and asterisk denotes a statistically significant difference (P<0.01) when compared with WT and *letS* PE bacteria.

Figure 2.5.
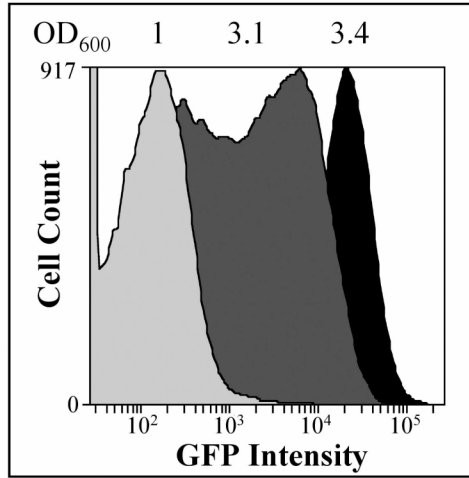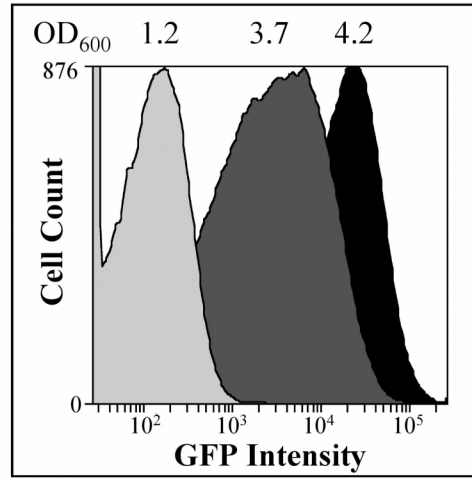
Figure 2.5. Flow cytometry indicates that eventually every *letS^T311M* cell in the population activates the *flaA* promoter to a similar level.
To determine what percentage of WT (A) and *letS^T311M* (B) populations expressed the pflaG reporter, cultures at various optical densities were washed and normalized to 5 × 10^5 in PBS. Promoter activity was analyzed by monitoring GFP fluorescence via flow cytometry. Shown are representative curves from one experiment, and the OD_{600} of each sample is denoted. Similar results were obtained in three separate experiments.

Table 2.3. Repressed genes for *letS*^{T311M} vs. WT for ODs 2 and 3

Gene ID	Name	Paris ID	Lens ID	Description	OD2[1]	OD3[1]
lpg1219	*flgE*	*lpp1227*	*lpl1227*	flagellar hook protein	-6.1	-
lpg1225	*flgK*	*lpp1233*	*lpl1233*	flagellar hook-associated protein	-4.9	-
lpg1226	*flgL*	*lpp1234*	*lpl1234*	flagellar hook-associated protein	-4.4	-
lpg1220	*flgF*	*lpp1228*	*lpl1228*	flagellar biosynthesis protein	-4.3	-
lpg0901	-	*lpp0962*	*lpl0932*	unknown	-3.8	-
lpg0902	-	*lpp0963*	*lpl0933*	unknown	-3.6	-
lpg0669	-	*lpp0725*	*lpl0705*	unknown	-3.6	-
lpg1168	-	*lpp1170*	*lpl1176*	regulatory protein (GGDEF and EAL domains)	-3.4	-
lpg1454	-	*lpp1410*	*lpl1590*	multidrug efflux protein	-3.2	-
lpg0277	-	*lpp0351*	*lpl0329*	regulatory protein (EAL domain)	-3.2	-
lpg1370	*fis2*	*lpp1324*	*lpl1321*	similar to DNA-binding protein Fis	-3.1	-
lpg1055	-	*lpp2327*	-	unknown	-3.0	-
lpg2028	*hemE*	*lpp2010*	*lpl2005*	uroporphyrinogen decarboxylase	-2.9	-
lpg2622	-	*lpp2675*	*lpl2547*	weakly similar to cysteine protease	-2.9	-
lpg1223	*flgI*	*lpp1231*	*lpl1231*	flagellar P-ring protein precursor	-2.9	-
lpg0426	*cspD*	*lpp0493*	*lpl0469*	cold shock-like protein	-2.9	-
lpg2105	-	-	-	transmembrane protein	-2.8	-
lpg0560	*phaB1*	*lpp0620*	*lpl0603*	acetoacetyl-CoA reductase	-2.8	-
lpg2106	-	-	-	unknown	-2.7	-
lpg1224	*flgJ*	*lpp1232*	*lpl1232*	flagellar biosynthesis protein	-2.6	-
lpg1667	-	*lpp1638*	*lpl1632*	similar to metallo-endopeptidases	-2.6	-
lpg0737	-	*lpp0802*	*lpl0773*	putative secreted protein	-2.6	-
lpg2579	-	*lpp2631*	*lpl2501*	unknown	-2.5	-
lpg2732	*lqsR*	*lpp2788*	*lpl2657*	LqsR response regulator	-2.5	-
lpg2837	-	*lpp2894*	*lpl2749*	similar to lysophospholipase A	-2.5	-
lpg2457	-	*lpp2523*	*lpl2376*	two-component response regulator (crystallized)	-2.4	-
lpg1908	*gst*	*lpp1883*	*lpl1874*	glutathione S-transferase	-2.4	-
lpg1218	*flgD*	*lpp1226*	*lpl1226*	flagellar basal-body rod modification protein	-2.4	-
lpg0733	-	*lpp0799*	*lpl0770*	unknown	-2.3	-
lpg1222	*flgH*	*lpp1230*	*lpl1230*	flagellar L-ring protein precursor	-2.3	-
lpg1059	*phaB3*	*lpp2322*	*lpl1056*	acetoacetyl-CoA reductase	-2.2	-
lpg2237	-	*lpp2190*	*lpl2163*	ABC-type multidrug transport system, ATPase and permease components	-2.2	-
lpg2950a[2]	-	*lpp3021*	*lpl2878*	unknown	-2.2	-
lpg2328	-	*lpp2276*	*lpl2248*	unknown - N-terminal similar to *Legionella* 33 kDa polypeptide	-2.2	-
lpg2258	-	*lpp2212*	*lpl2184*	unknown	-2.1	-
lpg1221	*flgG*	*lpp1229*	*lpl1229*	flagellar biosynthesis protein	-2.1	-
lpg0874	*pntB*	*lpp0937*	*lpl0907*	NAD(P) transhydrogenase subunit beta	-2.0	-
lpg0953	-	*lpp1015*	*lpl0982*	long-chain acyl-CoA synthetases (AMP-forming)	-2.0	-
lpg1655	-	*lpp1626*	*lpl1620*	LasB-like zinc metalloprotease (elastase)	-2.0	-
lpg2164	-	*lpp2102*	*lpl2091*	unknown	-1.9	-
lpg2999	*legP*	*lpp3071*	*lpl2927*	eukaryotic zinc metalloproteinase	-1.9	-
lpg1451	-	*lpp1406*	*lpl1593*	phosphatidyl/ethanolamine-binding protein	-1.9	-
lpg0623	-	*lpp0677*	*lpl0660*	predicted membrane protein	-1.9	-
lpg2373	-	-	-	unknown	-1.8	-
lpg2324	-	*lpp2272*	*lpl2244*	L-gulono-gamma-lactone oxidase	-1.8	-
lpg2401	-	*lpp2466*	*lpl2324*	putative secreted esterase	-1.8	-
lpg1759	*fliG*	*lpp1723*	*lpl1723*	flagellar motor switch protein	-1.8	-
lpg0803	-	*lpp0865*	*lpl0836*	acyl-CoA dehydrogenase/SOS response	-1.8	-
lpg1779	-	*lpp1743*	*lpl1743*	unknown	-1.8	-
lpg2192	-	-	-	molecular chaperone/heat shock protein	-1.8	-
lpg0561	*phaB2*	*lpp0621*	*lpl0604*	acetoacetyl-CoA reductase	-1.8	-

53

Gene ID	Name	Paris ID	Lens ID	Description	OD2[1]	OD3[1]
lpg3002	-	*lpp3074*	*lpl2930*	putative inner membrane protein translocase	-1.7	-
lpg0902a[2]	-	*lpp0964*	*lpl0934*	unknown	-1.7	-
lpg1758	*fliH*	*lpp1722*	*lpl1722*	polar flagellar assembly protein	-1.7	-
lpg0283	-	*lpp0359*	*lpl0335*	NAD+ formate/lactate dehydrogenase	-1.6	-
lpg1174a[2]	-	*lpp1177*	*lpl1183*	unknown	-5.8	-8.5
lpg0012	-	*lpp0012*	*lpl0012*	unknown	-3.2	-2.6
lpg1895	-	*lpp1864*	*lpl1859*	unknown	-1.9	-6.0
lpg0632	-	*lpp0686*	*lpl0669*	type IV fimbrial pilin related protein	-	-7.5
lpg2803	-	*lpp2849*	*lpl2718*	unknown	-	-6.4
lpg2569	-	-	-	unknown	-	-5.9
lpg0741	-	*lpp0806*	*lpl0777*	unknown	-	-5.5
lpg0586	-	*lpp0636*	*lpl0620*	putative transcriptional regulator	-	-5.4
lpg2315	-	*lpp2263*	*lpl2235*	unknown	-	-4.8
lpg0259	-	*lpp0329*	*lpl0312*	unknown	-	-4.7
lpg2187	-	*lpp2137*	*lpl2112*	unknown	-	-4.5
lpg1686	-	-	-	unknown	-	-4.3
lpg2862	*legC8*	-	-	cytotoxic glucosyltransferase Lgt2	-	-4.3
lpg2990	-	*lpp3061*	*lpl2918*	unknown	-	-4.1
lpg1340	*flaA*	*lpp1294*	*lpl1293*	flagellin	-	-4.0
lpg1577	*rpoE*	*lpp1535*	*lpl1448*	sigma factor RpoE (sigma 24)	-	-3.9
lpg0631	-	*lpp0685*	*lpl0668*	type IV fimbrial biogenesis protein PilV	-	-3.8
lpg1386	*enhA3*	*lpp1341*	*lpl1337*	similar to enhanced entry protein EnhA	-	-3.8
lpg0910	*enhA2*	*lpp0972*	*lpl0942*	similar to enhanced entry protein EnhA	-	-3.7
lpg2603	-	*lpp2656*	*lpl2526*	unknown	-	-3.6
lpg0672	-	*lpp0728*	*lpl0708*	acetoacetate decarboxylase (crystallized)	-	-3.6
lpg2582a[2]	-	*lpp2636*	*lpl2506*	unknown	-	-3.5
lpg2520	-	*lpp2588*	*lpl2442*	unknown	-	-3.5
lpg2364	-	-	-	weakly similar to NAD-dependent DNA ligase	-	-3.5
lpg0628	-	*lpp0682*	*lpl0665*	type IV fimbrial biogenesis PilY1-related protein	-	-3.4
lpg1121	-	*lpp1121*	*lpl1126*	unknown	-	-3.3
lpg0286a[2]	-	*lpp0364*	*lpl0339*	unknown - signal peptide predicted	-	-3.1
lpg2157	*sdeA*	*lpp2096*	*lpl2085*	SdeA- substrate of the Dot/Icm T4SS	-	-3.1
lpg0898	-	*lpp0959*	*lpl0929*	unknown	-	-3.0
lpg1491	-	*lpp1447*	-	some similarity with eukaryotic proteins	-	-3.0
lpg1339	-	*lpp1293*	*lpl1292*	unknown	-	-3.0
lpg0620	-	*lpp0674*	*lpl0657*	unknown	-	-3.0
lpg1158	-	*lpp1160*	-	some similarity with eukaryotic proteins	-	-3.0
lpg1669	-	*lpp1641*	*lpl1634*	unknown - alpha-amylase domain	-	-3.0
lpg2524	-	-	-	transcriptional regulator, LuxR family	-	-2.9
lpg1355	*sidG*	*lpp1309*	-	SidG - substrate of the Dot/Icm T4SS	-	-2.9
lpg2145	-	*lpp2083*	*lpl2073*	putative two-component response regulator	-	-2.9
lpg0629	-	*lpp0683*	*lpl0666*	Tfp pilus assembly protein PilX	-	-2.9
lpg0088	-	*lpp0102*	*lpl0087*	similar to arginine-binding periplasmic protein	-	-2.9
lpg2521	-	*lpp2589*	*lpl2443*	unknown - transmembrane protein	-	-2.8
lpg2527	-	*lpp2592*	*lpl2447*	unknown	-	-2.8
lpg0625	-	*lpp0679*	*lpl0662*	similar to unknown eukaryotic proteins	-	-2.8
lpg2146	*stuC*	*lpp2084*	*lpl2074*	sensor histidine kinase	-	-2.8
lpg1290	-	*lpp1253*	-	unknown	-	-2.8
lpg1963	-	-	-	unknown	-	-2.8
lpg2498a[2]	-	*lpp2567*	*lpl2421*	unknown	-	-2.7
lpg0673	-	*lpp0729*	*lpl0709*	unknown - signal peptide protein	-	-2.7
lpg1207	-	*lpp1209*	*lpl1215*	similar to YbaK/prolyl-tRNA synthetase associated region	-	-2.7
lpg2877	-	*lpp2936*	*lpl2790*	unknown	-	-2.7
lpg0627	*pilE*	*lpp0681*	*lpl0664*	type-IV pilin	-	-2.6
lpg0589	-	*lpp0639*	*lpl0623*	unknown	-	-2.6
lpg1968a[2]	-	*lpp1951*	*lpl1940*	unknown	-	-2.6
lpg0871	-	*lpp0934*	*lpl0903*	unknown	-	-2.6
lpg0614	-	*lpp0665*	*lpl0649*	unknown	-	-2.6

Gene ID	Name	Paris ID	Lens ID	Description	OD2[1]	OD3[1]
lpg1485	-	*lpp1441*	*lpl1543*	unknown	-	-2.5
lpg2181	*arcB*	*lpp2133*	*lpl2108*	putative histidine kinase/response regulator	-	-2.5
lpg0037	*artJ1*	*lpp0036*	*lpl0037*	similar to arginine 3rd transport system periplasmic binding protein	-	-2.5
lpg1115	*kaiC2*	*lpp1116*	*lpl1120a*	putative circadian clock protein KaiC	-	-2.5
lpg0258	-	*lpp0328*	*lpl0311*	unknown	-	-2.5
lpg2132	-	*lpp2071*	*lpl2061*	regulatory protein (GGDEF domain)	-	-2.5
lpg1113	-	*lpp1113*	*lpl1117*	unknown	-	-2.4
lpg2147	-	*lpp2086*	*lpl2075*	unknown	-	-2.4
lpg1496	-	*lpp1453*	*lpl1530*	some similarities with sidE protein	-	-2.4
lpg1080	-	-	-	putative deoxyguanosine triphosphate triphosphohydrolase	-	-2.4
lpg2907	-	*lpp2976*	*lpl2824*	unknown	-	-2.4
lpg2049	-	*lpp2032*	*lpl2027*	unknown	-	-2.4
lpg2719	-	*lpp2776*	*lpl2647*	unknown	-	-2.4
lpg0671	*ndh*	*lpp0727*	*lpl0707*	NADH dehydrogenase	-	-2.3
lpg2268	-	*lpp2222*	*lpl2194*	unknown	-	-2.3
lpg2246	-	*lpp2200*	*lpl2172*	unknown	-	-2.2
lpg0039	-	*lpp0040*	*lpl0039*	unknown	-	-2.2
lpg0587	*yqgF*	*lpp0637*	*lpl0621*	Holliday junction resolvase-like protein	-	-2.2
lpg1112	-	*lpp0639*	*lpl1116*	unknown	-	-2.2
lpg0245	-	*lpp0315*	*lpl0299*	NAD-glutamate dehydrogenase	-	-2.2
lpg2759	-	*lpp2807*	*lpl2676*	unknown	-	-2.2
lpg2093	-	-	-	unknown	-	-2.2
lpg2108	-	-	-	unknown	-	-2.2
lpg0121	-	*lpp0134*	*lpl0119*	ABC transporter, permease protein	-	-2.2
lpg0514a[2]	-	*lpp0577*	*lpl0553*	unknown	-	-2.1
lpg1793	-	*lpp1757*	*lpl1757*	unknown	-	-2.1
lpg0645	-	-	-	truncated structural toxin protein RtxA	-	-2.1
lpg2907	-	*lpp2976*	*lpl2824*	unknown	-	-2.1
lpg0527	-	*lpp0592*	*lpl0573*	signal transduction protein	-	-2.1
lpg2351	-	*lpp2300*	*lpl2273*	unknown	-	-2.1
lpg1114a[2]	-	*lpp1115*	*lpl1119*	KaiB-like circadian clock protein	-	-2.1
lpg1796	-	*lpp1760*	*lpl1760*	transcriptional regulator, LysR family	-	-2.0
lpg2075	-	-	-	DNA adenine methylase	-	-2.0
lpg0029	*rre41*	*lpp0029*	*lpl0030*	regulatory protein (GGDEF and EAL domains)	-	-1.9
lpg2426	*mdcA*	*lpp2493*	-	malonate decarboxylase- alpha subunit	-	-1.9
lpg2584	*sidF*	*lpp2637*	*lpl2507*	SidF - substrate of the Dot/Icm system	-	-1.9
lpg0550	-	*lpp0611*	*lpl0592abc*	similar to D-amino acid dehydrogenase with a C-terminal cAMP binding motif	-	-1.9
lpg2526	-	*lpp2591*	*lpl2446*	unknown	-	-1.7

[1] Fold Change (FC) at the corresponding OD. If no FC is indicated, the gene was either not differentially expressed or the statistical analyses failed due to FC variability.

[2] These genes were not predicted in the Philadelphia strain. Their ID therefore became the ID of the gene located upstream on the chromosome followed by "a". For the exact location and orientation of these genes see Table 2.S1.

Table 2.4. Subset of repressed genes in the *letS*[T311M] mutant as compared to WT

Family	Gene ID	Name	Paris ID	Lens ID	Description	OD2[1]	OD3[1]
Regulation	*lpg0277*	-	*lpp0351*	*lpl0329*	regulatory protein (EAL domain)	-3.2	-
	lpg1168	-	*lpp1170*	*lpl1176*	regulatory protein (GGDEF and EAL domains)	-3.4	-
	lpg2457	-	*lpp2523*	*lpl2376*	two-component response regulator (crystallized)	-2.4	-
	lpg2732	*lqsR*	*lpp2788*	*lpl2657*	LqsR response regulator	-2.5	-
Flagellum synthesis	*lpg1218*	*flgD*	*lpp1226*	*lpl1226*	flagellar basal-body rod modification protein	-2.4	-
	lpg1219	*flgE*	*lpp1227*	*lpl1227*	flagellar hook protein	-6.1	-
	lpg1220	*flgF*	*lpp1228*	*lpl1228*	flagellar biosynthesis protein	-4.3	-
	lpg1221	*flgG*	*lpp1229*	*lpl1229*	flagellar biosynthesis protein	-2.1	-
	lpg1222	*flgH*	*lpp1230*	*lpl1230*	flagellar L-ring protein precursor	-2.3	-
	lpg1223	*flgI*	*lpp1231*	*lpl1231*	flagellar P-ring protein precursor	-2.9	-
	lpg1224	*flgJ*	*lpp1232*	*lpl1232*	flagellar biosynthesis protein	-2.6	-
	lpg1225	*flgK*	*lpp1233*	*lpl1233*	flagellar hook-associated protein	-4.9	-
	lpg1226	*flgL*	*lpp1234*	*lpl1234*	flagellar hook-associated protein	-4.4	-
	lpg1758	*fliH*	*lpp1722*	*lpl1722*	polar flagellar assembly protein	-1.7	-
	lpg1759	*fliG*	*lpp1723*	*lpl1723*	flagellar motor switch protein	-1.8	-
Putatively involved in PHB synthesis	*lpg0560*	*phaB1*	*lpp0620*	*lpl0603*	acetoacetyl-CoA reductase	-2.8	-
	lpg0561	*phaB2*	*lpp0621*	*lpl0604*	acetoacetyl-CoA reductase	-1.8	-
	lpg1059	*phaB3*	*lpp2322*	*lpl1056*	acetoacetyl-CoA reductase	-2.2	-
Unknown	*lpg1174a*[2]	-	*lpp1177*	*lpl1183*	unknown	-5.8	-8.5
	lpg2803	-	*lpp2849*	*lpl2718*	unknown	-	-6.4
	lpg1895	-	*lpp1864*	*lpl1859*	unknown	-1.9	-6.0
	lpg2569	-	-	-	unknown	-	-5.9
	lpg0741	-	*lpp0806*	*lpl0777*	unknown	-	-5.5
Flagellum	*lpg1340*	*flaA*	*lpp1294*	*lpl1293*	flagellin	-	-4.0
Virulence	*lpg1355*	*sidG*	*lpp1309*	-	SidG - substrate of the Dot/Icm T4SS	-	-2.9
	lpg2157	*sdeA*	*lpp2096*	*lpl2085*	SdeA- substrate of the Dot/Icm T4SS	-	-3.1
	lpg2584	*sidF*	*lpp2637*	*lpl2507*	SidF - substrate of the Dot/Icm system	-	-1.9
	lpg2862	*legC8*	-	-	cytotoxic glucosyltransferase Lgt2	-	-4.3
	lpg0910	*enhA2*	*lpp0972*	*lpl0942*	similar to enhanced entry protein EnhA	-	-3.7
	lpg1386	*enhA3*	*lpp1341*	*lpl1337*	similar to enhanced entry protein EnhA	-	-3.8
Eukaryotic-like	*lpg0625*	-	*lpp0679*	*lpl0662*	similar to unknown eukaryotic proteins	-	-2.8
	lpg1491	-	*lpp1447*	-	some similarity with eukaryotic proteins	-	-3.0
	lpg1158	-	*lpp1160*	-	some similarity with eukaryotic proteins	-	-3.0
Regulation	*lpg1577*	*rpoE*	*lpp1535*	*lpl1448*	sigma factor RpoE (sigma 24)	-	-3.9
	lpg0586	-	*lpp0620*	-	putative transcriptional regulator	-	-5.4
	lpg1114a[2]	-	*lpp1115*	*lpl1119*	KaiB-like circadian clock protein	-	-2.1
	lpg1115	*kaiC2*	*lpp1116*	*lpl1120a*	putative circadian clock protein KaiC	-	-2.5
	lpg1796	-	*lpp1760*	*lpl1760*	transcriptional regulator. LysR family	-	-2.0
	lpg2145	-	*lpp2083*	*lpl2073*	putative two-component response regulator	-	-2.9
	lpg2146	*stuC*	*lpp2084*	*lpl2074*	sensor histidine kinase	-	-2.8
	lpg2181	*arcB*	*lpp2133*	*lpl2108*	putative histidine kinase/response regulator	-	-2.5
	lpg2524	-	-	-	transcriptional regulator. LuxR family	-	-2.9
	lpg0029	*rre41*	*lpp0029*	*lpl0030*	regulatory protein (GGDEF and EAL domains)	-	-1.9
	lpg2132	-	*lpp2071*	*lpl2061*	regulatory protein (GGDEF domain)	-	-2.5
Type IV pilus	*lpg0627*	*pilE*	*lpp0681*	*lpl0664*	type IV pilin	-	-2.6
	lpg0628	-	*lpp0682*	*lpl0665*	type IV fimbrial biogenesis PilY1-related protein	-	-3.4
	lpg0629	-	*lpp0683*	*lpl0666*	Tfp pilus assembly protein PilX	-	-2.9
	lpg0631	-	*lpp0685*	*lpl0668*	type IV fimbrial biogenesis protein PilV	-	-3.8
	lpg0632	-	*lpp0686*	*lpl0669*	type IV fimbrial pilin related protein	-	-7.5

[1] Fold Change (FC) at the corresponding OD. If no FC is indicated, the gene was either not differentially expressed or the statistical analyses failed due to FC variability.

[2] These genes were not predicted in the Philadelphia strain. Their ID therefore became the ID of the gene located upstream on the chromosome followed by "a". For the exact location and orientation of these genes see Table 2.S1.

Table 2.5. Induced genes for $letS^{T311M}$ vs. WT at ODs 2 and 3

Gene ID	Name	Paris ID	Lens ID	Description	OD2[1]	OD3[1]
lpg1489	-	*lpp1445*	*lpl1539*	unknown	2.3	-
lpg1776	-	*lpp1740*	*lpl1740*	unknown	2.0	-
lpg2002	*yajC*	*lpp1983*	*lpl1978*	preprotein translocase subunit YajC	2.0	-
lpg1136a[2]	-	*lpp1138*	*lpl1143*	unknown	1.9	-
lpg1966a[2]	-	*lpp1948*	*lpl1937*	unknown	1.9	-
lpg0420	*eda*	*lpp0487*	*lpl0463*	2-deydro-3-deoxyphosphogluconate aldolase / 4-hydroxy-2-oxoglutarate aldolase	1.9	-
lpg1593	-	*lpp1551*	*lpl1432*	similar to carbon storage regulator CsrA	1.9	-
lpg2001	*secD*	*lpp1982*	*lpl1977*	protein-export membrane protein SecD	1.8	-
lpg2000	*secF*	*lpp1981*	*lpl1976*	protein-export membrane protein SecF	1.7	-
lpg1853	*udk*	*lpp1820*	*lpl1819*	uridine kinase	1.6	-
lpg0915	-	*lpp0976*	*lpl0946*	similar to cell division protein FtsL	-	2.8
lpg0892	-	*lpp0953*	*lpl0923*	kynurenine 3-monooxygenase	-	2.7
lpg0024	*hbp*	*lpp0024*	*lpl0025*	hemin binding protein	-	2.3
lpg1364	*glnA*	*lpp1318*	*lpl1315*	glutamine synthetase	-	2.0
lpg0865	-	*lpp0928*	*lpl0897*	similar to outer membrane lipoprotein	-	1.8

[1] Fold Change (FC) at the corresponding OD. If no FC is indicated, the gene was either not differentially expressed or the statistical analyses failed due to FC variability.
[2] These genes were not predicted in the Philadelphia strain. Their ID therefore became the ID of the gene located upstream on the chromosome followed by "a". For the exact location and orientation of these genes see Table 2.S1.

Table 2.S1. Implementation of the Philadelphia strain annotation

Gene ID	Description	Strand	Start coordinates	Stop coordinates	Length (aa)
lpg0286a	unknown - signal peptide predicted	+	341722	341952	77
lpg0514a	unknown	+	556062	556325	88
lpg0902a	unknown	+	647400	647804	135
lpg1174a	unknown	+	1299590	1299835	82
lpg2498a	unknown	+	2816627	2816851	75
lpg2582a	unknown	+	2912984	2913163	60
lpg1114a	unknown	-	1221307	1221035	91
lpg1136a	unknown	-	1251794	1251573	74
lpg1966a	unknown	-	2206294	2206067	76
lpg1968a	unknown	-	2208173	2207934	80
lpg2950a	unknown	-	3339455	3339189	89

Figure 2.6. The LetA/LetS System acts as a rheostat to fine-tune its phenotypic profile.

While *L. pneumophila* are in the E phase of growth, the LetA/LetS system is either inactive, or may regulate a subset of unidentified genes. At this time point, genes that are essential for *L. pneumophila* replication are induced, for example the post-transcriptional regulator *csrA*.   When LetS receives an appropriate signal, the sensor kinase autophosphorylates, and as phosphate flows through the relay, the amount of LetA~P accumulates. It is predicted that the amount of LetA~P required to activate the Dot/Icm type IV secretion system and sodium sensitivity is low, as *letS^{T311M}* mutants are similar to WT for these traits. Perhaps intermediate levels of LetA~P are required to activate the PE phenotypes of infectivity, cytotoxicity and lysosomal avoidance as *letS^{T311M}* mutants exhibit intermediate phenotypes when compared to WT and *letS* null bacteria. Also, intermediate levels of LetA~P are likely needed to induce motility, since a kinetic defect was observed in genes of the flagellar cascade for the *letS^{T311M}* mutant. Presumably, substantial levels of LetA~P are required for pigmentation as *letS^{T311M}* mutants do not accumulate substantial levels of the soluble pigment. Likewise, high levels of LetA~P are probably required to induce *lpg0012*, *lpg1174* and *lpg1895*, since the *letS^{T311M}* mutant was repressed for these genes at both $OD_{600} = 2$ and $OD_{600} = 3$ when compared to WT *L. pneumophila*.

Figure 2.6.
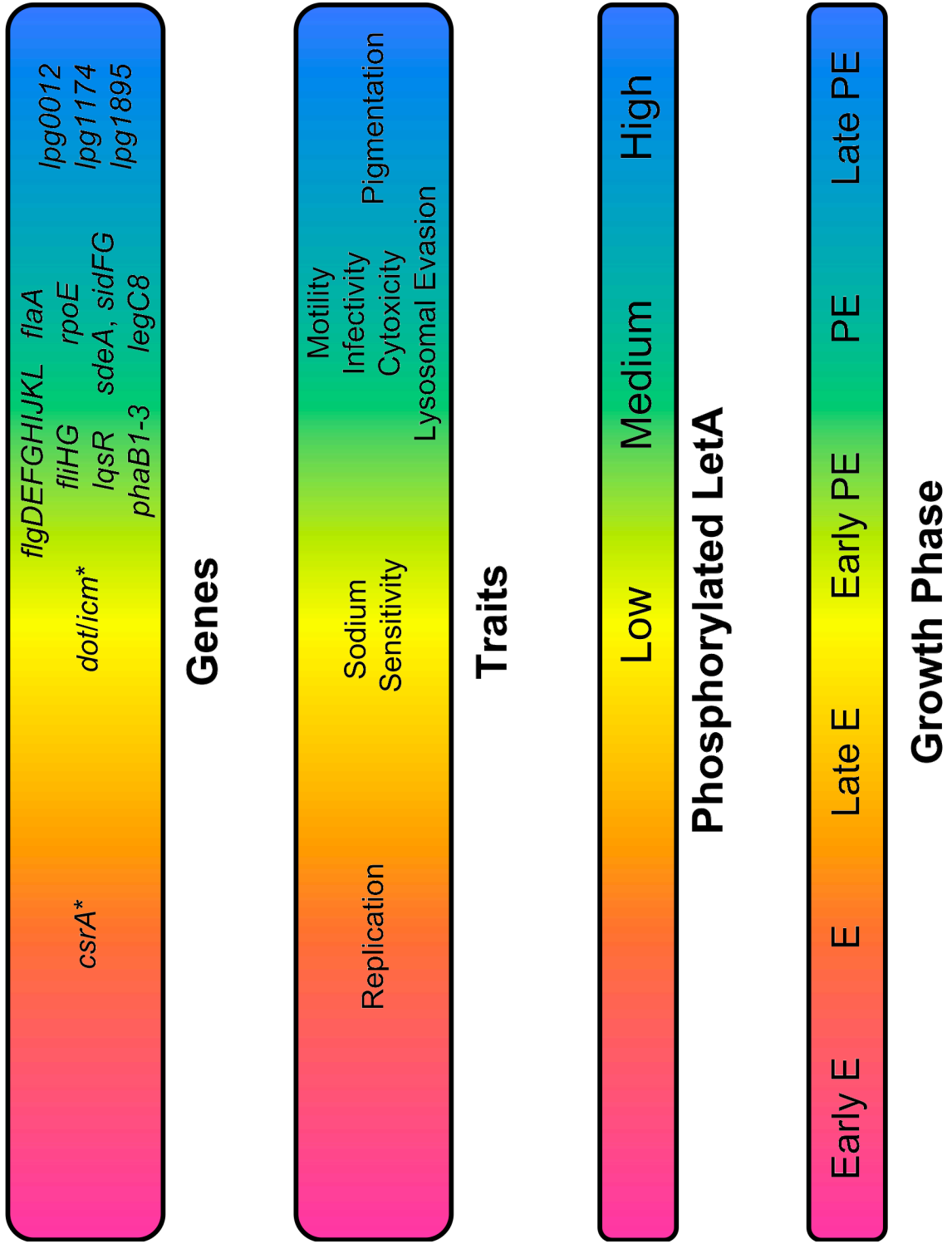
Figure 2.7. Model for LetA/LetS regulation.
Upon receiving an appropriate signal, LetS autophosphorylates on a histidine (H) residue located in the transmitter (T) domain. The signal is then transduced to an aspartic acid (D) in the receiver (R) and then to a second histidine (H) located in the histidine phosphotransfer domain (HPD) of LetS. Finally, the phosphoryl group is transferred to an aspartic acid (D) in the receiver (R) domain of LetA. Once phosphorylated, LetA binds DNA via a helix-turn-helix (HTH) motif to activate transcription of its targets, RsmY and RsmZ. CsrA binds near the ribosomal binding site of mRNAs, which destabilizes the transcripts and ultimately inhibits their translation. The presence of ample amounts of RsmY and RsmZ titrate CsrA away from its targets, which enables translation of the mRNAs. We postulate that the rate that phosphate flows through the relay controls the amount of phosphorylated LetA present in the cell, and likewise the amount of RsmY and RsmZ that are transcribed. This in turn affects the number of CsrA molecules that are removed from mRNA transcripts.

Figure 2.7.
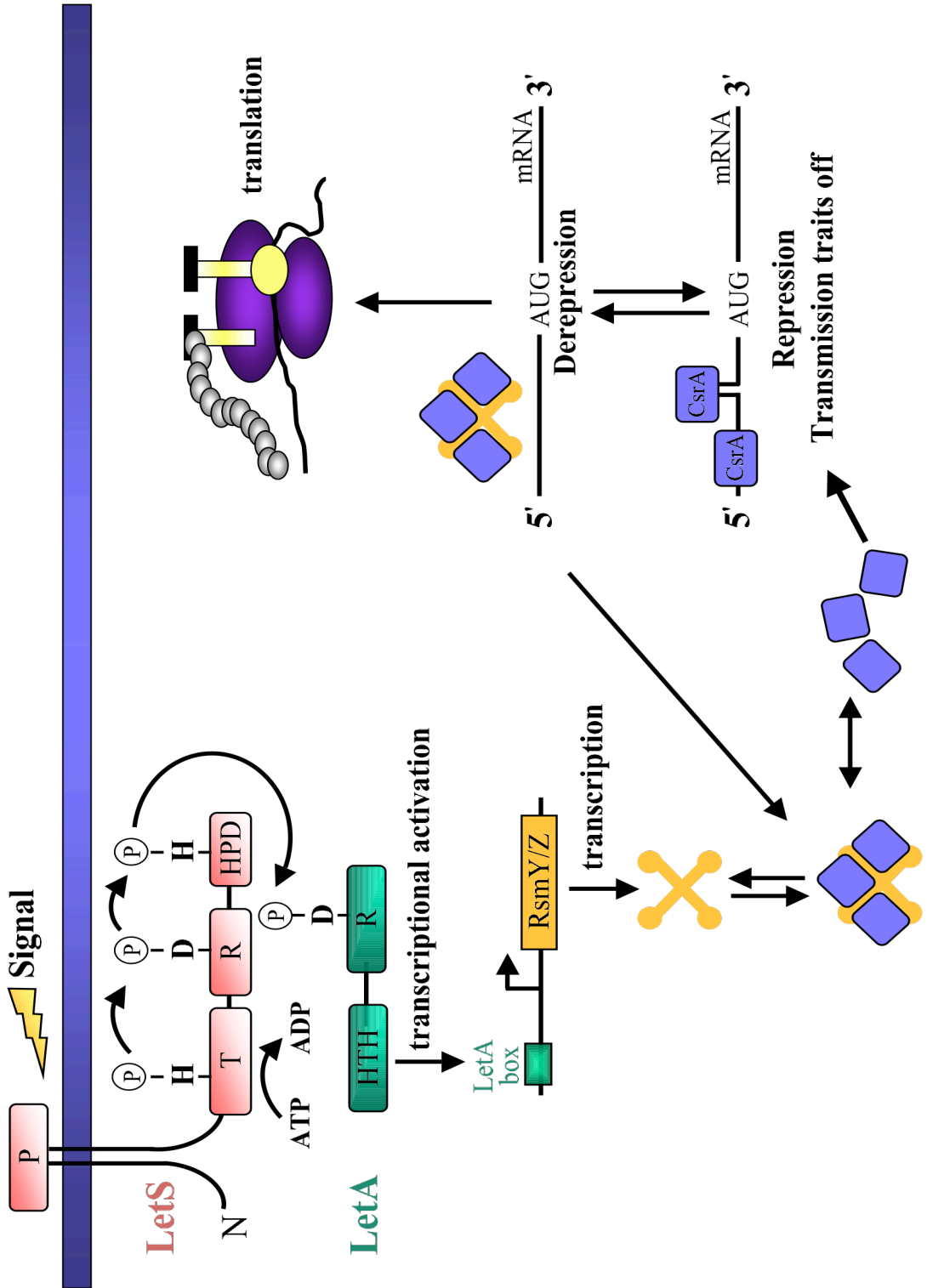
CHAPTER THREE

LEGIONELLA PNEUMOPHILA COUPLES FATTY ACID FLUX TO MICROBIAL DIFFERENTIATION AND VIRULENCE

Summary

Essential to the life cycle of *Legionella pneumophila* is its ability to alternate between at least two distinct phenotypes: a non-infectious, replicative form required for intracellular growth and an infectious, transmissive form that is vital for dissemination. Although amino acids are known to govern this developmental switch, we postulated that *L. pneumophila* could use other metabolic cues to regulate its differentiation. By applying phenotypic microarrays, we demonstrate that when replicative *L. pneumophila* encounter excess short chain fatty acids (SCFAs), the bacteria restrict growth and quickly activate transmissive traits. Their response to SCFAs is dependent on the two-component system LetA/LetS and the stringent response enzyme SpoT. Using the metabolic inhibitors cerulenin and TOFA, we deduced that alterations in the fatty acid biosynthetic pathway signal *L. pneumophila* to induce mechanisms that promote transmission. Moreover, western analysis determined that perturbations in fatty acid biosynthesis alter the distribution of acylated acyl carrier proteins in *L. pneumophila,* a process believed to be monitored by SpoT, an enzyme that generates the alarmone ppGpp which coordinately induces transmission traits. We propose that by coupling phase differentiation to its metabolic state, *L. pneumophila* can swiftly acclimate to environmental fluctuations or stresses encountered in its host, thereby enhancing its overall fitness.

Introduction

Legionella pneumophila is a promiscuous, gram-negative pathogen commonly found in freshwater systems. In these aquatic environments, *L. pneumophila* efficiently parasitizes at least 14 different species of amoebae, two species of ciliated protozoa, and one slime mold (Fields *et al.*, 2002). Moreover, *Legionella* can exist as a free-living microbe by establishing multispeciated biofilms in both natural and potable water systems, which often serve as reservoirs of contamination (Fields *et al.*, 2002). Consequently, if susceptible individuals inadvertently aspirate bacteria-laden aerosols, the bacteria can colonize alveolar macrophages to cause the severe pneumonia Legionnaires' disease. Due to the disparate conditions under which *L. pneumophila* can survive, the bacteria must utilize mechanisms to monitor their milieu and swiftly acclimate to their surroundings.

To tolerate environmental fluctuations, many bacteria alter their cellular physiology and morphology in a process known as differentiation. For example, the sexually transmitted bacterium *Chlamydia trachomatis* alternates between an extracellular, metabolically inert elementary body (EB) required for host transmission and an intracellular, metabolically active reticulate body (RB) that undergoes repeated cycles of cell division (Abdelrahman and Belland, 2005; Samuel *et al.*, 2003). Likewise, the etiologic agent of human Q fever, *Coxiella burnetii*, displays two morphological cell types, a replicative large cell variant (LCV) and a highly resistant small cell variant (Heinzen *et al.*, 1999). Within sessile biofilm communities, the opportunistic pathogen *Pseudomonas aeruginosa* alternates between distinct motile and non-motile cell types (Purevdorj-Gage *et al.*, 2005). By employing cellular differentiation, each of these bacterial pathogens can evade the defense mechanisms of their hosts, and likewise promote self-preservation.

Similar to the aforementioned pathogens, ground-breaking work by Rowbotham revealed that, within amoebae, *L. pneumophila* exhibits two distinct phenotypic states: a

63

nonmotile, thin-walled replicative form and a motile, thick-walled infectious form that contains stores of an energy-rich polymer β-hydroxybutyrate (Rowbotham, 1986). Subsequent studies have corroborated these early findings and determined that the replicative and transmissive phases of the *L. pneumophila* life cycle are reciprocal (Alli *et al.*, 2000; Byrne and Swanson, 1998; Hammer and Swanson, 1999; Molofsky and Swanson, 2003; Watarai *et al.*, 2001b; Wieland *et al.*, 2002). The current model suggests that when phagocytic cells engulf transmissive *Legionella*, the bacteria avoid lysosomal degradation by establishing vacuoles isolated from the endosomal network, a process mediated by the Dot/Icm type IV secretion system and the shedding of vesicles rich in lipopolysaccharide (Berger and Isberg, 1993; Berger *et al.*, 1994; Fernandez-Moreira *et al.*, 2006; Joshi *et al.*, 2001). If conditions in the vacuolar compartment are favorable, the post-transcriptional regulator CsrA and the sRNA chaperone Hfq repress transmissive traits, thereby enabling *L. pneumophila* to replicate profusely (Fettes *et al.*, 2001; McNealy *et al.*, 2005; Molofsky and Swanson, 2003). However, once nutrient supplies are exhausted, bacterial replication halts, and the progeny initiate a global change in their metabolism known as the stringent response (Gal-Mor *et al.*, 2002; Hammer and Swanson, 1999). Activation of this pathway generates the alarmone, ppGpp, which coordinates bacterial differentiation. In particular, a major shift in the *L. pneumophila* transcriptional profile is mediated by alternative sigma factors as the LetA/LetS two-component system relieves CsrA repression on transmissive traits (Bruggemann *et al.*, 2006; Hammer and Swanson, 1999; Hammer *et al.*, 2002; Molofsky and Swanson, 2003). As a consequence, *L. pneumophila* expresses a panel of traits that are vital for dissemination, including cytotoxicity, motility and lysosome evasion (Bachman and Swanson, 2001, 2004a, b; Hammer *et al.*, 2002; Jacobi *et al.*, 2004; Lynch *et al.*, 2003).

 L. pneumophila responds to metabolic cues to govern its phase differentiation. Amino acid concentrations appear to be critical, as fluctuations in their availability alter the developmental state of the microbe. For example, *L. pneumophila* relies on PhtA to

gauge whether the threonine supply in its vacuolar compartment is sufficient to sustain growth (Sauer *et al.*, 2005). Moreover, the macrophage amino acid transporter SLC1A5 (hATB$^{0,+}$) is required to support replication of intracellular *L. pneumophila* (Wieland *et al.*, 2005). Studies of broth cultures predict that when amino acid supplies are depleted, uncharged tRNAs accumulate, and the stringent response enzyme RelA produces the ppGpp signaling molecule, which triggers *L. pneumophila* differentiation (Gal-Mor *et al.*, 2002; Hammer and Swanson, 1999; Zusman *et al.*, 2002). However, since *L. pneumophila relA* mutants replicate as efficiently as WT within macrophages, other cues or regulators must contribute (Zusman *et al.*, 2002).

Since *Legionella* persist in diverse environments, we postulated that signals other than amino acids also induce its differentiation. Indeed, the *L. pneumophila* genome encodes SpoT, a second ppGpp synthetase that equips *Escherichia coli* to generate the alarmone in response to additional stresses, such as phosphate starvation or inhibition of fatty acid biosynthesis (Battesti and Bouveret, 2006; Gong *et al.*, 2002; Magnusson *et al.*, 2005; Seyfzadeh *et al.*, 1993; Zusman *et al.*, 2002). By screening hundreds of metabolites via phenotypic microarrays, and then applying a series of pharmacological, biochemical and genetic tests, we determined that, in response to perturbations in fatty acid biosynthesis, replicative *L. pneumophila* rely on SpoT to activate the stringent response pathway and coordinately express its transmissive traits, thereby coupling phase differentiation to its metabolic state.

Experimental procedures

Bacterial strains, culture conditions and reagents. *L. pneumophila* strain Lp02 (*thyA hsdR rpsL*; MB110), a virulent thymine auxotroph, was the parental strain for all mutants constructed (Berger and Isberg, 1993). MB355 contains the pflaG plasmid that encodes thymidylate synthetase as a selectable marker and a transcriptional fusion of the *flaA*

promoter to *gfp* (Hammer and Swanson, 1999; Hammer *et al.*, 2002). MB414 contains *letA-22* and MB417 encodes *letS-36*, mariner insertion alleles of *lpg2646* and *lpg1912*, respectively, that confer resistance to kanamycin (Hammer *et al.*, 2002). Both MB414 and MB417 contain the pflaG reporter plasmid. To obtain *letA* and *letS* mutants lacking pflaG, the mutant alleles from MB414 and MB417 were transferred onto the Lp02 chromosome by natural competence to generate MB413 and MB416, respectively (Hammer *et al.*, 2002). MB684 has a kanamycin cassette inserted into *relA* (*lpg1457*) and contains the pflaG reporter plasmid (Appendix A). MB685 has a gentamicin cassette inserted into *relA*, a kanamycin cassette inserted into *spoT* (*lpg2009*), and carries the pflaG plasmid (Appendix A).

   To construct a *pta ackA2* (*lpg2261* and *lpg2262*) deletion mutant, the 3.3 kb *pta ackA2* locus was amplified from Lp02 genomic DNA using forward primer 5′-GCAACTCGTATGCCATAC and reverse primer 5′-GTAAATCCATCGCTTTGGG. The PCR fragment was purified and ligated to pGEM-T (Promega), transformed into *E. coli* DH5α, and the resulting plasmid designated as pGEM-T-PtaAckA2 (MB619). A 1.8 kb region of the *pta ackA2* open reading frame was removed by digestion with *Xma*I and *Nhe*I, and the remaining pGEM-T-PtaAckA2 fragment was blunted with Klenow and treated with Antarctic phosphatase (New England Biolabs). The 1.3-kb kanamycin resistance cassette from pUC4K was removed via *Eco*RI digestion, blunted with Klenow and ligated into the digested pGEM-T-PtaAckA2 plasmid to create pGEM-T-PtaAckA2::Kan (MB681). After verification by PCR, the deletion/insertion alleles were transformed into Lp02 via natural competence and selected for by antibiotic resistance (Stone and Abu Kwaik, 1999). The incorporation of the desired mutation into the Lp02 background was confirmed by PCR and the resulting strain designated as MB641. To monitor the induction of the *flaA* promoter by fluorometry, MB641 was transformed with pflaG. Two independent isolates were tested and found similar in fluorometry assays; MB682 data are displayed.

Bacteria were cultured at 37°C in 5 ml aliquots of *N*-(2-acetamido)-2-aminoethanesulfonic acid (ACES; Sigma)-buffered yeast extract (AYE) broth and supplemented with 100 µg/ml thymidine when necessary. For all experiments, exponential (E) cultures were defined as having an optical density at 600 nm (OD_{600}) of 0.5 to 0.85 and post-exponential (PE) cultures as having an OD_{600} of 3.4 to 4.5. To obtain colony-forming units (CFU), *L. pneumophila* were plated on ACES-buffered charcoal-yeast extract agar supplemented with 100 µg/ml thymidine (CYET) and incubated at 37°C for 4-5 days.

Biolog Phenotype MicroArray™ Analysis. To discover novel compounds that induce *L. pneumophila* differentiation, Phenotype MicroArray™ (PM) plates were purchased from Biolog (San Diego). The 96-well plates screened (PM1, PM2A, PM3B, PM4A and PM5) contained sources of carbon, nitrogen, sulfur, phosphorous and various nutrients. 100 µl of E phase MB355 cultured in AYE media was added to each well of the Biolog plates, and the plates were incubated at 37°C while shaking. After 3 h, cultures were transferred to black, clear-bottom tissue culture plates (Costar), and the relative fluorescence intensity was quantified using a Synergy™ HT microplate reader (Bio-Tek). The settings for fluorescence measurements were 485 nm excitation, 530 nm emission and sensitivity of 50. To identify less potent triggers of *L. pneumophila* differentiation, the MicroArray™ plates were incubated for an additional 3 h and monitored for *flaAgfp* induction as described above. Inducers were defined as having a 1.2-7.8 fold increase in fluorescence at 6 h when compared to the negative control well of the Biolog plates in at least 3 independent experiments.

Fluorometry. To monitor expression of the flagellin promoter, *L. pneumophila* strains containing the *flaAgfp* reporter plasmid pflaG were cultured in AYE media. Cultures were supplemented with 10 mM acid, 0.5 µg/ml cerulenin (Sigma) or 5 µg/ml 5-

(tetradecyloxy)-2-furoic acid (TOFA; Cayman Chemical) when they reached $OD_{600} =$ 0.50-0.85 (T = 0). *L. pneumophila* cultures supplemented with water or DMSO served as negative and vehicle controls, respectively. At the times indicated, the cell density of each culture was measured as OD_{600}. To analyze similar bacterial concentrations, aliquots were collected by centrifugation, and the cell densities were normalized to OD_{600} = 0.01 in PBS. An aliquot of each sample (200 μL) was transferred to black 96-well plates (Costar), and the relative fluorescence intensity was measured using a Synergy™ HT microplate reader (485 nm excitation, 530 nm emission and sensitivity of 50).

Macrophage cultures. Macrophages were isolated from femurs of female A/J mice (Jackson Laboratory) and cultured in RPMI-1640 containing 10% heat-inactivated fetal bovine serum (RPMI/FBS; Gibco BRL) as described previously (Swanson and Isberg, 1995). Following a 7-day incubation in L-cell supernatant-conditioned media, macrophages were plated at either 5×10^4 or 2.5×10^5 per well for cytotoxicity and degradation assays, respectively.

Cytotoxicity. To measure contact-dependent cytotoxicity of *L. pneumophila* following macrophage infection, PE bacteria or E phase cultures supplemented with water or 10 mM fatty acids for 3 h were added to macrophage monolayers at the indicated multiplicities of infection (MOI). After centrifugation at $400 \times g$ for 10 min at 4°C (Molofsky *et al.*, 2005), the cells were incubated for 1 h at 37°C. For quantification of macrophage viability, RPMI/FBS containing 10% alamarBlue™ (Trek Diagnostic Systems) was added to the monolayers for 6-12 h, and the reduction of the colorimetric dye was measured spectrophotometrically as described (Byrne and Swanson, 1998; Hammer and Swanson, 1999; Molofsky *et al.*, 2005). Each sample was analyzed in triplicate wells in three or more independent experiments.

Lysosomal degradation. The percentage of intracellular *L. pneumophila* that remained intact after a 2 h macrophage infection was quantified by fluorescence microscopy. Briefly, macrophages were plated at 2.5×10^5 onto coverslips in 24 well plates. Then, PE bacteria or E phase microbes supplemented with either water or 10 mM fatty acids for 3 h were added to macrophage monolayers at an MOI ~ 1. The cells were centrifuged at 400 $\times$ g for 10 min at 4°C and then incubated for 2 h at 37°C. Uninternalized bacteria were removed by washing the monolayers with RPMI/FBS three times, and the macrophages were fixed, permeabilized and stained for *L. pneumophila* as described (Molofsky *et al.*, 2005). For each sample, duplicate coverslips were scored for intact rods versus degraded particles in three independent experiments (Bachman and Swanson, 2001; Molofsky and Swanson, 2003).

Sodium sensitivity. To calculate the percentage of *L. pneumophila* that are sensitive to sodium, PE bacteria or E cultures supplemented with either water or 10 mM fatty acids for 3 h were plated onto CYET and CYET containing 100 mM NaCl. After a 6-day incubation at 37°C, CFUs were enumerated and the percentage of sodium sensitive microbes calculated as described (Byrne and Swanson, 1998).

Analysis of L. pneumophila acyl-ACPs. For purification of acyl-ACPs, WT *L. pneumophila* were cultured to the E phase at 37°C on an orbital shaker in 250 ml AYE containing 100 μg/ml thymidine. Upon reaching an OD_{600} between 0.5-0.85, the cultures were supplemented with water, 10 mM fatty acid or 0.5 μg/ml cerulenin and then cultured for an additional 3 h at 37°C while shaking. After the incubation period, cells were harvested by centrifugation at 4,000 $\times$ g for 20 min at 4°C, and the cell pellets were stored at -80°C. The cells were thawed on ice, and the pellets were resuspended in 12.5 ml ACP buffer (200 mM NaCl, 20 mM Tris-HCl, pH 6, 1 mM EDTA). To prevent protein degradation, 1 tablet of a protease inhibitor cocktail (Roche) was added to each

12.5 ml suspension. Cells were lysed by sonication and the lysates cleared by centrifugation at 7,000 × g for 1 h at 4°C. Sequence data predicts that *L. pneumophila* contains three ACPs ranging from 8.6-15.3 kDa. Thus, large molecular weight proteins were easily removed from the lysates via 50K and 30K centrifugal filter devices (Amicon Ultra; Millipore). The remaining ACP fractions were concentrated with 5K centrifugal filter devices, which also removed small molecular weight proteins and salts from the samples (Amicon Ultra; Millipore). The protein concentration of each sample was determined using the Bio-Rad Protein Assay, and samples were stored at -20°C. To detect intracellular acyl-ACPs, purified *L. pneumophila* ACPs were separated on native polyacrylamide urea gels. Briefly, 13% nondenaturing gels were prepared, and urea was added to either 0.5 M or 2.5 M for short chain fatty acid (SCFA) or long chain fatty acid (LCFA) gels, respectively (Jackowski and Rock, 1983; Post-Beittenmiller *et al.*, 1991; Rock and Cronan, 1981). After electrophoresis in 192 mM glycine, 25 mM Tris buffer, samples were transferred to polyvinylidene difluoride (PVDF) membrane (Bio-Rad), and the membranes blocked in TBS-T (20 mM Tris-HCl, pH 7.5, 500 mM NaCl, 0.05% Tween 20) containing 5% nonfat milk. To detect ACP proteins from *L. pneumophila*, the membranes were probed with an *E. coli* primary ACP antibody (gift from C. O. Rock, Memphis, TN) diluted 1:500 and a secondary goat anti-rabbit antibody conjugated to horseradish peroxidase (Pierce) diluted 1:8000 (Jackowski and Rock, 1983) and then developed with SuperSignal® West Pico Chemiluminescent Substrate (Pierce).

Detection of ppGpp. Accumulation of the ppGpp signaling molecule in response to flux in fatty acid metabolism was detected by thin-layer chromatography (TLC) as described (Cashel, 1969, 1994; Hammer and Swanson, 1999). Briefly, E phase Lp02 cultures were diluted to an $OD_{600} = 0.25$ and labeled with approximately 100 µCi/ml carrier-free [^{32}P]-phosphoric acid (ICN Pharmaceuticals) for 6 h, or two generation times, at 37°C on a roller drum. After incorporation of the radioactive label, cultures were supplemented

with water, 10 mM acetic acid, 10 mM propionic acid or 0.5 µg/ml cerulenin and incubated for an additional 1.5 h at 37°C. For the PE control sample, 100 µCi/ml carrier-free [^{32}P]-phosphoric acid was added to late E phase Lp02, and the cultures incubated at 37°C on a roller drum until reaching PE, or approximately 6 h. To extract the nucleotides, 50 µl aliquots were removed from each culture and added to 13 M formic acid and then incubated on ice for 15 min. Samples were subjected to two freeze-thaw cycles and stored at -80°C until chromatography. Formic acid extracts (9 µL for PE samples and 25 µL for E samples) were applied to a PEI-cellulose TLC plate (20 × 20) and developed with 1.5 M KH_2PO_4, pH 3.4 as described (Cashel, 1969, 1994; Hammer and Swanson, 1999). TLC plates were exposed to autoradiography film for 72 h and developed in a phosphoimager. To monitor growth following water, fatty acid or cerulenin supplementation, optical densities were determined for non-radioactive cultures grown under identical conditions.

Results

Phenotype microarrays identify novel cues of L. pneumophila differentiation

To discern whether a variety of signals trigger *L. pneumophila* differentiation, we employed Biolog Phenotype MicroArray™ plates to screen a library containing sources of carbon, nitrogen, sulfur and phosphorous. Exponential (E) *L. pneumophila* carrying a *gfp* reporter for flagellin, a marker of transmissive bacteria, were cultured in the microarray plates, and the relative fluorescence was quantified over time. Of the 387 compounds screened, only 22 (6%) induced *flaAgfp* expression during the E phase of growth (Table 3.2). Among these were deoxyadenosine, deoxyribose, 2-deoxy-D-glucose-6-phosphate, dihydroxyacetone, nitrite, hydroxylamine, parabanic acid and methionine-alanine dipeptide. However, the predominant class of compounds (12 of 22) was carboxylic acids. In particular, the four SCFAs formic, acetic, propionic and butyric

71

acid all triggered *flaAgfp* expression. Also eliciting a positive response were two detergents, Tween 20 and Tween 80; however, it is noteworthy that both detergents also contain carboxylic acid groups: lauric and oleic acids, respectively (Table 3.2). High concentrations of formate, acetate, propionate and butyrate are known to inhibit the growth of many microorganisms (Meynell 1963 and Bohnhoff 1964), including *L. pneumophila* (Warren and Miller, 1979). Moreover, acetate, propionate and butyrate regulate *Salmonella typhimurium* invasion gene expression *in vitro* at concentrations that correlate with their relative abundance in the intestinal tract (Lawhon *et al.*, 2002). Therefore, we postulated that *L. pneumophila* monitors SCFAs to coordinate its life cycle.

Excess short chain fatty acids inhibit L. pneumophila growth and induce motility

　　　　To verify the results from the phenotypic microarrays, we performed quantitative assays with two SCFAs, acetic and propionic acid. As predicted from the Biolog screen, when E cultures were treated with either 10 mM acetic or propionic acid, *L. pneumophila* immediately activated the *flaA* promoter (Fig. 3.1B and D) and stopped replicating (Fig. 3.1A and C). In contrast, control cultures supplemented with water did not induce the *flaA* promoter until 9 h, a time when *L. pneumophila* normally transitions to the post-exponential (PE) phase (Fig. 3.1, circles). Microscopic examination revealed that the SCFAs also induced motility (data not shown), as expected (Hammer and Swanson, 1999). The growth inhibition of *L. pneumophila* was not attributed to a loss in viability, as judged by the constant CFU of the cultures (data not shown).

　　　　To determine whether the response by *L. pneumophila* to SCFAs was a consequence of alterations in pH, E bacteria were treated with two inorganic acids, hydrochloric or perchloric acid, and then monitored for growth and fluorescence. When added to a range of concentrations (1.25-20 mM), neither hydrochloric nor perchloric acid triggered growth inhibition or induction of the *flaAgfp* promoter (Fig. 3.1E and F;

also data not shown). Moreover, the pH of *Legionella* cultures supplemented with acetic

or propionic acid did not differ significantly from identical cultures supplemented with

water, nor did the pH of the fatty acid-treated cultures vary detectably over the course of

the experiment (data not shown). Finally, when E cultures were supplemented with non-

acidic forms of acetate, namely calcium acetate or magnesium acetate, *L. pneumophila*

replication halted, and the bacteria activated the flagellin promoter to a level similar to

that displayed after acetic acid addition (data not shown). Therefore, *L. pneumophila*

appear to respond to a signal generated by SCFAs that is distinct from pH.

Fatty acid supplementation stimulates L. pneumophila differentiation

Since both acetic and propionic acid induced motility and inhibited bacterial

replication, we next investigated whether the SCFAs also trigger other *L. pneumophila*

transmissive phase phenotypes, including cytotoxicity to phagocytic cells, the avoidance

of lysosomal degradation and sodium sensitivity (Byrne and Swanson, 1998). Indeed,

after supplementation with either acetic or propionic acid, E phase *L. pneumophila*

became as cytotoxic to bone marrow-derived macrophages as PE control cultures (Fig.

3.2A). Importantly, SCFAs alone were not cytotoxic (Table 3, *letA* and *letS* mutants; also

data not shown). Further, when E phase *L. pneumophila* were supplemented with

SCFAs, the majority of the bacteria also acquired the capacity to evade lysosomes, as

judged by immunofluorescence microscopy (Fig. 3.2B). Although only 15% of E phase

L. pneumophila avoided degradation (Fig 3.2B, water sample), greater than 50% of those

exposed to acetic or propionic acid escaped the lysosomal compartment (Fig. 3.2B).

Finally, 10 mM acetic or propionic acid also triggered sodium sensitivity in E phase

microbes (Fig. 3.2C). Thus, our Biolog screen accurately predicted that exposure to 10

mM SCFAs induces *L. pneumophila* differentiation to the transmissive phenotype.

Accordingly, we next tested two potential modes of action: Excess SCFA may either

generate high-energy intermediates that affect two-component phosphorelay systems or instead alter fatty acid metabolism.

To respond to fatty acids, L. pneumophila requires the LetA/LetS two-component system, but not generation of acetyl-phosphate and propionyl-phosphate

At the crux of *L. pneumophila's* differentiation circuitry is the two-component system LetA/LetS, which regulates all known transmissive phase phenotypes (Lynch *et al.*, 2003). To discern whether the response of *L. pneumophila* to the SCFAs is dependent on the signal transduction system, we cultured *letA* and *letS* mutants containing the *flaAgfp* reporter construct to the E phase, supplemented the cultures with 10 mM acetic or propionic acid, and then monitored both optical density and fluorescence of the cultures over time. When confronted with SCFAs, the *letA* and *letS* mutants resembled wild-type (WT) *L. pneumophila* in restricting their growth (Table 3.3). In contrast, *L. pneumophila* required the LetA/LetS system to induce flagellin expression in response to 10 mM acetic acid (Fig. 3.3A); albeit to a lesser degree, LetA/LetS also mediated the response to propionic acid, a SCFA that exerts a stronger effect on the flagellin promoter (Fig. 3.3B). Furthermore, microscopic examination demonstrated that *L. pneumophila* requires LetA/LetS to trigger motility in response to either 10 mM acetic or propionic acid (Table 3.3). Likewise, the two-component system was required for expression of three other transmissive traits: cytotoxicity, lysosome avoidance, and sodium sensitivity (Table 3.3). Therefore, when *L. pneumophila* encounters a sudden increase in SCFAs, a pathway that includes the LetA/LetS phosphorelay coordinates bacterial differentiation.

The response regulators of many two-component systems can use the high-energy intermediates acetyl-phosphate and propionyl-phosphate to catalyze their own phosphorylation (Wolfe, 2005). For example, acetyl-phosphate stimulates the *S. typhimurium* response regulator SirA to induce invasion gene expression (Lawhon *et al.*,

2002) and also activates the *Bordetella pertussis* BvgA response regulator independently of its cognate histidine kinase (Boucher *et al.*, 1994). Therefore, we tested whether exogenous acetic or propionic acid must be converted to acetyl- and propionyl-phosphate before activating the LetA/LetS signal transduction system. For this purpose, we constructed and analyzed a *L. pneumophila* mutant that lacks the two enzymes that synthesize the phosphate intermediates, phosphotransacetylase and acetyl kinase, encoded by the *pta* and *acka2* genes, respectively (McCleary *et al.*, 1993; Wolfe, 2005). By monitoring the induction of the flagellin promoter, it was evident that both the phosphotransacetylase and acetyl kinase enzymes were dispensable for *L. pneumophila* to differentiate when confronted by excess acetic or propionic acid (Fig. 3.4). Thus, SCFAs trigger *L. pneumophila* differentiation by a mechanism other than generating acetyl- and propionyl-phosphate intermediates that activate the LetA/LetS system.

When fatty acid biosynthesis is inhibited, a physical interaction between acyl carrier protein (ACP) and SpoT enables *E. coli* to enter stationary phase (Battesti and Bouveret, 2006). The stringent response alarmone ppGpp also coordinates *L. pneumophila* differentiation (Hammer and Swanson, 1999). Therefore, we investigated whether *L. pneumophila* monitors fatty acid metabolism to govern its life cycle.

Perturbations in fatty acid biosynthesis trigger L. pneumophila differentiation

The degradation and biosynthetic pathways of fatty acid metabolism are tightly controlled, as their simultaneous activation would be futile. The point of regulation lies in the irreversible conversion of acetyl-CoA to malonyl-CoA, which is governed by the acetyl-CoA carboxylase complex (ACC) (Magnuson *et al.*, 1993). In mammalian cells, the inhibitor 5-(tetradecyloxy)-2-furoic acid (TOFA) blocks the ACC complex and prevents acetate from being incorporated into fatty acids (McCune and Harris, 1979; Panek *et al.*, 1977). Accordingly, malonyl-CoA levels in the cell are significantly reduced, and fatty acid biosynthesis is halted (Cook *et al.*, 1978; McCune and Harris,

1979). Therefore, to begin to test the hypothesis that SCFA supplements impinge upon either fatty acid degradation or biosynthesis, we first investigated whether acetic and propionic acid still trigger *L. pneumophila* differentiation when the conversion of acetyl-CoA to malonyl-CoA is blocked by TOFA. As expected, E cultures supplemented with 10 mM acetic or propionic acid prematurely activated the flagellin promoter (Fig. 3.5B and C). However, when cultures were simultaneously supplemented with SCFAs and TOFA, which is predicted to inhibit ACC, the bacteria did not differentiate (Fig. 3.5B and C). When treated with TOFA alone, *L. pneumophila* growth was restricted (data not shown) but viability was maintained, as the number of CFU was similar between 0 and 24 h after TOFA treatment (data not shown). Since activity of the ACC complex was required for SCFAs to initiate *L. pneumophila* differentiation, we deduced that addition of 10 mM acetic or propionic acid likely affects the fatty acid biosynthetic pathway.

As an independent test of the model that perturbations in fatty acid biosynthesis trigger *L. pneumophila* differentiation, we exploited the antibiotic cerulenin, which irreversibly blocks two key fatty acid enzymes, FabB and FabF (Buttke and Ingram, 1978; Ulrich *et al.*, 1983; Vance *et al.*, 1972). As with TOFA, cerulenin treatment inhibits fatty acid biosynthesis. However, rather than depleting malonyl-CoA concentrations, cerulenin causes malonyl-CoA to accumulate in the cell (Heath and Rock, 1995). When WT *L. pneumophila* was cultured to the E phase and supplemented with 0.5 μg/ml cerulenin, bacterial replication stopped (data not shown), and the *flaA* promoter was activated (Fig. 3.5D). Similar to propionic acid (Fig. 3.3B), the response to cerulenin was partially dependent on the LetA/LetS two-component system (data not shown).

In eukaryotic cells, the simultaneous addition of cerulenin and TOFA decreases malonyl-CoA levels and blocks fatty acid biosynthesis (Pizer *et al.*, 2000). Therefore, to test the prediction that TOFA also negates the effect of cerulenin on prokaryotic cells, we treated E phase *L. pneumophila* with both inhibitors and then monitored flagellin promoter activity over time. Whereas cerulenin activates the *L. pneumophila flaA*

promoter, a marker of the transmissive phase (Fig. 3.5E), cultures treated with both cerulenin and TOFA did not differentiate (Fig. 3.5E). Taken together, the effects of both SCFA supplementation and the pharmacological inhibitors of particular fatty acid biosynthetic enzymes indicate that, when fatty acid biosynthesis is disrupted, *L. pneumophila* responds by differentiating to the transmissive phase.

Short chain fatty acid supplementation alters the L. pneumophila profile of acylated acyl carrier proteins

A critical component of fatty acid and lipid biosynthesis is ACP. This small, acidic protein is post-translationally modified by a 4′-phosphopantetheine group, which enables fatty acid intermediates to bind to the holo-protein through a thioester linkage (Magnuson *et al.*, 1993). Once modified, holo-ACP carries the growing fatty acid chain through successive rounds of fatty acid biosynthesis, elongating the fatty acid each cycle. To ascertain by a biochemical approach whether SCFA supplementation alters the fatty acid biosynthetic pathway, we analyzed *L. pneumophila* acyl-ACP pools by western analysis after their separation through native polyacrylamide gels designed either for SCFAs or long chain fatty acids (Post-Beittenmiller *et al.*, 1991; Rock and Cronan, 1981).

When E cultures were supplemented with 10 mM acetic or propionic acid for 3 h, the profiles of the acyl-ACPs were significantly different than identical cultures supplemented with water (Fig. 3.6). In fact, cultures treated with the SCFAs resembled the PE control, as similar ACP bands were depleted in each of the samples. Likewise, when cultures were supplemented with cerulenin, the ACP pools differed greatly from the water control and instead showed a substantial depletion in a majority of the ACP species (Fig. 3.6). Therefore, these biochemical data lend further support to the model that flux in fatty acid biosynthesis triggers *L. pneumophila* differentiation.

Alterations in the fatty acid biosynthetic pathway stimulates the stringent response

Many microbes produce ppGpp to adapt to nutritional and metabolic stresses such as deprivation of amino acids, carbon, iron, phosphorous and fatty acids (Srivatsan and Wang, 2008). Moreover, a regulatory role for ACP in the stringent response has recently been described: SpoT directly interacts with the functional form of ACP, and single amino acid substitutions that disrupt this interaction abrogates SpoT-dependent ppGpp accumulation when fatty acid biosynthesis is inhibited (Battesti and Bouveret, 2006). Accordingly, it has been suggested that SpoT senses an intermediate in fatty acid biosynthesis to trigger ppGpp accumulation in the cell (Battesti and Bouveret, 2006; DiRusso and Nystrom, 1998).

To ascertain whether WT *L. pneumophila* accumulates ppGpp in response to perturbations in fatty acid biosynthesis, nucleotide pools were labeled with ^{32}P during E phase growth, and then cultures were supplemented with water, acetic acid, propionic acid, or cerulenin for 1.5 h. Indeed, E cultures supplemented with propionic acid accumulated modest levels of ppGpp when compared to background levels of the alarmone in the water control (Fig. 3.7A). As expected from our phenotypic data (relative fluorescence in Fig. 3.1B and D), 10 mM acetic acid resulted in only trace levels of ppGpp, similar to the water control (Fig. 3.7A). Furthermore, when E cultures were treated with cerulenin, *L. pneumophila* produced detectable levels of the ppGpp alarmone, indicating that the stringent response pathway is induced when fatty acid biosynthesis is inhibited (Fig. 3.7A).

To test genetically whether *L. pneumophila* differentiation in response to perturbations in fatty acid biosynthesis was coordinated by ppGpp, we analyzed whether either the RelA or SpoT enzymes were required for the bacterial response to SCFAs. When E cultures were supplemented with either 10 mM acetic or propionic acid, *relA* mutant *L. pneumophila* differentiated, similar to WT (Fig. 3.7B and C). In contrast, *relA spoT* mutants were unable to trigger the phenotypic switch in response to 10 mM fatty

acids (Fig. 3.7B and C). Together, these data suggest that, when *L. pneumophila* encounter excess SCFAs, SpoT equips the bacteria to invoke the stringent response pathway to elicit swift changes in gene expression and rapidly adapt to metabolic stress.

Discussion

Since *L. pneumophila* persist within many different environments, we predicted that various metabolites cue its differentiation. To identify such metabolic triggers, we screened several hundred compounds via phenotype microarrays. Out of 387 compounds tested, only 22 triggered the premature transition from the replicative to the transmissive phase, with the majority being carboxylic acids (Table 3.2). Importantly, several of the compounds that elicited a positive response in the screen were independently verified to induce other transmissive phenotypes (Fig. 3.2, Table 3.3 and data not shown). Previous studies postulated that when amino acid concentrations are limited, uncharged tRNAs accumulate and the RelA enzyme synthesizes ppGpp, an alarmone that activates the regulatory cascade that governs *L. pneumophila* differentiation (Hammer and Swanson, 1999; Zusman *et al.*, 2002). Here we expand this paradigm by showing that ppGpp also accumulates when fatty acid biosynthesis is perturbed, perhaps due to a direct interaction between SpoT and ACP (Battesti and Bouveret, 2006). Indeed, preliminary genetic data indicate that when SpoT can no longer interact with ACP, *L. pneumophila* fails to differentiate in response to alterations in fatty acid biosynthesis (Appendix A). Thus, the stringent response machinery equips *L. pneumophila* to monitor both protein and fatty acid biosynthesis to judge when to exit one host and search for another.

Although the mechanism by which *L. pneumophila* detects fluctuations in fatty acid biosynthesis remains to be elucidated, it has been suggested that SpoT equips *E. coli* to sense either an accumulation or a depletion of an intermediate in this biosynthetic pathway (Battesti and Bouveret, 2006; DiRusso and Nystrom, 1998). Recent work with *Bacillus subtilis* demonstrated that a key regulator of lipid metabolism is malonyl-CoA, a

molecule that may act as a signal during stress and starvation (Schujman *et al.*, 2008). Similarly, our data using inhibitors of fatty acid biosynthesis indicate that malonyl-CoA levels may cue the phenotypic switch from the replicative to the transmissive form. E phase *L. pneumophila* immediately induce the *flaAgfp* reporter when treated with cerulenin, an inhibitor of fatty acid biosynthesis that causes malonyl-CoA to accumulate (Heath and Rock, 1995). Conversely, TOFA, which is predicted to deplete the levels of malonyl-CoA present in the cell, does not stimulate E phase *L. pneumophila* to activate the *flaA* promoter (Cook *et al.*, 1978; McCune and Harris, 1979). Therefore, *L. pneumophila* may monitor the levels of malonyl-CoA in the cell to regulate its phenotypic switch.

Alternatively, *L. pneumophila* may monitor the acyl chains attached to ACP. For example, the bacteria may recognize when acyl-ACPs levels are sparse or their ratio is altered, thereby leading to an accumulation or a depletion in one or more of the acyl-ACP species. Indeed, when E phase *L. pneumophila* were treated with either excess SCFAs or cerulenin, the acyl-ACPs in the cell were significantly depleted, as determined by western analysis (Fig. 3.6). Thus, *L. pneumophila* may monitor the depletion in acyl-ACPs via a SpoT-ACP interaction, which enables the cell to swiftly produce ppGpp when deemed appropriate. Since studies in *E. coli* suggest that fatty acid biosynthesis contains numerous intermediate compounds, more detailed studies are needed to determine which, if any, of the intermediates can trigger *L. pneumophila* differentiation. Furthermore, sequence data predict that *L. pneumophila* contains three ACPs (*lpg0359, lpg1396* and *lpg2233*) which each contain the critical serine residue that is likely modified by a 4'-phosphopantetheine moiety (Magnuson *et al.*, 1993). Our data do not address which ACP(s) are involved, as the specificity of the ACP antibody has not been determined (Fig. 3.6). Therefore, whether these ACPs are functionally redundant or whether each plays a unique role in the *Legionella* life cycle awaits further study.

We propose that by coupling the stringent response to fatty acid metabolism *L. pneumophila* can quickly alter its transcriptional profile. One important observation was that the levels of ppGpp observed in response to SCFAs and cerulenin was significantly less than that of PE bacteria (Fig. 3.7A). This is consistent with the previous report that *E. coli* produces low levels of ppGpp in response to fatty acid starvation (Seyfzadeh *et al.*, 1993). The low levels of ppGpp we observed also likely reflect our labeling conditions: Due to the fastidious nature of *L. pneumophila*, a phosphate-limited media, such as that used to label nucleotides efficiently in *E. coli* (Seyfzadeh *et al.*, 1993), was not a viable option for these studies. Nevertheless, since every PE trait is induced when E phase *L. pneumophila* are treated with excess SCFAs or cerulenin, even the modest level of ppGpp detected in the cell is sufficient to trigger differentiation (Fig. 3.2, Table 3.3). By analogy to *E. coli*, we favor a model by which sigma factor competition enables *L. pneumophila* to fine-tune its gene expression profile (Magnusson *et al.*, 2005). Perhaps when fatty acid biosynthesis is altered, the quantity of ppGpp produced by *L. pneumophila* is sufficient to recruit the appropriate cohort of its six alternative sigma factors to RNAP, thereby specifically inducing the PE traits necessary to promote host transmission and survival in the extracellular environment (Cazalet *et al.*, 2004; Chien *et al.*, 2004).

Compared with acetic acid, excess propionic acid consistently induced more robust *flaA* expression by *L. pneumophila* (Fig. 3.1B and D). In the same vein, propionic acid appeared to have a less stringent requirement for the LetA/LetS system than acetic acid did (Fig. 3.3). Nevertheless, when *letA* and *letS* mutants were treated with excess acetic or propionic acid, the mutants were equally defective for the early induction of PE phenotypes (Table 3.3). And, although *letA* and *letS* mutants treated with SCFAs were unable to trigger motility, cytotoxicity, lysosomal degradation or sodium sensitivity, the bacteria were still restricted for growth (Table 3.3). Thus, SCFAs likely affect the

bacteria similarly. On the other hand, growth inhibition in *L. pneumophila* occurs by a LetA/LetS independent mechanism that remains to be delineated.

While our *in vitro* data indicate that *L. pneumophila* monitors perturbations in fatty acid biosynthesis to regulate its differentiation, it is not known whether SCFAs also cue bacterial differentiation within the vacuolar compartment of phagocytic cells, as the composition of the *Legionella*-containing vacuole in freshwater protozoa and alveolar macrophages has yet to be elucidated. Although broth studies predict that *L. pneumophila* utilizes *relA* to produce ppGpp when amino acid supplies are exhausted, *relA* is dispensable for intracellular growth in both human macrophages and amoebae (Hammer and Swanson, 1999; Zusman *et al.*, 2002). In contrast, intracellular *L. pneumophila* do require SpoT to differentiate from the replicative to the transmissive phase and to initiate secondary infections in bone marrow-derived mouse macrophages (Appendix A). Therefore, *L. pneumophila* employs SpoT to monitor either fatty acids or other metabolites in the vacuolar compartment to regulate its differentiation and virulence.

There are several ways in which *L. pneumophila* could encounter alterations in the fatty acids that are present in its intracellular niche. For example, when the TCA cycle does not operate completely or when bacterial cells are flooded with excess carbon, microbes will excrete acetate into their extracellular milieu, a process known as acetogenesis (Wolfe, 2005). Perhaps when nutrients are abundant during the replicative phase, *L. pneumophila* excretes excess carbon as SCFAs, which accumulate in the vacuolar compartment. Upon reaching a certain threshold, the high concentrations of SCFAs present in the vacuole could serve as a signal for differentiation, escape, and subsequent host transmission. *L. pneumophila* also possesses lipolytic enzymes that may degrade either host or their own membranes to generate free fatty acids. When starved for essential nutrients, some bacteria do degrade phospholipids within their own cell membranes for use as internal stores of carbon and energy. Alternatively, *L.*

pneumophila may monitor external sources of fatty acids that are derived from the host plasma or phagosomal membranes. Consistent with this idea, within mouse macrophages *L. pneumophila* replicate within a lysosomal compartment (Sturgill-Koszycki and Swanson, 2000), the site for membrane degradation. Interestingly, alveolar macrophages can phagocytose pulmonary surfactant, which is rich in phosphatidylcholine, phosphatidylglycerol and palmitic acid (Grabner and Meerbach, 1991), and *L. pneumophila* can use a secreted phospholipase A enzyme to deplete phosphatidylcholine and phosphatidylglycerol from lung surfactant to release free fatty acids (Flieger *et al.*, 2000). By this scenario, the accidental human host may in fact exacerbate the infection process by stimulating synthesis of flagellin, which in turn provokes an inflammatory cell death pathway by macrophages (Molofsky *et al.*, 2005; Molofsky *et al.*, 2006; Ren *et al.*, 2006).

Due to limitations of our Biolog screen, we cannot rule out the possibility that additional metabolites present on the arrays also cue intracellular differentiation of *L. pneumophila*. Since the permeability of the *L. pneumophila* membrane for each of the compounds on the phenotypic microarrays is unknown, we cannot exclude the possibility that some compounds were unable to cross the cell membrane. Furthermore, titration curves indicate that the inducers may only trigger differentiation within a narrow concentration range (data not shown). In particular, in E phase *L. pneumophila*, the SCFAs induce *flaAgfp* expression only when present between 5-10 mM (data not shown). Since the phenotype microarrays have only one concentration of each compound on the plate, we cannot rule out that additional inducers of *L. pneumophila* differentiation might exist. Indeed, nicotinic acid, which is present on Biolog plate PM5 at 10 μM, did not cause growth restriction or induction of the *flaAgfp* reporter. However, both genomic microarray and phenotypic data indicate that 5 mM nicotinic acid triggers *L. pneumophila* differentiation (Chapter 4).

Since person-to-person transmission of *L. pneumophila* has never been documented, the capacity of *L. pneumophila* to mount a productive infection stems from its remarkable ability to exploit physiological and metabolic pathways that operate within both professional phagocytes and amoebae. In particular, *L. pneumophila* has evolved a mechanism to monitor fatty acid biosynthesis and use this information to regulate expression of its transmission traits, thereby enhancing its fitness when confronted by disparate environmental conditions.

Table 3.1. Bacterial strains and plasmids

Strain or Plasmid	Relevant genotype/phenotype	Reference or Source
Strains		
E. coli		
DH5α	F⁻ *endA1 hsdR17* (r⁻ m⁺) *supE44 thi-l recA1 gryA* (Nal^l) *relA1* Δ (*lacZYA-argF*⁻)$_{U169}$ φ80d*lacZ*Δ*M15* λ*pir*RK6	Laboratory collection
MB619	DH5α pGEM-T-PtaAckA2	This work
MB681	DH5α pGEM-T-PtaAckA2::Kan	This work
L. pneumophila		
MB110	wild type; *thyA hsdR rpsL*	(Berger and Isberg, 1993)
MB355	pflaG	(Hammer and Swanson, 1999)
MB413	*letA-22::kan*	(Hammer *et al.*, 2002)
MB414	*letA-22::kan* pflaG	(Hammer *et al.*, 2002)
MB416	*letS-36::kan*	(Hammer *et al.*, 2002)
MB417	*letS-36::kan* pflaG	(Hammer *et al.*, 2002)
MB641	*pta ackA2*::*kan*	This work
MB682	*pta ackA2*::*kan* pflaG	This work
MB684	*relA*::*kan* pflaG	Appendix A
MB685	*relA*::*gent spoT*::*kan* pflaG	Appendix A
Plasmids		
pGEM-T	Multiple cloning site within coding region of β-lactamase α fragment linearized with single-T overhangs; 3 kb; Amp^R	Promega
pflaG	150 bp *flaA* promoter fragment fused to GFP, encodes thymidylate synthetase; 10.5 kb; Amp^R	(Hammer and Swanson, 1999)
pGEM-T-PtaAckA2	pGEM-T containing 3.3 kb *pta ackA2 locus* PCR amplified from Lp02 chromosome and ligated into T overhangs; 6.3 kb; Amp^R	This work
pUC4K	pUC4 containing 1.3 kb kanamycin cassette	Pharmacia
pGEM-T-PtaAckA2::Kan	pGEM-T-PtaAckA2 with 1.3 kb kanamycin cassette inserted between *Xma*I and *Nhe*I sites in the *pta ackA2* ORF resulting in a 1.8 kb deletion	This work

Table 3.2. Compounds that trigger premature differentiation in *L. pneumophila*

Compound[*]	Biolog Plate
Carboxylic Acids	
Formic acid	PM1
Acetic acid	PM1
Propionic acid	PM1
Butyric acid	PM2A
α-Ketovaleric acid	PM2A
Caproic acid	PM2A
Itaconic acid	PM2A
Sorbic acid	PM2A
4-hydroxybenzoic acid	PM2A
m-hydroxy phenyl acetic acid	PM1
p-hydroxy phenyl acetic acid	PM1
Monomethyl succinate	PM1
Detergents	
Polyoxyethylene sorbitan monolaurate (Tween 20)	PM5
Polyoxyethylene sorbitan monooleate (Tween 80)	PM1
Other	
2-Deoxy D glucose-6-phosphate	PM4A
Deoxyadenosine	PM1
Deoxyribose	PM2A
Dihydroxyacetone	PM2A
Hydroxylamine	PM3B
Met-Ala dipeptide	PM3B
Nitrite	PM3B
Parabanic acid	PM3B

[*]Approximate concentrations: carbon sources 5-20 mM, nitrogen sources 2-5 mM, phosphorus and sulfur sources 0.1 to 2 mM.

Figure 3.1. Growth inhibition and the premature expression of motility are specific to fatty acid addition.
WT *L. pneumophila* carrying the *flaAgfp* reporter construct were cultured to the E phase and then supplemented with water or 10 mM acid. At the times indicated, samples were collected and optical density and relative fluorescence were analyzed. The addition of acetic acid (AA; closed squares) or propionic acid (PA; closed triangles) causes growth inhibition (A, C, E) and early motility (B, D, F), whereas cultures supplemented with hydrochloric acid (HCl; open squares) or perchloric acid ($HClO_4$; open triangles) do not (E and F). For all experiments, E cultures supplemented with water (H_2O; closed circles), which enter the PE phase around 9 h, served as a negative control. Shown are representative graphs from three or more independent experiments.

Figure 3.1.
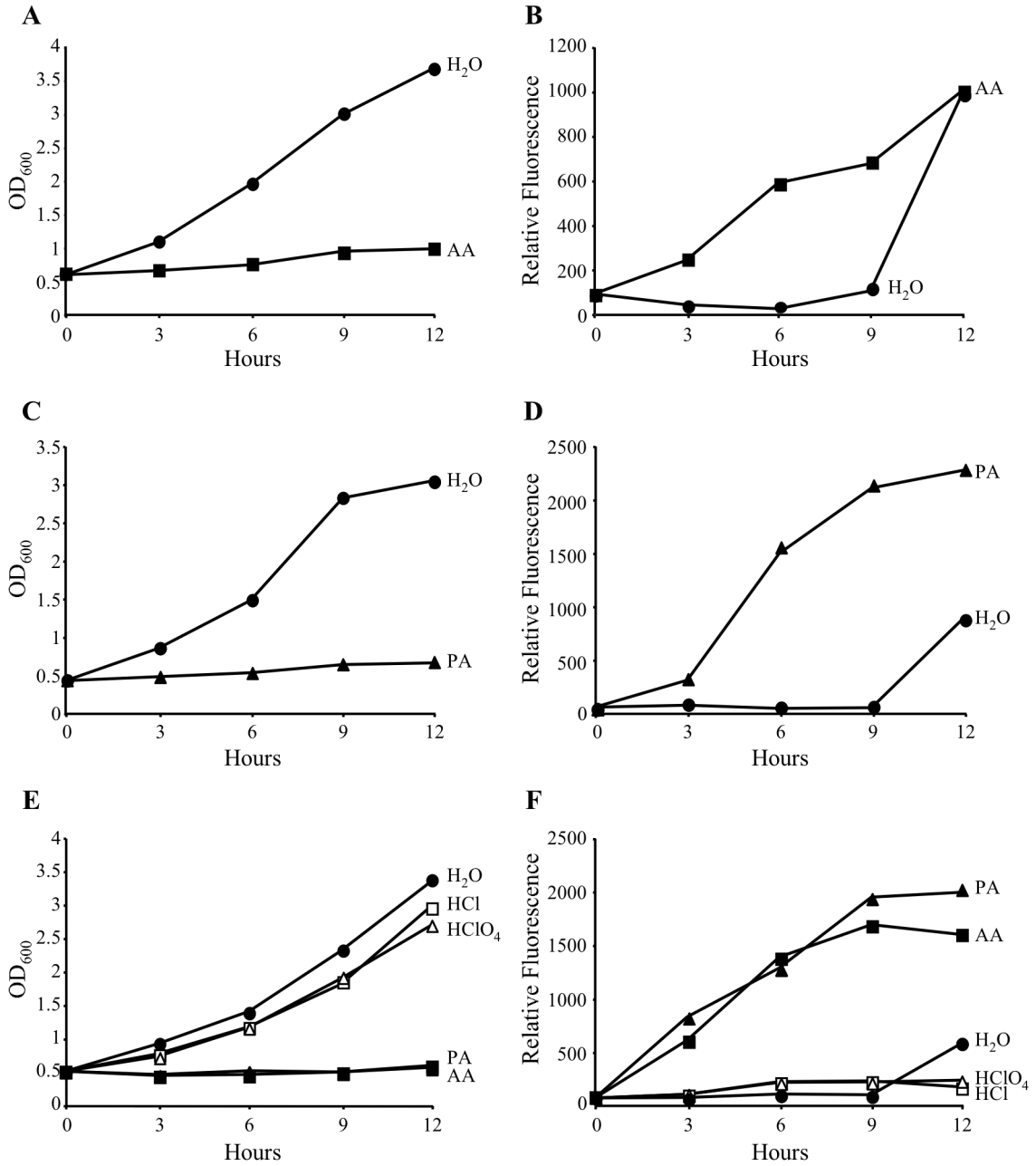
Figure 3.2.
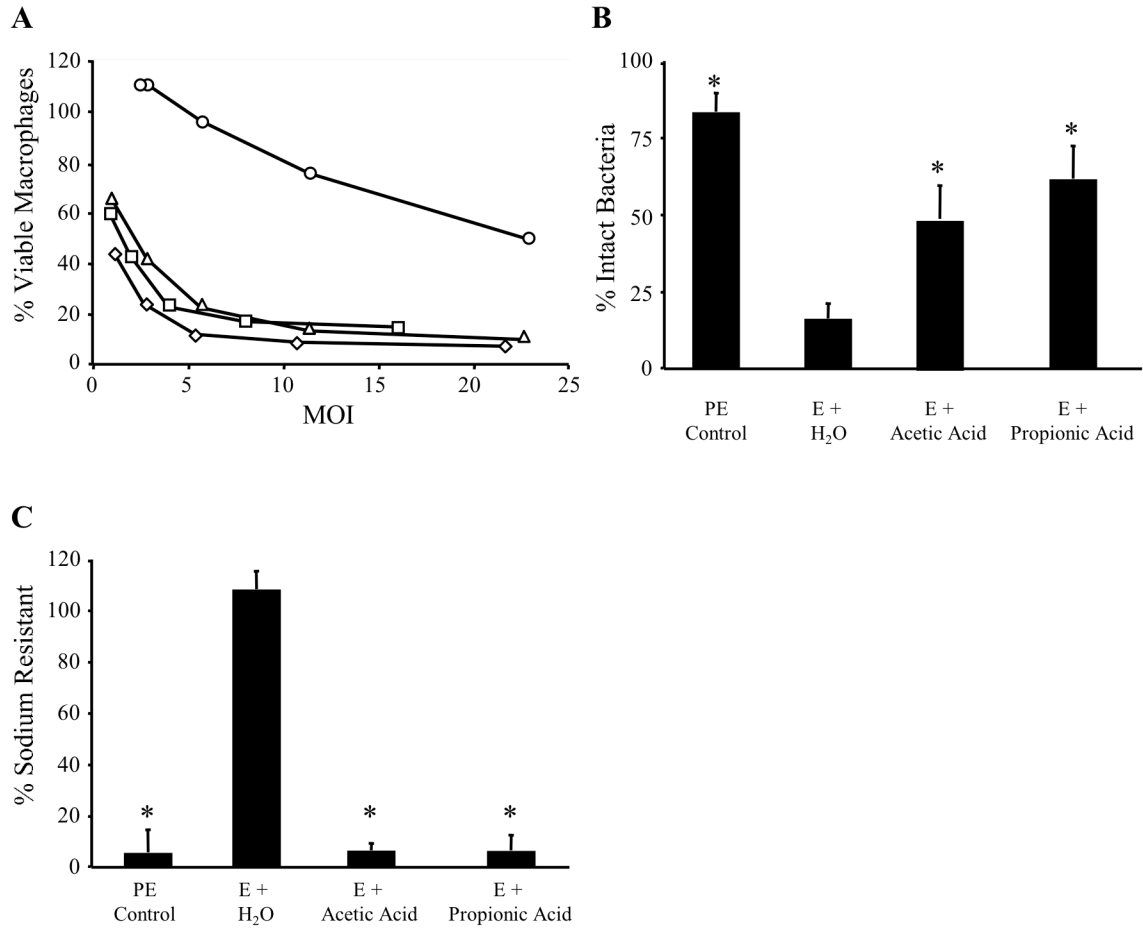
Figure 3.2. Fatty acid supplementation of WT *L. pneumophila* induces the early expression of multiple transmissive phase phenotypes.
(A) Macrophage viability was assessed by quantifying the reduction of the colorimetric dye alamarBlue™ following a 1 h incubation of macrophages with PE cultures (diamonds) or E cultures supplemented with water (circles), acetic acid (squares) or propionic acid (triangles). Shown is a representative graph from three independent experiments preformed in triplicate. (B) Lysosome evasion was determined by culturing *L. pneumophila* strains with macrophages at an MOI = 1 and quantifying the percent of intact bacteria following a 2-hour incubation by fluorescence microscopy. Displayed are the means from duplicate samples in three independent experiments. Error bars indicate SD and asterisks designate significant differences (P<0.01) when compared to water control. (C) The percent of sodium resistant bacteria was measured by plating cultures on media with or without 100 mM NaCl and then calculated as described (Byrne and Swanson, 1998). Shown are the means ± SD from duplicate samples in three independent experiments. Asterisks denote statistically significant differences (P<0.01) when compared to water control.

Figure 3.3.
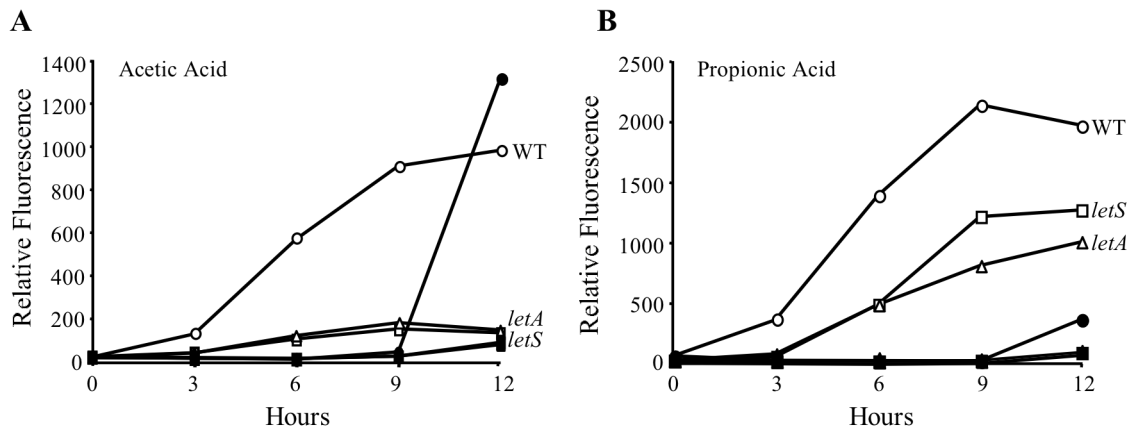
Figure 3.3. The LetA/LetS signal transduction system is required for full induction of premature motility.
WT (circles), *letA* (triangles) or *letS* (squares) *L. pneumophila* containing the *flaAgfp* reporter were grown to the E phase and then supplemented with water (closed symbols), 10 mM acetic acid (open symbols; Fig. 3.3A) or 10 mM propionic acid (open symbols; Fig. 3.3B). Samples were collected and analyzed for fluorescence at the times indicated. Shown are representative graphs from three independent experiments.

Table 3.3. Phenotypic response of *letA* and *letS* mutants 3 hours after fatty acid supplementation.

Strain	Culture conditions	Growth inhibition[a]	Motility[b]	Cytotoxicity[c]	Degradation[d]	Na sensitivity[e]
Wild-type	PE control	+	+++	+	+	+
	E + H₂O	–	–	–	–	–
	E + Acetic acid	+	++	+	+	+
	E + Propionic acid	+	++	+	+	+
letA	PE control	+	–	–	–	–
	E + H₂O	–	–	–	–	–
	E + Acetic acid	+	–	–	–	–
	E + Propionic acid	+	–	–	–	–
letS	PE control	+	–	–	–	–
	E + H₂O	–	–	–	–	–
	E + Acetic acid	+	–	–	–	–
	E + Propionic acid	+	–	–	–	–

a. Growth of *L. pneumophila* was monitored by measuring the OD_{600} of the cultures 3 h after supplementation. Although *letA* and *letS* cultures supplemented with fatty acids do not display PE phenotypes, bacterial growth is completely inhibited. Data represent at least three independent experiments.

b. Motility was assessed by phase-contrast microscopy and is based on numerous independent trials. (-) indicates cultures that were <10% motile, (+) indicates 10-25% motility, (++) indicates 25-75% motility, and (+++) indicates high levels of directed motility (>75%).

c. Cytotoxicity of *L. pneumophila* for macrophages was measured as described in Fig. 2. (+) indicates >50% of the macrophages were viable following incubation with bacteria at MOIs ranging from 0-20, whereas (-) represents <50% macrophage viability.   Data reported are from three independent experiments performed in triplicate.

d. The percent of bacteria that remain intact following a 2 h incubation within macrophages was determined as in Fig. 2. (+) indicates that >50% of the bacteria avoided lysosomal degradation, and (-) indicates that the number of bacteria remaining intact at 2 h did not significantly differ from exponential cultures supplemented with water (negative control). Data represent the mean ± SD from duplicate samples in three independent experiments.

e. The percent of sodium resistant bacteria was determined as described in Fig 2. The values represent the mean ± SD for three independent experiments performed in duplicate.

Figure 3.4.

A

B
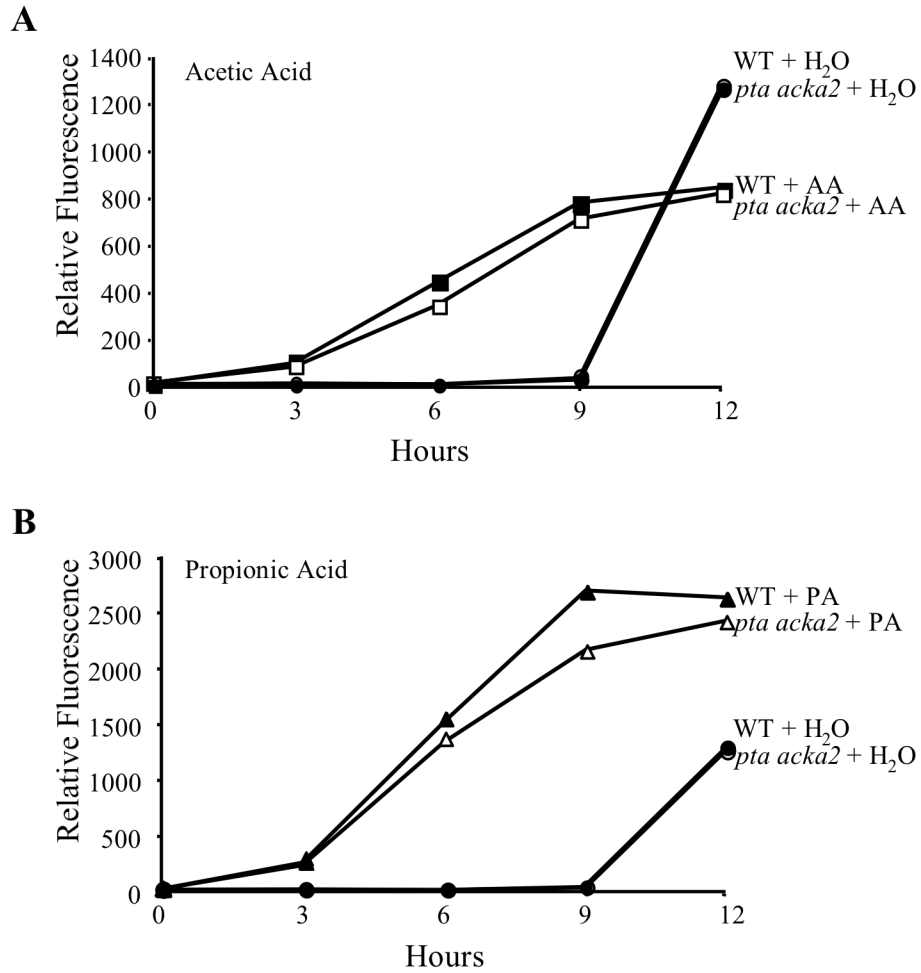
Figure 3.4. Induction of motility by fatty acid addition is independent of *pta ackA2*. Broth cultures of WT (closed symbols) or *pta ackA2* (open symbols) *L. pneumophila* containing pflaG were grown to the E phase and then supplemented with water (H_2O) (circles), 10 mM acetic acid (AA) (squares; Fig. 3.4A), or 10 mM propionic acid (PA) (triangles; Fig. 3.4B). Samples were taken at 3 h intervals and their relative fluorescence assessed by fluorometry. Displayed are representative graphs from three independent experiments.

Figure 3.5. Alterations in fatty acid biosynthesis induce *L. pneumophila* differentiation.

(A) Schematic of fatty acid metabolism indicating where TOFA and cerulenin inhibitors act. (B and C) Inhibition of the conversion of acetyl-CoA to malonyl-CoA abrogates the early differentiation that is triggered by fatty acid supplementation. E cultures containing pflaG were supplemented with either 10 mM acetic acid (AA; squares; Fig 3.5A) or 10 mM propionic acid (PA; triangles, Fig. 3.5B) with (open shapes) or without (closed shapes) the acetyl-CoA carboxylase inhibitor TOFA (5 µg/ml), and the fluorescence was monitored over time. Identical cultures supplemented with water (closed circles) or DMSO (vehicle control, data not shown) were analyzed as controls. Displayed are representative graphs from three independent experiments. (D) Inhibition of fatty acid biosynthesis stimulates early differentiation. E cultures of WT *L. pneumophila* carrying the *flaAgfp* plasmid were supplemented with the fatty acid biosynthesis inhibitor, cerulenin (Cer, 0.5 µg/ml; open circles), and the relative fluorescence monitored over time. Identical cultures supplemented with DMSO (closed circles) served as vehicle controls. A representative graph from three independent experiments is shown. (E) TOFA negates *L. pneumophila* differentiation triggered by cerulenin. WT *Legionella* containing pflaG were cultured to the E phase and then supplemented with cerulenin (Cer; closed squares) or cerulenin plus TOFA (open squares). Identical cultures treated with water (H_2O; closed circles) or TOFA alone (open circles) are shown as controls. Displayed is a representative graph from three independent experiments.

Figure 3.5.

Figure 3.6.

A   short chain acyl-ACPs   **B**   long chain acyl-ACPs

PE Control	E + H₂O	E + AA	E + PA	E + Cer

PE Control	E + H₂O	E + AA	E + PA	E + Cer
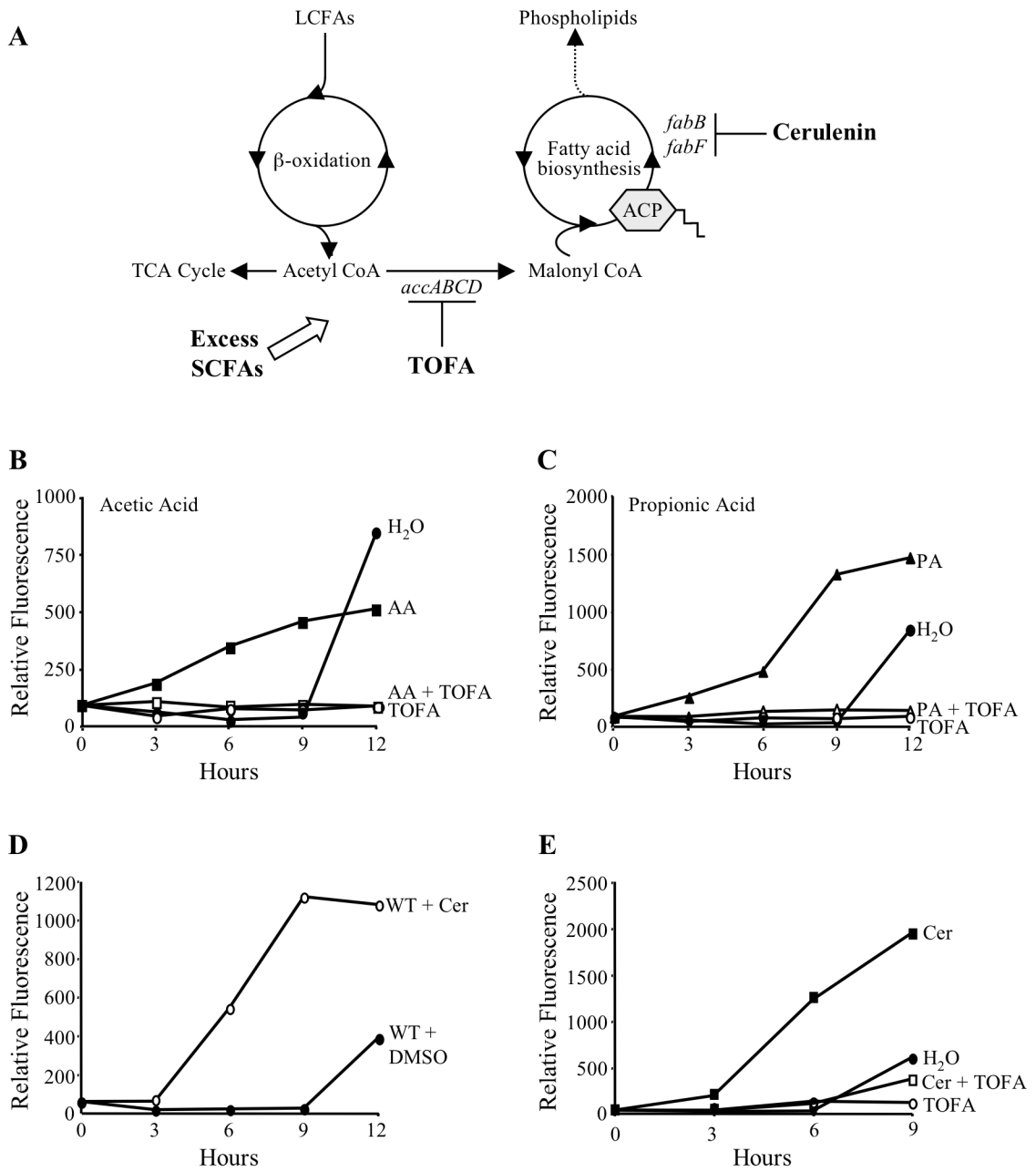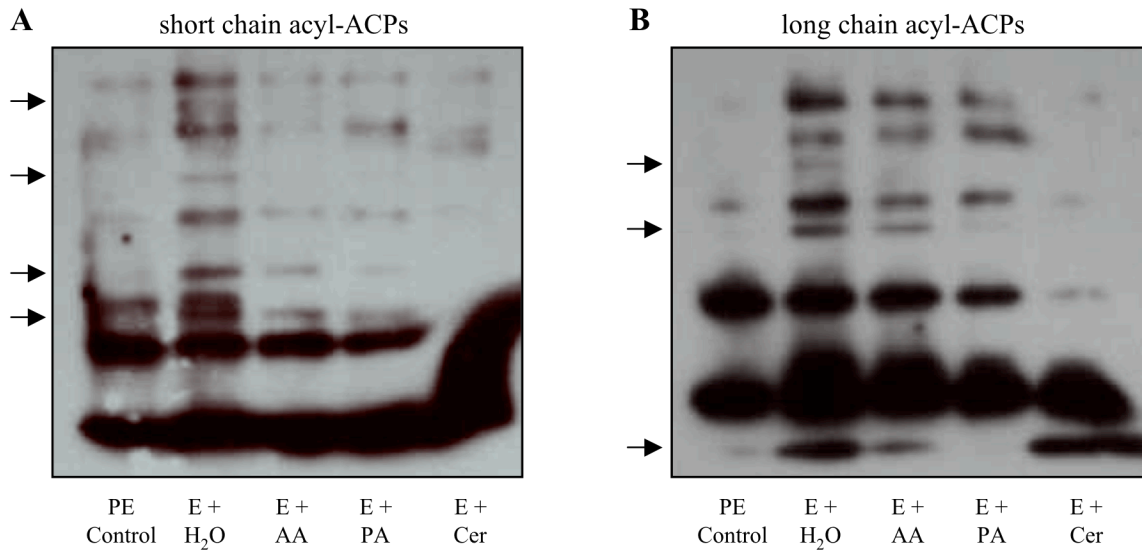
Figure 3.6. Perturbations in fatty acid biosynthesis alter *L. pneumophila* acyl-ACP profiles.
E phase *L. pneumophila* were incubated with water (H_2O), acetic acid (AA), propionic acid (PA), or cerulenin (Cer) for 3 h, then acyl-ACPs were extracted, purified and separated on 13% short chain fatty acid (A) or 13% long chain fatty acid (B) native polyacrylamide gels. ACP species were detected by western blotting. Arrows denote protein bands that differ between the E control and the treatment samples. Also shown are acyl-ACP pools from PE bacteria. Representative films from three independent experiments are displayed.

Figure 3.7.

A

GTP		
ppGpp		
Origin		

| PE | E + | E + | E + | E + |
| Control | Water | Acetic Acid | Propionic Acid | Cerulenin |

B

C
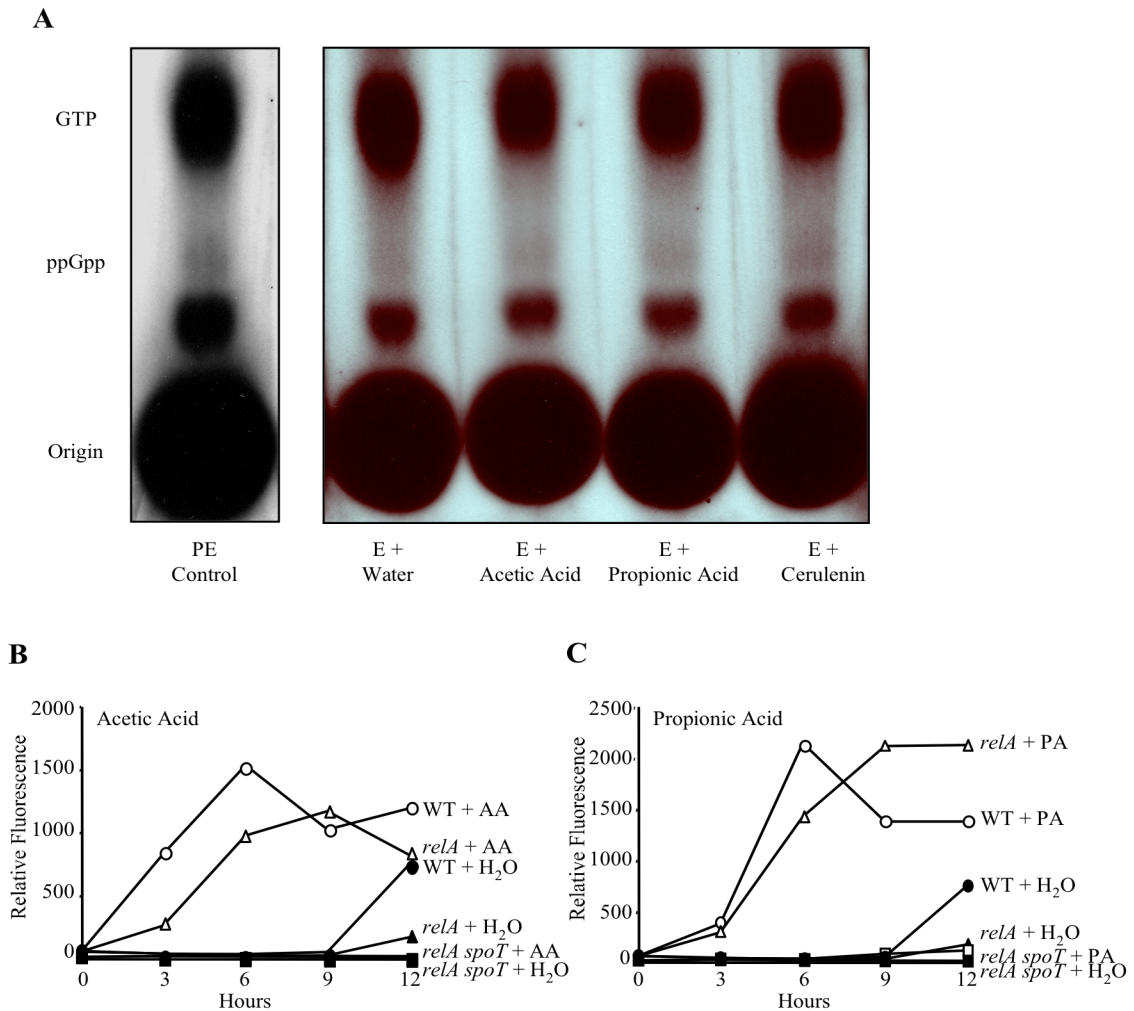
Figure 3.7. *L. pneumophila* **employs the stringent response to induce differentiation when fatty acid biosynthesis is altered.**
(A) Addition of fatty acids triggers ppGpp production in the E phase. After labeling nucleotide pools with ^{32}P, E cultures of WT *L. pneumophila* were supplemented with water, 10 mM SCFAs or 0.5 µg/ml cerulenin for 1.5 h to stimulate ppGpp synthesis. Extracts were prepared and nucleotides separated by TLC. For the PE control, late E phase cultures were labeled with ^{32}P until reaching the PE phase (approximately 6 h). Cell extracts and TLC were performed similar to E cultures. Representative chromatograms from two or more independent experiments are shown for each condition. (B and C) *L. pneumophila* requires SpoT to sense SCFAs. WT (circles), *relA* (triangles) or *relA spoT* (squares) *L. pneumophila* containing the *flaAgfp* reporter were cultured to the E phase and then supplemented with water (closed symbols), 10 mM acetic acid (open symbols; Fig. 3.7B) or 10 mM propionic acid (open symbols; Fig. 3.7C). At the times indicated, aliquots of the cultures were analyzed for fluorescence. Representative graphs from three independent experiments are shown.

Figure 3.8.

Limiting amino acids

Perturbations in fatty acid biosynthesis

RelA

SpoT ACP

ppGpp

Differentiation

Replication
(E)

Transmission
(PE)
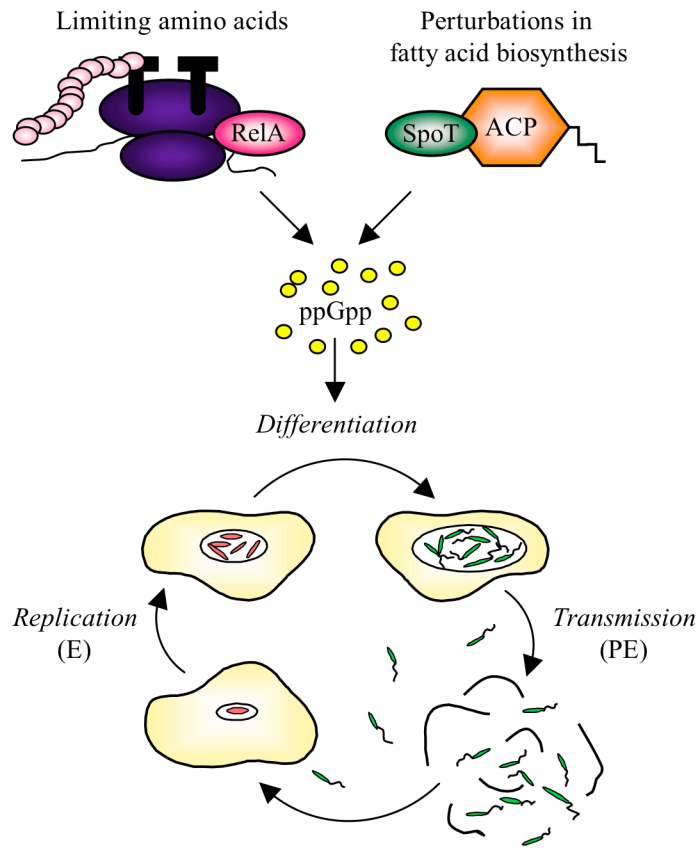
Figure 3.8. *L. pneumophila* **monitors flux in fatty acid biosynthesis to coordinate differentiation.**

CHAPTER FOUR

NICOTINIC ACID MODULATES *LEGIONELLA PNEUMOPHILA* GENE EXPRESSION AND VIRULENCE PHENOTYPES

Summary

When bacteria encounter various environmental fluctuations or stresses, they can activate transcriptional and phenotypic programs to coordinate an appropriate response. Indeed, the intracellular pathogen *Legionella pneumophila* converts from a non-infectious replicative form to an infectious transmissive form when the bacterium encounters alterations in either amino acid concentrations or fatty acid biosynthesis. Here we report that nicotinic acid (NA) also triggers *L. pneumophila* phase differentiation. In particular, when replicative *L. pneumophila* are supplemented with 5 mM NA, the bacteria induce numerous transmissive phase phenotypes, including motility, cytotoxicity towards macrophages, sodium sensitivity and lysosome avoidance. Moreover, transcriptional profile analysis determined that NA regulates a panel of genes similar to transmissive phase *L. pneumophila*. In addition, NA alters the expression of 246 genes that were unique for NA supplementation. While nearly 25% of these genes lack an assigned function, the most highly expressed gene following NA treatment is predicted to encode a membrane transporter. Since *Bordetella* and *E. coli* also differentiate in response to NA, knowledge of NA regulation by *L. pneumophila* will shed light on the mode of action and biological significance of this phenotypic modulator.

Introduction

Normally found in fresh water systems as a parasite of protozoa, *Legionella pneumophila* can also infect alveolar macrophages to cause the life-threatening pneumonia, Legionnaires' disease. Moreover, in aquatic environments *L. pneumophila* can exist as either a planktonic cell or persist within a sessile biofilm community. To survive within these diverse ecological niches, *L. pneumophila* has evolved methods to swiftly adapt to changing conditions by modifying its cellular physiology and morphology in a process known as differentiation. Under nutrient rich conditions, the post-transcriptional regulator CsrA suppresses transmissive traits and activates regulatory pathways that enable robust replication (Fettes *et al.*, 2001; Molofsky and Swanson, 2003). Once conditions deteriorate, proliferation halts and *L. pneumophila* initiates the stringent response to synthesize the second messenger, ppGpp (Hammer and Swanson, 1999; Zusman *et al.*, 2002). Simultaneously, the LetA/LetS two-component system is activated to relieve CsrA repression on transmissive traits (Hammer *et al.*, 2002; Molofsky and Swanson, 2003). As a result, *L. pneumophila* induces traits that promote transmission and survival in the harsh environment, including: motility, cytotoxicity towards phagocytic cells, sodium sensitivity, and the ability to avoid lysosomes (Bachman and Swanson, 2001, 2004a, b; Hammer *et al.*, 2002; Jacobi *et al.*, 2004; Lynch *et al.*, 2003).

To acclimate to its surroundings, *L. pneumophila* must monitor the external milieu and translate a perceived stimulus into a coordinated response. Indeed, when amino acids are depleted, the stringent response enzyme RelA senses the accumulation of uncharged tRNAs at the ribosome and produces the alarmone ppGpp (Hammer and Swanson, 1999; Zusman *et al.*, 2002). Additionally, *L. pneumophila* can monitor flux in fatty acid biosynthesis through an interaction between a second stringent response enzyme, SpoT, and a central component of fatty acid metabolism, acyl carrier protein (Battesti and Bouveret, 2006; Seyfzadeh *et al.*, 1993). Whether RelA or SpoT induces

the stringent response, the end result is the same. Thus, both enzymes enable *L. pneumophila* to assess its metabolic state and, when necessary, initiate transmission to a new niche. Since *L. pneumophila* persists in many different environments, it is conceivable that metabolic cues other than amino acids and fatty acids induce its differentiation.

One common way that microbes respond to external stimuli is via two-component signal transduction systems (Calva and Oropeza, 2006). For many two-component systems, the cues that initiate autophosphorylation and the subsequent phosphorelay are unknown. However, it is predicted that numerous environmental stimuli or conditions can activate these systems (Calva and Oropeza, 2006). At the core of *L. pneumophila's* differentiation circuitry is LetA/LetS, a two-component system that regulates all known transmission traits (Hammer *et al.*, 2002; Lynch *et al.*, 2003). Although the precise signal that activates the LetA/LetS system has not been identified, phenotypic studies indicate that multiple cues operate via the phosphorelay to trigger *L. pneumophila* phase differentiation.

The pyridine derivative nicotinic acid (NA) can activate microbial two-component systems, and consequently, modulate the genes and phenotypes that are governed by these regulatory proteins. Notably, studies in *Bordetella pertussis* have deduced that NA regulates a spectrum of gene expression states and virulence factors, such as pertussis toxin, adenylate cyclase toxin and filamentous hemagglutinin (Cotter and DiRita, 2000; Cummings *et al.*, 2006; McPheat *et al.*, 1983; Schneider and Parker, 1982). Moreover, the *Bordetella* two-component system BvgA/BvgS, which controls most known virulence and colonization factors, is modulated by the concentration of NA in the media (Miller *et al.*, 1989). Likewise, NA also regulates the *Escherichia coli* EvgA/EvgS system, which confers multi-drug resistance and acid tolerance (Eguchi *et al.*, 2003; Masuda and Church, 2002, 2003; Nishino and Yamaguchi, 2001; Nishino *et al.*, 2003; Utsumi *et al.*, 1994). Both the *B. pertussis* BvgA/BvgS and the *E. coli*

EvgA/EvgS systems belong to a family of proteins that employ a multi-step phosphorelay to activate their response pathways, but the mechanism by which NA modulates these two-component systems is not understood.

Since the LetA/LetS system belongs to the same family of signal transducing proteins as BvgA/BvgS and EvgA/EvgS, we postulated that NA might similarly modulate the expression of *L. pneumophila* transmission genes and phenotypes. To test this hypothesis, we performed phenotypic and transcriptional analyses of NA-treated *L. pneumophila*. Our data indicate that NA supplementation controls the expression of a unique cohort of genes and also triggers *L. pneumophila* differentiation. Moreover, NA activated the expression of a putative membrane transporter, which may help unravel the biochemical pathway by which NA modulates bacterial differentiation.

Experimental procedures

Bacterial strains, culture conditions and reagents. *L. pneumophila* strain Lp02 (*thyA hsdR rpsL*; MB110), a virulent thymine auxotroph derived from the serogroup 1 clinical isolate Philadelphia 1, was the parental strain for all mutants constructed (Berger and Isberg, 1993). MB355 contains the pflaG plasmid that encodes thymidylate synthetase as a selectable marker and a transcriptional fusion of the *flaA* promoter to *gfp* (Hammer and Swanson, 1999; Hammer *et al.*, 2002). MB414 contains *letA-22* and MB417 encodes *letS-36*, mariner insertion alleles of *lpg2646* and *lpg1912*, respectively, that confer resistance to kanamycin (Hammer *et al.*, 2002). Both MB414 and MB417 contain the pflaG reporter plasmid. For phenotypic assays, bacteria were cultured at 37°C in 5 ml of *N*- (2-acetamido)-2-aminoethanesulfonic acid (ACES; Sigma)-buffered yeast extract (AYE) broth. When necessary, cultures were supplemented with 100 µg/ml thymidine. In all experiments, replicative phase or exponential (E) cultures were defined as having an optical density at 600 nm (OD_{600}) of 0.5 to 0.85. Transmissive phase or post-

exponential (PE) cultures were defined as having an OD_{600} of 3.4 to 4.5. To obtain colony-forming units (CFU), *L. pneumophila* were plated on ACES-buffered charcoal-yeast extract agar supplemented with 100 µg/ml thymidine (CYET) and incubated for 4-5 days at 37°C.

Macrophage cultures. Bone marrow-derived macrophages were isolated from femurs of female A/J (Jackson Laboratory) mice and cultured in RPMI-1640 containing 10% heat-inactivated fetal bovine serum (RPMI/FBS; Gibco BRL) as previously described (Swanson and Isberg, 1995). Following a 7-day incubation in L-cell supernatant-conditioned media, macrophages were plated at either 2.5×10^5 or 5×10^4 per well for lysosomal degradation and cytotoxicity assays, respectively.

Fluorometry. To monitor expression of the flagellin promoter, *L. pneumophila* strain MB355, which contains the pflaG reporter plasmid, was cultured in AYE media without thymidine at 37°C on a rotating wheel. When cultures reached an $OD_{600} = 0.50$-0.85 (T = 0) they were supplemented with either 5 mM nicotinic acid or water, and at the times indicated, the cell density of each culture was measured at OD_{600}. To analyze similar bacterial concentrations, aliquots were collected by centrifugation, and the cell densities were normalized to $OD_{600} = 0.01$ in PBS. An aliquot of each sample (200 µL) was transferred to black 96-well plates (Costar), and the relative fluorescence intensity was measured using a Synergy™ HT microplate reader (485 nm excitation, 530 nm emission and sensitivity of 50).

Lysosomal degradation. The percentage of intracellular *L. pneumophila* that remained intact following a 2 h macrophage infection was quantified by fluorescence microscopy. Briefly, macrophages were plated at 2.5×10^5 onto coverslips in 24 well plates. Then, PE bacteria or E phase microbes supplemented with either water or 5 mM nicotinic acid for 3

h were added to macrophage monolayers at an MOI ~ 1. The cells were centrifuged at 400 × g for 10 min at 4°C and then incubated for 2 h at 37°C. Uninternalized bacteria were removed by washing the monolayers with RPMI/FBS three times, and the macrophages were fixed, permeabilized and stained for *L. pneumophila* as described (Molofsky *et al.*, 2005). For each sample, at least 100 macrophages on duplicate coverslips were scored for intact rods versus degraded particles in three independent experiments (Bachman and Swanson, 2001; Molofsky and Swanson, 2003).

Cytotoxicity. To determine contact-dependent cytotoxicity of *L. pneumophila* following macrophage infection, PE bacteria or E phase cultures supplemented with water or 5 mM nicotinic acid for 3 h were added to macrophage monolayers at the indicated multiplicities of infection (MOI). After centrifugation at 400 × g for 10 min at 4°C (Molofsky *et al.*, 2005), the cells were incubated at 37°C for 1 h. To quantify macrophage viability, RPMI/FBS containing 10% alamarBlue™ (Trek Diagnostic Systems) was added to the monolayers for 6-12 h, and the reduction of the colorimetric dye was measured spectrophotometrically as described (Byrne and Swanson, 1998; Hammer and Swanson, 1999; Molofsky *et al.*, 2005). Each sample was analyzed in triplicate wells in three or more independent experiments.

Sodium sensitivity. To calculate the percentage of *L. pneumophila* that are sensitive to sodium, PE bacteria or E cultures supplemented with either water or 5 mM nicotinic acid for 3 h were plated onto CYET and CYET containing 100 mM NaCl. After a 6-day incubation at 37°C, CFUs were enumerated and the percentage of sodium sensitive microbes calculated as described (Byrne and Swanson, 1998).

Statistical analyses for phenotypic assays. To calculate *p*-values for lysosomal degradation and sodium sensitivity assays, one-way analysis of variance (ANOVA) was used for at least 3 independent samples.

RNA isolation, RNA labeling and microarray hybridization. WT *L. pneumophila* were cultured on an orbital shaker at 37ºC to $OD_{600} = 0.65$ in 150 ml AYE containing 100 µg/ml thymidine. Upon reaching the appropriate optical density, cultures were supplemented with either water or 5 mM nicotinic acid, and then incubated for an additional 30 min or 3 h at 37ºC on an orbital shaker. Following the incubation period, 10 ml aliquots were centrifuged at $6000 \times$ g for 2 min at 4ºC. The culture supernatants were discarded and the pellets stored at -80ºC. Total RNA was extracted using TRIzol (Invitrogen) as described previously (Milohanic *et al.*, 2003). The RNA was reverse-transcribed and labeled with Cy3 or Cy5 according to the manufacture's instructions (Amersham Biosciences). The microarrays were designed to contain gene-specific 70mer oligonucleotides based on all predicted genes within the genome of *L. pneumophila* strain Paris (CR628336) and its plasmid (CR628338) as described previously (Bruggemann *et al.*, 2006). Hybridizations were performed following the manufacturers' recommendations (Corning) using 250 pmol of Cy3 and Cy5 labeled cDNA. Slides were scanned on a GenePix 4000A scanner (Axon Instruments) and the laser power and PMT were adjusted to balance the two channels. The resulting files were analyzed using Genepix Pro 5.0 software. Spots were excluded from analysis if they contained high background fluorescence, slide abnormalities or weak intensity. To obtain statistical data for the gene expression profiles, all microarrays were performed in duplicate with a dye swap.

Data and statistical analysis for microarrays. Data normalization and differential analysis were conducted using the R software (http://www.R-project.org). No

background subtraction was performed, but a careful graphical examination of all the slides was performed to ensure a homogeneous, low-level background in both channels. A loess normalization (Yang *et al.*, 2002) was performed on a slide-by-slide basis (BioConductor package marray; http://bioconductor.org/packages/2.2/bioc/html/marray.html). Differential analysis was carried out separately for each comparison between the two time points, using the VM method (VarMixt package (Delmar *et al.*, 2005)), together with the Benjamini and Yekutieli (Reiner *et al.*, 2003) p-value adjustment method. If not stated otherwise, only differently expressed genes with 1.4-fold-changes were taken into consideration. Empty and flagged spots were excluded from the data set, and only genes without missing values for the comparison of interest were analyzed.

Results

Nicotinic acid inhibits L. pneumophila growth and induces motility

To discern whether nicotinic acid (NA) triggers *L. pneumophila* differentiation, wild-type (WT) bacteria that contained the *flaAgfp* reporter construct were cultured to the exponential (E) phase and supplemented with either water or 5 mM NA. When E cultures were treated with NA, replication stopped (Fig. 4.1A, squares), and the bacteria immediately activated the *flaA* promoter (Fig. 4.1B, squares). In contrast, control cultures supplemented with water did not induce the *flaA* promoter until 9 h, a time when *L. pneumophila* normally transitions to the post-exponential (PE) phase (Fig. 4.1B, circles). In support of the fluorometry data, microscopic examination revealed that NA also triggered motility (data not shown). Thus, in response to a signal generated by NA, *L. pneumophila* induces its phenotypic switch.

NA supplementation stimulates L. pneumophila differentiation

To determine whether NA induces transmission traits apart from growth inhibition and motility induction, we tested NA-treated *L. pneumophila* for other PE phenotypes, including: the avoidance of lysosomal degradation, cytotoxicity to phagocytic cells and sodium sensitivity (Byrne and Swanson, 1998). Indeed, when E phase *L. pneumophila* were supplemented with 5 mM NA, the majority of the bacteria acquired the capacity to evade lysosomes, as judged by immunofluorescence microscopy (Fig. 4.2A). While less than 15% of E phase *Legionella* avoided degradation, greater than 70% of E bacteria exposed to 5 mM NA escaped the lysosomal compartment (Fig. 4.2A). Further, after NA treatment, E phase *L. pneumophila* became as cytotoxic to bone marrow-derived macrophages as PE control cultures (Fig. 4.2B). Finally, 5 mM NA also triggered sodium sensitivity of E phase microbes, albeit to a slightly less degree than PE *L. pneumophila* (Fig. 4.2C). Taken together, our phenotypic data suggest that 5 mM NA triggers *L. pneumophila* differentiation to the transmissive phenotype.

L. pneumophila requires the LetA/LetS two-component system to respond to NA

Work in *Bordetella* and *E. coli* indicates that NA elicits transcriptional and phenotypic responses through a two-component system. To analyze whether the response of *L. pneumophila* to NA is dependent on the homologous LetA/LetS signal transduction system, we cultured *letA* and *letS* mutants containing the *flaAgfp* reporter construct to the E phase, supplemented the cultures with 10 mM NA, and then monitored both optical density and fluorescence of the cultures over time. When treated with NA, the *letA* and *letS* mutants resembled WT *L. pneumophila* in restricting their growth (Fig. 4.3A). In contrast, *L. pneumophila* partially required the LetA/LetS system to completely induce flagellin expression in response to 10 mM NA (Fig. 4.3B). Furthermore, microscopic examination demonstrated that *L. pneumophila* requires LetA/LetS to trigger motility in response to NA (data not shown). Thus, our data indicate that the *L.*

pneumophila LetA/LetS two-component system is required to fully activate the *flaA* promoter and induce motility following NA supplementation.

Transcriptome analysis of replicative and transmissive L. pneumophila indicates that profound changes in gene expression exist between the phenotypic phases

To identify the transcriptional changes that occur when *L. pneumophila* transitions from the replicative to the transmissive phase, we employed multiple-genome DNA microarrays to analyze E and PE bacteria (Cazalet *et al.*, 2004; Chien *et al.*, 2004). Overall, 924 genes were more highly expressed in the PE phase (synonymously, repressed in the E phase; Fig. 4.4 and Table 4.S1) and 751 *L. pneumophila* genes were repressed in the PE phase (synonymously, elevated in the E phase; Fig. 4.4 and Table 4.S2). Importantly, our microarray data confirm transcriptional and regulatory data which indicate that *L. pneumophila* displays distinct gene expression patterns and phenotypes in the replicative and transmissive phases (Bruggemann *et al.*, 2006; Byrne and Swanson, 1998; Edwards and Swanson, 2006).

Several categories of genes were significantly induced in the PE phase when compared to the E phase. These include genes that are required for flagellum biosynthesis (Bruggemann *et al.*, 2006; Heuner and Steinert, 2003). In addition, numerous regulatory genes were activated in the PE phase, such as the sigma factors *rpoS* and *rpoE*, the transmission trait enhancer *letE*, and the stringent response enzyme *relA* (Bachman and Swanson, 2001, 2004a, b; Hales and Shuman, 1999; Hammer and Swanson, 1999; Zusman *et al.*, 2002). Other regulatory genes that were preferentially expressed in the PE phase include several two-component systems and members of the GGDEF/EAL family of proteins (Tables 4.1 and 4.S1). As expected, many genes of the Dot/Icm type IV secretion system had elevated levels of expression in the PE phase, notably *icmCPRSTV*, *dotV* and *sdbC* (Segal *et al.*, 2005). Finally, transcriptional analysis showed that the expression of genes encoding poly-hydroxybutyrate synthesis (*phaB1*

and *phaB2*), as well as several families of transporters and efflux pumps, were more highly expressed in PE phase when compared to E phase bacteria (Tables 4.1 and 4.S1).

Microarrays determine that NA regulates a panel of genes similar to PE L. pneumophila

Since NA supplementation triggers *L. pneumophila* differentiation, and transcriptional microarrays indicate that vastly different expression profiles are displayed between the replicative and transmissive phases, we predicted that the transcriptional program induced by NA supplementation would be quite extensive. To learn whether NA-treated *L. pneumophila* differ from PE phase microbes, we employed microarrays to compare E phase *L. pneumophila* treated with 5 mM NA to similar cultures supplemented with water. Indeed, when E phase bacteria were treated with NA, the expression levels of 714 genes were significantly elevated and 435 genes were repressed when compared to the water control (Fig. 4.4 and data not shown). Similar to PE *L. pneumophila*, when NA was added to E phase bacteria, 14 genes of the flagellar apparatus were induced, including: *flaA*, *fliADS*, *flgDFIJKLM*, *fleN*, *flhB* and *motB2* (Bruggemann *et al.*, 2006; Heuner and Steinert, 2003). Moreover, the expression of numerous genes involved in virulence was activated by NA supplementation, such as components of the Dot/Icm type IV secretion system (*icmBGOX*), substrates of the secretion system (*ralF*, *lidA*, *sdcA*, *sdhB1*, *sdbAB*, *sdeBCD*, *sidACDFGHH'*) and enhanced entry proteins *enhABC* (Segal *et al.*, 2005). By comparing the microarray data from PE bacteria to the transcriptional data from E phase *L. pneumophila* treated with NA, it was apparent that the profiles were comparable; bacteria from the two sample sets had 600 induced and 303 repressed genes in common (Fig. 4.4 and Tables 4.S3 and 4.S4). Accordingly, we conclude that the phenotypic switch triggered by NA supplementation is due to the induction of a transcriptional profile that is similar to that of PE *L. pneumophila*.

Transcriptional analysis identifies genes unique for NA modulation

While NA modulates the genotypic and phenotypic profiles of *B. pertussis* and *E. coli*, the mechanism by which NA elicits a response is not understood. To uncover the *L. pneumophila* genes and pathways controlled by NA supplementation, we analyzed the transcriptional profiles of E phase bacteria treated with 5 mM NA for 3 h compared to similar cultures supplemented with water. Using the microarray data set from replicative and transmissive phase *L. pneumophila* as a reference, we identified 246 genes that were uniquely regulated by NA supplementation (Fig. 4.4 and Tables 4.2 and 4.3). Of the genes that were highly induced following NA treatment, nearly 40% have no predicted function (44 genes out of 114 total, Table 4.2). Several regulatory genes had elevated expression levels, including the two-component regulator *lpg0098* and the transcriptional regulators from the MarR and LysR families, *lpg1212* and *lpg0274*, respectively (Table 4.2). Also, the induction of two virulence genes, *icmD/dotP* and *icmJ/dotN*, was particular to NA addition (Segal *et al.*, 2005).

The most striking observation was that the two genes with the highest level of transcriptional activation in response to NA lie in an operon; *lpg0272* and *lpg0273* were 9-fold and 35-fold elevated, respectively (Table 4.2 and Fig. 4.5). The *lpg0272* locus is predicted to encode a 14.6 kDa cysteine transferase, and *lpg0273* encodes a 44.9 kDa membrane protein belonging to the Major Facilitator Superfamily (MFS) of transporters (Fig. 4.5). Directly downstream of the *lpg0272-3* operon, but positioned in the opposite orientation, is the LysR transcriptional regulator (*lpg0274*), whose expression is elevated in response to NA, as described above (Fig. 4.5). Upstream of the *lpg0272-3* operon, but again in the opposite direction, are two genes involved in nicotinate and nicotinamide metabolism, *lpg0270-1* (Fig. 4.5). However, according to our microarray data, *lpg0270-1* are neither induced nor repressed following a 3 h treatment with NA when compared to the water control. Whether NA affects *lpg0270-1* expression at time points other than 3 h has not been assessed. Together, our transcriptional data indicate that NA regulates a

distinct set of *L. pneumophila* genes; furthermore, the phenotypic modulator might initiate differentiation through a membrane transporter.

Discussion

A variety of microbes sense NA concentrations to modulate their genotypic and phenotypic expression profiles. For example, the respiratory pathogen *B. pertussis* controls hundreds of genes and virulence traits depending on the concentration of NA that is present in the culture media (Cotter and DiRita, 2000; Cummings *et al.*, 2006; McPheat *et al.*, 1983; Schneider and Parker, 1982). Similarly, in *E. coli*, NA regulates the expression of motility, the outer membrane porin protein OmpC and the alcohol dehydrogenase protein AdhE (Han *et al.*, 1999; Leonardo *et al.*, 1996; Utsumi *et al.*, 1994). In addition, NA concentrations control the expression of adhesion genes in the urinary tract pathogen *Candida glabrata* (Domergue *et al.*, 2005).

Both amino acid and fatty acid concentrations are known to cue *L. pneumophila* differentiation; however, due to the variety of ecological locals this microbe can exploit, we postulated that NA might serve as an additional signal for its phenotypic switch. Indeed, when E phase *L. pneumophila* were treated with 5 mM NA, growth was restricted and the bacteria activated the flagellin promoter (Fig. 4.1). Moreover, microscopy indicated that NA induced motility 3 h after supplementation, thus corroborating the fluorometry data (Fig. 4.1 and data not shown). NA also modulates other *L. pneumophila* PE phenotypes: When NA was added to E phase cultures, the bacteria largely avoided degradation in the lysosomal compartment and became cytotoxic towards macrophages (Fig. 4.2). Additionally, NA-treated *L. pneumophila* were sensitive to sodium as indicated by a loss in CFU when compared to the E phase control (Fig. 4.2). Higher concentrations of NA failed to trigger *L. pneumophila* differentiation, as judged by a lack of lysosome avoidance and cytotoxicity, as well as salt tolerance (data not shown). At present, it is unclear whether high concentrations of NA directly represses genes that

govern phase differentiation or whether the viability of the bacteria is affected. Together, our phenotypic data determined that NA modulates PE-specific *L. pneumophila* phenotypes, and further validate the *flaAgfp* reporter construct as an indicator of *L. pneumophila* differentiation.

B. pertussis and *E. coli* respond to NA via the two-component systems BvgA/BvgS and EvgA/EvgS, respectively. While many two-component signal transduction systems use a two-step phosphorelay to activate gene expression, the *B. pertussis* and *E. coli* systems belong to a family of proteins that use a four-step phosphorelay to customize their expression profiles (Cotter and Miller, 1997). Importantly, the *L. pneumophila* LetA/LetS system, which regulates PE phenotypes, also belongs to this unorthodox family of signaling molecules. Similar to the BvgA/BvgS and EvgA/EvgS systems, NA also coordinates *L. pneumophila* differentiation through LetA/LetS. As indicated by fluorometry, complete induction of motility is dependent on both LetA and LetS (Fig. 4.3). Conversely, inhibition of *L. pneumophila* growth by NA occurs by a LetA/LetS independent mechanism (Fig. 4.3) that remains to be elucidated. Besides the aforementioned two-component systems, numerous microbes employ this family of signal transduction systems to regulate their response pathways, including: GacA/GacS of *Acinetobacter baumannii*, PigQ/PigW of *Serratia marcescens*, VarA/VarS of *Vibrio cholerae*, SirA/BarA of *Salmonella*, GacA/GacS of *Pseudomonas* and the UvrY/BarA and TorR/TorS systems of *E. coli* (Heeb and Haas, 2001; Lapouge *et al.*, 2008; Perraud *et al.*, 1999). Therefore, we predict that other members within this family of two-component systems may sense NA to regulate their genotypic and phenotypic expression profiles.

It is now well documented that the *L. pneumophila* life cycle includes two reciprocal phases (Bruggemann *et al.*, 2006; Byrne and Swanson, 1998; Molofsky and Swanson, 2004). When conditions are favorable, *L. pneumophila* suppresses its transmissive traits, and instead begins to multiply. However, once nutrients are

111

exhausted, replication halts, and the bacteria activate traits that promote efficient host transmission. Accordingly, *L. pneumophila* displays a pattern of genes and phenotypes that are unique for the replicative and transmissive phases (Bruggemann *et al.*, 2006; Molofsky and Swanson, 2004). To discern the gene expression profiles of the two phases of the *L. pneumophila* life cycle, we analyzed broth-grown microbes in the E and PE phases by microarrays. Remarkably, 1675 genes were differentially regulated between replicative and transmissive bacteria; 751 genes were repressed and 924 genes were induced in the PE phase when compared to E phase microbes (Fig. 4.4, Tables 4.S1 and 4.S2). As expected from phenotypic analyses, genes that encode components of the flagellar apparatus and the Dot/Icm type IV secretion system were highly expressed in the PE phase in comparison to E phase *L. pneumophila* (Byrne and Swanson, 1998; Segal *et al.*, 2005). Conversely, the post-transcriptional regulator CsrA, which represses all transmissive traits, was not expressed in PE bacteria (Table 4.S1). Moreover, genes for cell division, metabolic pathways and biosynthetic pathways were repressed in the PE phase as compared to E phase microbes (Table 4.S1). Thus, our transcriptional data support the model that *L. pneumophila* undergoes a radical shift in gene expression programs between the replicative and transmissive phases of its biphasic life cycle. In addition, our microarray data set supports the work of Brüggemann *et. al*., which demonstrated that other virulent strains of *L. pneumophila* undergo a dramatic change in their gene expression profiles both in liquid cultures and during amoebae infections, thus validating the model of the reciprocal phases of the *L. pneumophila* life cycle (Bruggemann *et al.*, 2006).

Since a large transcriptional program is induced upon entry into the PE phase (Bruggemann *et al.*, 2006), we predicted that the phenotypic switch triggered by NA would be due to an alteration in gene expression. To discern which *L. pneumophila* genes are controlled by NA, we compared the gene expression profiles of PE bacteria to E phase cultures that were supplemented with the phenotypic modulator. As expected,

the microarrays indicated that NA regulates the expression of 1149 genes, a large number of which are either induced or repressed in the PE phase (a total of 903 genes are shared between the two conditions tested; Fig. 4.4 and data not shown). Similar to PE bacteria, NA supplementation activated the expression of numerous components of the flagellar apparatus (Bruggemann *et al.*, 2006; Heuner and Steinert, 2003). This corroborates our phenotypic data, which deduced that E phase *L. pneumophila* activate motility 3 h after NA treatment (data not shown). Moreover, previous data indicate that both cytotoxicity and lysosome avoidance are mostly dependent upon motility (Molofsky *et al.*, 2005). Therefore, since our transcriptional data determined that most of the flagellar genes are induced by NA treatment, it was not surprising that when 5 mM NA was added to E phase *L. pneumophila*, the bacteria became cytotoxic towards macrophages and largely avoided the lysosomal compartment (Fig. 4.2 A and B and data not shown). In addition, the microarrays determined that NA activates the expression of several Dot/Icm type IV secretion genes (data not shown). The presence of the secretion system is thought to form a large pore by which sodium can enter the bacterial cell ((Byrne and Swanson, 1998; Sadosky *et al.*, 1993; Vogel *et al.*, 1996). Indeed, the expression of the apparatus correlated with the sodium sensitivity phenotype displayed by PE bacteria and E phase *L. pneumophila* supplemented with NA (Fig. 4.2C). Based on our data, we infer that the differentiation that is triggered by NA is largely dependent upon a shift in the transcriptional profile of the bacterium towards that of PE *L. pneumophila*.

Although data clearly indicate that NA controls microbial genes and phenotypes, the mode by which the modulator exerts its effect has not been elucidated. To determine the cohort of genes that are unique for NA regulation, we compared the transcriptional profile of PE genes to E phase *L. pneumophila* that were treated with 5 mM NA. While nearly 250 genes were specific for NA supplementation, genes within the *lpg0272-3* operon had the highest level of expression (Table 4.2). Preliminary data suggest that *lpg0272-3* is essential, as efforts to generate a double mutant have been unsuccessful

(data not shown). Since *lpg0272* encodes a cysteine transferase, and *L. pneumophila* requires cysteine for growth, this auxotrophy may account for our failed attempts to disrupt the operon (Fig. 4.5).

Sequence data predict that *lpg0273* encodes a membrane protein that belongs to the MFS of transporters (Fig. 4.5). We speculate that *lpg0273* may function either as an importer or exporter for small metabolites, a process which *L. pneumophila* monitors to control its differentiation. The transcriptional regulator *lpg0274*, which lies within the same region of the *L. pneumophila* chromosome as *lpg0272-3*, also showed elevated levels of gene expression after NA treatment (Fig. 4.5 and Table 4.2). The significance for the close proximity of transcriptional regulator to *lpg0272-3* has not been assessed. However, we postulate that *lpg0274* might be involved in the transcriptional and phenotypic changes that are elicited by NA. Finally, it is interesting to note that upstream of the *lpg0272-3* operon lie two genes involved in nicotinate and nicotinamide metabolism (*lpg0270-1*; Fig. 4.5). While the gene expression levels of *lpg0270-1* were not altered under the conditions tested, their contribution to the same metabolic pathways as NA lends further support to the hypothesis that *lpg0272-3* is directly involved in NA signaling.

One mechanism by which NA could exert its effect is by controlling a class of proteins known as sirtuins. These highly conserved nicotinamide adenine dinucleotide (NAD^+)-dependent deacetylase enzymes regulate a range of proteins by affecting the acetylation and deacetylation states of their particular substrates (Blander and Guarente, 2004). Moreover, it has been proposed that nicotinamide, the amide of NA, is the metabolite that controls sirtuin activity *in vivo* (Starai *et al.*, 2004). Recent work in *Salmonella enterica* has determined that microbes contain homologous of the sirtuin proteins (Starai *et al.*, 2002). In particular, *S. enterica* encodes the sirtuin CobB, which controls the activity of acetyl-coA synthetase (ACS), and likewise, the conversion of acetate to acetyl-coA (Starai *et al.*, 2002; Wolfe, 2005). Previous work from our lab

suggests that alterations in acetate concentrations can perturb the fatty acid biosynthetic pathway and trigger *L. pneumophila* differentiation (Chapter 3). Genome analysis indicates that almost all microbes contain a CobB homologue. Thus, we predict that *L. pneumophila* encodes a sirtuin that regulates acetate levels similar to *S. enterica*. According to this model, NA supplementation would affect a *L. pneumophila* sirtuin, which in turn impacts fatty acid biosynthesis and differentiation. While analyses of the *L. pneumophila* genome have not identified obvious sirtuin candidates, our transcriptional data predict that 44 genes of unknown function are induced following NA treatment. Therefore, we envision that one of these genes could encode a novel protein that has sirtuin-like activity (Table 4.2).

In summary, our data indicate that NA controls the genotypic and phenotypic profiles of *L. pneumophila* through the use of the LetA/LetS two-component system. Since numerous microbes employ analogous signal transduction systems to coordinate their response pathways, we predict that the repertoire of bacteria modulated by NA is larger than currently appreciated. Furthermore, our transcriptional analysis of the replicative and transmissive phases supports the model of the *L. pneumophila* biphasic life cycle. Finally, while our microarray studies demonstrate that NA induces an expression program largely similar to that of PE bacteria, we did identify a novel group of genes that are regulated by NA. We predict that this class of genes will provide a valuable resource for experimentalists to uncover the biochemical pathways that mediate NA signaling.

Figure 4.1.

A

B
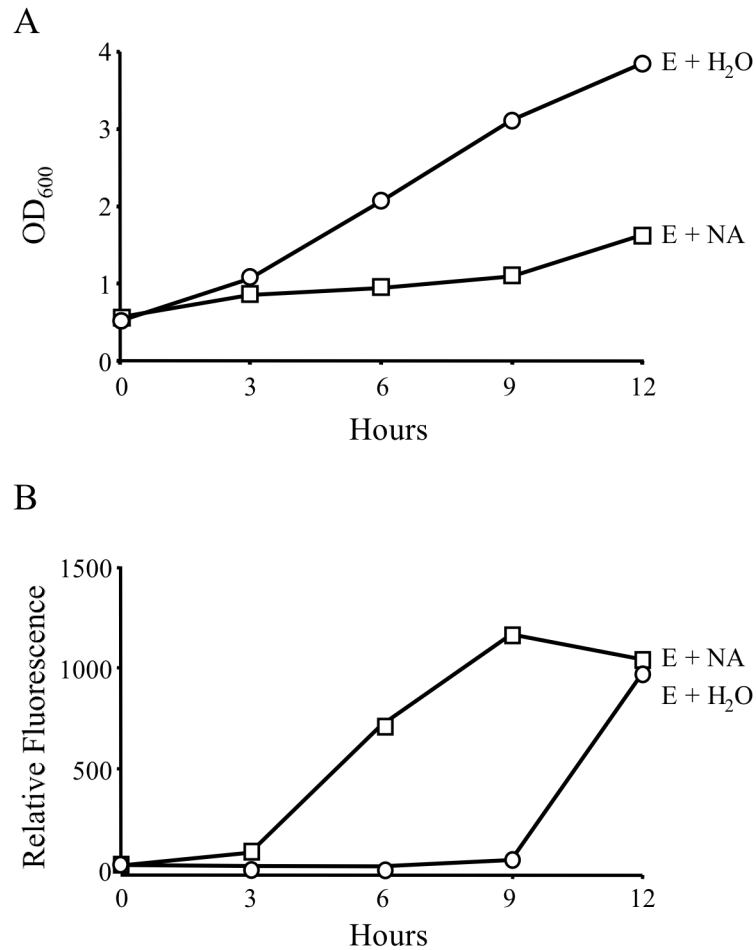
Figure 4.1. Nicotinic acid supplementation triggers growth inhibition and the premature expression of motility.
WT *L. pneumophila* carrying the *flaAgfp* reporter construct were cultured to the E phase and then supplemented with water (H_2O; circles) or 5 mM nicotinic acid (NA; squares). At the times indicated, samples were collected and optical density and relative fluorescence were analyzed. Whereas NA causes growth inhibition (A) and early motility (B), cultures supplemented with H_2O, do not enter the PE phase until 9 h following supplementation, as indicated by less growth (A) and induction of the *flaA* reporter (B) at this time point. Shown are representative graphs from three or more independent experiments.

Figure 4.2.
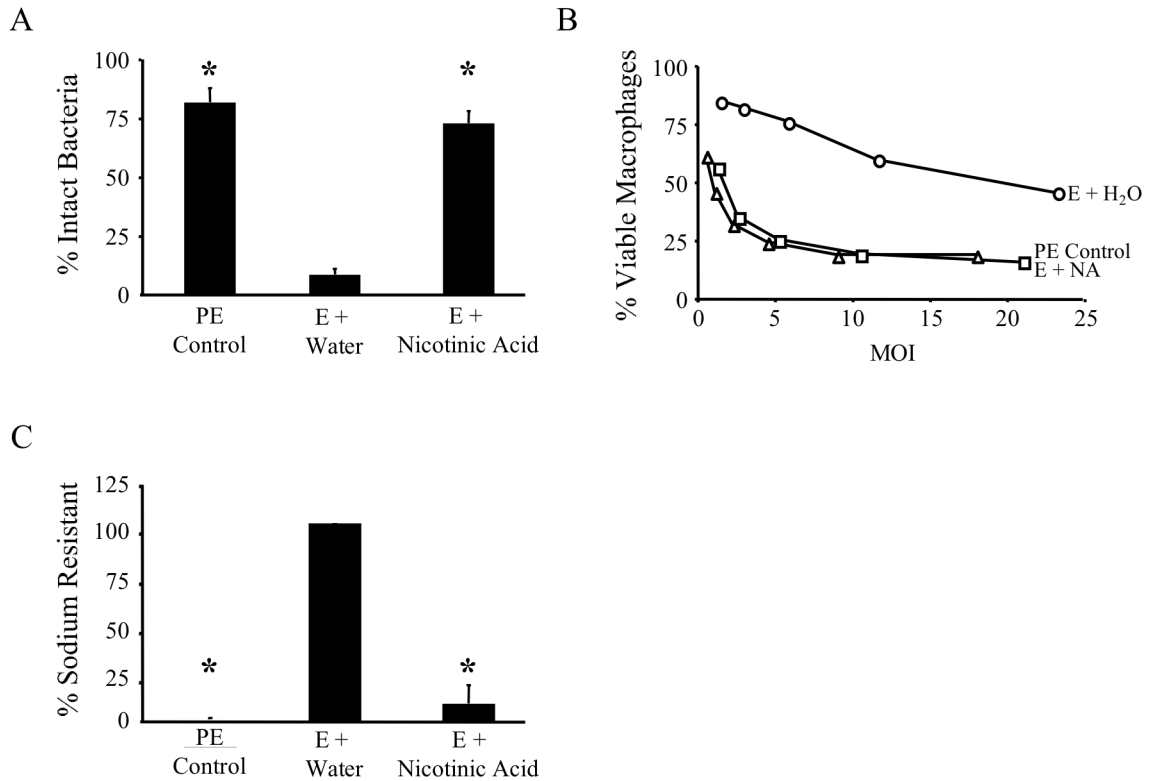
Figure 4.2. Nicotinic acid supplementation of WT *L. pneumophila* induces the early expression of multiple transmissive phase phenotypes.
(A) Lysosome evasion was determined by culturing *L. pneumophila* strains for 2 h with macrophages at an MOI = 1, and then quantifying the percent of intact bacteria by fluorescence microscopy.   Displayed are the means from duplicate samples in three independent experiments.   Error bars indicate SD, and asterisks designate significant differences (P<0.01) when compared to water control. (B) Macrophage viability was assessed by quantifying the reduction of the colorimetric dye alamarBlue™ following a 1-hour incubation of macrophages with PE cultures (triangles) or E cultures supplemented with water (H_2O; circles) or nicotinic acid (NA; squares).   Shown is a representative graph from three independent experiments preformed in triplicate.   (C) The percent of sodium resistant bacteria was measured by plating cultures on media with or without 100 mM NaCl, and then the viable CFU calculated as described (Byrne and Swanson, 1998).   Values shown = mean [(E + NA or PE control)/(E + H_2O) × 100%]. Error bars represent SD from duplicate samples in three independent experiments. Asterisks denote statistically significant differences (P<0.01) when compared to water control.

Figure 4.3

A

B
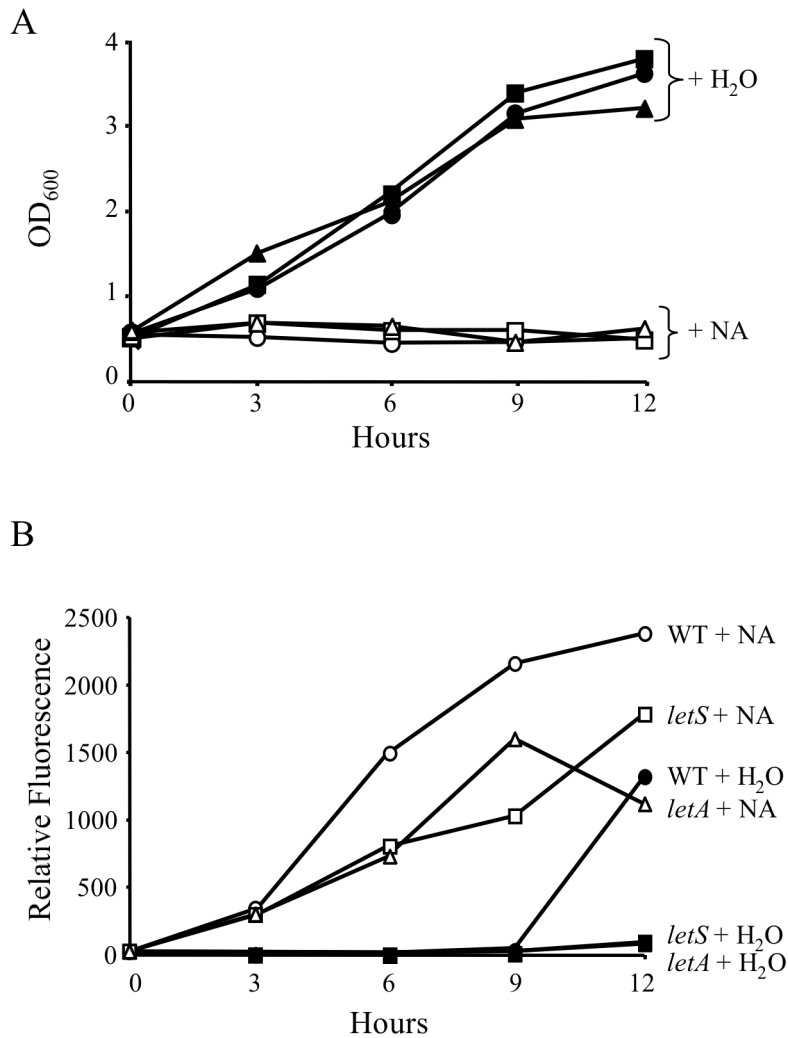
Figure 4.3. LetA/LetS is dispensable for growth inhibition, but required for full induction of motility following NA treatment.
WT (circles), *letA* (triangles) or *letS* (squares) *L. pneumophila* containing the *flaAgfp* reporter were grown to the E phase and then supplemented with water (closed symbols), or 10 mM NA (open symbols). Samples were collected and analyzed for OD_{600} (A) or fluorescence (B) at the times indicated. Shown are representative graphs from three independent experiments.

Table 4.1. Subset of genes induced in the PE phase as compared to the E phase

Family	Gene ID	Name	Paris ID	Lens ID	Gene product	FC[1]
Flagellum synthesis	*lpg1216*	*flgB*	*lpp1224*	*lpl1224*	flagellar basal-body rod protein FlgB	1.7
	lpg1217	*flgC*	*lpp1225*	*lpl1225*	flagellar basal-body rod protein FlgC	2.5
	lpg1219	*flgE*	*lpp1227*	*lpl1227*	flagellar hook protein FlgE	39.4
	lpg1784	*flhF*	*lpp1748*	*lpl1784*	flagellar biosynthesis protein FlhF	7.6
	lpg1221	*flgG*	*lpp1229*	*lpl1229*	flagellar biosynthesis protein FlgG	4.5
	lpg1222	*flgH*	*lpp1230*	*lpl1230*	flagellar L-ring protein precursor FlgH	4.3
	lpg1785	*flhA*	*lpp1749*	*lpl1749*	flagellar biosynthesis protein flhA	1.8
	lpg1761	*fliE*	*lpp1725*	*lpl1725*	flagellar hook-basal body complex protein FliE	2.6
	lpg1760	*fliF*	*lpp1724*	*lpl1724*	flagellar M-ring protein FliF	2.2
	lpg1759	*fliG*	*lpp1723*	*lpl1723*	flagellar motor switch protein FliG	2.2
	lpg1758	*fliH*	*lpp1722*	*lpl1722*	polar flagellar assembly protein FliH	2.0
	lpg1757	*fliI*	*lpp1721*	*lpl1721*	flagellum-specific ATP synthase FliI	1.6
	lpg1791	*fliN*	*lpp1755*	*lpl1755*	flagellar motor switch protein FliN	2.0
	lpg1789	*fliP*	*lpp1753*	*lpl1753*	flagellar biosynthetic protein FliP	1.7
	lpg1781	*motA1*	*lpp1745*	*lpl1745*	flagellar motor protein MotA	6.7
	lpg2962	-	*lpp3034*	*lpl2892*	similar to sodium-type flagellar protein MotY	6.5
Regulation	*lpg1284*	*rpoS*	*lpp1247*	*lpl1247*	RNA polymerase sigma factor RpoS (sigma 38)	1.9
	lpg1577	*rpoE*	*lpp1535*	*lpl1448*	sigma factor RpoE (sigma 24)	3.0
	lpg0537	*letE*	*lpp0602*	*lpl0583*	transmission trait enhancer protein LetE	1.8
	lpg1457	*relA*	*lpp1413*	*lpl1571*	GTP pyrophosphokinase	1.7
	lpg0853	*fleQ*	*lpp0915*	*lpl0884*	transcriptional regulator FleQ	1.9
	lpg0891	-	*lpp0952*	*lpl0922*	regulatory protein (GGDEF and EAL domains)	12.7
	lpg2655	-	*lpp2708*	*lpl2581*	sensory box protein (EAL and GGDEF domains)	2.9
	lpg0879	-	*lpp0942*	*lpl0912*	two-component response regulator (GGDEF domain)	2.3
	lpg1357	-	*lpp1311*	*lpl1308*	regulatory protein (GGDEF and EAL domains)	1.8
	lpg1173	*pilS*	*lpp1175*	*lpl1181*	sensor protein PilS	3.3
	lpg1762	*fleR*	*lpp1726*	*lpl1726*	similar to two-component response regulator	2.4
	lpg0714	-	*lpp0780*	*lpl0751*	similar to two-component sensor histidine kinase	1.6
	lpg2723	-	*lpp2780*	-	similar to transcriptional regulator - ArsR family	3.8
	lpg0280	-	*lpp0355*	*lpl0332*	similar to transcriptional regulator lysR family	1.7
Virulence	*lpg0453*	*icmC/dotE*	*lpp0519*	*lpl0495*	icmC/dotE	2.2
	lpg0445	*icmP/dotM*	*lpp0511*	*lpl0487*	icmP/dotM	2.4
	lpg0443	*icmR*	*lpp0509*	*lpl0485*	icmR	2.3
	lpg0442	*icmS*	*lpp0508*	*lpl0484*	icmS	2.1
	lpg0441	*icmT*	*lpp0507*	*lpl0483*	icmT	3.9
	lpg2687	*icmV*	*lpp2741*	*lpl2614*	icmV	1.9
	lpg0472	*dotV*	*lpp0537*	*lpl0513*	dotV	2.1
	lpg2391	*sdbC*	*lpp2458*	*lpl2315*	SdbC proteins - substrate of the Dot/Icm system	2.3
Involved in PHB synthesis	*lpg0560*	*phaB1*	*lpp0620*	*lpl0603*	acetoacetyl-CoA reductase	2.3
	lpg0561	*phaB2*	*lpp0621*	*lpl0604*	acetoacetyl-CoA reductase	1.9
Transporters	*lpg0610*	-	*lpp0661*	*lpl0645*	similar to major facilitator family transporter	3.8
	lpg1893	-	*lpp1860*	*lpl1855*	similar to major facilitator family transporter	2.6
	lpg1404	-	*lpp1359*	*lpl1355*	similar to major facilitator family transporter	2.0
	lpg2237	*abcT3*	*lpp2190*	*lpl2163*	similar to multidrug resistance ABC transporter	3.3
	lpg1008	*helA*	*lpp2371*	*lpl1046*	similar to cation efflux system protein CzcA	1.8
	lpg2481	-	*lpp2545*	*lpl2401*	membrane protein- similar to metabolite efflux pump	2.8
	lpg2178	*mexF2*	*lpp2130*	*lpl2104*	similar to RND multidrug efflux transporter	2.5
	lpg2193	-	*lpp2142*	*lpl2117*	similar to sulfate transporters	2.0
	lpg1063	*proP6*	*lpp1082*	*lpl1060*	proline/betaine transporter	1.7
	lpg1007	*helB*	*lpp2372*	*lpl1045*	cation efflux system HelB	1.7
	lpg0430	-	*lpp0497*	*lpl0473*	similar to multidrug resistance efflux pump	1.6
	lpg1479	-	*lpp1435*	*lpl1549*	similar to potassium efflux system kefA	1.6
	lpg0231	-	*lpp0301*	*lpl0284*	similar to cation transport ATPase	1.6
	lpg0949	-	*lpp1011*	*lpl0978*	predicted membrane protein- similar to transporter	1.6

[1] Fold Change (FC)

Table 4.2. Genes induced by 5 mM NA when compared to PE *L. pneumophila*

Gene ID	Name	Paris ID	Lens ID	Description	FC[1]
lpg0273	-	*lpp0347*	*lpl0325*	similar to transporter of the major facilitator superfamily (MFS)	35.0
lpg0272	-	*lpp0346*	*lpl0324*	cysteine transferase	9.3
lpg1121	-	*lpp1121*	*lpl1126*	unknown	6.1
lpg0689	-	*lpp0744*	*lpl0725*	weakly similar to DNA-binding ferritin-like protein (oxidative damage protectant)	5.0
lpg2350	-	*lpp2299*	*lpl2272*	similar to alkyl hydroperoxide reductase AhpC	4.8
lpg0436	*legA11*	*lpp0503*	*lpl0479*	ankyrin repeat protein	4.6
lpg1697	-	*lpp1662*	*lpl1656*	conserved hypothetical protein	3.6
lpg1230	-	*lpp1038*	*lpl1003*	similar to conserved hypothetical protein	3.5
lpg2392	*legL6*	*lpp2459*	*lpl2316*	leucine-rich repeat-containing protein	3.5
lpg2217	-	*lpp2169*	*lpl2142*	similar to chitinase	3.3
lpg0213	-	*lpp0272*	*lpl0267*	similar to membrane protein LrgB	3.1
lpg2315	-	*lpp2263*	*lpl2235*	unknown	3.0
lpg1136a[2]	-	*lpp1138*	*lpl1143*	unknown	2.9
lpg2166	-	*lpp2104*	*lpl2093*	unknown	2.9
lpg1716	-	*lpp1681*	*lpl1675*	unknown	2.8
lpg2621	-	*lpp2674*	*lpl2544*	similar to acid phosphatase- class B	2.7
lpg1489	-	*lpp1445*	*lpl1539*	unknown	2.7
lpg1966a[2]	-	*lpp1948*	*lpl1937*	unknown	2.6
lpg0075	-	*lpp0089*	*lpl0077*	similar to conserved hypothetical protein	2.4
lpg0086	-	*lpp0100*	*lpl0085*	putative membrane protein	2.4
lpg2762	-	*lpp2810*	*lpl2679*	unknown	2.3
lpg0044	-	*lpp0045*	-	similar to sterol desaturase	2.3
lpg0750	*hisH*	*lpp0816*	*lpl0787*	similar to imidazole glycerol phosphate synthase subunit HisH	2.3
lpg0171	*legU1*	*lpp0233*	*lpl0234*	protein with a F-box domain	2.2
lpg1550	-	*lpp1507*	*lpl1476*	conserved hypothetical protein	2.2
lpg0986	-	*lpp1057*	*lpl1019*	putative membrane protein similar to conserved hypothetical protein	2.2
lpg2414	-	*lpp2483*	*lpl2338*	unknown	2.2
lpg2665	-	*lpp2719*	*lpl2592*	similar to dienelactone hydrolase family protein	2.1
lpg0454	*icmD/dotP*	*lpp0520*	*lpl0496*	icmD/dotP	2.1
lpg2813	*vipE*	*lpp2865*	*lpl2728*	vipE	2.1
lpg0098	-	*lpp0112*	*lpl0098*	two-component sensor and regulator, histidine kinase response regulator	2.1
lpg0722	-	*lpp0788*	*lpl0759*	unknown	2.0
lpg2353	*yrfE*	*lpp2302*	*lpl2275*	similar to MutT/nudix family protein	2.0
lpg1631	-	*lpp1601*	-	similar to 3-oxoacyl-[acyl-carrier-protein] synthase III	2.0
lpg1124	-	*lpp1125*	*lpl1129*	unknown	2.0
lpg2937	*fum*	*lpp3005*	*lpl2866*	fumarate hydratase- class II	2.0
lpg1710	-	*lpp1675*	*lpl1669*	weakly similar to cytochrome c5	2.0
lpg2850	-	*lpp2908*	*lpl2762*	similar to cold shock protein	1.9
lpg1580	-	*lpp1538*	*lpl1445*	some similarities to cytochrome B561	1.9
lpg0286	-	*lpp0362*	*lpl0338*	similar to oxidoreductase- short chain dehydrogenase/reductase family	1.9
lpg0154	-	*lpp0218*	*lpl0215*	unknown	1.9
lpg2218	-	*lpp2170*	*lpl2143*	similar to choline monooxygenase	1.9
lpg2600	-	*lpp2653*	*lpl2523*	similar to membrane bound acyltransferase	1.9
lpg0301	-	*lpp0379*	*lpl0354*	similar to eukaryotic proteins	1.8
lpg1927	-	*lpp1902*	*lpl1891*	similar to conserved hypothetical protein	1.8
lpg1147	-	*lpp1149*	*lpl1153*	similar to acetyltransferase	1.8
lpg0819	-	*lpp0038*	-	similar to transposase (IS4 family)	1.8
lpg0526	-	*lpp0591*	*lpl0572*	unknown	1.8
lpg1212	-	*lpp1214*	*lpl1220*	similar to transcriptional regulator- MarR family	1.8
lpg2194	-	*lpp2143*	*lpl2118*	similar to carbonic anhydrase proteins	1.8
lpg1390	-	*lpp1345*	*lpl1341*	unknown	1.8
lpg0374	-	*lpp0441*	*lpl0417*	unknown	1.7
lpg1735	*gatC*	*lpp1700*	*lpl1699*	glutamyl-tRNA (Gln) amidotransferase (subunit C)	1.7
lpg0677	-	*lpp0733*	*lpl0713*	unknown	1.7
lpg2198	-	*lpp2148*	*lpl2122*	similar to transporters	1.7

Gene ID	Name	Paris ID	Lens ID	Description	FC[1]
lpg2929	*panD*	*lpp2996*	*lpl2856*	aspartate-1-decarboxylase	1.7
lpg2889	*gidA2*	*lpp2948*	*lpl2802*	highly simislar to glucose-inhibited division protein A GidA	1.7
lpg1896	*ychJ*	*lpp1865*	*lpl1860*	similar to hypothetical protein	1.7
lpg0455	*icmJ/dotN*	*lpp0521*	*lpl0497*	icmJ/dotN	1.7
lpg2398	-	*lpp2464*	*lpl2321*	similar to aminoglycoside 6-N-acetyltransferase	1.7
lpg2008	-	*lpp1989*	*lpl1984*	similar to putative endoribonuclease L-PSP	1.7
lpg2970	-	*lpp3042*	*lpl2900*	similar to glycerophosphoryl diester phosphodiesterase (ATA start codon)	1.6
lpg1679	-	*lpp1651*	*lpl1644*	similar to hypothetical proteins	1.6
lpg0588	*pyrB*	*lpp0638*	*lpl0622*	similar to aspartate carbamoyltransferase	1.6
lpg0554	*dinP*	*lpp0614*	*lpl0597*	similar to DNA damage inducible protein P	1.6
lpg0627	*pilE3*	*lpp0681*	*lpl0664*	type-IV pilin	1.6
lpg2648	*cinA*	*lpp2701*	*lpl2573*	belong to the CinA protein family	1.6
lpg2877	-	*lpp2936*	*lpl2790*	unknown	1.6
lpg1204	*pyrE*	*lpp1206*	*lpl1212*	orotate phosphoribosyltransferase	1.6
lpg2014	-	*lpp1996*	*lpl1991*	similar to conserved hypothetical protein	1.5
lpg1488	*legC5*	*lpp1444*	*lpl1540*	unknown	1.5
lpg0543	*prsA*	*lpp0607*	*lpl0588*	ribose-phosphate pyrophosphokinase	1.5
lpg0877	-	*lpp0940*	*lpl0910*	similar to uncharacterized proteins	1.5
lpg2413	-	*lpp2482*	*lpl2337*	unknown	1.5
lpg1824	-	*lpp1787*	*lpl1788*	similar to acyl-CoA dehydrogenase	1.5
lpg1858	*hubB*	*lpp1826*	*lpl1822*	similar to DNA-binding protein HU-beta	1.5
lpg0882	-	*lpp0944*	*lpl0914*	predicted transmembrane protein	1.5
lpg1850	-	*lpp1817*	*lpl1816*	hypothetical protein (rhodanese domain)	1.5
lpg1835	-	*lpp1798*	*lpl1799*	29 kDa immunogenic protein	1.5
lpg0534	*sucC*	*lpp0599*	*lpl0580*	succinyl-CoA synthetase- beta subunit	1.5
lpg0274	-	*lpp0348*	*lpl0326*	transcriptional regulator, LysR family	1.5
lpg1954	-	*lpp1936*	-	unknown	1.5
lpg2623	-	*lpp2676*	*lpl2548*	unknown membrane protein	1.5
lpg2358	*rpsU*	*lpp2307*	*lpl2280*	30S ribosomal protein S21	1.5
lpg1364	*glnA*	*lpp1318*	*lpl1315*	glutamine synthetase	1.5

[1] Fold Change (FC)

Table 4.3. Genes repressed by 5 mM NA when compared to PE *L. pneumophila*

Gene ID	Name	Paris ID	Lens ID	Description	FC Ratio[1]
lpg0913	-	*lpp0974*	*lpl0944*	MraZ protein	-3.4
lpg1763	*flrB*	*lpp1727*	*lpl1727*	similar to sensor histidine kinase	-3.0
lpg2328	-	*lpp2276*	*lpl2248*	unknown- N-terminal similar to *Legionella* 33 kDa polypeptide	-2.7
lpg2517	-	*lpp2585*	*lpl2439*	similar to transcriptional regulator of the Lrp family	-2.6
lpg0097	-	*lpp0111*	*lpl0097*	similar to unknown protein- truncated	-2.4
lpg2045	-	*lpp2028*	*lpl2023*	similar to ABC-type transport system used for resistance to organic solvents	-2.4
lpg2675	*dotC*	*lpp2729*	*lpl2602*	defect in organelle trafficking lipoprotein DotC	-2.3
lpg2514	*lprN*	*lpp2582*	-	similar to outer membrane efflux protein (RND multidrug efflux)	-2.3
lpg1792	*fliM*	*lpp1756*	*lpl1756*	flagellar motor switch protein FliM	-2.2
lpg0449	*icmL/dotI*	*lpp0515*	*lpl0491*	icmL/dotI	-2.1
lpg1320	*lspD*	*lpp1275*	*lpl1274*	type II protein secretion LspD	-2.1
lpg0451	*icmE/dotG*	*lpp0517*	*lpl0493*	icmE/dotG	-2.1
lpg2703	*petC*	*lpp2758*	*lpl2631*	similar to ubiquinol-cytochrome c oxydoreductase- cytochrome c1	-2.1
lpg0979	*aacA42*	-	-	aminoglycoside N(6')acetyltransferase, similar to *aacA41*	-2.1
lpg0447	*lphA/dotK*	*lpp0513*	*lpl0489*	lphA/dotK	-2.1
lpg0092	*rnr/lidP, vacB*	*lpp0106*	*lpl0091*	similar to exoribonuclease RNase R	-2.0
lpg0920	-	*lpp0981*	*lpl0951*	phosphatidylglycerophosphatase B	-2.0
lpg0660	-	*lpp0715*	*lpl0697*	similar to ABC transporter (permease)	-2.0
lpg1063	*proP6*	-	*lpl1060*	proline/betaine transporter ProP6	-2.0
lpg0448	*icmM/dotJ*	*lpp0514*	*lpl0490*	icmM/dotJ	-2.0
lpg0895	-	*lpp0956*	*lpl0926*	unknown	-2.0
lpg0950	-	*lpp1012*	*lpl0979*	similar to hydrolase	-2.0
lpg1681	-	*lpp1654*	*lpl1647*	unknown	-1.9
lpg2698	*amiB*	*lpp2753*	*lpl2626*	similar to N-acetylmuramoyl-L-alanine amidase	-1.9
lpg1706	*astA*	*lpp1671*	*lpl1665*	arginine N-succinyltransferase- beta chain	-1.9
lpg0552	*sugE*	*lpp0613*	*lpl0595*	similar to suppressor of groEL	-1.9
lpg0175	-	*lpp0237*	*lpl0237*	similar to pyoverdine biosynthesis protein PvcB	-1.9
lpg0957	-	*lpp1019*	*lpl0986*	similar to hypothetical protein	-1.9
lpg2439	-	*lpp2506*	*lpl2360*	similar to conserved hypothetical protein	-1.9
lpg0093	-	*lpp0107*	*lpl0092*	similar to RNA methyltransferase	-1.9
lpg1006	*helC*	*lpp2373*	*lpl1044*	efflux protein presumed to function with HelB and HelA	-1.9
lpg0002	*dnaN*	*lpp0002*	*lpl0002*	DNA polymerase III- beta chain	-1.9
lpg1788	*fliQ*	*lpp1752*	*lpl1752*	flagellar biosynthetic protein FliQ	-1.8
lpg0025	*rcp*	*lpp0025*	*lpl0026*	Rcp protein- confers resistance to cationic antimicrobial peptides and promotes intracellular infection	-1.8
lpg1652	*iolG*	*lpp1623*	*lpl1618*	similar to myo-inositol 2-dehydrogenase	-1.8
lpg0766	-	*lpp0831*	*lpl0807*	unknown	-1.8
lpg1557	*pabB*	*lpp1514*	*lpl1469*	similar to para-aminobenzoate synthase- component I	-1.8
lpg0831	-	*lpp0893*	*lpl0862*	similar to flavin-containing monooxygenases	-1.8
lpg2802	-	*lpp2848*	*lpl2717*	similar to DnaA- ATPase involved in DNA replication initiation	-1.8
lpg1707	*aruD*	*lpp1672*	*lpl1666*	succinylglutamic semialdehyde dehydrogenase	-1.8
lpg0247	-	*lpp0317*	*lpl0301*	unknown	-1.8
lpg2809	*pepN2*	*lpp2855*	*lpl2724*	aminopeptidase N	-1.8
lpg0466	*dcoA*	*lpp0531*	*lpl0507*	oxaloacetate decarboxylase alpha-chain	-1.8
lpg1730	*ugpE*	*lpp1695*	*lpl1694*	similar to glycerol-3-phosphate ABC transporter- permease component	-1.8
lpg0932	*aroK*	*lpp0994*	*lpl0963*	shikimate kinase I	-1.8
lpg0828	-	*lpp0890*	*lpl0859*	similar to unknown proteins	-1.8
lpg1459	*yfdZ*	*lpp1415*	*lpl1569*	similar to putative aminotransferase	-1.8
lpg0699	-	*lpp0754*	*lpl0736*	similar to outer membrane protein TolC	-1.8
lpg2980	*parC*	*lpp3051*	*lpl2908*	DNA topoisomerase IV- A subunit	-1.8
lpg2175	-	*lpp2127*	*lpl2101*	similar to hypothetical hydrolase proteins	-1.7

Gene ID	Name	Paris ID	Lens ID	Description	FC Ratio[1]
lpg1426	-	lpp1381	lpl1377	unknown	-1.7
lpg1416	-	lpp1371	lpl1367	similar to purine nucleoside phosphorylase proteins	-1.7
lpg0964	-	lpp1026	lpl0993	membrane protein- similar to 4-hydroxybenzoate octaprenyltranferase	-1.7
lpg2340	kdtA	lpp2288	lpl2261	3-deoxy-D-manno-oct-2-ulosonic acid transferase/LPS core biosynthesis	-1.7
lpg1867	-	lpp1832	lpl1829	similar to site specific recombinase- phage integrase family	-1.7
lpg2782	nuoH	lpp2829	lpl2698	NADH-quinone oxidoreductase chain H	-1.7
lpg2448	-	-	-	transposase, ISSod6	-1.7
lpg1432	-	lpp1387	lpl1609	similar to oxidase	-1.7
lpg0283	-	lpp0359	lpl0335	similar to NAD+-dependent formate dehydrogenase	-1.7
lpg1766	ftsK	lpp1730	lpl1730	similar to cell division protein FtsK	-1.7
lpg2029	folB	lpp2011	lpl2006	similar to dihydroneopterin aldolase	-1.7
lpg2892	parB2	lpp2951	lpl2805	similar to chromosome partitioning protein parB	-1.7
lpg0255	-	lpp0325	lpl0308	similar to outer membrane protein	-1.7
lpg1533	ydgR	lpp1490	lpl1493	similar to peptide transport proteins	-1.7
lpg2858	-	lpp2916	lpl2770	similar to unknown protein	-1.7
lpg1334	-	lpp1288	lpl1287	similar to 2-methylthioadenine synthetase	-1.7
lpg2678	-	lpp2732	lpl2605	similar to unknown protein	-1.7
lpg1293	ispZ	lpp1256	lpl1255	similar to intracellular septation protein	-1.7
lpg2341	djlA	lpp2289	lpl2262	similar to DnaJ-like protein	-1.7
lpg0742	-	lpp0807	lpl0778	similar to unknown proteins	-1.7
lpg2033	recG1	lpp2015	lpl2010	ATP-dependent DNA helicase RecG	-1.7
lpg2734	-	lpp2790	lpl2659	similar to signal transduction histidine kinase	-1.6
lpg2618	murF	lpp2671	lpl2541	UDP-N-acetylmuramoyl-tripeptide-D-alanyl-D-alanine ligase	-1.6
lpg1789	fliP	lpp1753	lpl1753	flagellar biosynthetic protein FliP	-1.6
lpg0264	-	lpp0335	lpl0316	weakly similar to amidase	-1.6
lpg2731	-	lpp2788	lpl2657	putative response regulator	-1.6
lpg0956	-	lpp1018	lpl0985	unknown	-1.6
lpg0774	-	lpp0839	lpl0815	unknown	-1.6
lpg2832	-	lpp2889	lpl2744	unknown	-1.6
lpg2854	-	lpp2912	lpl2766	hypothetical tetratricopeptide repeat protein	-1.6
lpg0692	dppF	lpp0747	lpl0728	similar to ABC transporter ATP-binding protein	-1.6
lpg0141	prlC	lpp0156	lpl0141	oligopeptidase A	-1.6
lpg0681	-	-	lpl0718	putative lipoprotein	-1.6
lpg1276	-	lpp1239	lpl1239	similar to electron transfer flavoprotein-ubiquinone oxidoreductase	-1.6
lpg2596	-	lpp2649	lpl2519	similar to unknown protein	-1.6
lpg1608	-	lpp1573	-	similar to MutT/nudix family protein	-1.6
lpg0174	pvcA	lpp0236	lpl0236	similar to pyoverdine biosynthesis protein PvcA	-1.6
lpg2072	-	-	-	unknown	-1.6
lpg2379	-	-	-	unknown	-1.6
lpg2620	smc	lpp2673	lpl2543	similar to chromosome partition protein smc	-1.6
lpg2825	-	lpp2321 lpp2878	lpl1057 lpl2740	similar to cold shock protein	-1.6
lpg0187	-	lpp0248	-	similar to Zn metalloprotein	-1.6
lpg0450	icmK/dotH	lpp0516	lpl0492	icmK/dotH	-1.6
lpg2031	argS	lpp2013	lpl2008	arginine tRNA synthetase	-1.6
lpg2252	-	lpp2206	lpl2178	similar to glutamine synthase	-1.6
lpg1506	-	lpp1463	lpl1520	putative membrane protein	-1.6
lpg2697	mutL	lpp2752	lpl2625	DNA mismatch repair protein MutL	-1.6
lpg0929	pilO	lpp0991	lpl0960	Tfp pilus assembly protein PilO	-1.6
lpg1562	merA	lpp1519	lpl1464	putative pyruvate/2-oxoglutarate dehydrogenase complex- dihydrolipoamide dehydrogenase (E3) component	-1.6
lpg0514	-	-	lpl0552	unknown	-1.6
lpg2044	-	lpp2027	lpl2022	similar to conserved hypothetical protein	-1.6
lpg1675	purC	lpp1647	lpl1640	phosphoribosylamidoimidazole-succinocarboxamide synthase	-1.6

Gene ID	Name	Paris ID	Lens ID	Description	FC Ratio[1]
lpg0106	-	*lpp0120*	*lpl0106*	similar to putative xanthine/uracil permeases	-1.6
lpg0708	-	*lpp0763*	*lpl0745*	weakly similar to *L. pneumophila* IcmL protein	-1.6
lpg0426	*cspD*	*lpp0493*	*lpl0469*	similar to cold shock-like protein CspD	-1.5
lpg0914	*mraW*	*lpp0975*	*lpl0945*	similar to S-adenosyl-methyltransferase MraW	-1.5
lpg2875	*glmU*	*lpp2934*	*lpl2788*	bifunctional- UDP-N-acetylglucosamine pyrophosphorylase and glucosamine-1-phosphate N-acetyltransferase	-1.5
lpg0117	*gcvH*	*lpp0131*	*lpl0116*	similar to glycine cleavage system H protein	-1.5
lpg1417	*gyrA*	*lpp1372*	*lpl1368*	DNA gyrase- subunit A- type II topoisomerase	-1.5
lpg1836[a]	-	*lpp1800*	*lpl1801*	unknown	-1.5
lpg1188	*kup21*	*lpp1190*	*lpl1196*	similar to low affinity potassium transport system protein Kup	-1.5
lpg0746	*iraB*	*lpp0812*	*lpl0783*	di/tripeptide transporter homolog IraB iron acquisition	-1.5
lpg1794	-	*lpp1758*	*lpl1758*	similar to oxidoreductase	-1.5
lpg0947	-	*lpp1009*	*lpl0976*	similar to 2-oxoglutarate ferredoxin oxidoreductase alpha subunit	-1.5
lpg0224	-	*lpp0283*	*lpl0278*	similar to toxin secretion ABC transporter ATP-binding protein	-1.5
lpg0925	*ponA*	*lpp0987*	*lpl0956*	similar to peptidoglycan synthetase; penicillin-binding protein 1A	-1.5
lpg1425	*pyrF*	*lpp1380*	*lpl1376*	orotidine 5`-phosphate decarboxylase	-1.5
lpg1626	-	*lpp1596*	*lpl1397*	putative copper efflux ATPase	-1.5
lpg2866	*priA*	*lpp2924*	*lpl2778*	primosomal protein N (replication factor Y)	-1.5
lpg0483	*legA12*	*lpp0547*	*lpl0523*	protein with ankyrin domain	-1.5
lpg2797	*rrmJ*	*lpp2843*	*lpl2712*	ribosomal RNA large subunit methyltransferase (cell division protein FtsJ)	-1.5
lpg0916	*pbpB*	*lpp0977*	*lpl0947*	peptidoglycan synthetase FtsI precursor	-1.5
lpg0427	-	*lpp0494*	*lpl0470*	similar to N-terminus of diadenosine tetraphosphate (Ap4A) hydrolase	-1.5
lpg2842	-	*lpp2901*	*lpl2754*	similar to PhoH protein	-1.5
lpg2634	-	*lpp2687*	*lpl2559*	similar to aminopeptidase	-1.5
lpg0059	-	*lpp0062*	*lpl0061*	unknown	-1.5
lpg0813	*mreD*	*lpp0875*	*lpl0846*	rod shape-determining protein MreD	-1.5
lpg1035	*pcoA*	*lpp2345*	-	similar to copper efflux ATPase	-1.5
lpg2718	-	*lpp2775*	*lpl2646*	unknown	-1.5
lpg1868	-	*lpp1833*	*lpl1830*	similar to ABC transporter- ATP-binding protein	-1.5

[1] Fold Change (FC)

Figure 4.4.
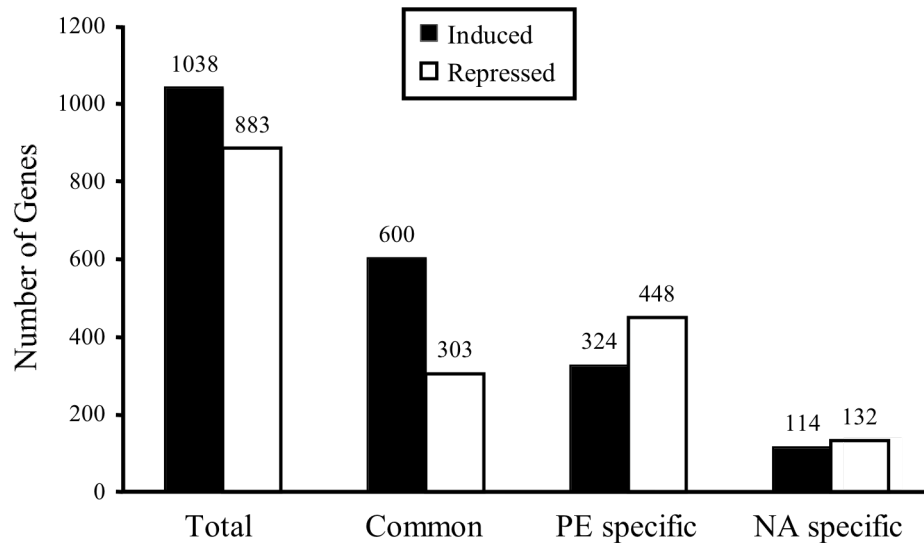
Figure 4.4. Comparison of genes regulated in the PE phase and NA-supplemented _L. pneumophila._
Black bars indicated genes with high levels of transcriptional activation, while white bars denote repressed genes. Together, 1038 are induced and 883 genes are repressed in both the PE phase and NA-treated E phase _L. pneumophila_. Transcriptional analysis indicates that only a subset of the regulated genes is shared between the two conditions tested. Specific to PE bacteria, 324 genes are highly activated, while 448 genes are repressed. Microarrays predict that 246 genes are uniquely regulated by NA following a 3 h treatment with the modulator.

Figure 4.5.
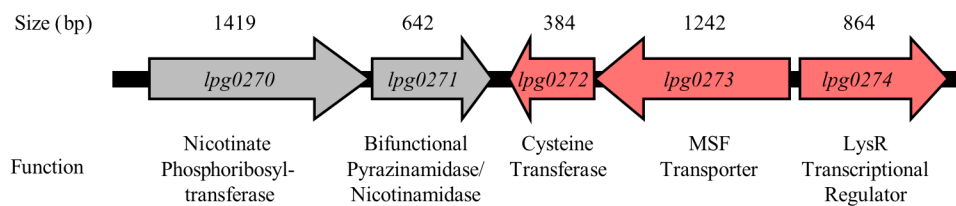
Figure 4.5. Region of the _L. pneumophila_ chromosome that contains _lpg0272-3._
Arrows indicate orientation of the genes. Sizes (bp) of the genes are indicated above, while the predicted function of each gene is listed below. Red indicates genes with significantly elevated expression levels when treated with 5 mM NA. Gray indicates genes that are not regulated by NA at 3 h.

Table 4.S1. Genes induced in PE phase as compared to E phase *L. pneumophila*

Gene ID	Name	Paris ID	Lens ID	Description	FC[1]
lpg1219	*flgE*	*lpp1227*	*lpl1227*	flagellar hook protein FlgE	39.4
lpg0891	-	*lpp0952*	*lpl0922*	regulatory protein (GGDEF and EAL domains)	12.7
lpg0623	-	*lpp0677*	*lpl0660*	unknown	7.8
lpg1784	*flhF*	*lpp1748*	*lpl1784*	flagellar biosynthesis protein FlhF	7.6
lpg0848	-	*lpp0910*	*lpl0879*	similar to conserved hypothetical protein	7.3
lpg2952	-	*lpp3023*	*lpl2881*	unknown	7.2
lpg1781	*motA1*	*lpp1745*	*lpl1745*	flagellar motor protein MotA	6.7
lpg2962	-	*lpp3034*	*lpl2892*	similar to sodium-type flagellar protein MotY	6.5
lpg0550	-	*lpp0611*	-	weakly similar to D-amino acid dehydrogenase- C-terminal cAMP binding motif	6.1
lpg0012	-	*lpp0012*	*lpl0012*	unknown	5.5
lpg0804	-	*lpp0866*	*lpl0837*	similar to hydrolase	5.5
lpg0871	-	*lpp0934*	*lpl0903*	unknown	5.5
lpg2324	-	*lpp2272*	*lpl2244*	L-gulono-gamma-lactone oxidase	4.9
lpg2818	-	*lpp2871*	*lpl2734*	similar to hypothetical protein	4.8
lpg0953	-	*lpp1015*	*lpl0982*	similar to long-chain-fatty-acid-CoA ligase	4.6
lpg1221	*flgG*	*lpp1229*	*lpl1229*	flagellar biosynthesis protein FlgG	4.5
lpg0034	-	*lpp0033*	*lpl0034*	unknown	4.5
lpg2210	-	*lpp2161*	*lpl2135*	unknown	4.4
lpg0426	*cspD*	*lpp0493*	*lpl0469*	similar to cold shock-like protein CspD	4.4
lpg1222	*flgH*	*lpp1230*	*lpl1230*	flagellar L-ring protein precursor FlgH	4.3
lpg2401	-	*lpp2466*	*lpl2324*	unknown	4.2
lpg0733	-	*lpp0799*	*lpl0770*	unknown	4.0
lpg0441	*icmT*	*lpp0507*	*lpl0483*	icmT	3.9
lpg0038	*legA10*	*lpp0037*	*lpl0038*	ankyrin repeat-containing protein	3.9
lpg2723	-	*lpp2780*	-	similar to transcriptional regulator- ArsR family	3.8
lpg0469	-	*lpp0534*	*lpl0510*	endonuclease/exonuclease/phosphatase family protein	3.8
lpg0610	-	*lpp0661*	*lpl0645*	similar to major facilitator family transporter	3.8
lpg2333	-	*lpp2281*	*lpl2253*	similar to membrane-associated metalloprotease proteins	3.7
lpg1752	-	*lpp1716*	*lpl1716*	unknown	3.5
lpg1660	*legL3*	*lpp1631*	*lpl1625*	leucine-rich repeat-containig protein	3.5
lpg1173	*pilS*	*lpp1175*	*lpl1181*	sensor protein PilS	3.3
lpg0915	-	*lpp0976*	*lpl0946*	similar to cell division transmembrane protein FtsL	3.3
lpg2385	-	*lpp2447*	*lpl2303*	some similarity with eukaryotic proteins	3.3
lpg2237	*abcT3*	*lpp2190*	*lpl2163*	similar to multidrug resistance ABC transporter ATP-binding protein	3.3
lpg1667	-	*lpp1638*	*lpl1632*	unknown	3.3
lpg1183	-	*lpp1186*	*lpl1192*	unknown	3.2
lpg0236	-	*lpp0306*	*lpl0290*	unknown	3.2
lpg1427	-	*lpp1382*	*lpl1378*	similar to short-chain dehydrogenase	3.2
lpg0883	-	*lpp0945*	*lpl0915*	unknown	3.1
lpg2038	-	*lpp2021*	*lpl2016*	similar to cell division protein ftsB homolog	3.0
lpg1577	*rpoE*	*lpp1535*	*lpl1448*	sigma factor RpoE (sigma 24)	3.0
lpg2186	*pksJ*	*lpp2136*	*lpl2111*	polyketide synthase, type I	2.9
lpg2655	-	*lpp2708*	*lpl2581*	sensory box protein, EAL and GGDEF domain	2.9
lpg1293	*ispZ*	*lpp1256*	*lpl1255*	intracellular septation protein A	2.9
lpg1146	-	*lpp1148*	*lpl1152*	similar to thermostable carboxypeptidase 1	2.8
lpg0824	-	*lpp0886*	*lpl0855*	rhomboid family protein	2.8
lpg1044	-	*lpp2337*	-	similar to NADH oxidoreductase	2.8
lpg1108	-	*lpp1108*	*lpl1108*	putative lipase	2.8
lpg2481	-	*lpp2545*	*lpl2401*	integral membrane protein- similar to metabolite efflux pump	2.8
lpg2681	-	*lpp2735*	*lpl2608*	similar to aldolase	2.8
lpg0609	*alaS*	*lpp0660*	*lpl0644*	similar to a domain of alanyl-tRNA synthetase	2.8
lpg1750	*clpB*	*lpp1714*	*lpl1714*	endopeptidase Clp ATP-binding chain B (ClpB)	2.7
lpg2016	-	*lpp1998*	*lpl1993*	hypothetical gene, YGGT family protein	2.7
lpg2953	-	*lpp3024*	*lpl2882*	unknown	2.7

Gene ID	Name	Paris ID	Lens ID	Description	FC[1]
lpg2410	-	*lpp2479*	*lpl2334*	similar to conserved hypothetical protein	2.7
lpg1176	-	*lpp1179*	*lpl1185*	Zn-dependent protease	2.6
lpg2530	*aroF*	*lpp2595*	*lpl2451*	phospho-2-dehydro-3-deoxyheptonate aldolase	2.6
lpg1893	-	*lpp1860*	*lpl1855*	similar to major facilitator family transporter (MFS)	2.6
lpg1056	-	*lpp2325*	*lpl1053*	guanylate cyclase	2.6
lpg2851	*hemG*	*lpp2909*	*lpl2763*	protoporphyrinogen oxidase	2.6
lpg2883	-	*lpp2942*	*lpl2796*	3-octaprenyl-4-hydroxybenzoate carboxy-lyase	2.6
lpg1761	*fliE*	*lpp1725*	*lpl1725*	flagellar hook-basal body complex protein	2.6
lpg2204	-	*lpp2155*	*lpl2129*	similar to alginate o-acetyltransferase AlgI	2.6
lpg0614	-	*lpp0665*	*lpl0649*	similar to hypothetical protein	2.6
lpg2348	*sodC*	*lpp2297*	*lpl2270*	superoxide dismutase [Cu-Zn] precursor	2.6
lpg1702	-	*lpp1667*	*lpl1661*	unknown	2.6
lpg0365	-	*lpp0430*	*lpl0406*	unknown	2.6
lpg0798	-	*lpp0860*	*lpl0831*	similar to unknown proteins	2.6
lpg0697	*sul1*	*lpp0752*	*lpl0734*	similar to inorganic transporter and to carbonic anhydrase (bi-functional)	2.6
lpg1745	-	*lpp1709*	*lpl1709*	similar to iron-sulpher cluster proteins NifU	2.5
lpg2733	-	*lpp2789*	*lpl2658*	putative membrane protein	2.5
lpg2837	-	*lpp2894*	*lpl2749*	phospholipase/lecithinase/hemolysin, lysophospholipase A, glycerophospholipid-cholesterol acyltransferase	2.5
lpg2178	*mexF2*	*lpp2130*	*lpl2104*	similar to RND multidrug efflux transporter	2.5
lpg2531	-	*lpp2596*	*lpl2452*	similar to chorismate mutase (N-terminal part)	2.5
lpg1217	*flgC*	*lpp1225*	*lpl1225*	flagellar basal-body rod protein FlgC	2.5
lpg0445	*icmP/dotM*	*lpp0511*	*lpl0487*	icmP/dotM	2.4
	-	*lpp2413*		weakly similar to serine/threonine protein kinase	2.4
lpg2405	*mutT*	*lpp2470*	*lpl2328*	mutator MutT protein	2.4
lpg0874	*pntB*	*lpp0937*	*lpl0907*	NAD(P) transhydrogenase subunit beta	2.4
lpg1762	*fleR*	*lpp1726*	*lpl1726*	similar to two-component response regulator	2.4
lpg1668	-	*lpp1639*	*lpl1633*	unknown	2.3
lpg2391	*sdbC*	*lpp2458*	*lpl2315*	SdbC proteins- putative substrate of the Dot/Icm system	2.3
lpg0560	*phaB1*	*lpp0620*	*lpl0603*	acetoacetyl-CoA reductase	2.3
lpg2225	-	*lpp2176*	*lpl2150*	similar to other proteins	2.3
lpg0443	*icmR*	*lpp0509*	*lpl0485*	icmR	2.3
lpg2532	*aspB*	*lpp2598*	*lpl2454*	similar to aspartate aminotransferase	2.3
lpg1150	-	*lpp1152*	*lpl1156*	similar to *E. coli* Ada protein (O-6-methylguanine-DNA methyltransferase)	2.3
lpg0879	-	*lpp0942*	*lpl0912*	two-component response regulator with GGDEF domain	2.3
lpg2239	-	*lpp2192*	-	unknown	2.3
lpg1054	*atpD1*	*lpp2328*		ATP synthase F1, beta chain	2.3
lpg2997	-	*lpp3068*	*lpl2925*	similar to alkane monooxygenase	2.2
lpg0823	-	*lpp0885*	*lpl0854*	hypothetical gene	2.2
lpg1413	*glpD*	*lpp1368*	*lpl1364*	glycerol-3-phosphate dehydrogenase	2.2
lpg2664	-	*lpp2718*	*lpl2591*	similar to biotin carboxylase (A subunit of acetyl-CoA carboxylase)	2.2
lpg1674	*purF*	*lpp1646*	*lpl1639*	amidophosphoribosyltransferase	2.2
lpg1130	*cyaA4*	*lpp1131*	*lpl1135*	adenylate cyclase	2.2
lpg0453	*icmC/dotE*	*lpp0519*	*lpl0495*	icmC/dotE	2.2
lpg2307	*grxC*	*lpp2255*	*lpl2226*	similar to glutaredoxin Grx	2.2
lpg1655	*lasB*	*lpp1626*	*lpl1620*	class 4 metalloprotease	2.2
lpg2298	*legC7*	*lpp2246*	*lpl2217*	inclusion membrane protein A	2.2
lpg1759	*fliG*	*lpp1723*	*lpl1723*	flagellar motor switch protein	2.2
lpg1890	*legLC8*	*lpp1857*	*lpl1852*	unknown	2.2
lpg1634	-	*lpp1604*	-	similar to oxidoreductase proteins	2.2
lpg1760	*fliF*	*lpp1724*	*lpl1724*	flagellar M-ring protein	2.2
lpg2195	-	*lpp2144*	*lpl2119*	hypothetical gene	2.2
lpg0246	-	*lpp0316*	*lpl0300*	unknown	2.2
lpg1900	-	*lpp1873*	*lpl1864*	unknown	2.2
lpg2424	-	*lpp2489*	*lpl2347*	unknown	2.2
lpg0803	-	*lpp0865*	*lpl0836*	similar to acyl-CoA dehydrogenase	2.2
lpg1568	*thiDE*	*lpp1526*	*lpl1457*	similar to phosphomethylpyrimidine kinase/thiamin-phosphate pyrophosphorylase	2.1
lpg1401	*pilZ*	*lpp1356*	*lpl1352*	similar to type 4 fimbrial biogenesis protein PilZ	2.1
lpg2874	-	*lpp2933*	*lpl2787*	unknown	2.1

Gene ID	Name	Paris ID	Lens ID	Description	FC[1]
lpg1136	-	*lpp1137*	*lpl1142*	similar to hypothetical protein	2.1
lpg2382	-	*lpp2444*	*lpl2300*	unknown	2.1
lpg0442	*icmS*	*lpp0508*	*lpl0484*	icmS	2.1
lpg1248	*virB9*	*lpp0177*	*lpl0159*	*Legionella* vir homologue protein	2.1
lpg1888	-	*lpp1855*	*lpl1850*	unknown	2.1
lpg0026	-	*lpp0026*	*lpl0027*	similar to amino acid permease	2.1
lpg1066	-	*lpp1085*	*lpl1063*	unknown	2.1
lpg0472	*dotV*	*lpp0537*	*lpl0513*	dotV	2.1
lpg1632	-	*lpp1602*	-	similar to glycosyltransferase	2.0
lpg1368	-	*lpp1322*	*lpl1319*	unknown	2.0
lpg0203	*yfhG*	*lpp0263*	*lpl0258*	similar to hypothetical protein	2.0
lpg1617	-	*lpp1587*	*lpl1406*	weakly similar to cytochrome C family proteins	2.0
lpg2048	-	*lpp2031*	*lpl2026*	unknown	2.0
lpg2436	-	*lpp2503*	*lpl2357*	putative membrane protein	2.0
lpg2682	-	*lpp2736*	*lpl2609*	similar to hypothetical proteins	2.0
lpg1758	*fliH*	*lpp1722*	*lpl1722*	polar flagellar assembly protein FliH	2.0
lpg2193	-	*lpp2142*	*lpl2117*	similar to sulfate transporters	2.0
lpg2806	-	*lpp2852*	*lpl2721*	unknown	2.0
lpg0262	-	*lpp0333*	*lpl0314*	bacteriophage-related DNA polymerase	2.0
lpg2828	-	*lpp2882*	*lpl2743*	unknown	2.0
lpg1791	*fliN*	*lpp1755*	*lpl1755*	flagellar motor switch protein FliN	2.0
lpg1404	-	*lpp1359*	*lpl1355*	similar to major facilitator membrane proteins	2.0
lpg0210	-	*lpp0269*	*lpl0264*	unknown	2.0
lpg1892	-	*lpp1859*	*lpl1854*	signal peptide predicted	2.0
lpg1450	-	*lpp1405*	-	similar to oxidoreductase	2.0
lpg1907	-	*lpp1882*	*lpl1871*	unknown	2.0
lpg1048	-	*lpp2334*	-	similar to ATP synthase alpha chain	2.0
lpg1169	-	*lpp1171*	*lpl1177*	similar to unknown protein	2.0
lpg0561	*phaB2*	*lpp0621*	*lpl0604*	acetoacetyl-CoA reductase	1.9
lpg0249	-	*lpp0319*	*lpl0303*	similar to fatty acid desaturase	1.9
lpg2019	-	*lpp2001*	*lpl1996*	similar to serine protease	1.9
lpg0663	-	*lpp0720*	*lpl0700*	similar to soluble lytic murein transglycosylase	1.9
lpg0853	*fleQ*	*lpp0915*	*lpl0884*	transcriptional regulator FleQ	1.9
lpg1721	*yfhC*	*lpp1686*	*lpl1685*	deaminase	1.9
lpg1322	*cyaA*	*lpp1277*	*lpl1276*	adenylate cyclase 1 protein	1.9
lpg2687	*icmV*	*lpp2741*	*lpl2614*	intracellular multiplication protein IcmV	1.9
lpg1722	*guaA*	*lpp1687*	*lpl1686*	similar to GMP synthetase (glutamine-hydrolyzing)	1.9
lpg0058	-	*lpp0061*	*lpl0060*	similar to glutaredoxin	1.9
lpg1891	-	*lpp1858*	*lpl1853*	similar to hypothetical protein	1.9
lpg1773	-	*lpp1737*	*lpl1737*	unknown	1.9
lpg0850	-	*lpp0912*	*lpl0881*	similar to conserved hypothetical protein	1.9
lpg1524	*pilD*	*lpp1481*	*lpl1502*	type 4 prepilin-like proteins leader peptide processing enzyme	1.9
lpg1297	*folD*	*lpp1261*	*lpl1260*	methylenetetrahydrofolate dehydrogenase/methenyltetrahydrofolate cyclohydrolase	1.9
lpg1284	*rpoS*	*lpp1247*	*lpl1247*	RNA polymerase sigma factor RpoS	1.9
lpg2491	-	*lpp2556*	*lpl2412*	similar to conserved hypothetical protein	1.9
lpg0217	*purK*	*lpp0276*	*lpl0271*	phosphoribosylaminoimidazole carboxylase- ATPase subunit	1.8
lpg1947	-	*lpp1930*	-	unknown	1.8
lpg2468	-	*lpp2533*	*lpl2388*	similar to coenzyme F42 unknown-reducing hydrogenase- gamma subunit	1.8
lpg1785	*flhA*	*lpp1749*	*lpl1749*	flagellar biosynthesis protein flhA	1.8
lpg1289	-	*lpp1252*	*lpl1252*	unknown	1.8
lpg2972	-	*lpp3044*	*lpl2902*	similar to putative translation initiation protein	1.8
lpg2412	*ampC*	*lpp2481*	*lpl2336*	similar to beta-lactamase precursor (cephalosporinase)	1.8
lpg1430	*ubiA*	*lpp1385*	*lpl1381*	similar to 4-hydroxybenzoate-octaprenyltransferase	1.8
lpg0079	-	*lpp0093*	*lpl0081*	similar to monooxygenase	1.8
lpg1250	*virB6*	*lpp0175*	*lpl0157*	*Legionella* vir homologue protein	1.8
lpg1128	-	*lpp1129*	*lpl1134*	similar to guanine deaminase	1.8
lpg0537	*letE*	*lpp0602*	*lpl0583*	transmission trait enhancer protein LetE	1.8

Gene ID	Name	Paris ID	Lens ID	Description	FC[1]
lpg2579	-	lpp2631	lpl2501	unknown	1.8
lpg1008	helA	lpp2371	lpl1046	similar to cation efflux system protein CzcA- may function with HelC and HelB	1.8
lpg1449	-	lpp1404	-	unknown	1.8
lpg2170	-	lpp2108	lpl2097	predicted membrane protein	1.8
lpg1357	-	lpp1311	lpl1308	regulatory protein (GGDEF and EAL domains)	1.8
lpg0103	vipF	lpp0117	lpl0103	N-terminal acetyltransferase, GNAT family	1.8
lpg2226	-	lpp2177	lpl2151	isovaleryl CoA dehydrogenase	1.7
lpg0997	-	lpp1068	lpl1030	unknown	1.7
lpg2389	katB	lpp2454	lpl2313	catalase-peroxidase KatB	1.7
lpg1789	fliP	lpp1753	lpl1753	flagellar biosynthetic protein FliP	1.7
lpg2683	dlpA	lpp2737	lpl2610	DlpA protein (isocitrate and isopropylmalate dehydrogenases family protein)	1.7
lpg1937	-	lpp1918	lpl1907	similar to conserved hypothetical protein	1.7
lpg1172	lidL	lpp1174	lpl1180	similar to conserved hypothetical protein- similar to C-terminal part of EnhC protein	1.7
lpg0496	argF	lpp0558	lpl0534	ornithine carbamoyltransferase	1.7
lpg1822	-	lpp1785	lpl1786	predicted transmembrane protein	1.7
lpg2975	-	lpp3047	lpl2904	unknown	1.7
lpg1665	-	lpp1636	lpl1630	similar to putative membrane proteins	1.7
lpg1063	proP6	lpp1082	lpl1060	proline/betaine transporter	1.7
lpg1874	-	lpp1839	lpl1836	similar to general secretion pathway protein L	1.7
lpg1457	relA	lpp1413	lpl1571	GTP pyrophosphokinase	1.7
lpg0280	-	lpp0355	lpl0332	similar to transcriptional regulator lysR family	1.7
lpg1104	-	lpp1103	lpl1103	unknown	1.7
lpg0963	-	lpp1025	lpl0992	unknown	1.7
lpg2349	-	lpp2298	lpl2271	similar to alkyl hydroperoxide reductase AhpD	1.7
lpg1022	deoA	lpp2359		similar to thymidine/pyrimidine-nucleoside phosphorylase	1.7
lpg2235	-	lpp2188	lpl2161	similar to sterol desaturase-related protein	1.7
lpg1603	plaB	lpp1568	lpl1422	phospholipase	1.7
lpg1216	flgB	lpp1224	lpl1224	flagellar basal-body rod protein FlgB	1.7
lpg2179	-	lpp2131	-	similar to peptide synthase	1.7
lpg1806	-	lpp1769	lpl1770	similar to hypothtical proteins	1.7
lpg1405	-	lpp1360	lpl1356	similar to multidrug translocase	1.7
lpg1370	fis2	lpp1324	lpl1321	similar to DNA-binding protein Fis	1.7
lpg1007	helB	lpp2372	lpl1045	cation efflux system HelB	1.7
lpg0196	-	lpp0254	lpl0252	unknown	1.7
lpg0837	-	lpp0899	lpl0868	similar to conserved hypothetical protein	1.7
lpg0271	pncA	lpp0345	lpl0323	nicotinamidase/pyrazinamidase	1.6
lpg2485	-	lpp2549	lpl2405	protein with TPR motifs (protein-protein interaction motif)	1.6
lpg0716	-	lpp0782	lpl0753	unknown	1.6
lpg0999	-	lpp1070	lpl1032	similar to conserved hypothetical protein	1.6
lpg0990	-	lpp1061	lpl1023	similar to unknown proteins	1.6
lpg0714	-	lpp0780	lpl0751	similar to two-component sensor histidine kinase	1.6
lpg2796	ftsH	lpp2842	lpl2711	cell division protease ftsH	1.6
lpg0430	-	lpp0497	lpl0473	similar to multidrug resistance efflux pump	1.6
lpg1737	gatB	lpp1702	lpl1701	glutamyl-tRNA (Gln) amidotransferase (subunit B)	1.6
lpg2738	hemY	lpp2794	lpl2663	protoporphyrinogen IX and coproporphyrinogen III oxidase HemY	1.6
lpg0935	-	lpp0997	lpl0966	similar to universal stress protein A	1.6
lpg2875	glmU	lpp2934	lpl2788	bifunctional GlmU protein- UDP-N-acetylglucosamine pyrophosphorylase and glucosamine-1-phosphate N-acetyltransferase	1.6
lpg1479	-	lpp1435	lpl1549	similar to potassium efflux system kefA	1.6
lpg0876	pntAa	lpp0939	lpl0909	pyridine nucleotide transhydrogenase- alpha subunit	1.6
lpg0231	-	lpp0301	lpl0284	similar to cation transport ATPase	1.6
lpg0949	-	lpp1011	lpl0978	predicted membrane protein- similar to transporter	1.6
lpg1955	-	lpp1937	lpl1924	similar to other protein	1.6
lpg1757	fliI	lpp1721	lpl1721	flagellum-specific ATP synthase FliI	1.6
lpg0734	-	lpp0800	lpl0771	similar to glutamine-dependent NAD(+) synthetase	1.6
lpg0140	-	lpp0155	lpl0140	unknown	1.6
lpg1723	guaB	lpp1688	lpl1687	similar to IMP dehydrogenase/GMP reductase	1.6
lpg2013	pilT	lpp1995	lpl1990	twitching motility protein PilT	1.6
lpg0563	-	lpp0623	lpl0606	unknown	1.6
lpg2342	-	lpp2290	lpl2263	unknown	1.6
lpg2824	recN2	lpp2877	lpl2739	DNA repair protein recN	1.6
lpg2614	murC	lpp2667	lpl2537	UDP-N-acetylmuramate--L-alanine ligase	1.6
lpg2676	dotB	lpp2730	lpl2603	defect in organelle trafficking protein DotB (ATPase)	1.6
lpg2959	-	lpp3030	lpl2888	conserved hypothetical protein	1.6
lpg2737	hemX	lpp2793	lpl2662	similar to uroporphyrinogen III methylase HemX	1.5

Gene ID	Name	Paris ID	Lens ID	Description	FC[1]
lpg2852	*amiC*	*lpp2910*	*lpl2764*	similar to amidase	1.5
lpg1480	*mutH*	*lpp1436*	*lpl1548*	similar to DNA mismatch repair protein mutH	1.5
lpg2177	-	*lpp2129*	*lpl2103*	hlyD family secretion protein	1.5
lpg0011	*resA*	*lpp0011*	*lpl0011*	thiol-disulfide oxidoreductase resA	1.5
lpg1743	*fis3*	*lpp1707*	*lpl1707*	similar to DNA-binding protein fis	1.5
lpg2613	*murB*	*lpp2666*	*lpl2536*	UDP-N-acetylenolpyruvoylglucosamine reductase	1.5
lpg2423	-	*lpp2488*	*lpl2346*	unknown	1.5
lpg1542	-	*lpp1499*	*lpl1484*	conserved hypothetical protein	1.5
lpg2533	*tehB*	*lpp2599*	*lpl2455*	similar to tellurite resistance protein TehB	1.5
lpg0738	*dnaB*	*lpp0803*	*lpl0774*	replicative DNA helicase	1.5
lpg0695	*legA8*	*lpp0750*	*lpl0732*	ankyrin repeat protein	1.5
lpg1440	-	*lpp1395*	*lpl1601*	similar to conserved hypothetical protein	1.5
lpg2622	-	*lpp2675*	*lpl2547*	weakly similar to cysteine protease	1.5

[1] Fold Change (FC)

Table 4.S2. Genes repressed in PE phase as compared to E phase *L. pneumophila*

Gene ID	Name	Paris ID	Lens ID	Description	FC Ratio[1]
lpg2002	*yajC*	*lpp1983*	*lpl1978*	similar to preprotein translocase	-14.5
lpg0063	*aroH*	-	-	phospho-2-dehydro-3-deoxyheptonate aldolase	-14.2
lpg0064	-	-	-	unknown	-11.2
lpg0479	*rpmB*	*lpp0544*	*lpl0520*	50S ribosomal protein L28	-10.3
lpg2489	*radC*	*lpp2553*	*lpl2409*	DNA repair protein RadC	-7.0
lpg1997	-	*lpp1978*	*lpl1973*	unknown	-6.7
lpg0067	-	-	-	YdeN-like	-6.0
lpg2653	*pth*	*lpp2706*	*lpl2578*	similar to peptidyl-tRNA hydrolase	-5.9
lpg1862	*tig*	*lpp1830*	*lpl1826*	peptidyl-prolyl cis-trans isomerase (trigger factor)	-5.8
lpg2651	*rplU*	*lpp2704*	*lpl2576*	50S ribosomal protein L21	-5.6
lpg0478	*rpL33*	*lpp0543*	*lpl0519*	50S ribosomal subunit protein L33	-5.5
lpg0260	-	*lpp0332*	*lpl0313*	unknown	-5.5
lpg0320	*rplJ*	*lpp0385*	*lpl0360*	50S ribosomal subunit protein L1 unknown	-5.3
lpg1592	*rpsF*	*lpp1550*	*lpl1433*	30S ribosomal protein S6	-4.9
lpg2988	*atpB*	*lpp3059*	*lpl2916*	highly similar to H+-transporting ATP synthase chain a	-4.8
lpg1590	-	*lpp1548*	*lpl1435*	similar to unknown protein	-4.7
lpg2329	*xseB*	*lpp2277*	*lpl2249*	similar to exodeoxyribonuclease VII- small subunit	-4.6
lpg0542	*fis1*	*lpp0606*	*lpl0587*	similar to DNA-binding proteins Fis	-4.5
lpg2101	*merA12*	-	-	similar to *merA1*, mercuric reductase	-4.4
lpg1591	*rpsR*	*lpp1549*	*lpl1434*	30S ribosomal subunit protein S18	-4.3
lpg2213	-	*lpp2164*	*lpl2138*	similar to hemin binding protein Hbp	-4.3
lpg2636	*rpsT*	*lpp2689*	*lpl2561*	30S ribosomal subunit protein S2 unknown	-4.2
lpg1422	-	*lpp1377*	*lpl1373*	similar to conserved hypothetical protein	-4.2
lpg1832	-	*lpp1795*	*lpl1796*	similar to unknown proteins	-4.1
lpg0068	-	-	-	transmembrane protein	-4.1
lpg0172	-	*lpp0234*	-	unknown	-4.1
lpg1520	-	*lpp1477*	*lpl1506*	similar to hypothetical protein	-4.0
lpg0342	*rpsN*	*lpp0407*	*lpl0382*	30S ribosomal protein S14	-3.9
lpg2989	*atpI*	*lpp3060*	*lpl2917*	similar to ATP synthase subunit i	-3.9
lpg0042	-	*lpp0042*	*lpl0041*	unknown	-3.8
lpg3005	*rpmH*	*lpp3077*	*lpl2933*	50S ribosomal protein L34	-3.8
lpg2650	*rpmA*	*lpp2703*	*lpl2575*	50S ribosomal protein L27	-3.8
lpg0358	-	*lpp0423*	*lpl0399*	similar to 3-oxoacyl-[acyl-carrier protein] reductase	-3.8
lpg3003	-	*lpp3075*	*lpl2931*	similar to conserved hypothetical protein	-3.8
lpg0335	*rpsC*	*lpp0400*	*lpl0375*	30S ribosomal protein S3	-3.7
lpg1982	-	*lpp1963*	*lpl1957*	some similarity with eukaryotic proteins / Shorter in phila	-3.7
lpg2694	*legD1*	*lpp2748*	*lpl2621*	similar to eukaryotic phytanoyl-CoA dioxygenase	-3.7
lpg0408[a]	-	*lpp0475*	*lpl0451*	similar to putative transmembrane proteins	-3.6
lpg0732	-	*lpp0798*	*lpl0769*	weakly similar to outer membrane protein	-3.6
lpg0922	*etfB*	*lpp0984*	*lpl0953*	electron transfer flavoprotein beta-subunit (Beta-ETF)	-3.6
lpg0339	*rplN*	*lpp0404*	*lpl0379*	50S ribosomal protein L14	-3.6
lpg2707	*rplM*	*lpp2762*	*lpl2635*	50S ribosomal subunit protein L13	-3.6
lpg0507	-	*lpp0570*	*lpl0546*	similar to putative outer membrane proteins	-3.5
lpg0353	*rpsD*	*lpp0418*	*lpl0394*	30S ribosomal subunit protein S4	-3.5
lpg1546	-	*lpp1503*	*lpl1480*	similar to fimbrial biogenesis and twitching motility protein (type 4)	-3.4
lpg0287	*efp*	*lpp0365*	*lpl0340*	similar to elongation factor P	-3.4
lpg1749	*sppA*	*lpp1713*	*lpl1713*	similar to putative signal peptide peptidases	-3.4
lpg1556	-	*lpp1513*	*lpl1470*	similar to unknown protein /MutT/nudix family protein	-3.4
lpg1776	-	*lpp1740*	*lpl1740*	unknown	-3.4
lpg0345	*rplR*	*lpp0410*	*lpl0385*	50S ribosomal subunit protein L18	-3.4
lpg1921	-	*lpp1896*	*lpl1885*	similar to conserved hypothetical protein	-3.3
lpg0582	-	*lpp0632*	*lpl0616*	unknown	-3.3

Gene ID	Name	Paris ID	Lens ID	Description	FC Ratio[1]
lpg0601	*ycf24*	*lpp0652*	*lpl0636*	similar to ABC transporter- permease component	-3.3
lpg2864	-	*lpp2922*	*lpl2776*	similar to conserved hypothetical protein	-3.3
lpg0600	-	*lpp0651*	*lpl0635*	similar to conserved hypothetical protein	-3.3
lpg2981	*atpC*	*lpp3052*	*lpl2909*	highly similar to H+-transporting ATP synthase epsilon chain	-3.3
lpg1396	*acpP2*	*lpp1351*	*lpl1347*	acyl carrier protein (ACP)	-3.3
lpg0325	*rps7*	*lpp0390*	*lpl0365*	30S ribosomal protein S7	-3.2
lpg1519	*ppt*	*lpp1476*	*lpl1507*	putative pyrimidine phosphoribosyl transferase	-3.2
lpg1558	-	*lpp1515*	*lpp1468*	similar to pyruvate dehydrogenase- (E1 alpha subunit)	-3.2
lpg2912	-	*lpp2980*	*lpl2830*	unknown	-3.1
lpg2094	*csrA*	*lpp0845*	*lpl0820*	global regulator CsrA	-3.1
lpg2727	*tgt2*	*lpp2784*	*lpl2653*	similar to queuine tRNA-ribosyltransferase	-3.1
lpg0351	*rpsM*	*lpp0416*	*lpl0392*	30S ribosomal protein S13	-3.1
lpg0474	*pssA*	*lpp0539*	*lpl0515*	similar to CDP-diacylglycerol-serine O-phosphatidyltransferase (phosphatidylserine synthase)	-3.1
lpg2765	*hit*	*lpp2813*	*lpl2682*	similar to HIT (histidine triad nucleotide-binding protein) family protein	-3.1
lpg2838	-	*lpp2897*	*lpl2750*	similar to unknown protein	-3.1
lpg0100	*lpxD*	*lpp0114*	*lpl0100*	similar to UDP-3-O-(R-3-hydroxymyristoyl)-glucosamine N-acyltransferase/Lipid A biosynthesis; third step	-3.1
lpg0650	*rpmE*	*lpp0704*	*lpl0686*	50S ribosomal protein L31	-3.1
lpg2706	*rpsI*	*lpp2761*	*lpl2634*	30S ribosomal subunit protein S9	-3.0
lpg0484	*hflK*	*lpp0548*	*lpl0524*	protease subunit HflK	-3.0
lpg2487	*dut*	*lpp2551*	*lpl2407*	deoxyuridine 5 -triphosphate nucleotidohydrolase (dUTPase)	-3.0
lpg2662	*panC*	*lpp2716*	*lpl2589*	similar to pantothenate synthetases	-3.0
lpg2714	*thrS*	*lpp2770*	*lpl2643*	threonyl tRNA synthetase	-3.0
lpg2712	*rplT*	*lpp2767*	*lpl2640*	50S ribosomal protein L2 unknown	-3.0
lpg2043	*pal*	*lpp2026*	*lpl2021*	peptidoglycan-associated lipoprotein precursor (19 kDa surface antigen) (PPL)	-2.9
lpg2308	*secB*	*lpp2256*	*lpl2227*	similar to protein-export protein SecB	-2.9
lpg2661	*panB*	*lpp2715*	*lpl2588*	similar to 3-methyl-2-oxobutanoatehydroxymethyltransferase	-2.9
lpg0328	*rpsJ*	*lpp0393*	*lpl0368*	30S ribosomal subunit protein S1 unknown	-2.9
lpg1803	-	*lpp1766*	*lpl1766*	unknown	-2.9
lpg0085	-	*lpp0099*	*lpl0084*	putative secreted protein	-2.9
lpg1167	-	*lpp1169*	*lpl1175*	similar to conserved hypothetical protein	-2.9
lpg0777	*lag-1*	*lpp0841*	*lpl0816*	O-acetyltransferase	-2.9
lpg0372	*smpA*	*lpp0437*	*lpl0413*	similar to other protein	-2.9
lpg1162	-	*lpp1164*	*lpl1170*	similar to other proteins	-2.9
lpg0769	-	*lpp0834*	*lpl0810*	unknown	-2.8
lpg1689	-	*lpp1658*	*lpl1652*	unknown	-2.8
lpg0640	*hslV*	*lpp0694*	*lpl0677*	peptidase component of the HslUV protease (heat shock protein)	-2.8
lpg0602	-	*lpp0653*	*lpl0637*	similar to ABC transporter ATP-binding protein	-2.8
lpg0811	*mreB*	*lpp0873*	*lpl0844*	rod shape-determining protein MreB	-2.8
lpg2999	*legP*	*lpp3071*	*lpl2927*	similar to eukaryotic zinc metalloproteinase	-2.8
lpg0330	*rplD*	*lpp0395*	*lpl0370*	50S ribosomal subunit protein L4	-2.8
lpg1840	*glyQ*	*lpp1804*	*lpl1805*	glycyl-tRNA synthetase alpha chain	-2.8
lpg0354	*rpoA*	*lpp0419*	*lpl0395*	DNA-directed RNA polymerase alpha chain	-2.7
lpg1658	-	*lpp1629*	*lpl1623*	similar to amino acid transporter	-2.7
lpg2956	*dcd*	*lpp3027*	*lpl2885*	deoxycytidine triphosphate deaminase	-2.7
lpg1005	*lvrA*	*lpp1076*	*lpl1038*	lvrA	-2.7
lpg2598	-	*lpp2651*	*lpl2521*	similar to unknown protein	-2.6
lpg2359	*lporfX*	*lpp2308*	*lpl2281*	similar to conserved hypothetical protein	-2.6
lpg1593	-	*lpp1551*	*lpl1432*	similar to carbon storage regulator CsrA	-2.6
lpg2577	-	*lpp2629*	*lpl2499*	unknown	-2.6
lpg0606	-	*lpp0657*	*lpl0641*	similar to conserved hypothetical protein	-2.6
lpg2935	*trxA*	*lpp3003*	*lpl2864*	highly similar to thioredoxin	-2.6
lpg1535	-	*lpp1492*	*lpl1491*	similar to rubredoxin protein	-2.6
lpg2713	*infC*	*lpp2769*	*lpl2642*	translation initiation factor IF-3	-2.6
lpg0855	-	*lpp0917*	*lpl0886*	similar to protease	-2.6
lpg0370	-	*lpp0435*	*lpl0411*	similar to conserved hypothetical proteins	-2.5
lpg2840	-	*lpp2899*	*lpl2752*	highly similar to bacterioferritin comigratory protein	-2.5

Gene ID	Name	Paris ID	Lens ID	Description	FC Ratio[1]
lpg2462	-	*lpp2528*	*lpl2381*	similar to hypothetical protein	-2.5
lpg0296	-	*lpp0374*	*lpl0349*	similar to conserved hypothetical protein	-2.5
lpg0475	*ptsH*	*lpp0540*	*lpl0516*	similar to sugar transport PTS phosphocarrier protein Hpr	-2.5
lpg1314	-	*lpp2055*	-	unknown	-2.5
lpg0282	-	*lpp0358*	*lpl0334*	some similarity with eukaryotic proteins	-2.5
lpg1770	*infA*	*lpp1734*	*lpl1734*	translation initiation factor IF-1	-2.5
lpg2116	-	-	-	transposase	-2.5
lpg2644	*sclB*	*lpp2697*	*lpl2569*	similar to putative protein from Stx2 converting bacteriophage I	-2.5
lpg2695a	-	*lpp2750*	*lpl2623*	similar to unknown proteins	-2.5
lpg2339	-	*lpp2287*	*lpl2260*	unknown	-2.5
lpg0482	-	*lpp0546*	*lpl0522*	similar to endo-1-4-beta-glucanase (hypothetical)	-2.5
lpg0856	*ccmA*	*lpp0918*	*lpl0887*	heme exporter protein CcmA	-2.5
lpg3004	*rnpA*	*lpp3076*	*lpl2932*	similar to ribonuclease P protein component (RNase P)	-2.5
lpg0724	-	*lpp0790*	*lpl0761*	similar to predicted periplasmic or secreted lipoprotein	-2.5
lpg0485	*hflC*	*lpp0549*	*lpl0525*	membrane protease subunit HflC	-2.5
lpg1585	-	*lpp1543*	*lpl1440*	unknown	-2.5
lpg0486	*purA*	*lpp0550*	*lpl0526*	adenylosuccinate synthetase (IMP-aspartate ligase) (AdSS) (AMPSase)	-2.4
lpg2121	-	*lpp2041*	*lpl2039*	similar to cold shock protein	-2.4
lpg1966	-	*lpp1947*	-	unknown	-2.4
lpg2827	-	*lpp2881*	*lpl2742*	similar to conserved hypothetical protein	-2.4
lpg2474	*hypF*	*lpp2539*	*lpl2394*	hydrogenase maturation protein HypF	-2.4
lpg0819	-	*lpp1851*	*lpp0038*	similar to transposase (IS4 family)	-2.4
lpg0149	-	-	-	hypothetical protein	-2.4
lpg2417	-	-	*lpl2340*	hypothetical protein	-2.4
lpg2448	-	-	-	transposase, ISSod6	-2.4
lpg0773	*wzt*	*lpp0838*	*lpl0814*	ABC transporter of LPS O-antigen- Wzt	-2.4
lpg1138	*potD*	*lpp1140*	*lpl1145*	similar to spermidine/putrescine-binding periplasmic protein precursor potD	-2.4
lpg0324	*rpsL*	*lpp0389*	*lpl0364*	30S ribosomal protein S12	-2.4
lpg1383	*rnhA*	*lpp1338*	*lpl1334*	similar to ribonuclease HI	-2.4
lpg1999	-	*lpp1980*	*lpl1975*	similar to pterin-4-alpha-carbinolamine dehydratase phhB	-2.4
lpg2463	-	*lpp2530*	*lpl2383*	similar to aspartyl/asparaginyl beta-hydroxylase	-2.4
lpg2774	-	*lpp2822*	*lpl2691*	similar to conserved hypothetical protein	-2.4
lpg1163	-	*lpp1165*	*lpl1171*	similar to permeases of the major facilitator superfamily (MFS)	-2.4
lpg1395	*fabG*	*lpp1350*	*lpl1346*	3-oxoacyl-[acyl-carrier protein] reductase (3-ketoacyl-acyl carrier protein reductase)	-2.4
lpg0329	*rplC*	*lpp0394*	*lpl0369*	50S ribosomal subunit protein L3	-2.3
lpg2631	*pepA*	*lpp2684*	*lpl2556*	similar to leucine aminopeptidase	-2.3
lpg1920	*lpxK*	*lpp1895*	*lpl1884*	similar to hypothetical protein	-2.3
lpg2960	-	*lpp3031*	*lpl2889*	similar to major outer membrane protein precursor	-2.3
lpg1510	*ala*	*lpp1467*	*lpl1516*	similar to D-alanine aminotransferase	-2.3
lpg1142	-	*lpp1144*	-	hypothetical protein- similar to endonuclease	-2.3
lpg1200	*hisG*	*lpp1202*	*lpl1208*	ATP phosphoribosyltransferase	-2.3
lpg2825	-	*lpp2878*	*lpl1057*	similar to cold shock protein CspC	-2.3
lpg2769	*rpsO*	*lpp2817*	*lpl2686*	30S ribosomal protein S15	-2.3
lpg1333	*rluD*	*lpp1287*	*lpl1286*	ribosomal large subunit pseudouridine synthase D (uracil hydrolyase)	-2.3
lpg2026	*grpE*	*lpp2008*	*lpl2003*	heat-shock protein GrpE (HSP-7 unknown cofactor)	-2.3
lpg2568	-	-	-	hypothetical protein	-2.3
lpg0065	-	-	-	unknown	-2.3
lpg1529	*prpD*	*lpp1486*	*lpl1497*	2-methylcitrate dehydratase	-2.3
lpg1854	*fabI*	*lpp1821*	*lpl1820*	similar to enoyl-[acyl-carrier-protein] reductase	-2.3
lpg2548	-	*lpp2617*	*lpl2469*	predicted transmembrane protein	-2.3
lpg1800	*recX*	*lpp1764*	*lpl1764*	regulatory protein RecX	-2.3
lpg1703	*umuC*	*lpp1668*	*lpl1662*	similar to error-prone repair protein	-2.2
lpg1410	-	*lpp1365*	*lpl1361*	similar to unknown protein	-2.2
lpg1919	*kdsB*	*lpp1894*	*lpl1883*	3-deoxy-manno-octulosonate cytidylyltransferase	-2.2
lpg2717	-	*lpp2773*	*lpl2645*	unknown	-2.2
lpg0815	-	*lpp0877*	*lpl0848*	unknown	-2.2
lpg0690	-	*lpp0745*	*lpl0726*	similar to conserved hypothetical protein- predicted membrane protein	-2.2
lpg1589	*rplI*	*lpp1547*	*lpl1436*	50S ribosomal protein L9	-2.2

Gene ID	Name	Paris ID	Lens ID	Description	FC Ratio[1]
lpg1923	-	*lpp1898*	*lpl1887*	similar to ferredoxin	-2.2
lpg1975	-	-	-	unknown	-2.2
lpg0133	*proQm*	*lpp0148*	*lpl0133*	similar to N-terminus of ProQ- activator of ProP osmoprotectant transporter	-2.2
lpg2860	-	*lpp2918*	*lpl2772*	unknown	-2.2
lpg1534	*hemL*	*lpp1491*	*lpl1492*	similar to glutamate-1-semialdehyde-2-1-aminomutase	-2.2
lpg0605	-	*lpp0656*	*lpl0640*	NifU protein family- possibly involved in formation or repair of [Fe-S] clusters	-2.2
lpg1101	-	*lpp1101*	*lpl1100*	unknown	-2.2
lpg1943	-	*lpp1924*	*lpl1913*	similar to hypothetical protein	-2.2
lpg0919	-	*lpp0980*	*lpl0950*	unknown	-2.1
lpg1649	*iolE*	*lpp1620*	*lpl1615*	similar to myo-inositol catabolism protein iolE	-2.1
lpg2284	-	*lpp2238*	*lpl2210*	similar to ATP-binding component of ABC transporter	-2.1
lpg0758	*rmlB*	*lpp0824*	*lpl0795*	dTDP-D-glucose 4-6-dehydratase rhamnose biosynthesis	-2.1
lpg1662	-	*lpp1633*	*lpl1627*	similar to putative transport proteins- MFS family	-2.1
lpg1418	*serC*	*lpp1373*	*lpl1369*	similar to phosphoserine aminotransferase	-2.1
lpg0755	*yvfE*	*lpp0821*	*lpl0792*	similar to polysaccharide biosynthesis protein	-2.1
lpg0858	*ccmC*	*lpp0920*	*lpl0889*	heme exporter protein CcmC	-2.1
lpg1392	*plsX*	*lpp1347*	*lpl1343*	fatty acid/phospholipid synthesis protein	-2.1
lpg1996	-	*lpp1977*	*lpl1972*	unknown	-2.1
lpg0973	-	*lpp1034*	*lpl1001*	unknown	-2.1
lpg2763	-	*lpp2811*	*lpl2680*	similar to unknown protein	-2.1
lpg1193	*hisI*	*lpp1195*	*lpl1201*	phosphoribosyl-AMP cyclohydrolase (PRA-CH)/phosphoribosyl-ATP pyrophosphatase (PRA-PH)	-2.1
lpg0434	-	*lpp0501*	*lpl0477*	unknown	-2.1
lpg2695	-	*lpp2749*	*lpl2622*	similar to glycosyltransferase	-2.1
lpg2702	*sspA*	*lpp2757*	*lpl2630*	similar to stringent starvation protein A	-2.1
lpg0727	*nusB*	*lpp0793*	*lpl0764*	similar to N utilization substance protein B homolog	-2.1
lpg2949	*wbm1*	-	-	asparagine synthase	-2.1
lpg1998	*hisC2*	*lpp1979*	*lpl1974*	similar to histidinol-phosphate aminotransferase	-2.1
lpg2293	*pgsA*	*lpp2240*	*lpl2212*	similar to CDP-diacylglycerol- glycerol-3-phosphate 3-phosphatidyltransferase	-2.1
lpg0860	*ccmE*	*lpp0922*	*lpl0891*	cytochrome c-type biogenesis protein CcmE	-2.1
lpg0125	-	*lpp0139*	*lpl0124*	similar to GTP-binding protein	-2.0
lpg1384	*dnaQ*	*lpp1339*	*lpl1335*	similar to DNA polymerase III- epsilon chain	-2.0
lpg1476	-	*lpp1432*	*lpl1552*	similar to conserved hypothetical protein	-2.0
lpg2036	-	*lpp2019*	*lpl2014*	similar to septum formation protein Maf	-2.0
lpg0137	*pgk*	*lpp0152*	*lpl0137*	phosphoglycerate kinase	-2.0
lpg1281	-	*lpp1244*	*lpl1244*	unknown	-2.0
lpg2900	*capM2*	*lpp2965*	*lpl2815*	similar to glycosyltransferases	-2.0
lpg0603	-	*lpp0654*	*lpl0638*	similar ABC transporter- permease component	-2.0
lpg2931a	-	*lpp2999*	*lpl2860*	unknown	-2.0
lpg0396	*trmD*	*lpp0464*	*lpl0440*	highly similar to tRNA (guanine-N1)-methyltransferase	-2.0
lpg2022	*metK*	*lpp2004*	*lpl1999*	S-adenosylmethionine synthetase	-2.0
lpg2632	*holC*	*lpp2685*	*lpl2557*	similar to DNA polymerase III- chi subunit	-2.0
lpg2115	-	-	-	hypothetical phage AbiD protein	-2.0
lpg2158	*pmtA*	*lpp2097*	*lpl2086*	similar to methyltransferase	-2.0
lpg1198	*hisC*	*lpp1200*	*lpl1206*	histidinol-phosphate aminotransferase (imidazole acetol-phosphate transaminase)	-2.0
lpg0052	-	*lpp0054*	*lpl0052*	similar to probable methylisocitrate lyase	-2.0
lpg1860	*clpX*	*lpp1828*	*lpl1824*	ATP-dependent Clp protease ATP-binding subunit ClpX	-2.0
lpg1186	-	*lpp1188*	*lpl1194*	similar to competence lipoprotein comL precursor	-2.0
lpg2967	*sodB*	*lpp3039*	*lpl2897*	superoxide dismutase-iron	-2.0
lpg1119	*map*	*lpp1120*	*lpl1124*	major acid phosphatase Map (histidine-acid phosphatase)	-2.0
lpg1482	-	*lpp1438*	*lpl1546*	unknown	-2.0
lpg2882	*metG_1*	*lpp2941*	*lpl2795*	methionyl-tRNA synthetase	-2.0
lpg1391	*rpmF*	*lpp1346*	*lpl1342*	50S ribosomal subunit protein L32	-2.0
lpg1472	*bioB*	*lpp1428*	*lpl1556*	biotin synthase	-2.0
lpg2507	-	*lpp2575*	*lpl2429*	unknown	-2.0
lpg0604	-	*lpp0655*	*lpl0639*	similar to cysteine desulfurase and to selenocysteine lyase	-2.0
lpg2172	-	*lpp2110*	-	similar to adenosylhomocysteinase	-1.9
lpg0568	*tyrS*	*lpp0628*	*lpl0611*	tyrosyl-tRNA synthetase	-1.9
lpg2710	*pheT*	*lpp2765*	*lpl2638*	phenylalanyl-tRNA synthetase- beta subunit	-1.9

Gene ID	Name	Paris ID	Lens ID	Description	FC Ratio[1]
lpg1399	*tmk*	*lpp1354*	*lpl1350*	similar to thymidylate kinase	-1.9
lpg0008	-	*lpp0008*	*lpl0008*	unknown	-1.9
lpg0504	*cdsA*	*lpp0567*	*lpl0543*	phosphatidate cytidylyltransferase	-1.9
lpg2306	-	*lpp2254*	*lpl2225*	similar to conserved hypothetical protein	-1.9
lpg0868	-	*lpp0931*	*lpl0900*	similar to acyl-CoA dehydrogenase	-1.9
lpg1447	*rluB*	*lpp1402*	*lpl1594*	similar to ribosomal large subunit pseudouridine synthase B	-1.9
lpg2553	*uhpC*	*lpp2623*	*lpl2474*	similar to hexose phosphate transport protein	-1.9
lpg2881	-	*lpp2940*	*lpl2794*	similar to electron transport complex protein rnfB	-1.9
lpg0400	*ffh*	*lpp0467*	*lpl0443*	similar to signal recognition particle protein Ffh	-1.9
lpg2944	*lpxD2*	*lpp3015*	*lpl2873*	similar to UDP-3-O-[3-hydroxymyristoyl] glucosamine N-acyltransferase	-1.9
lpg2791	*secG*	*lpp2837*	*lpl2706*	protein export membrane protein secG (preprotein translocase subunit)	-1.9
lpg0821	-	*lpp0883*	*lpl0852*	similar to lipopolysaccharide biosynthesis glycosyltransferase	-1.9
lpg1445	*scpA*	*lpp1400*	*lpl1596*	similar to segregation and condensation protein A	-1.9
lpg0510	*fabZ*	*lpp0572*	*lpl0548*	(3R)-hydroxymyristoyl-[acyl carrier protein] dehydratase	-1.9
lpg1841	*com1*	*lpp1805*	*lpl1806*	similar to outer membrane protein	-1.9
lpg1831	*mrp*	*lpp1776*	*lpl1777*	similar to unknown protein	-1.9
lpg1471	*bioA*	*lpp1427*	*lpl1557*	adenosylmethionine-8-amino-7-oxononanoate aminotransferase	-1.9
lpg2021	*ahcY*	*lpp2003*	*lpl1998*	adenosylhomocysteinase (S-adenosyl-L-homocysteinehydrolase)	-1.9
lpg0541	-	*lpp0605*	*lpl0586*	C-terminal part similar to unknown virulence protein	-1.9
lpg0406	-	*lpp0472*	*lpl0448*	similar to conserved hypothetical proteins	-1.9
lpg0786	*mesJ*	*lpp0850*	*lpl0825*	similar to cell cycle protein MesJ	-1.9
lpg0946	*pdxJ*	*lpp1008*	*lpl0975*	pyridoxal phosphate biosynthetic protein pdxJ	-1.9
lpg2321	*sdaC*	*lpp2269*	*lpl2241*	similar to serine transporter	-1.9
lpg2047	-	*lpp2030*	*lpl2025*	similar to ABC transporter permease protein	-1.8
lpg0780	-	*lpp0844*	*lpl0819*	similar to glyoxalase II	-1.8
lpg1227	-	*lpp1235*	*lpl1235*	unknown	-1.8
lpg0799	*nadA*	*lpp0861*	*lpl0832*	similar to quinolinate synthetase A	-1.8
lpg1801	*recA*	*lpp1765*	*lpl1765*	RecA protein	-1.8
lpg2277	-	*lpp2231*	*lpl2203*	similar to O-methyltransferase	-1.8
lpg0424	-	*lpp0491*	*lpl0467*	similar to hypothetical proteins	-1.8
lpg0229	-	*lpp0288*	*lpl0282*	unknown	-1.8
lpg0098	-	*lpp0112*	*lpl0098*	weakly similar to putative response regulator	-1.8
lpg0367[a]	-	*lpp0432*	*lpl0408*	putative lipopeptide	-1.8
lpg0046	-	*lpp0047*	*lpl0045*	unknown	-1.8
lpg1103	-	*lpp1102*	*lpl1102b*	putative secreted protein	-1.8
lpg0756	*rmlC*	*lpp0822*	*lpl0793*	dTDP-4-dehydrorhamnose 3-5-epimerase	-1.8
lpg2898	-	*lpp2963*	*lpl2821*	similar to cytochrome c	-1.8
lpg1661	-	*lpp1632*	*lpl1626*	similar to conserved hypothetical proteins	-1.8
lpg0789	-	*lpp0853*	*lpl0827*	alginate O-acetyltransferase AlgI	-1.8
lpg0731	-	*lpp0797*	*lpl0768*	some similarity with outer surface protein	-1.8
lpg1620	-	*lpp1590*	*lpl1403*	similar to transcriptional regulator (MarR family)	-1.8
lpg1657	-	*lpp1628*	*lpl1622*	similar to dimethylarginine dimethylaminohydrolase	-1.8
lpg2136	*ceaC*	*lpp2075*	*lpl2065*	chemiosmotic efflux system protein C-like protein	-1.8
lpg2004	*queA*	*lpp1985*	*lpl1980*	S-adenosylmethionine: tRNA ribosyltransferase-isomerase	-1.8
lpg0295	-	*lpp0373*	*lpl0348*	similar to nucleotidyltransferase family protein	-1.8
lpg1553	*minC*	*lpp1510*	*lpl1473*	similar to cell division inhibitor MinC (septum placement)	-1.8
lpg0651	-	*lpp0705*	*lpl0687*	similar to NADP-dependent malic enzyme	-1.8
lpg1548	*ndk*	*lpp1505*	*lpl1478*	similar to nucleoside diphosphate kinase	-1.8
lpg0748	-	*lpp0814*	*lpl0785*	similar to LPS biosynthesis protein	-1.8
lpg1319	*lspE*	*lpp1274*	*lpl1273*	type II protein secretion ATPase LspE	-1.8
lpg2322	*legA5*	*lpp2270*	*lpl2242*	ankyrin repeat protein	-1.8
lpg0413	-	*lpp0480*	*lpl0456*	similar to hypothetical proteins	-1.8
lpg2558	-	-	-	integrase of prophage CP-933C	-1.8
lpg1507	-	*lpp1464*	*lpl1519*	similar to sodium/hydrogen antiporter family protein	-1.8
lpg0129[a]	-	*lpp0144*	*lpl0129*	weakly similar to conserved hypothetical protein	-1.8
lpg0040	-	*lpp0041*	*lpl0040*	similar to conserved hypothetical protein	-1.8
lpg0251	-	*lpp0321*	-	similar to N-terminal part of eukaryotic RNA-binding protein precursor	-1.8
lpg1764	-	*lpp1728*	*lpl1728*	conserved hypothetical protein	-1.8
lpg2276	-	*lpp2230*	*lpl2202*	similar to leucine dehydrogenase	-1.8

Gene ID	Name	Paris ID	Lens ID	Description	FC Ratio[1]
lpg0322	*rpoB*	*lpp0387*	*lpl0362*	RNA polymerase B-subunit	-1.8
lpg0691	*parE*	*lpp0746*	*lpl0727*	DNA topoisomerase IV subunit B	-1.8
lpg2701	*sspB*	*lpp2756*	*lpl2629*	similar to stringent starvation protein B	-1.8
lpg2580	*gcdH*	*lpp2632*	*lpl2502*	similar to glutaryl-CoA dehydrogenase	-1.8
lpg1371	*lpxB1*	*lpp1325*	*lpl1322*	similar to lipid-A-disaccharide synthase	-1.7
lpg0366	*dapF*	*lpp0431*	*lpl0407*	diaminopimelate epimerase	-1.7
lpg0832	-	*lpp0894*	*lpl0863*	similar to oxidoreductases- short-chain dehydrogenase/reductase family	-1.7
lpg1587	-	*lpp1545*	*lpl1438*	similar to unknown protein	-1.7
lpg1443	-	*lpp1398*	*lpl1598*	similar to putative translation factor	-1.7
lpg2522	-	*lpp2590*	*lpl2444*	similar to other protein	-1.7
lpg2003	*tgt*	*lpp1984*	*lpl1979*	unknown	-1.7
lpg2411	-	*lpp2480*	*lpl2335*	unknown	-1.7
lpg1015	*yueD*	*plpp0120*	-	conserved gene, perhaps benzil (sepiapterin, ketoacyl) reductase	-1.7
lpg1477	-	*lpp1433*	*lpl1551*	similar to conserved hypothetical protein	-1.7
lpg267	-	*lpp2690*	*lpl2562*	unknown	-1.7
lpg2484	-	*lpp2548*	*lpl2404*	similar to conserved hypothetical protein	-1.7
lpg2337	*hemK*	*lpp2285*	*lpl2258*	similar to methyltransferase hemK	-1.7
lpg0613	-	*lpp0664*	*lpl0648*	unknown	-1.7
lpg0184	-	-	-	unknown	-1.7
lpg2278	*hpd*	*lpp2232*	*lpl2204*	4-hydroxyphenylpyruvate dioxygenase (legiolysin)	-1.7
lpg2361	*rpoD*	*lpp2310*	*lpl2283*	RNA polymerase sigma factor rpoD (sigma-7 unknown)	-1.7
lpg2356	-	*lpp2305*	*lpl2278*	predicted membrane protein	-1.7
lpg2963	*pyrC*	*lpp3035*	*lpl2893*	similar to dihydroorotase- homodimeric type	-1.7
lpg2913	-	-	-	hypothetical protein	-1.7
lpg2679	-	*lpp2733*	*lpl2606*	similar to oxidoreductase	-1.7
lpg0726	-	*lpp0792*	*lpl0763*	similar to unknown proteins	-1.7
lpg2898[a]	-	*lpp2964*	*lpl2814*	similar to ferredoxin component of dioxygenase	-1.7
lpg0089	-	*lpp0103*	*lpl0088*	conserved hypothetical protein	-1.7
lpg0470	-	*lpp0535*	*lpl0511*	similar to fructose-bisphosphate aldolase	-1.7
lpg2420	-	-	*lpl2343*	hypothetical protein	-1.7
lpg0618	*tag*	*lpp0672*	*lpl0656*	similar to 3-methyladenine-DNA glycosylase I	-1.7
lpg1872	*lepA1*	*lpp1837*	*lpl1834*	similar to GTP-binding elongation factor	-1.7
lpg1826	-	*lpp1789*	*lpl1790*	hypothetical gene	-1.7
lpg2670	*ftsY*	*lpp2724*	*lpl2597*	similar to C-terminal part of signal recognition particle GTPase- FtsY	-1.7
lpg1586	-	*lpp1544*	*lpl1439*	unknown- possibly truncated	-1.7
lpg0858	*ccmD*	*lpp0921*	*lpl0890*	heme exporter protein CcmD	-1.7
lpg1286	-	*lpp1249*	*lpl1249*	similar to conserved hypothetical protein	-1.7
lpg1808	*hemB*	*lpp1771*	*lpl1772*	similar to delta-aminolevulinic acid dehydratases (porphobilinogen synthase)	-1.7
lpg2454	-	*lpp2520*	*lpl2373*	similar to unknown protein	-1.7
lpg2968	*argD*	*lpp3040*	*lpl2898*	similar to ornithine/acetylornithine aminotransferase	-1.7
lpg0481	-	*lpp0545*	*lpl0521*	similar to S-adenosylmethionine-dependent methyltransferase	-1.7
lpg0369	-	*lpp0434*	*lpl0410*	similar to phospholipase/carboxylesterase	-1.7
lpg0664	*rpe*	*lpp0721*	*lpl0701*	ribulose-phosphate 3-epimerase	-1.7
lpg2059	-	-	-	hypothetical phage repressor	-1.7
lpg2358	*rpsU*	*lpp2307*	*lpl2280*	30S ribosomal protein S21	-1.7
lpg2902	-	*lpp2969*	*lpl2817*	similar to conserved hypothetical protein	-1.7
lpg2330	*ispA*	*lpp2278*	*lpl2250*	similar to geranyltranstransferase; farnesyl-diphosphate synthase	-1.6
lpg2657	*feoB*	*lpp2711*	*lpl2584*	ferrous iron transporter B	-1.6
lpg2567	-	-	-	ISI400 transposase B	-1.6
lpg0615	-	*lpp0666*	-	similar to polypeptide deformylase	-1.6
lpg2496	-	*lpp2563*	*lpl2417*	similar to rRNA methylase	-1.6
lpg1897	-	*lpp1866*	*lpl1861*	similar to glutathione-regulated potassium-efflux system protein KefC	-1.6
lpg2453	-	*lpp2519*	*lpl2372*	unknown	-1.6
lpg1704	*umuD*	*lpp1669*	*lpl1663*	similar to error-prone repair: SOS-response transcriptional repressors	-1.6
lpg2009[a]	*rpoZ*	*lpp1991*	*lpl1986*	RNA polymerase omega subunit	-1.6
lpg1547	-	*lpp1504*	*lpl1479*	similar to conserved hypothetical protein	-1.6
lpg1486	-	*lpp1442*	*lpl1542*	similar to transcriptional regulator (Lrp family)	-1.6
lpg1991	-	*lpp1972*	*lpl1967*	predicted membrane protein	-1.6
lpg1576	*ruvB*	*lpp1534*	*lpl1449*	highly similar to holliday junction DNA helicase RuvB	-1.6

136

Gene ID	Name	Paris ID	Lens ID	Description	FC Ratio[1]
lpg0421	ywtG	lpp0488	lpl0464	similar to sugar transport protein	-1.6
lpg2085	traU	-	-	TraU	-1.6
lpg1844	dtD	lpp1808	lpl1809	similar to D-tyrosyl-tRNA (Tyr) deacylase	-1.6
lpg0778	-	lpp0842	lpl0817	similar to glycosyltransferase	-1.6
lpg2970	ubiE	lpp2970	lpl2818	ubiquinone/menaquinone biosynthesis methyltransferase	-1.6
lpg2770	truB	lpp2818	lpl2687	tRNA pseudouridine synthase B	-1.6
lpg1305	trpA	lpp1269	lpl1268	tryptophan synthase- alpha subunit	-1.6
lpg2754	dnaZX	lpp2802	lpl2671	DNA polymerase III- gamma and tau subunits	-1.6
lpg0513	serS	lpp0575	lpl0551	seryl-tRNA synthetase	-1.6
lpg1883	-	lpp1847	lpl1844	putative membrane protein	-1.6
lpg0077	pepP	lpp0091	lpl0079	similar to proline aminopeptidase P II	-1.6
lpg2839	smpB	lpp2898	lpl2751	similar to SsrA-binding protein	-1.6
lpg2285	-	lpp2239	lpl2211	similar to ABC transporter- permease component	-1.6
lpg2173	tnpA2	lpp1566	lpl0196	TnpA transposase (partial in Lens)	-1.6
lpg0694	proS	lpp0749	lpl0731	prolyl-tRNA synthetase (proline-tRNA ligase) (global RNA synthesis factor)	-1.6
lpg0148	-	-	-	hypothetical protein	-1.6
lpg1544	hisS	lpp1501	lpl1482	histidyl-tRNA synthetase	-1.6
lpg1823	-	lpp1786	lpl1787	similar to conserved hypothetical protein	-1.6
lpg0633	-	lpp0687	lpl0670	similar to peptidoglycan GlcNAc deacetylase proteins	-1.6
lpg0593	-	lpp0643	lpl0627	similar to 5-formyltetrahydrofolate cyclo-ligase	-1.6
lpg2886	-	lpp2945	lpl2799	highly similar to transcriptional regulator ExsB	-1.6
lpg1545	-	lpp1502	lpl1481	hypothetical protein	-1.6
lpg1285	hmgA	lpp1248	lpl1248	homogentisate 1-2-dioxygenase	-1.6
lpg0404	-	lpp0470	lpl0446	similar to amino acid antiporter	-1.6
lpg2249	-	lpp2203	lpl2175	similar to amidotransferase	-1.6
lpg1304	trpB	lpp1268	lpl1267	tryptophan synthase beta subunit	-1.6
lpg2282	asnS	lpp2236	lpl2208	asparagine tRNA synthetase	-1.6
lpg2848	-	lpp2906	lpl2760	similar to ribonuclease	-1.6
lpg1873	-	lpp1838	lpl1835	similar to membrane-bound lytic murein transglycosylase B precursor	-1.6
lpg0298	surA	lpp0376	lpl0351	similar to peptidyl-prolyl cis-trans isomerase SurA	-1.6
lpg1922	-	lpp1897	lpl1886	similar to ATP-dependent DNA helicase	-1.6
lpg0533	sucB	lpp0598	lpl0579	dihydrolipoamide succinyltransferase- E2 subunit	-1.6
lpl1530	prpC	lpp1487	lpl1496	2-methylcitrate synthase	-1.6
lpg0891	-	lpp0881	-	similar to transposase (IS4 family)	-1.5
lpg0131	dapB	lpp0146	lpl0131	similar to dihydrodipicolinate reductase proteins	-1.5
lpg1855	ppiD	lpp1825	lpl1821	similar to peptidyl-prolyl cis-trans isomerase D	-1.5
lpg1871	lepB1	lpp1836	lpl1833	signal peptidase I	-1.5
lpg2206	-	lpp2157	lpl2131	unknown	-1.5
lpg2184	-	-	-	hypothetical protein	-1.5
lpg1509	-	lpp1466	lpl1517	similar to penicillin-binding protein precursor (D-alanyl-D-alaninecarboxypeptidase fraction C)	-1.5
lpg0371	-	lpp0436	lpl0412	similar to conserved hypothetical proteins	-1.5
lpg1644	-	lpp1614	lpl1382	similar to putative outer membrane proteins	-1.5
lpg1303	trpF	lpp1267	lpl1266	N-(5-phosphoribosyl) anthranilate isomerase	-1.5
lpg2371	-	-	-	hypothetical protein	-1.5
lpg1197	hisB	lpp1199	lpl1205	histidinol-phosphatase/imisazoleglycerol-phosphate dehydratase	-1.5
lpg0323	rpoC	lpp0388	lpl0363	RNA polymerase beta subunit	-1.5
lpg2788	nuoB2	lpp2835	lpl2704	NADH dehydrogenase I chain B	-1.5
lpg0800	nadB1	lpp0862	lpl0833	L-aspartate oxidase	-1.5
lpg0120	-	lpp0134	lpl0119	some similarity with *L. pneumophila* IcmL/DotI	-1.5
lpg2936	-	lpp3004	lpl2865	unknown	-1.5
lpg0043	-	lpp0043	lpl0042	similar to conserved hypothetical protein	-1.5
lpg2951	cysK	lpp3022	lpl2880	highly similar to cystathionine beta-synthase	-1.5
lpg2286	-	-	-	pirin	-1.5
lpg2471	hypE	lpp2536	lpl2391	hydrogenase expression/formation protein HypE	-1.5
lpg2286	-	-	-	pirin/signal transduction	-1.5
lpg1448	-	lpp1403	-	similar to transcriptional regulator- LuxR family	-1.5
lpg2604	-	lpp2657	lpl2527	similar to unknown protein	-1.5
lpg2542	-	lpp2608	lpl2463	unknown	-1.5

Gene ID	Name	Paris ID	Lens ID	Description	FC Ratio[1]
lpg1625	-	*lpp1595*	*lpl1398*	unknown	-1.5
lpg2184	-	-	-	hypothetical protein	-1.5
lpg2525	-	-	-	hypothetical protein	-1.5
lpg1504	*aceE*	*lpp1461*	*lpl1522*	pyruvate dehydrogenase (decarboxylase component) E1p	-1.5
lpg1347	-	*lpp1301*	*lpl1300*	similar to rare lipoprotein B RlpB	-1.5
lpg1429	-	*lpp1384*	*lpl1380*	unknown	-1.5
lpg1346	*holA*	*lpp1300*	*lpl1299*	similar to DNA polymerase III- delta subunit HolA	-1.5
lpg1748	*suhB*	*lpp1712*	*lpl1712*	similar to inositol-1-monophosphatase	-1.5
lpg2696	*miaA*	*lpp2751*	*lpl2624*	similar to tRNA delta (2)-isopentenylpyrophosphate transferase	-1.5
lpg1772	-	*lpp1736*	*lpl1736*	similar to conserved hypothetical protein	-1.5
lpg1716	-	*lpp1681*	*lpl1675*	unknown	-1.5
lpg1466	-	*lpp1422*	*lpl1562*	similar to conserved hypothetical protein	-1.5
lpg1141	*potA*	*lpp1143*	*lpl1148*	similar to spermidine/putrescine transport system ATP-binding protein PotA	-1.5
lpg1843	*pip*	*lpp1807*	*lpl1808*	similar to proline iminopeptidase	-1.5
lpg2184	-	-	-	hypothetical protein	-1.5
lpg0041	-	-	-		-1.5
lpg0191	-	*lpp0251*	-	unknown	-1.5
lpg1945	-	*lpp1926*	*lpl1916*	similar to 3-5-cyclic-nucleotide phosphodiesterase precursor (CpdP)	-1.5
lpg1575	-	*lpp1533*	*lpl1450*	hypothetical protein	-1.5
lpg2451	-	*lpp2516*	*lpl2369*	similar to N-hydroxyarylamine O-acetyltransferase	-1.4
lpg0007	-	*lpp0007*	*lpl0007*	putative carbon-nitrogen hydrolase family protein	-1.4
lpg2834	-	*lpp2891*	*lpl2746*	similar to transcriptional accessory protein	-1.4
lpg2571	-	-	-	hypothetical protein	-1.4
lpg0078	*ubiH*	*lpp0092*	*lpl0080*	similar to 2-octaprenyl-6-methoxyphenol hydroxylase	-1.4
lpg1027	*ceaC2*	*lpp2353*	*lpl2065*	chemiosmotic efflux system C protein C	-1.4
lpg1834	*metI*	*lpp1797*	*lpl1798*	similar to ABC transporter permease protein	-1.4
lpg0188	-	*lpp0249*	*lpl0248*	similar to predicted acyl-CoA transferases	-1.4

[1] Fold Change (FC)

Table 4.S3. Induced genes shared between PE phase and NA-treated *L. pneumophila*

Gene ID	Name	Paris ID	Lens ID	Description	PE FC[1]	NA FC[1]
lpg1340	*flaA*	*lpp1294*	*lpl1293*	flagellin	104.5	144.1
lpg1160	-	*lpp1162*	*lpl1168*	unknown	88.2	83.2
lpg2493	-	*lpp2559*	*lpl2414*	similar to small heat shock protein	86.3	74.5
lpg2157	*sdeA*	*lpp2096*	*lpl2085*	sdeA	75.0	70.1
lpg1339	-	*lpp1293*	*lpl1292*	unknown	71.7	90.0
lpg1496	-	*lpp1453*	*lpl1530*	some similarities with sidE protein	60.1	35.0
lpg2395	-	*lpp2461*	*lpl2318*	unknown	55.5	15.2
lpg2222	-	*lpp2174*	*lpl2147*	similar to unknown protein	47.9	45.9
lpg1206	-	*lpp1208*	*lpl1214*	similar to unknown protein	43.4	36.7
lpg0901	-	*lpp0962*	*lpl0932*	unknown	43.0	16.3
lpg0910	-	*lpp0972*	*lpl0942*	to enhanced entry protein EnhA	40.8	56.0
lpg2246	-	*lpp2200*	*lpl2172*	unknown	40.0	40.9
lpg0088	-	*lpp0102*	*lpl0087*	similar to arginine-binding periplasmic protein	35.3	22.9
-	-	*lpp0052*	*lpl0050*	unknown	34.6	17.3
lpg1336	-	*lpp1290*	*lpl1289*	similar to enhanced entry protein EnhA	33.3	12.3
lpg0672	-	*lpp0728*	*lpl0708*	similar to acetoacetate decarboxylase	32.9	37.4
lpg2181	-	*lpp2133*	*lpl2108*	similar to response regulator	27.7	31.8
lpg0499	-	*lpp0561*	*lpl0537*	similar to carboxy-terminal protease family protein	27.5	14.6
lpg1669	-	*lpp1641*	*lpl1634*	unknown	27.3	17.5
-	*sdeB*	-	*lpl2084*	SdeB	27.3	25.1
lpg0644	-	-	-	hypothetical protein	25.5	11.5
-	-	*lpp2869*	*lpl2732*	hypothetical gene	23.7	32.2
lpg0673	-	*lpp0729*	*lpl0709*	similar to unknown protein	23.4	17.8
lpg0969	-	*lpp1031*	*lpl0998*	unknown	23.3	9.5
lpg2268	-	*lpp2222*	*lpl2194*	putative membrane protein	23.1	4.5
lpg1337	*fliS*	*lpp1291*	*lpl1290*	similar to flagellar protein FliS	22.7	11.9
lpg2509	*sdeD*	*lpp2577*	*lpl2431*	SdeD protein (substrate of the Dot/Icm system)	22.4	25.0
lpg0383	-	*lpp0450*	*lpl0426*	unknown	22.3	5.8
lpg0902	-	*lpp0963*	*lpl0933*	unknown	22.2	12.9
lpg2957	-	*lpp3028*	*lpl2886*	similar to protease	22.1	17.5
lpg1960	-	*lpp1942*	*lpl1934*	unknown	22.0	18.9
lpg1038	-	*lpp2343*	-	unknown	21.5	5.2
lpg2990	-	*lpp3061*	*lpl2918*	unknown	21.4	23.6
lpg2153	*sdeC*	*lpp2092*	*lpl2081*	SdeC protein- substrate of the Dot/Icm system	21.2	16.0
lpg0644	-	-	-	hypothetical protein	21.0	15.3
lpg2529	-	*lpp2594*	*lpl2449*	unknown	20.9	18.4
lpg1338	*fliD*	*lpp1292*	*lpl1291*	similar to flagellar hook-associated protein 2 (flagellar capping protein)	20.9	13.4
lpg1793	-	*lpp1757*	*lpl1757*	unknown	20.8	6.0
lpg1226	*flgL*	*lpp1234*	*lpl1234*	flagellar hook-associated protein FlgL	20.6	11.8
-	-	*lpp0364*	*lpl0339*	signal peptide predicted	20.5	9.5
lpg0245	-	*lpp0315*	*lpl0299*	similar to C-terminal part of conserved hypothetical protein	20.5	15.1
lpg0967	-	*lpp1029*	*lpl0996*	unknown	20.4	7.2
lpg0644	-	-	-	hypothetical protein	19.7	8.0
lpg2511	*sidC*	*lpp2579*	*lpl2433*	SidC protein (substrate of the Dot/Icm system)	19.7	20.2
lpg1683	-	-	-	hypothetical protein	19.6	14.3
lpg0878	-	*lpp0941*	*lpl0911*	unknown	19.3	12.2
lpg1298	-	*lpp1262*	*lpl1261*	unknown	19.1	2.4
lpg1485	-	*lpp1441*	*lpl1543*	similar to unknown protein	19.1	4.3
lpg2049	-	*lpp2032*	*lpl2027*	unknown	18.9	3.0
lpg1491	-	*lpp1447*	*lpl1537*	some similarity with eukaryotic proteins	18.8	10.9
lpg2803	-	*lpp2849*	*lpl2718*	similar to putative coproporphyrinogen oxidase A	18.8	8.5
lpg2334	-	*lpp2282*	*lpl2254*	unknown	18.7	15.3
lpg2351	-	*lpp2300*	*lpl2273*	unknown	18.1	20.2

					PE	NA
Gene ID	Name	Paris ID	Lens ID	Description	FC[1]	FC[1]
lpg2666	-	*lpp2720*	*lpl2593*	similar to unknown protein	17.9	7.5
lpg0644	-	-	-	hypothetical protein	17.9	21.0
lpg1876	-	*lpp1841*	*lpl1838*	similar to unknown protein	17.7	13.4
lpg1111	-	*lpp1112*	*lpl1115*	unknown	17.7	11.9
-	-	*lpp1110*	*lpl1113*	hypothetical protein	17.6	11.4
-	-	*lpp1260*	*lpl1259*	unknown	17.6	9.1
lpg1895	-	*lpp1864*	*lpl1859*	unknown	17.0	3.6
lpg0393	-	*lpp0460*	*lpl0436*	unknown	16.6	6.3
lpg1290	-	*lpp1253*	-	unknown	16.2	3.3
lpg1115	-	*lpp1116*	*lpl1121*	similar to other protein- ATP binding site	16.1	12.5
lpg1686	-	-	-	hypothetical protein	15.6	15.9
lpg0671	-	*lpp0727*	*lpl0707*	similar to NADH-ubiquinone oxidoreductase	15.6	10.4
-	-	-	*lpl1530*	hypothetical protein	15.5	9.8
lpg2578	-	*lpp2630*	*lpl2500*	unknown	15.3	2.9
-	-	-	*lpl2384*	hypothetical protein	15.3	14.1
lpg0620	-	*lpp0674*	*lpl0657*	unknown	15.2	6.3
-	-	-	*lpl2295*	hypothetical protein	14.6	2.9
lpg2641	*enhA*	*lpp2694*	*lpl2566*	enhanced entry protein EnhA	14.6	4.0
lpg2076	-	-	-	hypothetical protein	14.4	10.5
lpg1782	*fliA*	*lpp1746*	*lpl1746*	sigma factor 28	14.3	4.7
lpg2457	-	*lpp2523*	*lpl2376*	similar to two-component response regulator	14.2	2.5
lpg2482	*sdbB*	*lpp2546*	*lpl2402*	SdbB protein (putative substrate of the Dot/Icm system)	14.0	7.3
lpg0279	-	*lpp0354*	*lpl0331*	similar to conserved hypothetical protein	13.7	5.8
lpg0741	-	*lpp0806*	*lpl0777*	similar to conserved hypothetical protein	13.6	13.4
lpg1636	-	*lpp1606*	*lpl1390*	similar to acetyltransferase- GNAT family	13.4	5.1
lpg1117	-	*lpp1118*	*lpl1123*	similar to *B. subtilis* PaiA transcriptional repressor of sporulation	13.3	8.5
lpg0037	-	*lpp0036*	*lpl0037*	similar to arginine transport system periplasmic binding protein	13.2	11.6
lpg2971	-	*lpp3043*	*lpl2901*	similar to NAD-linked malate dehydrogenase (malic enzyme)	13.1	14.5
lpg1135	-	*lpp1136*	*lpl1141*	similar to transcriptional regulator- TetR family	12.7	5.2
-	-	*lpp2567*	*lpl2421*	unknown	12.4	3.9
lpg2149	-	*lpp2088*	*lpl2077*	unknown	12.3	11.1
lpg1207	-	*lpp1209*	*lpl1215*	similar to conserved hypothetical protein	12.3	10.2
lpg0968	-	*lpp1030*	*lpl0997*	unknown	12.1	3.7
lpg1102	-	-	-	hypothetical protein	12.0	2.0
lpg1495	-	*lpp1452*	*lpl1531*	unknown	11.8	10.9
lpg1220	*flgF*	*lpp1228*	*lpl1228*	flagellar biosynthesis protein FlgF	11.7	4.3
lpg2510	*sdcA*	-	-	sdcA	11.7	12.2
lpg2105	-	-	-	transmembrane protein	11.6	4.5
lpg2464	-	-	-	hypothetical protein	11.6	6.7
lpg0244	-	*lpp0314*	*lpl0298*	similar to oxydoreductase	11.6	8.7
lpg2527	-	*lpp2592*	*lpl2447*	unknown	11.3	8.1
lpg1385	-	*lpp1340*	*lpl1336*	unknown	11.3	7.3
lpg2258	-	*lpp2212*	*lpl2184*	putative membrane protein	11.3	2.7
lpg0717	-	*lpp0783*	*lpl0754*	unknown	11.2	4.0
lpg2106	-	-	-	hypothetical protein	11.2	3.7
lpg2459	-	*lpp2525*	*lpl2378*	similar to guanylate cyclase-related protein	11.2	2.2
-	-	-	*lpl1116*	hypothetical protein	11.1	4.3
lpg1253	*lvhB4*	*lpp0171*	*lpl0154*	*Legionella* vir homologue protein putative type IV secretion protein	11.0	8.3
lpg1225	*flgK*	*lpp1233*	*lpl1233*	flagellar hook-associated protein 1	11.0	2.8
lpg0380	-	*lpp0447*	*lpl0423*	unknown	10.9	4.6
lpg2510	*sdcA*	*lpp2578*	*lpl2432*	SdcA protein- paralog of SidC (substrate of the Dot/Icm system)	10.8	7.5
-	-	*lpp2998*	*lpl2859*	similar to conserved hypothetical protein	10.8	3.9
lpg1950	*ralF*	*lpp1932*	*lpl1919*	RalF protein- translocated into host cells by the Dot/Icm system	10.7	12.3
lpg2209	-	*lpp2160*	*lpl2134*	similar to conserved hypothetical protein	10.6	3.7
lpg1055	-	-	-	hypothetical protein	10.5	6.5
lpg1356	-	*lpp1310*	*lpl1307*	similar to unknown protein	10.4	7.5
lpg2640	*enhB*	*lpp2693*	*lpl2565*	enhanced entry protein EnhB	10.4	5.4
lpg0009	-	*lpp0009*	*lpl0009*	similar to host factor-1 protein	10.3	7.7
-	-	*lpp0352*	-	regulatory protein (GGDEF domain)	10.1	4.9

					PE	NA
Gene ID	Name	Paris ID	Lens ID	Description	FC[1]	FC[1]
lpg0196	-	*lpp0253*	*lpl0252*	unknown	10.0	8.0
lpg2147	-	*lpp2086*	*lpl2075*	unknown	10.0	9.9
lpg1887	-	*lpp1854*	*lpl1849*	Q-rich protein	10.0	12.4
lpg2759	-	*lpp2807*	*lpl2676*	unknown	10.0	3.2
lpg1885	-	*lpp1849*	*lpl1846*	unknown	9.9	3.4
-	-	*lpp2976*	*lpl2824*	unknown	9.9	4.1
lpg2393	-	*lpp2460*	*lpl2317*	similar to bacterioferritin	9.8	3.7
lpg2958	-	*lpp3029*	*lpl2887*	transmembrane protein- similar to membrane-bound serine protease	9.7	5.1
lpg0846	-	*lpp0908*	*lpl0877*	similar to conserved hypothetical protein	9.7	5.2
lpg2465	*sidD*	-	-	sidD	9.7	16.1
lpg2639	*enhC*	*lpp2692*	*lpl2564*	enhanced entry protein EnhC	9.7	6.2
lpg1112	-	-	-	hypothetical protein	9.6	3.2
lpg2862	*legC8*	-	-	coiled-coil containing protein	9.6	8.3
lpg0415	-	*lpp0482*	*lpl0458*	similar to hypothetical proteins	9.5	8.7
lpg1925	-	*lpp1900*	*lpl1891*	unknown	9.5	6.6
lpg2207	-	*lpp2158*	*lpl2132*	similar to unknown protein	9.5	7.2
lpg2831	-	*lpp2888*	-	unknown	9.4	3.7
lpg0670	-	*lpp0726*	*lpl0706*	similar to predicted esterae	9.3	8.6
lpg2520	-	*lpp2588*	*lpl2442*	unknown	9.2	3.9
lpg0847	*murA*	*lpp0909*	*lpl0878*	UDP-N-acetylglucosamine 1-carboxyvinyltransferase	9.1	8.9
lpg1918	-	*lpp1893*	*lpl1884*	weakly similar to endoglucanase	9.1	7.4
lpg0147	-	-	-	transposase	9.1	4.6
lpg0737	-	*lpp0802*	*lpl0773*	similar to conserved hypothetical protein	9.1	3.9
lpg0907	*flgM*	*lpp0969*	*lpl0939*	similar to negative regulator of flagellin synthesis (Anti-sigma-28 factor)	9.1	4.1
lpg1039	-	*lpp2342*	-	similar to unknown protein	9.1	6.4
lpg2316	-	*lpp2264*	*lpl2236*	similar to 3-hydroxybutyrate dehydrogenase	8.9	8.8
lpg2402	-	*lpp2467*	*lpl2325*	similar to transcriptional regulator- LysR family	8.9	4.1
-	-	*lpp1115*	*lpl1119*	similar to other proteins	8.8	5.4
lpg2426	-	*lpp2493*	-	similar to malonate decarboxylase- alpha subunit	8.7	5.0
lpg1993	-	*lpp1974*	*lpl1969*	similar to putative polysaccharide deacetylase-related protein	8.7	7.4
lpg1309	-	*lpp1273*	*lpl1272*	unknown	8.6	4.1
lpg0674	-	*lpp0730*	*lpl0710*	similar to adenylate cyclase	8.6	3.3
lpg1455	-	*lpp1411*	*lpl1573*	similar to *Legionella pneumophila* putative phospholipase C	8.5	7.4
lpg2017	-	*lpp1999*	*lpl1994*	unknown	8.5	3.9
lpg1161	-	*lpp1163*	*lpl1169*	similar to predicted phosphoribosyl transferase	8.5	2.9
lpg0527	-	*lpp0592*	*lpl0573*	similar to conserved hypothetical protein	8.4	3.9
lpg1145	-	*lpp1147*	*lpl1151*	unknown	8.3	6.4
lpg1058	-	*lpp2323*	*lpl1055*	similar to polyhydroxyalkanoic-acid-synthase	8.2	5.0
lpg2187	-	*lpp2137*	*lpl2112*	unknown	8.2	5.8
lpg2442	-	*lpp2509*	*lpl2362*	unknown	8.1	5.0
lpg2075	*dam*	-	-	DNA adenine methylase	8.1	5.2
lpg2820	-	*lpp2873*	-	similar to predicted oxidoreductase	8.1	8.3
lpg0632	-	*lpp0686*	*lpl0669*	similar to type-4 fimbrial pilin related protein	8.0	2.4
lpg1796	-	*lpp1760*	*lpl1760*	similar to transcriptional regulator (LysR family)	7.9	5.8
lpg1168	-	*lpp1170*	*lpl1176*	regulatory protein (GGDEF and EAL domains)	7.9	5.3
lpg1223	*flgI*	*lpp1231*	*lpl1231*	flagellar P-ring protein precursor FlgI	7.9	1.8
lpg2311	-	*lpp2259*	*lpl2230*	unknown	7.8	6.4
lpg2257	-	*lpp2211*	*lpl2183*	unknown	7.7	4.3
lpg1116	-	*lpp1117*	*lpl1122*	similar to chitinase	7.7	7.0
lpg2323	-	*lpp2271*	*lpl2243*	similar to type II secretion system protein-like protein and twitching mobility pr	7.7	4.7
-	-	*lpp2368*	-	unknown	7.7	6.3
lpg2583	-	*lpp2635*	*lpl2505*	similar to FlhB protein- part of export apparatus for flagellar proteins	7.6	2.7
lpg0277	-	*lpp0351*	*lpl0329*	regulatory protein (EAL domain)	7.6	6.3
lpg0278	-	*lpp0353*	*lpl0330*	similar to two-component sensor histidine kinase	7.6	4.1
lpg2138	-	*lpp2077*	*lpl2067*	similar to transcriptional regulator- LysR family	7.6	2.6
lpg1083	-	-	-	hypothetical protein	7.6	4.7
lpg0151	-	-	-	hypothetical protein	7.6	5.0
-	-	*lpp2958*	*lpl2807*	unknown	7.4	1.6
lpg2427	-	*lpp2494*	-	similar to malonate decarboxylase- beta subunit	7.4	4.7

| | | | | | PE | NA |
Gene ID	Name	Paris ID	Lens ID	Description	FC[1]	FC[1]
lpg1092	-	*lpp1093*	*lpl1096*	similar to beta-phosphoglucomutase	7.4	5.2
-	-	-	*lpl2385*	hypothetical protein	7.3	12.4
-	-	*lpp0216*	*lpl0211*	hypothetical protein	7.3	4.3
lpg2561	-	-	-	hypothetical protein	7.2	3.2
lpg0669	-	*lpp0725*	*lpl0705*	similar to hypothetical protein	7.1	8.9
-	*sidH'*	*lpp2886*	-	substrates of the *Legionella pneumophila* Dot/Icm system	7.1	8.4
lpg1944	-	*lpp1925*	*lpl1914*	similar to conserved hypothetical protein	7.1	5.5
lpg2406	*lidE*	*lpp2472*	*lpl2329*	lidE	7.1	4.0
-	-	*lpp1177*	*lpl1183*	unknown	7.1	4.0
lpg1123	-	*lpp1124*	*lpl1128*	similar to amino acid ABC transporter (amino acid binding protein)	7.1	2.1
-	-	*lpp0208*	-	some similarity with nucleoside hydrolase	7.1	3.9
lpg1046	-	*lpp2336*	-	unknown	7.0	3.8
lpg1110	-	*lpp1111*	*lpl1114*	unknown	7.0	3.6
-	-	*lpp2988*	*lpl2846*	highly similar to putative lytic murein transglycosylase	7.0	5.4
lpg1032	-	*lpp2348*	-	unknown	7.0	4.7
lpg1639	-	*lpp1609*	*lpl1387*	unknown	7.0	5.8
lpg1985	-	*lpp1966*	*lpl1960*	similar to guanine deaminase	7.0	3.9
lpg1490	-	*lpp1446*	*lpl1538*	similar to adenylate cyclase- family 3	6.9	5.2
lpg0817	-	*lpp0879*	*lpl0850*	similar to ATP-dependent Clp protease adaptor protein ClpS	6.9	2.2
lpg1025	-	*lpp2355*	-	regulatory protein (GGDEF domain)	6.9	4.1
lpg2107	-	-	-	hypothetical protein	6.9	3.4
lpg2721	-	*lpp2778*	*lpl2649*	similar to unknown protein	6.8	4.4
lpg0165	-	*lpp0226*	*lpl0228*	similar to conserved hypothetical protein	6.8	5.0
lpg0156	-	*lpp0219*	*lpl0220*	regulatory protein (GGDEF domain)	6.7	10.8
lpg2719	-	*lpp2776*	*lpl2647*	similar to conserved hypothetical protein	6.7	3.2
lpg2829	*sidH*	*lpp2883*	-	substrate of the *Legionella pneumophila* Dot/Icm system	6.7	2.3
lpg2154	-	*lpp2093*	*lpl2082*	similar to *L. pneumophila* SdeA protein	6.6	9.7
lpg2955	*himD*	*lpp3026*	*lpl2884*	highly similar to integration host factor- beta subunit	6.6	2.9
lpg1454	-	*lpp1410*	*lpl1590*	similar to probable multidrug efflux protein	6.6	6.3
lpg0854	-	*lpp0916*	*lpl0885*	unknown	6.5	2.8
lpg0233	*mdlC*	-	-	benzoylformate decarboxylase	6.5	3.9
lpg1903	-	*lpp1876*	*lpl1867*	similar to hypothetical protein	6.4	5.9
lpg0818	*clpA*	*lpp0880*	*lpl0851*	ATP-dependent Clp protease ATP-binding subunit ClpA	6.4	5.1
lpg0157	-	*lpp0220*	*lpl0221*	regulatory protein (EAL domain)	6.4	4.4
lpg0074	-	*lpp0088*	*lpl0076*	similar to other proteins	6.3	3.7
lpg2441	-	*lpp2508*	-	similar to hypothetical proteins	6.3	3.7
lpg2192	-	-	-	small HspC2 heat shock protein	6.3	4.4
lpg1659	-	*lpp1630*	*lpl1624*	similar to hypothetical proteins	6.2	3.7
lpg2191	*gspA*	*lpp2141*	*lpl2116*	global stress protein GspA	6.2	3.5
lpg2830	-	*lpp2887*	-	conserved ubiquitin conjugation factor E4 family domain (U-box)	6.2	3.5
lpg1055	-	*lpp2327*	-	unknown	6.1	4.7
lpg1154	-	*lpp1156*	*lpl1161*	unknown	6.1	4.8
lpg1125	-	*lpp1126*	*lpl1130*	similar to amino acid ABC transporter	6.1	3.9
lpg0892	-	*lpp0953*	*lpl0923*	similar to kynurenine 3-monooxygenase	6.0	3.5
lpg2761	-	*lpp2809*	*lpl2678*	unknown	6.0	18.2
lpg2317	-	*lpp2265*	*lpl2237*	similar to conserved hypothetical protein	6.0	5.4
lpg1224	*flgJ*	*lpp1232*	*lpl1232*	flagellar biosynthesis protein FlgJ	5.9	2.6
lpg1095	-	-	-	chemiosmotic efflux system B protein B	5.9	6.1
lpg1622	-	*lpp1592*	*lpl1401*	unknown	5.9	2.0
lpg0906	-	*lpp0968*	*lpl0938*	similar to unknown protein	5.9	2.9
lpg1915	-	*lpp1890*	*lpl1881*	similar to type IV pilin PilA	5.9	5.0
lpg1670	-	*lpp1642*	*lpl1635*	unknown	5.9	6.8
lpg2495	-	*lpp2562*	*lpl2416*	similar to homospermidine synthase	5.8	5.6
lpg2028	*hemE*	*lpp2010*	*lpl2005*	uroporphyrinogen decarboxylase	5.8	4.7
lpg1030	*cecA1*	*lpp2350*	-	chemiosmotic efflux system C protein A	5.8	3.4
lpg0940	*lidA*	*lpp1002*	*lpl0971*	LidA protein- substrate of the Dot/Icm system	5.8	5.0
lpg2161	-	*lpp2100*	*lpl2089*	similar to conserved hypothetical protein	5.8	2.3
lpg2364	-	-	-	hypothetical protein	5.8	2.8
lpg1282	*surE*	*lpp1245*	*lpl1245*	acid phosphatase SurE (Stationary phase survival protein)	5.8	3.5

					PE	NA
Gene ID	Name	Paris ID	Lens ID	Description	FC[1]	FC[1]
lpg1951	-	*lpp1933*	*lpl1920*	weakly similar to sphingosine kinase	5.7	2.6
lpg1355	*sidG*	*lpp1309*	-	SidG protein- substrate of the Dot/Icm system	5.7	4.6
lpg2720	-	*lpp2777*	*lpl2648*	putative cAMP/cGMP binding protein	5.7	2.0
lpg0586	-	*lpp0636*	*lpl0620*	similar to conserved hypothetical protein	5.7	3.3
lpg2108	-	-	-	hypothetical protein	5.7	3.3
lpg2327	-	*lpp2275*	*lpl2247*	unknown	5.6	5.5
lpg1360	*lspI*	*lpp1314*	*lpl1311*	type II secretory pathway protein LspI	5.6	5.6
-	-	*lpp1640*	-	unknown	5.6	15.7
lpg2528	-	*lpp2593*	*lpl2448*	weakly similar to alpha-glucosidase	5.6	4.6
lpg2642	-	*lpp2695*	*lpl2568*	regulatory protein (GGDEF and EAL domains)	5.6	4.4
lpg1218	*flgD*	*lpp1226*	*lpl1226*	flagellar basal-body rod modification protein FlgD	5.6	2.4
lpg1151	-	*lpp1153*	*lpl1157*	unknown	5.5	3.0
lpg0631	-	*lpp0685*	*lpl0668*	weakly similar with pre-pilin leader sequence	5.5	4.7
lpg1415	*gltA*	*lpp1370*	*lpl1366*	citrate synthase	5.5	4.8
lpg3000	-	*lpp3072*	*lpl2928*	unknown	5.5	3.1
lpg2132	-	*lpp2071*	*lpl2061*	regulatory protein (GGDEF domain)	5.4	1.7
lpg1926	-	*lpp1901*	*lpl1892*	similar to conserved hypothetical protein	5.4	4.6
lpg1155	-	*lpp1157*	*lpl1162*	similar to eukaryotic pyruvate decarboxylase	5.4	4.2
lpg1024	*copA1*	*lpp2356*	-	similar to copper efflux ATPase	5.4	5.3
lpg1635	-	*lpp1605*	*lpl1391*	similar to hypothetical proteins	5.4	4.5
lpg2582	-	*lpp2634*	*lpl2504*	similar to hypothetical proteins	5.3	1.8
lpg0227	-	*lpp0286*	*lpl0281*	unknown	5.3	3.7
lpg2422	-	*lpp2487*	*lpl2345*	some similarity with eukaryotic proteins	5.3	4.8
lpg1170	-	*lpp1172*	*lpl1178*	similar to Pyruvate formate-lyase activating enzyme	5.3	1.5
lpg2248	-	*lpp2202*	*lpl2174*	unknown	5.2	4.2
lpg2492	-	*lpp2558*	*lpl2413*	similar to alcohol dehydrogenase	5.2	2.3
lpg2508	-	*lpp2576*	*lpl2430*	unknown	5.2	3.9
lpg0267	-	*lpp0341*	*lpl0319*	similar to magnesium and cobalt transport proteins	5.2	2.2
lpg1525	-	*lpp1482*	*lpl1501*	putative cAMP/cGMP binding protein	5.1	2.7
lpg1098	-	*lpp1094*	*lpl1097*	unknown	5.1	2.9
lpg2099	-	-	-	methionine sulfoxide reductase B	5.1	3.7
lpg2976	-	*lpp3048*	*lpl2905*	unknown	5.1	3.4
lpg1643	*thrC*	*lpp1613*	*lpl1383*	similar to threonine synthase ThrC	5.1	2.2
-	-	*lpp1762*	*lpl1762*	unknown	5.0	3.3
lpg2111	-	-	-	methionine sulfoxide reductase B	5.0	2.5
lpg2267	-	*lpp2221*	*lpl2193*	similar to imidazolonepropionase and related amidohydrolases	5.0	3.5
lpg2148	-	*lpp2087*	*lpl2076*	unknown	5.0	5.0
lpg2383	-	*lpp2445*	*lpl2301*	similar to transcriptional regulator- LysR family	5.0	5.0
lpg2199	-	*lpp2149*	*lpl2123*	unknown	5.0	6.1
lpg1040	-	*lpp2341*	-	predicted membrane protein- similar to hypothetical protein	5.0	4.2
lpg1105	-	*lpp1104*	*lpl1104*	similar to Peptide methionine sulfoxide reductase msrB	5.0	2.2
lpg2318	*motA2*	*lpp2266*	*lpl2238*	similar to proton conductor component of motor- chemotaxis and motility protein	5.0	2.3
lpg0666	-	*lpp0723*	*lpl0703*	similar to conserved hypothetical protein	4.9	4.4
lpg2196	-	*lpp2146*	*lpl2121*	similar to ketosteroid isomerase homolog	4.9	7.2
lpg2969	-	*lpp3041*	*lpl2899*	similar to conserved hypothetical protein	4.9	2.2
lpg1540	-	*lpp1497*	*lpl1486*	similar to universal stress protein A UspA	4.7	3.6
lpg0589	-	*lpp0639*	*lpl0623*	unknown	4.7	2.5
lpg2228	-	*lpp2180*	*lpl2153*	similar to 3-oxoacyl-[acyl-carrier-protein] synthase III	4.7	2.0
lpg2521	-	*lpp2589*	*lpl2443*	unknown	4.6	3.7
lpg1783	*fleN*	*lpp1747*	*lpl1747*	similar to flagellar synthesis regulator	4.6	2.3
lpg2396	-	*lpp2462*	*lpl2319*	similar to conserved hypothetical protein	4.6	2.3
lpg0926	-	*lpp0988*	*lpl0957*	unknown	4.6	6.6
lpg1948	*legLC4*	-	-	leucine-rich repeat and coiled coil-containing protein	4.6	4.0
lpg2229	-	*lpp2181*	*lpl2154*	similar to acyl-CoA synthetase	4.5	3.0
lpg1522	*pilB*	*lpp1479*	*lpl1504*	pilus assembly protein PilB	4.5	4.6
lpg0873	-	*lpp0936*	*lpl0906*	unknown	4.5	1.7
lpg2526	-	*lpp2591*	*lpl2446*	unknown	4.5	4.8
lpg2155	-	*lpp2094*	*lpl2083*	unknown	4.5	5.2

					PE	NA
Gene ID	Name	Paris ID	Lens ID	Description	FC[1]	FC[1]
lpg2180	-	*lpp2132*	-	similar to two component sensor histidine kinase	4.5	1.9
lpg1949	-	*lpp1931*	*lpl1918*	unknown	4.5	1.7
lpg1671	-	*lpp1643*	*lpl1636*	unknown	4.5	2.9
lpg2409	-	*lpp2476*	*lpl2332*	unknown	4.4	4.7
lpg2888	-	*lpp2947*	*lpl2801*	unknown	4.4	4.7
lpg0073	-	*lpp0087*	*lpl0075*	regulatory protein (GGDEF and EAL domains)	4.4	2.2
-	-	*lpp0964*	*lpl0934*	similar to hypothetical protein	4.4	3.1
lpg1984	-	*lpp1965*	*lpl1959*	similar to hydantoin-racemase	4.3	2.3
lpg2428	-	*lpp2495*	-	similar to malonate decarboxylase- gamma subunit	4.3	4.2
-	-	*lpp2316*	-	similar to hydrolase	4.3	2.7
-	-	*lpp2636*	*lpl2506*	unknown	4.3	3.1
lpg2724	-	*lpp2781*	*lpl2650*	some simillarity with eukaryotic proteins	4.3	5.0
lpg2524	-	-	-	transcriptional regulator, LuxR family	4.3	3.8
lpg2073	-	-	-	hypothetical protein	4.3	3.8
lpg0013	-	*lpp0013*	*lpl0013*	similar to other protein	4.3	3.9
lpg1127	-	*lpp1128*	*lpl1133*	similar to long-chain acyl-CoA synthetase	4.2	3.9
lpg2098	-	-	-	MsrA3 - peptide methionine sulfoxide reductase	4.2	2.3
lpg1977	-	*lpp1960*	*lpl1954*	similar to putative intracellular protease/amidase	4.2	1.7
lpg2074	-	-	-	4-diphosphocytidyl-2-methyl-D-erithritol synthase	4.2	4.1
lpg0625	-	*lpp0679*	*lpl0662*	similar to unknown eukaryotic proteins	4.2	6.9
lpg1908	*gst*	*lpp1883*	*lpl1874*	glutathione S-transferase	4.2	4.9
lpg1279	-	*lpp1242*	*lpl1242*	unknown	4.2	3.5
-	-	*lpp0564*	*lpl0540*	unknown	4.2	3.3
lpg1451	-	*lpp1406*	*lpl1593*	similar to unknown protein	4.1	2.5
lpg1898	-	*lpp1871*	*lpl1862*	similar to MoxR-like ATPases- putative regulator	4.1	3.0
lpg2849	-	*lpp2907*	*lpl2761*	similar to unknown proteins	4.1	2.9
lpg1515	*lssB*	*lpp1473*	*lpl1510*	*Legionella* secretion system protein B	4.1	1.9
lpg0010	-	*lpp0010*	*lpl0010*	similar to GTP-binding protein HflX	4.1	3.6
lpg0585	-	*lpp0635*	*lpl0619*	similar to hypothetical protein	4.1	1.7
lpg0903	-	*lpp0965*	*lpl0935*	similar to protease	4.1	2.1
lpg1278	-	*lpp1241*	*lpl1241*	similar to conserved hypothetical protein	4.1	1.8
lpg1687	-	*lpp1656*	*lpl1650*	unknown	4.0	3.3
lpg2195	-	*lpp2145*	*lpl2120*	similar to ornithine cyclodeaminase	4.0	4.6
lpg1386	-	*lpp1341*	*lpl1337*	some similarity with EnhA protein	4.0	4.6
lpg1080	-	-	-	deoxyguanosinetriphosphate triphosphohydrolase-like protein	4.0	2.8
lpg2301	-	*lpp2249*	*lpl2220*	unknown	4.0	1.6
lpg0113	-	*lpp0126*	*lpl0111*	Ankyrin repeat protein	4.0	3.0
lpg2200	-	*lpp2150*	*lpl2124*	unknown	4.0	8.8
lpg1134	-	*lpp1135*	*lpl1140*	similar to 2-nitropropane dioxygenase	4.0	3.0
lpg1174	*pilR*	*lpp1176*	*lpl1182*	similar to type 4 fimbriae expression regulatory protein PilR (two-component response regulator)	4.0	1.7
lpg2319	*motB2*	*lpp2267*	*lpl2239*	similar to flagellar motor protein	3.9	2.0
lpg2584	*sidF*	*lpp2637*	*lpl2507*	substrate of the Dot/Icm system	3.9	1.8
lpg0893	-	*lpp0954*	*lpl0924*	similar to unknown proteins	3.9	5.7
lpg2205	-	*lpp2156*	*lpl2130*	predicted integral membrane protein	3.9	2.0
lpg2145	-	*lpp2083*	*lpl2073*	similar to two-component response regulator	3.9	3.7
lpg2811	-	*lpp2857*	*lpl2726*	similar to conserved hypothetical protein	3.9	2.0
-	-	*lpp2293*	*lpl2266*	unknown	3.9	2.5
lpg1688	-	*lpp1657*	*lpl1651*	some similarity with flagellar hook-length control protein FliK	3.9	2.0
lpg1523	*pilC*	*lpp1480*	*lpl1503*	pilus assembly protein PilC	3.8	2.9
lpg2018	-	*lpp2000*	*lpl1995*	similar to conserved hypothetical protein	3.8	2.7
-	-	*lpp0577*	*lpl0553*	unknown	3.8	3.8
-	-	*lpp1951*	*lpl1940*	hypothetical gene	3.8	3.0
lpg2310	*murI*	*lpp2258*	*lpl2229*	similar to glutamate racemase	3.8	4.9
lpg2087	*traC*	-	-	TraC	3.8	3.9
lpg2917	-	-	-	hypothetical protein	3.8	4.2
lpg1831	-	*lpp1794*	*lpl1795*	similar to acetyl-coenzyme A synthetase	3.8	3.2
lpg0744	-	*lpp0809*	*lpl0780*	regulatory protein (GGDEF domain)	3.8	2.4
lpg2709	*himA*	*lpp2764*	*lpl2637*	similar to integration host factor- alpha subunit	3.8	1.6

					PE	NA
Gene ID	Name	Paris ID	Lens ID	Description	FC[1]	FC[1]
lpg1779	-	*lpp1743*	*lpl1743*	similar to hypothetical poteins	3.7	3.3
lpg2146	*stuC*	*lpp2084*	*lpl2074*	sensor histidine kinase	3.7	2.4
lpg2532	-	*lpp2597*	*lpl2453*	similar to chorismate mutase (C-terminal part)	3.7	1.6
lpg1555	-	*lpp1512*	*lpl1471*	similar to arginine 3rd transport system periplasmic binding protein	3.7	4.0
lpg0525	*lvgA*	*lpp0590*	*lpl0571*	unknown virulence protein	3.7	2.4
lpg1690	*acnA*	*lpp1659*	*lpl1653*	aconitate hydratase	3.6	4.0
lpg2190	-	*lpp2140*	*lpl2115*	present a domain similar to IcmL prtein	3.6	1.7
-	-	*plpp0012*	-	similar to molybdenum cofactor synthesis protein 3	3.6	1.8
lpg2116	-	-	-	transposase, IS4 family TnpA	3.6	2.0
lpg0845	-	*lpp0907*	*lpl0876*	weakly similar to anti-anti-sigma factor	3.5	2.4
lpg2821	-	*lpp2874*	-	similar to unknown protein	3.5	3.2
lpg1518	*lssE*	*lpp1475*	*lpl1508*	regulatory protein (GGDEF and EAL domains)	3.5	2.3
lpg0894	-	*lpp0955*	*lpl0925*	similar to eukaryotic cytokinin oxidase	3.5	1.7
lpg0842	-	*lpp0904*	*lpl0873*	similar to permease of ABC transporter	3.5	2.0
lpg0665	-	*lpp0722*	*lpl0702*	predicted membrane protein	3.5	3.1
lpg0629	-	*lpp0683*	*lpl0666*	similar to Tfp pilus assembly protein PilX	3.5	2.1
lpg2500	-	*lpp2569*	*lpl2423*	similar to carbonic anhydrase	3.5	4.0
lpg0023	-	*lpp0023*	*lpl0024*	putative membrane protein	3.5	5.4
lpg2810	-	*lpp2856*	*lpl2725*	similar to conserved hypothetical protein	3.4	3.0
lpg2793	*lepA*	*lpp2839*	*lpl2708*	effector protein A- substrate of the Dot/Icm secretion system	3.4	3.3
lpg2816	*rep*	*lpp2868*	*lpl2731*	ATP-dependent DNA helicase Rep	3.4	2.1
-	-	-	*lpl2445*	hypothetical protein	3.4	2.6
lpg0029	-	*lpp0029*	*lpl0030*	regulatory protein (GGDEF and EAL domains)	3.4	2.1
-	-	-	-	structural toxin protein RtxA	3.3	4.4
lpg2112	-	-	-	24 kDa macrophage-induced major protein	3.3	6.2
lpg0723	-	*lpp0789*	*lpl0760*	unknown	3.3	1.6
lpg1983	-	*lpp1964*	*lpl1958*	unknown	3.3	2.2
lpg1551	-	*lpp1508*	*lpl1475*	unknown	3.3	2.9
lpg0200	*qxtA*	*lpp0259*	*lpl0255*	similar to cytochrome d ubiquinol oxidase subunit I	3.3	2.7
lpg1641	-	*lpp1611*	*lpl1385*	similar to acylaminoacyl-peptidase proteins	3.2	2.7
lpg1158	-	*lpp1160*	*lpl1165*	some similarity with eukaryotic proteins	3.2	3.9
lpg0473	-	*lpp0538*	*lpl0514*	conserved hypothetical protein	3.2	3.5
lpg1097	*phbC*	-	-	polyhydroxyalkanoic synthase	3.2	2.0
lpg2212	-	*lpp2163*	*lpl2137*	unknown	3.2	1.7
lpg2399	-	*lpp2465*	*lpl2322*	C-terminal part similar to *Legionella* unknown virulence protein	3.2	6.9
lpg0446	*icmO/dotL*	*lpp0512*	*lpl0488*	icmO/dotL	3.2	2.0
lpg0790	*sdhL*	*lpp0854*	*lpl0828*	similar to L-serine dehydratase	3.2	3.5
lpg0844	-	*lpp0906*	*lpl0875*	similar to unknown protein	3.2	2.8
lpg1106	-	*lpp1105*	*lpl1105*	unknown	3.1	3.0
lpg1987	-	*lpp1968*	*lpl1962*	similar to phosphohistidine phosphatase SixA	3.1	2.0
lpg2812	-	*lpp2858*	*lpl2727*	similar to unknown protein	3.1	2.4
lpg2126	-	*lpp2064*	*lpl2054*	similar to potassium uptake protein	3.1	1.8
lpg1148	-	*lpp1150*	*lpl1154*	putative coiled-coil protein	3.1	3.3
lpg1526	-	*lpp1483*	*lpl1500*	unknown	3.1	2.8
lpg2152	-	*lpp2091*	*lpl2080*	similar to multidrug resistance ABC transporter ATP-binding protein	3.1	2.5
lpg0628	-	*lpp0682*	*lpl0665*	weakly similar to type 4 fimbrial biogenesis protein PilY1	3.1	1.9
lpg0825	-	*lpp0887*	*lpl0856*	similar to peptidase proteins	3.1	2.3
lpg1672	*purN*	*lpp1644*	*lpl1637*	phosphoribosylglycinamide formyltransferase	3.0	2.5
lpg0696	-	*lpp0751*	*lpl0733*	unknown	3.0	2.0
lpg2429	-	*lpp2496*	-	similar to phosphoribosyl-dephospho-CoA transferase	3.0	2.9
lpg2143	-	*lpp2081*	*lpl2071*	unknown	3.0	3.5
lpg1685	-	-	-	hypothetical protein	3.0	2.8
lpg0136	*sdhB1*	*lpp0150*	*lpl0135*	SdhB protein- substrate of the Dot/Icm system	3.0	1.7
-	*0*	*plpp0029*	-	weakly similar to TrbI protein	3.0	2.8
lpg1378	-	*lpp1333*	*lpl1329*	similar to proton/peptide symporter family protein	3.0	1.8
-	-	*lpp1652*	*lpl1645*	unknown	3.0	2.2
lpg1043	-	*lpp2338*	-	similar to unknown protein	3.0	1.6
lpg0056	-	*lpp0058*	*lpl0056*	unknown	3.0	3.0
lpg1701	-	*lpp1666*	*lpl1660*	unknown	3.0	1.7

					PE	NA
Gene ID	Name	Paris ID	Lens ID	Description	FC[1]	FC[1]
lpg0796	-	*lpp0859*	-	unknown	3.0	3.1
lpg2128	-	*lpp2068*	*lpl2058*	unknown	2.9	3.4
lpg2264	-	*lpp2218*	*lpl2190*	similar to unknown protein	2.9	2.9
lpg0269	-	*lpp0343*	*lpl0321*	similar to conserved hypothetical protein	2.9	1.8
lpg0242	-	*lpp0312*	*lpl0296*	similar to D-3 phosphoglycerate dehydrogenase SerA	2.9	3.3
lpg2300	-	*lpp2248*	*lpl2219*	similar to ankyrin repeat domain protein	2.9	2.4
lpg0035	-	*lpp0034*	*lpl0035*	unknown	2.9	2.1
lpg2689	*icmX*	*lpp2743*	*lpl2616*	intracellular multiplication protein IcmX	2.9	2.9
lpg1292	-	*lpp1255*	*lpl1254*	similar to two component response regulator	2.9	2.2
lpg0414	-	*lpp0481*	*lpl0457*	similar to ribosomal protein S6 modification enzyme	2.9	2.5
lpg0192	-	-	-	heat shock hsp20	2.8	2.6
-	-	*lpp2560*	-	predicted membrane protein	2.8	4.2
lpg1684	-	-	-	hypothetical protein	2.8	3.6
lpg0843	-	*lpp0905*	*lpl0874*	similar to unknown protein	2.8	2.3
-	-	*lpp2357*	-	unknown	2.8	2.4
lpg0386	-	*lpp0453*	*lpl0429*	highly similar to *C. burnetii* heat shock protein HtpX	2.8	1.9
lpg0238	-	*lpp0308*	*lpl0292*	similar to betaine aldehyde dehydrogenase BetB	2.8	1.8
lpg2458	*shkA*	*lpp2524*	*lpl2377*	similar to two-component sensor histidine kinase	2.8	3.5
lpg2312	-	*lpp2260*	*lpl2231*	unknown	2.8	1.7
lpg2440	-	*lpp2507*	*lpl2361*	similar to conserved hypothetical protein	2.8	4.7
lpg0476	-	*lpp0541*	*lpl0517*	similar to putative sigma-54 modulation protein	2.8	2.6
lpg2431	-	*lpp2498*	-	similar to malonyl-CoA acyl-carrier-protein transacylase	2.8	2.1
lpg2159	-	*lpp2098*	*lpl2087*	similar to (hydroxyindole) O-methyltransferase	2.8	2.4
lpg0276	-	*lpp0350*	*lpl0328*	unknown	2.7	2.3
lpg1961	-	*lpp1943*	*lpl1935*	unknown	2.7	2.3
lpg2916	-	*lpp2985*	*lpl2844*	unknown	2.7	1.9
lpg1726	-	*lpp1691*	*lpl1690*	similar to acyl-CoA dehydrogenase	2.7	2.3
lpg1596	-	*lpp1554*	*lpl1429*	similar to α subunit of fatty-acid oxidation complex-3-hydroxyacyl-CoA dehydrogenase	2.7	2.5
lpg1836	-	*lpp1799*	*lpl1800*	some similarity with eukaryotic protein	2.7	2.6
lpg2731	-	*lpp2787*	*lpl2656*	similar to 2-amino-3-ketobutyrate coenzyme A ligase	2.7	1.7
lpg2216	-	*lpp2167*	*lpl2141*	some similarity with eukaryotic protein	2.7	2.3
lpg2979	-	*lpp3050*	*lpl2907*	hypothetical protein	2.7	2.5
-	-	-	*lpl2845*	hypothetical protein	2.7	1.9
lpg0081	-	*lpp0095*	-	unknown	2.7	2.8
lpg1942	-	*lpp1923*	*lpl1912*	similar to 3-hydroxybutyryl-CoA dehydrogenase	2.7	1.9
lpg1175	-	*lpp1178*	*lpl1184*	similar to putative hydrolase	2.7	3.0
lpg1715	-	*lpp1680*	*lpl1674*	16 kD immunogenic protein	2.7	2.8
lpg0619	-	*lpp0673*	-	unknown	2.7	5.9
lpg1875	-	*lpp1840*	*lpl1837*	similar to putative general secretion pathway protein	2.7	3.0
lpg1468	-	*lpp1424*	*lpl1560*	unknown	2.7	1.7
lpg2909	-	*lpp2978*	-	similar to hypothetical protein	2.6	4.3
lpg1021	-	*lpp2360*	-	similar to metallo-beta-lactamase superfamily proteins	2.6	1.7
lpg1851	-	*lpp1818*	*lpl1817*	unknown	2.6	3.1
lpg0782	-	*lpp0846*	*lpl0821*	similar to O-antigen acetylase	2.6	4.5
lpg2908	-	*lpp2977*	*lpl2825*	highly similar to peptide methionine sulfoxide reductase	2.6	2.3
lpg2376	-	*lpp2441*	-	similar to transcriptional regulator- LysR family	2.6	1.9
lpg0241	-	*lpp0311*	*lpl0295*	similar to glutaminase	2.5	2.0
lpg2110	-	-	-	hypothetical protein	2.5	3.5
lpg2355	-	*lpp2304*	*lpl2277*	similar to amidase	2.5	2.3
lpg0743	-	*lpp0808*	*lpl0779*	similar to unknown proteins	2.5	2.2
lpg2519	-	*lpp2587*	*lpl2441*	unknown	2.5	9.4
lpg2118	-	-	-	transposase TnpA	2.5	2.7
lpg2189	-	*lpp2138*	*lpl2113*	similar to putative transport proteins	2.5	2.1
lpg1780	*motB*	*lpp1744*	*lpl1744*	similar to chemotaxis MotB protein	2.5	1.5
lpg0456	*icmB/dotO*	*lpp0522*	*lpl0498*	icmB/dotO	2.5	1.6
lpg1114	-	*lpp1114*	*lpl1118*	regulatory protein (GGDEF and EAL domains)	2.5	1.6
lpg2606	-	*lpp2659*	*lpl2529*	similar to unknown protein	2.5	3.0
lpg0645	*rtxA-1*	*lpp0699*	*lpl0681*	structural toxin protein RtxA	2.5	3.1

					PE	NA
Gene ID	Name	Paris ID	Lens ID	Description	FC[1]	FC[1]
lpg1132	-	*lpp1134*	*lpl1139*	unknown	2.4	1.8
lpg1042	-	*lpp2339*	-	similar to putative cytochrome c family protein	2.4	1.8
-	-	*lpp2183*	*lpl2156*	similar to acyl carrier protein (ACP)	2.4	2.9
lpg1583	-	*lpp1541*	*lpl1442*	similar to aldehyde dehydrogenase	2.4	2.4
lpg1972	-	*lpp1955*	*lpl1950*	unknown	2.4	3.0
lpg2467	-	*lpp2532*	*lpl2387*	similar to coenzyme F42 unknown-reducing hydrogenase- α subunit	2.4	1.7
lpg1973	-	*lpp1957*	*lpl1951*	unknown	2.4	2.8
lpg0621	*sidA*	*lpp0675*	*lpl0658*	SidA protein- substrate of the Dot/Icm transport system	2.4	2.0
lpg2156	*sdeB*	*lpp2095*	*lpl2084*	substrates of the *Legionella pneumophila* Dot/Icm system SdeB	2.4	2.3
lpg0275	*sdbA*	*lpp0349*	*lpl0327*	SdbA protein- putative substrate of the Dot/Icm system	2.4	1.8
lpg1484	-	*lpp1440*	*lpl1544*	weak similarity to myosin	2.4	2.2
lpg0153	-	*lpp0215*	*lpl0210*	unknown	2.4	2.9
lpg1317	-	-	-	hypothetical protein	2.4	2.3
lpg2741	-	*lpp2797*	*lpl2666*	similar to oligoribonuclease	2.4	2.2
lpg1192	-	*lpp1194*	*lpl1200*	similar to unknown proteins	2.4	2.1
lpg1718	-	*lpp1683*	*lpl1682*	ankyrin repeat protein	2.3	2.4
lpg2039	-	*lpp2022*	*lpl2017*	similar to mevalonate kinase	2.3	1.6
lpg2516	*smlA*	*lpp2584*	*lpl2438*	major facilitator superfamily (MFS) transporter	2.3	2.2
lpg0294	-	*lpp0372*	*lpl0347*	unknown	2.3	1.7
lpg1889	-	*lpp1856*	*lpl1851*	similar to esterase/lipase	2.3	2.5
lpg0452	*icmG/dotF*	*lpp0518*	*lpl0494*	icmG/dotF	2.3	1.5
lpg2262	*ack*	*lpp2216*	*lpl2188*	acetate kinase	2.3	1.8
lpg2925	-	*lpp2991*	*lpl2851*	conserved lipoprotein	2.3	1.6
lpg1126	-	*lpp1127*	*lpl1131*	some similarity with eukaryotic proteins	2.3	1.8
lpg0402	-	*lpp0469*	*lpl0445*	ankyrin repeat protein	2.3	2.3
lpg2256	-	*lpp2210*	*lpl2182*	similar to metallo-beta-lactamase superfamily proteins	2.3	2.1
lpg2435	-	*lpp2502*	*lpl2356*	unknown	2.3	1.5
lpg2460	-	*lpp2526*	*lpl2379*	unknown	2.3	2.1
-	-	*lpp0255*	-	similar to conserved hypothetical protein	2.3	2.2
lpg2742	*cca*	*lpp2798*	*lpl2667*	tRNA nucleotidyltransferase	2.3	1.9
lpg1673	*purD*	*lpp1645*	*lpl1638*	phosphoribosylamine-glycine ligase	2.3	2.1
lpg2794	*msrA*	*lpp2840*	*lpl2709*	similar to phosphoglucomutase	2.3	2.0
lpg2261	*pta*	*lpp2215*	*lpl2187*	similar to phosphotransacetylase	2.3	1.9
lpg0487	-	*lpp0551*	*lpl0527*	similar to hypothetial proteins	2.3	2.0
lpg1041	-	*lpp2340*	-	predicted membrane protein	2.2	2.3
lpg2799	-	*lpp2845*	*lpl2714*	similar to O-acetyltransferase	2.2	1.5
lpg1914	-	*lpp1889*	*lpl1880*	similar to type IV pilin PilA	2.2	1.5
lpg1003	-	*lpp1074*	*lpl1036*	similar to carbon storage regulator	2.2	2.9
lpg1597	-	*lpp1555*	*lpl1428*	similar to β-subunit of fatty acid oxidation complex-3-keto-acyl-CoA-thiolase	2.2	2.8
lpg2129	-	-	-	hypothetical protein	2.2	2.0
-	-	*lpp0617*	*lpl0600*	hypothetical protein	2.2	2.6
lpg2231	-	*lpp2184*	*lpl2157*	similar to 3-oxoacyl-[acyl-carrier protein] reductase	2.2	2.5
lpg0540	-	*lpp0604*	*lpl0585*	similar to putative transport proteins	2.2	2.0
lpg2550	-	*lpp2619*	*lpl2471*	unknown	2.2	2.0
-	-	*lpp0158*	*lpl0143*	unknown	2.2	1.9
lpg1940	-	*lpp1921*	*lpl1910*	similar to peptide antibiotic synthetase	2.2	1.7
lpg0642	-	*lpp0696*	*lpl0679*	unknown	2.1	2.1
lpg2739	-	*lpp2795*	*lpl2664*	similar to cation-efflux system membrane protein	2.1	1.8
lpg0014	-	*lpp0014*	*lpl0014*	similar to conserved hypothetical protein	2.1	1.5
lpg1941	-	*lpp1922*	*lpl1911*	similar to acyl-coA dehydrogenase	2.1	2.0
lpg2879	-	*lpp2938*	*lpl2792*	unknown	2.1	2.1
lpg2498	-	*lpp2566*	*lpl2420*	unknown	2.1	2.0
-	-	*lpp2518*	*lpl2371*	unknown	2.1	1.8
lpg1630	-	*lpp1600*	-	similar to 3-beta hydroxysteroid dehydrogenase/isomerase	2.1	1.8
-	-	*lpp3009*	-	unknown	2.1	1.9
lpg1453	-	*lpp1409*	*lpl1591*	unknown	2.1	4.3
lpg1029	*cecA2*	*lpp2351*	-	chemiosmotic efflux system protein A-like protein	2.1	2.2
lpg2201	-	*lpp2151*	*lpl2125*	similar to unknown proteins	2.1	1.9
lpg0270	*pncB*	*lpp0344*	*lpl0322*	nicotinate phosphoribosyltransferase	2.0	1.8

					PE	NA
Gene ID	Name	Paris ID	Lens ID	Description	FC[1]	FC[1]
lpg0788	-	*lpp0852*	*lpl0826*	unknown	2.0	2.4
lpg0214	-	*lpp0273*	*lpl0268*	predicted membrane protein- similar to conserved hypothetical protein LrgA	2.0	4.1
lpg0385	-	*lpp0452*	*lpl0428*	similar to LemA from *Coxiella burnetii*	2.0	3.6
lpg2227	-	*lpp2178*	*lpl2152*	similar to propionyl-CoA carboxylase beta chain	2.0	1.7
lpg2050	-	*lpp2033*	*lpl2028*	unknown	2.0	2.0
lpg1648	-	*lpp1619*	*lpl1614*	putative secreted protein	2.0	1.8
lpg2466	-	*lpp2531*	*lpl2386*	similar to hydrogenase 1 maturation protease	2.0	1.9
-	-	-	*plpl0026*	conjugal pilus assembly protein TraF	2.0	2.0
lpg0428	-	*lpp0495*	*lpl0471*	similar to hypothetical proteins	2.0	2.8
lpg1050	-	*lpp2332*	-	similar to ATP synthase C chain	2.0	1.8
lpg0070	-	*lpp0085*	*lpl0073*	similar to aspartate aminotransferase	2.0	2.3
lpg0841	-	*lpp0903*	*lpl0872*	similar to ABC transporter- ATP-binding protein	2.0	1.6
lpg1274	-	*lpp1237*	*lpl1237*	similar to conserved hypothetical protein	1.9	3.4
lpg1037	-	-	-	hypothetical protein	1.9	1.7
lpg2545	-	*lpp2612*	*lpl2467*	unknown	1.9	1.8
lpg0930	*pilP*	*lpp0992*	*lpl0961*	Tfp pilus assembly protein PilP	1.9	1.9
lpg0477	*rpoN*	*lpp0542*	*lpl0518*	RNA polymerase sigma-54 factor (sigma-L)	1.9	1.6
lpg1318	-	-	-	hypothetical protein	1.9	2.0
lpg0667	-	*lpp0724*	*lpl0704*	similar to conserved hypothetical protein	1.9	2.8
lpg1031	-	*lpp2349*	-	unknown	1.9	1.7
lpg1501	-	*lpp1458*	*lpl1525*	similar to acetyltransferase	1.9	2.0
lpg0401	-	*lpp0468*	*lpl0444*	unknown	1.9	2.6
lpg1497	-	*lpp1454*	*lpl1529*	similar to aminopeptidase N	1.9	2.1
lpg2607	-	*lpp2660*	*lpl2530*	similar to peptidase	1.9	1.7
lpg1059	-	*lpp2322*	*lpl1056*	similar to acetoacetyl-CoA reductase	1.9	1.6
lpg2455	-	*lpp2521*	*lpl2374*	unknown	1.9	2.6
lpg2740	-	*lpp2796*	*lpl2665*	similar to conserved hypothetical protein	1.9	2.2
lpg1959	-	*lpp1941*	*lpl1932*	unknown	1.9	2.0
lpg1057	-	*lpp2324*	*lpl1054*	regulatory protein (GGDEF and EAL domains)	1.9	2.6
-	-	-	*lpl0168*	hypothetical protein	1.9	1.9
lpg2081	*traF*	-	-	sex pilus assembly TraF, thiol-disulfide isomerase and thioredoxins	1.9	1.6
-	-	-	-	RNA polymerase sigma-32 factor	1.8	1.7
lpg0995	-	*lpp1066*	*lpl1028*	unknown	1.8	1.9
lpg2352	*mdh*	*lpp2301*	*lpl2274*	malate dehydrogenase	1.8	2.7
lpg1171	-	*lpp1173*	*lpl1179*	unknown	1.8	3.3
-	-	*lpp2147*	-	unknown	1.8	2.1
lpg0166	-	*lpp0227*	*lpl0229*	similar to conserved hypothetical protein	1.8	4.5
lpg0566	-	*lpp0626*	*lpl0609*	similar to uncharacterized membrane protein- similar to *Bacillus subtilis* spore maturation protein B	1.8	1.8
lpg0944	-	*lpp1006*	-	unknown	1.8	1.9
lpg1744	-	*lpp1708*	*lpl1708*	similar to HesB/YadR/YfhF family proteins	1.8	1.5
lpg0050	-	*lpp0051*	*lpl0049*	putative integral membrane protein	1.8	1.9
lpg2430	-	*lpp2497*	-	similar to 2-(5-triphosphoribosyl)-3-dephosphocoenzyme-A synthase	1.8	2.0
lpg1825	-	*lpp1788*	*lpl1789*	similar to acetyl-CoA acetyltransferase	1.8	2.1
lpg2685	*sbpA*	*lpp2739*	*lpl2612*	small basic protein SbpA	1.8	2.1
-	-	*lpp2069*	*lpl2059*	unknown	1.8	1.7
lpg2546	-	*lpp2615*	-	unknown	1.8	1.5
lpg2547	-	*lpp2616*	*lpl2468*	similar to protein secretion chaperonin CsaA	1.7	1.5
-	*cadA1*	*lpp2369*	-	similar to cadmium-transporting ATPase (C-terminal part)	1.7	1.8
lpg1581	-	*lpp1539*	*lpl1444*	weakly similar to NADP-specific glutamate dehydrogenase	1.7	1.6
lpg2537	-	*lpp2603*	-	similar to conserved hypothetical protein	1.7	1.9
lpg2503	-	-	-	hypothetical protein	1.7	1.5
lpg1928	-	*lpp1903*	*lpl1895*	similar to conserved hypothetical protein	1.7	2.0
lpg2230	-	*lpp2182*	*lpl2155*	similar to acyl-CoA synthetase	1.7	1.7
lpg1882	-	*lpp1846*	*lpl1843*	similar to lactoylglutathione lyase	1.7	1.8
lpg1091	-	*lpp1092*	*lpl1095*	unknown	1.7	2.4
lpg1343	-	*lpp1297*	*lpl1296*	similar to conserved hypothetical protein	1.7	1.9
lpg1933	-	*lpp1914*	*lpl1903*	unknown	1.7	41.5
lpg2518	-	*lpp2586*	*lpl2440*	unknown	1.7	3.9

					PE	NA
Gene ID	Name	Paris ID	Lens ID	Description	FC[1]	FC[1]
lpg0532	*sucA*	*lpp0597*	*lpl0578*	2-oxoglutarate dehydrogenase- E1 subunit	1.7	1.8
lpg2302	*asd*	*lpp2250*	*lpl2221*	aspartate-semialdehyde dehydrogenase	1.7	2.1
lpg0898	-	*lpp0959*	*lpl0929*	unknown	1.6	21.9
lpg0433	-	*lpp0500*	*lpl0476*	putative transcriptional regulator	1.6	1.8
lpg2483	-	*lpp2547*	*lpl2403*	similar to hypothetical protein	1.6	1.5
lpg2667	*rpoH*	*lpp2721*	*lpl2594*	RNA polymerase sigma-32 factor	1.6	1.5
lpg1582	-	*lpp1540*	*lpl1443*	similar to unknown proteins	1.6	1.6
lpg0556	-	*lpp0615*	*lpl0598*	similar to hypothetical proteins	1.6	1.6
lpg1159	-	*lpp1161*	*lpl1167*	similar to putative drug metabolite transport protein (DMT family)	1.6	1.8
lpg0630	-	*lpp0684*	*lpl0667*	similar to Tfp pilus assembly protein PilW	1.6	7.4
lpg2680	-	*lpp2734*	*lpl2607*	similar to D-alanine-D-alanine ligase (N-terminal part)	1.6	1.6
lpg2599	*topA*	*lpp2652*	*lpl2522*	DNA topoisomerase I	1.6	1.6
lpg1564	-	*lpp1521*	*lpl1462*	unknown	1.6	1.6
lpg0518	-	*lpp0581*	*lpl0557*	unknown	1.5	3.5
lpg0253	-	*lpp0323*	*lpl0306*	similar to putative acetyltransferase	1.5	1.6

[1] Fold Change (FC)

Table 4.S4. Repressed genes shared between PE phase and NA-treated *L. pneumophila*

Gene ID	Name	Paris ID	Lens ID	Description	PE FC Ratio[1]	NA FC Ratio[1]
lpg0810	-	*lpp0872*	*lpl0843*	similar to other proteins	-45.0	-23.3
-	-	*lpp2554*	*lpl2410*	hypothetical gene	-23.9	-3.1
lpg1713	*tsf*	*lpp1678*	*lpl1672*	elongation factor Ts (EF-Ts)	-8.7	-3.1
lpg2985	*atpH*	*lpp3056*	*lpl2913*	highly similar to H+-transporting ATP synthase chain delta	-7.1	-3.7
lpg2884	-	*lpp2943*	*lpl2797*	unknown	-6.6	-1.9
lpg2950	-	-	-	hypothetical protein	-6.4	-3.4
lpg0316	*secE*	*lpp0381*	*lpl0356*	preprotein translocase secE subunit	-6.2	-2.0
lpg2652	-	*lpp2705*	*lpl2578*	similar to 50S ribosomal subunit protein L25- RplY	-6.2	-1.9
lpg0319	*rplA*	*lpp0384*	*lpl0359*	50S ribosomal protein L1	-6.0	-3.2
lpg0321	*rplL*	*lpp0386*	*lpl0361*	50S ribosomal subunit protein L7/L12	-6.0	-2.8
lpg0397	*rimM*	*lpp0465*	*lpl0441*	similar to 16S rRNA processing protein RimM	-5.9	-3.0
lpg0419	*glk*	*lpp0486*	*lpl0462*	similar to glucokinase	-5.9	-3.5
lpg2986	*atpF*	*lpp3057*	*lpl2914*	highly similar to H+-transporting ATP synthase chain b	-5.9	-2.1
lpg2983	*atpG*	*lpp3054*	*lpl2911*	highly similar to H+-transporting ATP synthase chain gamma	-5.8	-3.5
lpg2987	*atpE*	*lpp3058*	*lpl2915*	highly similar to H+-transporting ATP synthase chain c	-5.7	-2.4
lpg0395	*rplS*	*lpp0463*	*lpl0439*	50S ribosomal protein L19	-5.7	-1.9
lpg0318	*rplK*	*lpp0383*	*lpl0358*	50S ribosomal protein L11	-5.4	-2.9
lpg2948	-	-	-	hypothetical protein	-5.2	-2.2
lpg0590	-	*lpp0640*	*lpl0624*	similar to competence protein comM	-5.1	-1.9
lpg2726	*ppiB*	*lpp2783*	*lpl2652*	peptidyl-prolyl cis-trans isomerase B (cyclophilin-type PPIase family)	-5.1	-2.1
lpg2984	*atpA*	*lpp3055*	*lpl2912*	highly similar to H+-transporting ATP synthase chain alpha	-5.1	-3.1
lpg0399	*rpsP*	*lpp0466*	*lpl0442*	highly similar to 30S ribosomal protein S16	-5.0	-1.8
lpg0416	*zwf*	*lpp0483*	*lpl0459*	similar to Glucose-6-phosphate 1-dehydrogenase	-4.9	-1.9
lpg0420	*eda*	*lpp0487*	*lpl0463*	similar to 2-deydro-3-deoxyphosphogluconate aldolase/4-hydroxy-2-oxoglutarate aldolase	-4.8	-2.5
lpg0391	-	*lpp0458*	*lpl0434*	similar to prolyl/lysyl hydroxylase	-4.7	-1.9
lpg0349	*secY*	*lpp0414*	*lpl0389*	preprotein translocase- SecY subunit	-4.6	-3.0
lpg2982	*atpD*	*lpp3053*	*lpl2910*	highly similar to H+-transporting ATP synthase beta chain	-4.6	-3.0
lpg0317	*nusG*	*lpp0382*	*lpl0357*	transcription antitermination protein NusG	-4.5	-1.8
lpg0394	-	*lpp0462*	*lpl0438*	similar to methylated-DNA-protein-cysteine S-methyltransferase	-4.5	-1.7
lpg0462	*accC*	*lpp0528*	*lpl0504*	biotin carboxylase (A subunit of acetyl-CoA carboxylase)	-4.5	-3.5
-	*rpmI*	*lpp2768*	*lpl2641*	50S ribosomal protein L35	-4.4	-2.3
lpg2773	*nusA*	*lpp2821*	*lpl2690*	transcription elongation protein nusA	-4.4	-2.5
lpg0340	*rplX*	*lpp0405*	*lpl0380*	50S ribosomal protein L24	-4.2	-1.6
lpg0923	*etfA*	*lpp0985*	*lpl0954*	electron transfer flavoprotein- alpha subunit	-4.2	-2.2
lpg0418	*edd*	*lpp0485*	*lpl0461*	similar to 6-phosphogluconate dehydratase	-4.1	-2.5
lpg0594	-	*lpp0644*	*lpl0628*	similar to unknown protein	-4.1	-2.3
lpg0422	-	*lpp0489*	*lpl0465*	similar to eukaryotic glucoamylase precursor	-4.1	-2.6
lpg0508	*lpxD2*	*lpp0571*	*lpl0547*	UDP-3-O-[3-hydroxymyristoyl] glucosamine N-acyltransferase	-4.1	-1.7
lpg0334	*rplV*	*lpp0399*	*lpl0374*	50S ribosomal subunit protein L22	-4.1	-2.2
lpg1712	*pyrH*	*lpp1677*	*lpl1671*	uridylate kinase (UK) (Uridine monophosphate kinase)	-4.0	-2.6
lpg0595	-	*lpp0645*	*lpl0629*	similar to aminodeoxychorismate lyase (PabC)	-4.0	-2.1
lpg0338	*rpsQ*	*lpp0403*	*lpl0378*	30S ribosomal protein S17	-3.9	-1.5
lpg0343	*rpsH*	*lpp0408*	*lpl0383*	30S ribosomal protein S8	-3.9	-2.2
lpg0341	*rplE*	*lpp0406*	*lpl0381*	50S ribosomal protein L5	-3.8	-1.7
lpg0747	*iraA*	*lpp0813*	*lpl0784*	small-molecule methyltransferase IraA iron acquisition	-3.8	-2.2
lpg3001	-	*lpp3073*	*lpl2929*	similar to GTPase for tRNA modification trmE	-3.8	-1.7
lpg0388	-	*lpp0455*	*lpl0431*	highly similar to ATP-binding component of ABC transporter	-3.8	-2.8
lpg0753	*neuC*	*lpp0819*	*lpl0790*	N-acylglucosamine 2-epimerase/LPS O-antigen biosynthesis	-3.7	-2.0
lpg2000	*secF*	*lpp1981*	*lpl1976*	similar to protein-export membrane protein SecF	-3.7	-2.9
lpg0924	*ald*	*lpp0986*	*lpl0955*	similar to alanine dehydrogenase	-3.6	-2.4
lpg0333	*rpsS*	*lpp0398*	*lpl0373*	30S ribosomal subunit protein S19	-3.6	-2.2
lpg0463	*accB*	*lpp0529*	*lpl0505*	acetyl-CoA carboxylase biotin carboxyl carrier protein	-3.6	-2.3
lpg1714	*rpsB*	*lpp1679*	*lpl1673*	30S ribosomal protein S2	-3.6	-1.8
lpg1606	-	*lpp1571*	*lpl1419*	similar to conserved hypothetical proteins	-3.6	-1.9
lpg1853	*udk*	*lpp1820*	*lpl1819*	uridine kinase	-3.6	-1.5

					PE	NA
Gene ID	Name	Paris ID	Lens ID	Description	FC Ratio[1]	FC Ratio[1]
lpg2943	*lpxA2*	*lpp3016*	-	similar to acyl-[acyl carrier protein]-UDP-N-acetylglucosamine O-acyltransferase	-3.5	-2.3
lpg0171	-	*lpp0232*	*lpl0234*	similar to hypothetical ABC transporter (permease)	-3.5	-2.5
lpg0344	*rplF*	*lpp0409*	*lpl0384*	50S ribosomal subunit protein L6	-3.5	-2.4
lpg0352	*rpsK*	*lpp0417*	*lpl0393*	30S ribosomal protein S11	-3.5	-1.6
lpg0135	-	*lpp0149*	*lpl0134*	similar to hypothetical protein	-3.5	-2.5
lpg1971	-	*lpp1954*	*lpl1949*	similar to organic hydroperoxide resistance protein	-3.4	-1.5
lpg0336	*rplP*	*lpp0401*	*lpl0376*	50S ribosomal protein L16	-3.4	-1.8
lpg0347	*rpmD*	*lpp0412*	*lpl0387*	50S ribosomal subunit protein L3unknown	-3.4	-1.9
lpg0417	*pgl*	*lpp0484*	*lpl0460*	similar to 6-phosphogluconolactonase	-3.4	-2.1
lpg1209	-	*lpp1211*	*lpl1217*	similar to conserved hypothetical protein	-3.3	-2.9
lpg0617	-	*lpp0671*	*lpl0655*	similar to *L. pneumophila* major outer membrane protein	-3.3	-2.5
-	*tufA2*	*lpp0392*	*lpl0367*	translation elongation factor Tu	-3.3	-1.9
lpg0041	-	-	-	hypothetical protein	-3.3	-3.7
lpg1946	-	*lpp1927*	*lpl1917a*	similar to transcriptional regulator- LuxR family	-3.3	-1.8
lpg0084	-	*lpp0098*	*lpl0083*	similar to unknown proteins	-3.2	-2.6
lpg2419	-	-	-	hypothetical protein	-3.2	-2.1
lpg0754	-	*lpp0820*	*lpl0791*	similar to acetyl transferase	-3.2	-2.6
lpg0812	*mreC*	*lpp0874*	*lpl0845*	rod shape-determining protein MreC	-3.2	-2.3
lpg0752	*neuB*	*lpp0818*	*lpl0789*	N-acetylneuraminic acid condensing enzyme peptidoglycan biosynthesis	-3.2	-1.6
lpg1393	*fabH*	*lpp1348*	*lpl1344*	3-oxoacyl-[acyl-carrier-protein] synthase III	-3.1	-2.3
lpg1559	-	*lpp1516*	*lpl1467*	similar to pyruvate dehydrogenase E1 (beta subunit)	-3.1	-2.2
lpg1552	-	*lpp1509*	*lpl1474*	similar to UDP-2-3-diacylglucosamine hydrolase	-3.1	-2.0
lpg1433	*deoC*	*lpp1388*	*lpl1608*	similar to 2-deoxyribose-5-phosphate aldolase	-3.1	-2.5
lpg0461	*prmA*	*lpp0527*	*lpl0503*	ribosomal protein L11 methyltransferase	-3.1	-2.7
lpg2254	-	*lpp2208*	*lpl2180*	similar to conserved hypothetical protein	-3.1	-2.1
lpg0331	*rplW*	*lpp0396*	*lpl0371*	50S ribosomal subunit protein L23	-3.1	-1.6
lpg0460	*purH*	*lpp0526*	*lpl0502*	similar to phosphoribosylaminoimidazolecarboxamide formyltransferase and IMP cyclohydrolase (bifunctionnal)	-3.1	-2.9
lpg0751	*neuA*	*lpp0817*	*lpl0788*	CMP-N-acetylneuraminic acid synthetase peptidoglycan biosynthesis	-3.0	-2.1
lpg0099	*polA*	*lpp0113*	*lpl0099*	DNA polymerase I	-3.0	-2.6
lpg2934	*ubiD*	*lpp3001*	*lpl2862*	highly similar to 3-polyprenyl-4-hydroxybenzoate decarboxylase	-3.0	-1.8
lpg1350	-	*lpp1304*	*lpl1303*	similar to dehydrogenase	-3.0	-1.9
lpg0337	*rpmC*	*lpp0402*	*lpl0377*	50S ribosomal subunit protein L29	-3.0	-1.6
-	-	-	*lpl2342*	hypothetical protein	-3.0	-2.1
lpg2595	*def*	*lpp2648*	*lpl2518*	similar to polypeptide deformylase	-2.9	-2.1
lpg2569	-	-	-	hypothetical protein	-2.9	-1.6
lpg0512	-	*lpp0574*	*lpl0550*	similar to membrane protein involved in chromosome condensation	-2.9	-2.4
lpg1140	*potB*	*lpp1142*	*lpl1147*	similar to spermidine/putrescine transport system permease protein PotB	-2.9	-2.0
lpg0346	*rpsE*	*lpp0411*	*lpl0386*	30S ribosomal subunit protein S5	-2.9	-2.4
lpg1460	-	*lpp1416*	*lpl1568*	similar to unknown protein	-2.9	-2.5
lpg1215	*hemF*	*lpp1223*	*lpl1223*	oxygen-dependent coproporphyrinogen III oxidase	-2.8	-1.6
lpg0767	-	*lpp0832*	*lpl0808*	unknown	-2.8	-2.6
lpg2057	*intD*	-	-	prophage dlp12 integrase	-2.8	-1.5
lpg1351	-	*lpp1305*	*lpl1304*	similar to aldehyde dehydrogenase	-2.8	-2.1
lpg0332	*rplB*	*lpp0397*	*lpl0372*	50S ribosomal subunit protein L2	-2.8	-2.0
lpg1421	*rpsA*	*lpp1376*	*lpl1372*	30S ribosomal protein S1	-2.8	-1.9
lpg1560	-	*lpp1517*	*lpl1466*	pyruvate dehydrogenase E2 (dihydrolipoamide acetyltransferase)	-2.8	-2.2
-	-	*lpp3017*	-	unknown	-2.8	-1.7
lpg0187	-	*lpp0247*	*lpl0247*	similar to conserved hypothetical protein	-2.8	-2.1
lpg0348	*rplO*	*lpp0413*	*lpl0388*	50S ribosomal subunit protein L15	-2.8	-1.9
lpg0787	-	*lpp0851*	-	unknown	-2.7	-1.6
lpg0749	*hisF1*	*lpp0815*	*lpl0786*	similar to imidazole glycerol phosphate synthase subunit HisF	-2.7	-1.9
lpg1434	*xapA*	*lpp1389*	*lpl1607*	similar to xanthosine phosphorylase	-2.7	-1.8
-	-	*lpp0240*	-	similar to hypothetical protein	-2.7	-2.0
lpg2386	-	*lpp2451*	*lpl2310*	unknown	-2.7	-2.0
lpg0596	-	*lpp0646*	*lpl0630*	similar to conserved hypothetical protein- predicted membrane protein	-2.7	-2.0
lpg2643	-	*lpp2696*	*lpl2569*	unknown	-2.7	-1.7
lpg2711	*pheS*	*lpp2766*	*lpl2639*	phenylalanyl-tRNA synthetase- alpha subunit	-2.7	-1.7

					PE	NA
Gene ID	Name	Paris ID	Lens ID	Description	FC Ratio[1]	FC Ratio[1]
lpg1719	-	*lpp1684*	*lpl1683*	similar to methionine aminopeptidase- type I	-2.7	-1.6
lpg0511	*lpxA1*	*lpp0573*	*lpl0549*	UDP-N-acetylglucosamine acyltransferase	-2.7	-1.8
lpg0090	-	*lpp0104*	*lpl0089*	unknown	-2.6	-2.4
lpg0768	-	*lpp0833*	*lpl0809*	similar to sialic acid synthase	-2.6	-1.7
lpg2597	-	*lpp2650*	*lpl2520*	similar to *E. coli* Smf protein	-2.6	-1.8
lpg2659	-	*lpp2713*	*lpl2586*	similar to predicted ATPase	-2.6	-1.9
lpg2554	-	*lpp2624*	*lpl2475*	similar to N-terminal part of rare lipoprotein A	-2.6	-1.6
lpg2674	*dotD*	*lpp2728*	*lpl2601*	lipoprotein DotD	-2.6	-2.0
lpg0423	-	*lpp0490*	*lpl0466*	similar to transcriptional regulator (XRE-family)	-2.6	-1.5
lpg2297	*rne*	*lpp2244*	*lpl2216*	ribonuclease E	-2.6	-2.6
lpg0327	*tufB*	-	-	Elongation factor Tu	-2.5	-2.0
lpg0060	-	-	-	methylase	-2.5	-2.0
lpg0548	-	*lpp0609*	*lpl0590*	similar to phosphopantetheine adenylyltransferase	-2.5	-2.9
lpg0700	-	*lpp0755*	*lpl0737*	similar to L-isoaspartate carboxylmethyltransferase protein pcm	-2.5	-2.0
lpg1332	-	*lpp1286*	*lpl1285*	similar to conserved hypothetical protein	-2.5	-2.3
lpg2772	*infB*	*lpp2820*	*lpl2689*	translation initiation factor IF-2	-2.5	-2.5
lpg1747	-	*lpp1711*	*lpl1711*	similar to putative tRNA/rRNA methyltransferase	-2.5	-2.4
lpg1578	-	*lpp1536*	*lpl1447*	conserved hypothetical protein	-2.5	-1.7
lpg1342	*folC*	*lpp1296*	*lpl1295*	similar to dihydrofolate:folylpolyglutamate synthetase FolC	-2.5	-2.0
lpg0506	-	*lpp0569*	*lpl0545*	similar to protective surface antigen	-2.5	-1.7
lpg2730	-	*lpp2786*	*lpl2655*	similar to cytochrome c5	-2.4	-2.0
lpg0363	-	*lpp0428*	*lpl0404*	similar to lipid A biosynthesis acyltransferase	-2.4	-2.1
lpg0852	-	*lpp0914*	*lpl0883*	unknown	-2.4	-1.7
lpg2771	*rbfA*	*lpp2819*	*lpl2688*	ribosome-binding factor A	-2.4	-2.5
lpg2929	*ksgA*	*lpp2995*	*lpl2855*	similar to dimethyladenosine transferase (16S rRNA dimethylase)	-2.4	-2.0
lpg0292	-	*lpp0370*	*lpl0345*	unknown	-2.4	-2.2
lpg2994	-	*lpp3065*	*lpl2922*	similar to conserved hypothetical protein	-2.4	-2.5
lpg0654	*dam*	*lpp0708*	*lpl0690*	DNA adenine methylase	-2.4	-1.8
lpg1845	-	*lpp1809*	*lpl1810*	conserved lipoprotein	-2.4	-2.3
lpg2728	-	*lpp2785*	*lpl2654*	similar to disulfide bond formation protein DsbB	-2.4	-1.8
lpg1420	*kcy*	*lpp1375*	*lpl1371*	cytidylate kinase	-2.4	-1.5
lpg1195	*hisA*	*lpp1197*	*lpl1203*	phosphoribosylformimino-5-aminoimidazole carboxamide ribotide isomerase	-2.3	-1.5
lpg1974	-	*lpp1958*	*lpl1952*	major outer membrane protein	-2.3	-1.5
-	-	*lpp0214*	*lpl0209*	similar to hypothetical protein	-2.3	-1.7
lpg0728	*thiL*	*lpp0794*	*lpl0765*	thiamine-monophosphate kinase	-2.3	-1.5
lpg0355	*rplQ*	*lpp0420*	*lpl0396*	50S ribosomal protein L17	-2.3	-1.9
lpg2880	*nth*	*lpp2939*	*lpl2793*	endonuclease III	-2.3	-1.9
lpg1380	*hutH*	*lpp1335*	*lpl1331*	similar to histidine ammonia-lyase (Histidase)	-2.3	-1.5
lpg0094	-	*lpp0108*	*lpl0093*	highly similar to ribose 5-phosphate isomerase RpiA	-2.3	-1.7
lpg2593	-	*lpp2646*	*lpl2516*	similar to rRNA methylase (sun protein)	-2.3	-2.2
lpg2476	*hypA*	*lpp2541*	*lpl2396*	hydrogenase nickel incorporation protein HypA	-2.3	-1.9
lpg1570	-	*lpp1528*	*lpl1455*	some similarities to 3 -nucleotidase/nuclease	-2.3	-1.9
lpg2176	-	*lpp2128*	*lpl2102*	similar to eukaryotic sphingosine-1-phosphate lyase 1	-2.2	-2.0
lpg2601	-	*lpp2654*	*lpl2524*	similar to conserved hypothetical protein	-2.2	-1.9
lpg2801	-	*lpp2847*	*lpl2716*	similar to phosphatidylglycerophosphate synthase	-2.2	-2.1
lpg1379	*hutU*	*lpp1334*	*lpl1330*	similar to urocanate hydratase (imidazolonepropionate hydrolase)	-2.2	-1.9
lpg1196	*hisH2*	*lpp1198*	*lpl1204*	imidazole glycerol phosphate synthase subunit HisH (IGP synthase glutamine amidotransferase subunit)	-2.2	-1.7
lpg0698	-	*lpp0753*	*lpl0735*	similar to conserved hypothetical protein	-2.2	-1.8
lpg1906	-	*lpp1881*	*lpl1872*	similar to conserved hypothetical protein	-2.2	-1.5
lpg0111	-	*lpp0124*	*lpl0110*	similar to farnesyl-diphosphate farnesyltransferase (Squalene synthetase)	-2.2	-1.6
lpg0297	-	*lpp0375*	*lpl0350*	similar to organic solvent tolerance protein	-2.2	-1.9
lpg1956	-	*lpp1938*	*lpl1925*	similar to chloromuconate cycloisomerase	-2.2	-1.8
lpg0636	*tdk*	*lpp0690*	*lpl0673*	similar to thymidine kinase	-2.2	-1.6
lpg1419	*aroA*	*lpp1374*	*lpl1370*	3-phosphoshikimate 1-carboxyvinyltransferase	-2.2	-1.9
lpg0195	*katG*	*lpp0252*	*lpl0251*	catalase-peroxidase	-2.2	-1.7
lpg0053	-	*lpp0055*	*lpl0053*	similar to hypothetical protein	-2.2	-2.6
lpg0360	-	*lpp0425*	*lpl0401*	similar to hydroxymyristoyl-(acyl carrier protein) dehydratase	-2.2	-2.0

					PE	NA
Gene ID	Name	Paris ID	Lens ID	Description	FC Ratio[1]	FC Ratio[1]
lpg2658	*feoA*	*lpp2712*	*lpl2585*	ferrous iron transporter A	-2.1	-1.9
lpg0864	-	*lpp0926*	*lpl0895*	similar to cytochrome c-type biogenesis protein	-2.1	-2.1
lpg1328	-	*lpp1283*	*lpl1282*	some similarities with eukaryotic protein	-2.1	-1.7
lpg0459	*dotU*	*lpp0525*	*lpl0501*	dotU	-2.1	-1.8
lpg1329	-	*lpp1284*	*lpl1283*	unknown	-2.1	-1.8
lpg2669	*ftsE*	*lpp2723*	*lpl2596*	highly similar to cell division ABC transporter- ATP-binding protein FtsE	-2.1	-1.9
-	-	-	*lpl2343*	hypothetical protein	-2.1	-1.8
lpg0054	-	*lpp0056*	*lpl0054*	unknown	-2.1	-2.3
lpg1962	-	*lpp1946*	*lpl1936*	similar to peptidyl-prolyl cis-trans isomerase proteins	-2.1	-1.8
lpg1818	*lpxK*	*lpp1781*	*lpl1782*	similar to tetraacyldisaccharide 4-kinase	-2.1	-2.1
lpg1861	*clpP*	*lpp1829*	*lpl1825*	ATP-dependent Clp protease proteolytic subunit	-2.1	-1.5
-	-	-	*lpl0818*	similar to glycosyl transferase	-2.1	-1.6
lpg2208	-	*lpp2159*	*lpl2133*	similar to oxidoreductase	-2.1	-1.8
lpg0326	*fusA*	*lpp0391*	*lpl0366*	translation elongation factor G	-2.1	-2.3
lpg0101	-	*lpp0115*	*lpl0101*	unknown	-2.1	-1.8
lpg0608	-	*lpp0659*	*lpl0643*	similar to methyltransferase	-2.1	-1.8
lpg2757	-	*lpp2805*	*lpl2674*	similar to hypothetical protein	-2.1	-1.8
lpg2872	-	*lpp2931*	*lpl2785*	similar to probable (di)nucleoside polyphosphate hydrolase NudH	-2.1	-2.8
lpg3002	-	*lpp3074*	*lpl2930*	putative inner membrane protein	-2.1	-2.2
lpg1521	-	*lpp1478*	*lpl1505*	similar to conserved hypothetical protein	-2.1	-3.2
lpg1194	*hisF2*	*lpp1196*	*lpl1202*	imidazole glycerol phosphate synthase subunit HisF	-2.1	-1.7
lpg1995	-	*lpp1976*	*lpl1971*	unknown	-2.1	-1.5
lpg2786	*nuoD*	*lpp2833*	*lpl2702*	NADH dehydrogenase I chain D	-2.1	-1.8
lpg0139	*gap*	*lpp0153*	*lpl0138*	glyceraldehyde 3-phosphate dehydrogenase	-2.1	-1.7
lpg0145	*ccrB*	-	-	site specific recombinase	-2.0	-1.9
lpg1075	-	-	-	hypothetical protein	-2.0	-1.5
-	-	*lpp2044*	-	unknown	-2.0	-2.0
lpg0783	*birA*	*lpp0847*	*lpl0822*	biotin-[acetylCoA carboxylase] holoenzyme synthetase and biotin operon repressor	-2.0	-1.8
lpg1700	-	*lpp1665*	*lpl1659*	similar to Uracil-DNA glycosylase	-2.0	-1.9
lpg2211	-	*lpp2162*	*lpl2136*	similar to conserved hypothetical protein	-2.0	-1.8
lpg0759	*gpi*	*lpp0825*	*lpl0796*	glucose-6-phosphate isomerase	-2.0	-2.1
lpg0867	-	*lpp0930*	*lpl0899*	similar to ATP-dependent DNA helicase RecQ	-2.0	-1.8
lpg1852	-	*lpp1819*	*lpl1818*	similar to putative alkaline phosphatase	-2.0	-1.5
lpg0105	-	*lpp0119*	*lpl0105*	similar to conserved hypothetical protein- predicted membrane protein	-2.0	-1.8
lpg2768	*pnp*	*lpp2816*	*lpl2685*	polynucleotide phosphorylase (PNPase)	-2.0	-2.2
lpg2856	-	*lpp2914*	*lpl2768*	similar to unknow protein	-2.0	-2.3
lpg0003	*recF*	*lpp0003*	*lpl0003*	RecF recombinational DNA repair ATPase	-2.0	-1.8
lpg2705	*petA*	*lpp2760*	*lpl2633*	similar to ubiquinol-cytochrome c reductase- iron-sulfur subunit	-2.0	-1.9
lpg0110	-	*lpp0123*	*lpl0109*	unknown	-2.0	-1.5
lpg0005	-	*lpp0005*	*lpl0005*	similar to peptidylarginine deiminase and related enzymes	-2.0	-1.6
lpg1739	-	*lpp1704*	*lpl1703*	similar to Adenylate cyclase 1	-2.0	-1.5
lpg0109	-	*lpp0122*	*lpl0108*	unknown	-2.0	-4.2
lpg2116	-	-	-	transposase, IS4 family TnpA	-2.0	-1.5
lpg0362	-	*lpp0427*	*lpl0403*	similar to 3-oxoacyl-[acyl-carrier-protein] synthase beta chain	-2.0	-1.8
lpg0137	-	*lpp0151*	*lpl0136*	similar to pyruvate kinase II PykA- glucose stimulated	-2.0	-1.9
lpg0598	-	*lpp0648*	*lpl0632*	similar to unknown protein	-2.0	-2.0
-	-	-	*lpl2341*	hypothetical protein	-2.0	-2.1
lpg0889	-	*lpp0950*	*lpl0920*	similar to acetyltransferase	-1.9	-2.0
lpg0547	-	*lpp0608*	*lpl0589*	similar to putative outer membrane lipoproteins	-1.9	-2.5
lpg2654	-	*lpp2707*	*lpl2580*	similar to GTP-binding protein	-1.9	-1.6
lpg1508	-	*lpp1465*	*lpl1518*	similar to rare lipoprotein A RlpA	-1.9	-1.6
lpg0514	-	-	-	hypothetical protein	-1.9	-1.6
lpg1711	*rrf*	*lpp1676*	*lpl1670*	ribosome recycling factor	-1.9	-1.8
lpg0083	-	*lpp0097*	*lpl0082*	similar to unknown proteins	-1.9	-2.0
lpg1296	-	*lpp1259*	*lpl1258*	similar to conserved hypothetical protein	-1.9	-1.7
lpg1699	*ubiG*	*lpp1664*	*lpl1658*	3-demethylubiquinone-9 3-methyltransferase	-1.9	-1.9
lpg1869	*rnc*	*lpp1834*	*lpl1831*	similar to ribonuclease III	-1.9	-1.7
lpg0838	-	*lpp0900*	*lpl0869*	similar to conserved hypothetical protein	-1.9	-1.9

Gene ID	Name	Paris ID	Lens ID	Description	PE FC Ratio[1]	NA FC Ratio[1]
lpg2477	-	*lpp2542*	*lpl2397*	weakly similar to high-affinity nickel-transport protein NixA	-1.9	-1.7
lpg2660	-	*lpp2714*	*lpl2587*	similar to unknown protein	-1.9	-1.6
lpg1394	*fabD*	*lpp1349*	*lpl1345*	malonyl CoA-acyl carrier protein transacylase	-1.9	-1.5
lpg2506	-	*lpp2574*	*lpl2428*	similar to sensor histidine kinase/response regulator	-1.9	-1.8
lpg0051	-	*lpp0053*	*lpl0051*	unknown	-1.9	-2.2
lpg0170	-	*lpp0231*	*lpl0233*	similar to C-terminal part of paraquat-inducible protein	-1.9	-2.0
lpg0772	*wzm*	*lpp0837*	*lpl0813*	ABC transporter of LPS O-antigen- Wzm	-1.8	-1.8
lpg2785	*nuoE*	*lpp2832*	*lpl2701*	NADH dehydrogenase I chain E	-1.8	-1.7
lpg2594	*fmt*	*lpp2647*	*lpl2517*	similar to methionyl-tRNA formyltransferase	-1.8	-1.9
lpg0807	*nadC*	*lpp0869*	*lpl0840*	nicotinate-nucleotide pyrophosphorylase	-1.8	-2.0
lpg2784	*nuoF*	*lpp2831*	*lpl2700*	NADH dehydrogenase I chain F	-1.8	-1.8
lpg0863	*ccmH*	*lpp0925*	*lpl0894*	cytochrome c-type biogenesis protein CcmH	-1.8	-2.0
lpg1424	-	*lpp1379*	*lpl1375*	similar to polysaccharide biosynthesis protein	-1.8	-1.6
lpg0226	-	*lpp0285*	*lpl0280*	similar to outer membrane component of multidrug efflux pump	-1.8	-2.2
lpg1164	-	*lpp1166*	*lpl1172*	similar to acetylornithine deacetylase	-1.8	-1.6
lpg2865	-	*lpp2923*	*lpl2777*	similar to unknown protein	-1.8	-1.6
lpg1436	-	*lpp1391*	*lpl1605*	unknown	-1.8	-1.5
lpg1306	*glnS*	*lpp1270*	*lpl1269*	glutamine tRNA synthetase	-1.8	-2.1
lpg2165	-	*lpp2103*	*lpl2092*	unknown	-1.8	-2.5
lpg0412	-	*lpp0479*	*lpl0455*	similar to Polyprenyltransferase (cytochrome oxidase assembly factor)	-1.8	-1.7
lpg2314	*dapA*	*lpp2262*	*lpl2234*	dihydrodipicolinate synthase	-1.8	-2.2
lpg1538	*pcnB*	*lpp1495*	*lpl1488*	poly(A) polymerase (PAP) (Plasmid copy number protein)	-1.8	-2.1
lpg0361	-	*lpp0426*	*lpl0402*	similar to 3-oxoacyl-[acyl-carrier-protein]synthase II	-1.8	-1.9
lpg1149	-	*lpp1151*	*lpl1155*	unknown	-1.8	-2.0
lpg2933	-	*lpp3000*	*lpl2861*	similar to C-terminal part of NAD(P)H-flavin reductase	-1.8	-1.6
lpg1970	-	*lpp1953*	*lpl1948*	similar to glutathione S-transferase	-1.8	-1.6
lpg0167	-	*lpp0228*	*lpl0230*	similar to conserved hypothetical protein	-1.8	-1.6
lpg0125	-	*lpp0138*	*lpl0123*	similar to cytochrome c4	-1.8	-1.8
lpg1463	*secA*	*lpp1419*	*lpl1565*	preprotein translocase- secretion protein SecA subunit	-1.7	-2.1
lpg0095	-	*lpp0109*	*lpl0094*	similar to 5 -nucleotidase	-1.7	-1.5
lpg2895	*ctaG*	*lpp2960*	*lpl2809*	cytochrome c oxidase assembly protein	-1.7	-2.1
lpg0830	-	*lpp0892*	*lpl0861*	unknown	-1.7	-1.5
lpg2795	*folP*	*lpp2841*	*lpl2710*	dihydropteroate synthase	-1.7	-1.6
lpg2787	*nuoC*	*lpp2834*	*lpl2703*	NADH dehydrogenase I chain C	-1.7	-1.8
lpg0140	*tkt*	*lpp0154*	*lpl0139*	similar to transketolase	-1.7	-1.6
lpg2867	-	*lpp2925*	*lpl2779*	similar to unknown protein	-1.7	-1.7
lpg1709	-	*lpp1674*	*lpl1668*	similar to unknown proteins	-1.7	-1.5
lpg0117	*gcsA*	*lpp0130*	*lpl0115*	glycine dehydrogenase [decarboxylating] subunit 1 (glycine decarboxylase) (glycine cleavage system P-protein)	-1.7	-1.5
lpg1088	-	*lpp1089*	-	unknown	-1.7	-1.6
lpg1536	-	*lpp1493*	*lpl1490*	similar to conserved hypothetical protein	-1.7	-1.8
lpg2993	-	*lpp3064*	*lpl2921*	similar to phosphoheptose isomerase	-1.7	-2.0
lpg1462	-	*lpp1418*	*lpl1566*	similar to tRNA-dihydrouridine synthase A DusA	-1.7	-1.6
lpg1989	-	*lpp1970*	*lpl1964*	putative membrane protein	-1.6	-1.6
lpg0491	-	*lpp0553*	*lpl0529*	similar to putative glutamine-binding periplasmic protein precursor	-1.6	-8.8
lpg0808	*murG*	*lpp0870*	*lpl0841*	(pentapeptide)pyrophosphoryl-undecaprenol N-acetylglucosamine transferase	-1.6	-1.7
lpg0653	-	*lpp0707*	*lpl0689*	similar to major facilitator family transporter	-1.6	-1.7
lpg0185	-	-	-	ABC sugar transporter, ATP binding protein	-1.6	-1.6
lpg0760	*rmlA*	*lpp0826*	*lpl0797*	glucose-1-phosphate thymidylyltransferase /rhamnose biosynthesis	-1.6	-1.8
lpg2581	-	*lpp2633*	*lpl2503*	similar to pyruvate/2-oxoglutarate dehydrogenase complex-dehydrogenase (E1) component- eukaryotic type- beta subunit	-1.6	-1.8
lpg1814	-	*lpp1777*	*lpl1778*	similar to conserved hypothetical protein	-1.6	-1.6
lpg0784	-	*lpp0848*	*lpl0823*	similar to phosphopantetheinyl transferase	-1.6	-1.6
lpg2995	-	*lpp3066*	*lpl2923*	conserved hypothetical protein- putative lipoprotein	-1.6	-1.6
lpg0505	*ecfE*	*lpp0568*	*lpl0544*	similar to putative membrane-associated Zn-dependent protease EcfE	-1.6	-1.8
lpg0792	-	*lpp0856*	*lpl0830*	similar to AmpG protein	-1.6	-1.8
lpg0857	*ccmB*	*lpp0919*	*lpl0888*	heme exporter protein CcmB	-1.6	-1.6
lpg1543	-	*lpp1500*	*lpl1483*	similar to conserved hypothetical protein	-1.6	-1.7

Gene ID	Name	Paris ID	Lens ID	Description	PE FC Ratio[1]	NA FC Ratio[1]
lpg1815	*oxyR*	*lpp1778*	*lpl1779*	hydrogen peroxide-inducible genes activator	-1.6	-1.5
lpg1273	-	*lpp1236*	*lpl1236*	unknown	-1.6	-1.5
lpg2781	*nuoI*	*lpp2828*	*lpl2697*	NADH-quinone oxidoreductase chain I	-1.6	-1.5
lpg0006	*speA*	*lpp0006*	*lpl0006*	similar to biosynthetic arginine decarboxylase	-1.5	-1.8
lpg0861	*ccmF*	*lpp0923*	*lpl0892*	cytochrome C-type biogenesis protein CcmF	-1.5	-1.7
lpg0458	*icmF*	*lpp0524*	*lpl0500*	icmF	-1.5	-1.8
lpg1411	*adk*	*lpp1366*	*lpl1362*	adenylate kinase	-1.5	-1.5
lpg2450	-	*lpp2515*	*lpl2368*	predicted integral membrane protein	-1.5	-2.7
lpg2861	-	*lpp2919*	*lpl2773*	similar to tRNA-dihydrouridine synthase B	-1.5	-1.5
lpg2777	*nuoM*	*lpp2824*	*lpl2693*	NADH-quinone oxidoreductase chain M	-1.5	-1.6
lpg2635	-	*lpp2688*	*lpl2560*	similar to integral membrane protein MviN	-1.5	-1.7
lpg0806	-	*lpp0868*	*lpl0839*	similar to Na(+)/H(+) antiporter	-1.5	-2.2
lpg2475	*hypB*	*lpp2540*	*lpl2395*	hydrogenase nickel incorporation protein HypB	-1.5	-1.6
lpg2780	*nuoJ*	*lpp2827*	*lpl2696*	NADH-quinone oxidoreductase chain J	-1.5	-1.7
lpg0836	-	*lpp0898*	*lpl0867*	similar to ABC transporter- ATP-binding protein	-1.5	-1.5
lpg0257	-	*lpp0327*	*lpl0310*	similar to multidrug resistance proteins	-1.5	-2.3
lpg2897	*coxB*	*lpp2962*	*lpl2811*	cytochrome c oxidase- subunit II	-1.4	-1.8
lpg0107	-	*lpp0121*	*lpl0107*	similar to conserved hypothetical protein	-1.4	-1.6

[1] Fold Change (FC)

CHAPTER FIVE

CONCLUSION

Summary of work presented

To combat various metabolic and environmental stresses, many microbes alter their cellular physiology in a process known as differentiation. Accordingly, when nutrients are abundant, *L. pneumophila* induces a cohort of genes that promote proliferation. However, once nutrients are depleted, replication halts and *L. pneumophila* activates an arsenal of traits to facilitate host transmission and survival in the harsh environment. My thesis work has examined both the regulatory proteins and the metabolic cues that regulate *L. pneumophila* phase differentiation. Based on genetics in conjunction with phenotypic and transcriptional analysis, I postulate that the complexity of the LetA/LetS two-component system enables *L. pneumophila* to customize a panel of traits that are suitable for the local conditions. Furthermore, I have uncovered several novel metabolites that govern the *L. pneumophila* developmental switch. In particular, my data indicate that perturbations in fatty acid biosynthesis activate the stringent response pathway via an interaction between SpoT and ACP, which ultimately leads to *L. pneumophila* differentiation. Finally, by comparing the transcriptional profiles of replicative and transmissive phase *L. pneumophila* to the genes that are regulated by nicotinic acid (NA), I have identified a set of genes that are unique to this phenotypic modulator. Taken together, my data establish that *L. pneumophila* swiftly acclimates to environmental stresses by monitoring metabolic fluctuations and employing a regulatory cascade that enables the bacteria to coordinate an appropriate response.

Future directions

Establishing whether LetA and LetS are partners within the same two-component system

The *L. pneumophila* LetA/LetS two-component system was originally identified by screening a library for mutants that were unable to activate flagellin expression (Hammer *et al.*, 2002). Surprisingly, genome analysis indicates that LetA and LetS do not reside within an operon or within the same region of the *Legionella* chromosome. Thus, it was an assumption that LetA and LetS are partners. However, phenotypic analysis indicates that every PE trait regulated by LetA is similarly controlled by LetS, including: the ability to infect both macrophages and *A. castellanii* and to avoid phagosome-lysosome fusion, macrophage cytotoxicity, motility, sodium sensitivity, stress resistance and pigmentation (Bachman and Swanson, 2004a; Hammer *et al.*, 2002; Lynch *et al.*, 2003). Moreover, microarray analysis of *letA* and *letS* mutants revealed that both regulate the same cohort of genes, apart from genes involved in arginine uptake and biosynthesis (*lpg0553-lpg0555*; Sahr *et. al*., unpublished). Taken together, the phenotypic and transcriptional data indicate that LetA and LetS likely work together to regulate PE genes and traits. To further bolster the argument that LetA and LetS are partners within a single two-component system, biochemical studies could analyze the transfer of phosphate from LetS to LetA.

Determining the kinetics of the LetA/LetS phosphorelay

Work in *Bordetella* indicates that the BvgA/BvgS two-component system regulates at least four classes of genes based upon the consensus sequences located in the promoter region of Bvg-regulated genes, the rate that phosphate flows through the relay, and the intracellular concentrations of phosphorylated BvgA (Cotter and Jones, 2003). Slow rates of phospho-transfer leads to low levels of BvgA~P, which is only sufficient to activate genes that contain high affinity BvgA binding sites (Cotter and Jones, 2003).

High rates of phospho-transfer results in high levels of BvgA~P, a pool that is sufficient to bind promoters containing both high and low affinity binding sites (Cotter and Jones, 2003). It has been suggested that the expression of the intermediate class of Bvg-regulated genes is dependent upon intermediate levels of phospho-transfer and intermediate concentrations of BvgA~P in the cell (Jones *et al.*, 2005; Williams *et al.*, 2005). Similarly, I predict that in *Legionella*, different flow rates in the phosphorelay affect the amount of phosphorylated LetA (LetA~P), which in turn impacts what targets LetA binds and which genes are transcribed.

At present, the biochemistry of the LetA/LetS phosphorelay has not been analyzed. While my data predict that histidine 307 is the autophosphorylation site (Chapter 2), the other residues in LetA and LetS that are predicted to participate in the phosphorelay need to be tested. Moreover, using purified LetA and LetS proteins, the contribution each signaling domain makes to the relay can be analyzed. Finally, the kinetics of the wild-type phosphorelay can be established by reconstituting the LetA/LetS system *in vitro*.

As described in Chapter 2, I generated a mutation in LetS (designated as *letS*^{T311M}) that demonstrated that a hierarchy exists among the *L. pneumophila* LetA/LetS regulated genes and phenotypes. I infer that the expression of the different transcriptional and phenotypic profiles is partially dependent on the rate that phosphate flows through the relay and the intracellular concentrations of LetA~P. Although this prediction is in accordance with the BvgA/BvgS model, the kinetics of the phosphorelay in the *letS*^{T311M} mutant has not been examined. Therefore, further biochemical analyses can test directly the prediction that LetA/LetS regulates expression through the concentration and flow of phosphate through the system.

Identifying LetA and CsrA targets

Whereas the BvgA/BvgS system controls the various classes of genes through the binding affinities of BvgA~P to different consensus sequences located in Bvg-regulated promoters, a stringent genome-wide pattern search in *L. pneumophila* only identified the LetA consensus sequence TNAGAAATTTCTNA upstream of the small RNAs, RsmY and RsmZ (Kulkarni *et al.*, 2006). Although microarray data indicate that LetA regulates 324 different genes, both bioinformatic and biochemical data suggest that the two regulatory RNAs are probably the only targets of LetA (Sahr *et. al.*, unpublished). Additional studies are required to determine whether LetA can also bind genes with less stringent or entirely different consensus sequences.

Unlike *Bordetella*, the *L. pneumophila* regulatory cascade that governs differentiation includes both the LetA/LetS and the CsrA/RsmY/RsmZ systems (Fettes *et al.*, 2001; Hammer *et al.*, 2002; Lynch *et al.*, 2003; Molofsky and Swanson, 2003). By incorporating the Csr system into the rheostat model of regulation, I predict that when LetS receives an appropriate signal, it autophosphorylates, and then transfers the phosphoryl group along the relay to LetA. Once LetA is phosphorylated, it binds upstream of RsmY and RsmZ and initiates their transcription. The small RNAs then relieve CsrA repression on mRNAs by titrating the protein away from its respective targets. RNA polymerase is then free to access and transcribe the mRNAs (Chapter 2).

Similar to the *Bordetella* system, I expect that the rate and efficiency of the LetA/LetS phosphorelay controls the level of LetA~P, and likewise, the amount of RsmY and RsmZ transcribed. Since more than one CsrA molecule can bind target mRNAs, perhaps different classes of mRNAs have different amounts of CsrA bound. Thus, some mRNAs would need high levels of RsmY and RsmZ to relieve CsrA repression, whereas mRNAs that have only one CsrA bound would need less RsmY and RsmZ transcribed. It is also possible that CsrA has different affinities for particular mRNA sequences. Accordingly, some mRNAs would contain consensus sequences where RsmY and RsmZ

159

would easily remove CsrA from its targets. Conversely, other mRNAs would have CsrA more tightly bound and would require more RsmY and RsmZ to relieve CsrA repression. Therefore, the amount of RsmY and RsmZ transcribed would then affect the order in which mRNAs are relieved from CsrA repression. This design is similar to *Bordetella*, but the *L. pneumophila* model contains an additional layer of regulation. Since only one CsrA target has been identified to date, future studies will be required to uncover other CsrA targets, to determine whether the consensus sequences differ between the mRNAs, and if different amounts of RsmY and RsmZ affect the affinity of CsrA for particular mRNA sequences (C. Buchrieser, personal communication).

Additional metabolites that cue L. pneumophila differentiation

In Chapter 3, I identified 22 novel triggers of *L. pneumophila* differentiation by screening hundreds of small molecules via phenotypic microarrays. The short chain fatty acids (SCFAs) formic, acetic, propionic and butyric acid were among the compounds that elicited a positive response. My data suggest that excess SCFAs perturb the balance in fatty acid biosynthesis, which ultimately triggers the stringent response pathway and *L. pneumophila* differentiation.

Other fatty acids: The Biolog screen identified eight additional carboxylic acids, and I postulate that these may similarly induce the phenotypic switch by altering fatty acid metabolism. Indeed, preliminary data indicate that α-ketovaleric acid may impact branched chain fatty acid metabolism and alter the acetyl-CoA levels in the cell (Fonseca and Swanson, unpublished). Moreover, several of the carboxylic acids could be degraded into SCFAs, which would then alter fatty acid biosynthesis similar to acetic and propionic acid (Chapter 3). For example, caproic acid (hexanoic acid) was identified by the phenotypic microarrays and was subsequently shown to inhibit growth and induce motility (data not shown). Caproic acid can be broken down by β-oxidation into 3 acetyl-

160

CoA molecules. As described in Chapter 3, acetyl-CoA can then be converted into malonyl-CoA, which can perturb the fatty acid biosynthetic pathway (Magnuson *et al.*, 1993). Similarly, the 12-carbon carboxylic acid lauric acid triggered *L. pneumophila* differentiation, as determined by growth inhibition and activation of the flagellin promoter (data not shown). However, the response of *L. pneumophila* to lauric acid was not as rapid or robust as the response induced by shorter chain fatty acids (data not shown). This phenomenon might be attributed to the six rounds of β-oxidation that must occur for the release of the 6 acetyl-CoA molecules. Whether additional long chain fatty acids also induce *L. pneumophila* differentiation has not been examined, since the phenotypic microarrays did not contain a panel of long chain fatty acids. Therefore, directed studies will be required to deduce whether the other carboxylic acids cue differentiation via activation of the stringent response and amplification by the LetA/LetS two-component system.

Tween detergents: In addition to the carboxylic acids, two detergents, Tween 20 and Tween 80, also induced *L. pneumophila* differentiation. It is possible that the detergents disrupt membrane integrity, which initiates a stress response and activates the regulatory pathways that govern phase differentiation. However, it is important to note that both detergents contain carboxylic acid groups: lauric and oleic acids, respectively. Thus, Tween 20 and Tween 80 may act as carboxylic acids to trigger *L. pneumophila* differentiation. However, the two related detergents Tween 40 and Tween 60 were present on the microarray plates, but neither inhibited growth or activated the *flaA* reporter construct. Tween 40 and Tween 60 also contain carboxylic acid moieties, palmitic and stearic acid, respectively. I did not test whether Tween 40 and Tween 60 truly fail to trigger *L. pneumophila* differentiation or if the concentrations of these detergents were outside the optimal range. Therefore, future studies can explore if other

concentrations of the detergents can initiate the phenotypic switch, and whether palmitic and stearic acid alone can trigger differentiation.

Nitrite: An additional cue of *L. pneumophila* differentiation that was identified by the phenotypic microarrays was nitrite. Nitrate, however, was unable to induce a response. Nitrite can be reduced to nitric oxide, a toxic compound that is released by macrophages to eliminate invading pathogens. Data suggest that nitric oxide is sensed by obligate aerobes through H-NOX (<u>H</u>eme-<u>N</u>itric Oxide and/or <u>Ox</u>ygen binding) domains, which leads to activation or repression of nitric oxide-regulated genes (Boon and Marletta, 2005). Recently, *L. pneumophila* was found to encode two H-NOX proteins (*lpg1056* and *lpg2459*), and a double deletion renders the bacteria nonmotile (Boon and Marletta, 2005). Therefore, *L. pneumophila* may use its H-NOX proteins to regulate its differentiation and virulence traits when confronted by host defenses.

Hydroxylamine: Hydroxylamine is an extremely reactive intermediate in nitrification, the process by which ammonia is oxidized into nitrite (Richardson and Watmough, 1999). Thus, hydroxylamine may operate similar to nitrite as describe above. Alternatively, hydroxylamine also acts as an antioxidant for fatty acids (Drysdale and Lardy, 1953). Since fatty acid degradation and biosynthesis are tightly coupled, the prevention of β-oxidation could shift the balance towards fatty acid biosynthesis, thereby disrupting flux in fatty acid metabolism (Chapter 3).

Other metabolites identified by phenotype microarrays: Perhaps the most enticing set of compounds to inhibit *L. pneumophila* growth and activate the *flaA* promoter are the six additional metabolites that have no obvious mechanism to elicit phase differentiation. These include: dihydroxyacetone, parabanic acid, deoxyadenosine, deoxyribose, 2-deoxy-D-glucose-6-phosphate and the methionine-alanine dipeptide. I postulate that

because dihydroxyacetone looks remarkable similar to a carboxylic acid, it may function similar to the aforementioned SCFAs. Finally, of the 12 dipeptides screened, only the methionine-alanine dipeptide was identified as a potent inducer of *L. pneumophila* differentiation. Importantly, single amino acids, including methionine and alanine, failed to generate a positive response (data not shown). Subsequent studies will be necessary to discern whether other dipeptide combinations can activate *L. pneumophila* differentiation and the mechanisms by which they elicit a response.

Nicotinic acid: Studies in *Bordetella* have demonstrated that the concentration of NA modulates different classes of Bvg-regulated genes and phenotypes (Schneider and Parker, 1982). Due to the similarities displayed between BvgA/BvgS and the LetA/LetS systems, I postulated that NA would also control the genotypic and phenotypic profiles of *L. pneumophila*. As described in Chapter 4, when E phase *L. pneumophila* were supplemented with 5 mM NA the bacteria induced numerous transmissive phase phenotypes including: motility, cytotoxicity towards macrophages, lysosomal avoidance and sodium sensitivity. Moreover, transcriptional analysis determined that the addition of NA regulated a panel of genes similar to PE *L. pneumophila* (Chapter 4). Importantly, the addition of NA activated the expression of 114 genes and inhibited the expression of 132 genes unique to NA supplementation (Chapter 4). While the mode of action for NA modulation has yet to be determined, the most highly expressed genes 3 h after supplementation were *lpg0272* and *lpg0273* (Chapter 4). These two genes lie within an operon, and transcriptional activation of *lpg0272-3* has never been observed under a variety of other conditions (C. Buchrieser, personal communication).

While *lpg0272* is predicted to encode a cysteine transferase, sequence analysis indicates that *lpg0273* encodes a transporter within the Major Facilitator Superfamily (MFS). One hypothesis is that *lpg0273* may function as an importer of NA and other similar compounds. If correct, I predict that a deletion in *lpg0273* would render the strain

blind to NA modulation, and likewise, the strain would fail to induce PE genes and phenotypes following supplementation. Alternatively, *lpg0273* may serve as an exporter of NA or other toxic compounds. According to this model, I anticipate that a deletion in *lpg0273* would create a strain that is more sensitive to NA. Therefore, the strain may respond to a lower concentration of NA or may lose viability when treated with the modulator. Since attempts to construct a double deletion of *lpg0272-3* have been unsuccessful, the operon may be essential. To further study *lpg0272-3*, I recommend constructing a conditional null and analyzing the mutant for its sensitivity to NA. In addition, whether *lpg0272-3* is required for intracellular growth can be assessed by analyzing the conditional *L. pneumophila* mutant during macrophage infections.

Potential sources of fatty acids during the L. pneumophila life cycle

Although the Biolog screen determined that SCFAs trigger the switch between the replicative and transmissive phases, it is unclear where *L. pneumophila* would encounter alterations in the fatty acids present in its environment. One possibility is that SCFAs are generated by *Legionella* itself. For example, when the TCA cycle does not operate completely, or when bacterial cells are overloaded with their preferred carbon source, they can excrete acetate and propionate into their extracellular milieu as a form of overflow metabolism (Wolfe, 2005). To cope with abundant nutrients during the replicative phase of growth, *L. pneumophila* may excrete SCFAs into the vacuolar compartment, where they would accumulate over time. Eventually, the high concentrations of SCFAs present in the vacuole could signal for differentiation, escape, and subsequent host transmission. It has not been determined whether *L. pneumophila* secretes acetic and propionic acid during intracellular growth or in broth cultures. Since SCFAs readily diffuse across membranes, isolating *Legionella*-containing vacuoles to monitor intracellular concentrations of the SCFAs would be nearly impossible, as significant losses in the fatty acids would occur. However, relatively simple mass

164

spectrometry of broth cultures could determine the presence of the SCFAs at different times during the *L. pneumophila* growth curve.

Alternatively, *L. pneumophila* may monitor external sources of fatty acids that are derived from the host plasma or phagosomal membranes. Consistent with this idea, *L. pneumophila* replicates within a lysosomal compartment, which is also the site for membrane degradation (Sturgill-Koszycki and Swanson, 2000). While the lysosomes themselves contain lipases and phospholipases that aid membrane degradation, *L. pneumophila* also possesses lipolytic enzymes that may degrade host cell membranes into free fatty acids. Furthermore, studies indicate that *L. pneumophila* secretes outer membrane vesicles during extra- and intracellular growth, and proteomic data suggest that the outer membrane vesicles contain several lipases including PlcB (*lpg1455*), PlaC (*lpg2837*), PlcA (*lpg0502*), PlaA (*lpg2343*) and Mip (Debroy *et al.*, 2006; Fernandez-Moreira *et al.*, 2006; Galka *et al.*, 2008). Moreover, sequence data predict that *L. pneumophila* contains *fadL* (*lpg1810*) and *fadD* (*lpg1554*), which likely facilitate the transport of exogenous long chain fatty acids across the cell membrane. I hypothesize that degradation of host membranes may release fatty acids into the lysosomal compartment, which accumulate over time, ultimately triggering *L. pneumophila* differentiation.

Conversely, when starved for essential nutrients, some bacteria will degrade phospholipids within their own cell membrane and use these internal stores for carbon and energy. For example, during the adaptation phase of starvation, the environmental water-borne pathogen *Mycobacterium avium* undergoes cell wall rearrangements, activation of β-oxidation enzymes and a depletion of internal cellular lipids (Archuleta *et al.*, 2005). Likewise, upon starvation the aquatic pathogen *Vibrio cholerae* alters its cell wall, adopts a coccoid morphology and depletes 99.8% of total lipids in the cell (Hood *et al.*, 1986). In accordance with this model, when *L. pneumophila* transitions from the replicative to the transmissive phase, the bacteria switch from a rod-shaped morphology

to a more coccobacillary shape as evident by phase-contrast microscopy (Bachman and Swanson, 2004a; Fettes *et al.*, 2001; Hammer and Swanson, 1999; Molofsky and Swanson, 2003). Although the precise phospholipid and fatty acid content in E and PE phase bacteria have not been analyzed, data indicate that the *L. pneumophila* surface is differentially regulated (Fernandez-Moreira *et al.*, 2006). Additionally, a previous report suggested that the fatty acid composition of *L. pneumophila* differs depending upon nutrient availability and during intracellular growth in *Acanthamoeba polyphaga* (Barker *et al.*, 1993). My data indicate that both an excess and a depletion in the SCFAs cue *L. pneumophila* differentiation (Chapter 3). Thus, when nutrients become limiting *L. pneumophila* may modify its cellular membrane and convert its internal lipid stores to free fatty acids for energy, a process that could also stimulate its phenotypic switch.

Acetyl- and propionyl-phosphate may regulate two-component systems other than LetA/LetS

Microbes can convert acetic and propionic acid to the high-energy intermediates, acetyl- and propionyl-phosphate, via the enzymes phosphotransacetylase (Pta) and acetyl kinase (AckA2) (McCleary *et al.*, 1993; Wolfe, 2005). Once generated, two-component systems can use these intermediates to phosphorylate the response regulator and activate transcription (Wolfe, 2005). My data indicate that the ability of *L. pneumophila* to differentiate when confronted by excess SCFAs was dependent upon the LetA/LetS two-component system (Chapter 3). Accordingly, I tested whether acetic and propionic acid were being converted to acetyl- and propionyl-phosphate to active LetA/LetS, and likewise, initiate the switch between the replicative and transmissive phases. By constructing a *L. pneumophila* mutant that lacks both the Pta and AckA2 enzymes, I determined that neither enzyme was required to induce differentiation in response to excess acetic or propionic acid (Chapter 3). I inferred that the SCFAs must trigger *L.*

pneumophila differentiation by a mechanism other than generating acetyl- and propionyl-phosphate intermediates.

Besides the LetA/LetS system, *L. pneumophila* is predictd to contain an additional 12 histidine kinases and 13 response regulators (Cazalet *et al.*, 2004; Chien *et al.*, 2004). Thus, acetyl- and propionyl-phosphate may directly phosphorylate one of these two-component systems to activate transcription and regulate response pathways. Since the other *L. pneumophila* two-component systems and the genes they govern are not well understood, it will be difficult to ascertain whether acetyl- and propionyl-phosphate can induce other *L. pneumophila* genes and phenotypes when confronted by excess acetate or propionate.

Determining the role of ACP in the L. pneumophila life cycle

Work in *E. coli* suggests that SpoT directly interacts with the functional form of ACP, as disruption of this interaction abrogates SpoT-dependent ppGpp accumulation when fatty acid biosynthesis is inhibited (Battesti and Bouveret, 2006). Data presented in Chapter 3 indicate that perturbations in fatty acid biosynthesis alter the ACP profiles present in *L. pneumophila* and induce the stringent response pathway via SpoT. Moreover, a *L. pneumophila* mutant that contains a single amino acid substitution in SpoT that is predicted to prevent its association with ACP fails to induce PE traits when fatty acid biosynthesis is altered (Appendix A).

While *E. coli* encodes only one ACP, sequence data suggest that *L. pneumophila* contains three ACPs (*lpg0359*, *lpg1396* and *lpg2233*) which all contain the serine residue that is modified by a 4'-phosphopantetheine moiety (Magnuson *et al.*, 1993). Using western analysis and mass spectrometry, attempts to identify which *L. pneumophila* ACPs are modified following perturbations in fatty acid biosynthesis have been unsuccessful (data not shown). Perhaps genetic analysis of the ACPs may determine

whether these ACPs are functionally redundant, or whether the ACPs are specific for different environments or phases of the *Legionella* life cycle.

In addition to playing a key role in the synthesis of fatty acids, many organisms use an ACP protein to generate polyketides. These secondary metabolites are produced using acetyl and propionyl subunits in a process that resembles fatty acid biosynthesis (Weissman, 2004). Based on the known pathways for polyketide synthesis, *L. pneumophila* is not predicted to produce this particular class of metabolites. However, due to the diversity that is displayed among the polyketides, a myriad of synthases and pathways are used for their generation, including many that have yet to be identified (Weissman, 2004). Therefore, *L. pneumophila* may use one of its ACPs to produce polyketides via a novel set of genes and metabolic pathways.

Identifying the precise fatty acid cue that triggers L. pneumophila differentiation

To monitor flux in fatty acid metabolism, it has been suggested that bacteria sense either an accumulation or a depletion of a key intermediate in the fatty acid biosynthetic pathway (Battesti and Bouveret, 2006; DiRusso and Nystrom, 1998). Using inhibitors of fatty acid biosynthesis, my data indicate that *L. pneumophila* may assess malonyl-CoA levels in the cell to regulate its differentiation (Chapter 3). For example, the cerulenin inhibitor causes malonyl-CoA levels to accumulate, while TOFA is predicted to deplete the levels of malonyl-CoA present in the cell (Cook *et al.*, 1978; Heath and Rock, 1995; McCune and Harris, 1979). When E phase *L. pneumophila* were treated with cerulenin, the bacteria immediately induced motility. However, TOFA treatment failed to trigger this phenotypic switch (Chapter 3). To deduce whether malonyl-CoA is the critical intermediate that governs *L. pneumophila* differentiation, the levels of the metabolite could be analyzed by HPLC during different phase of growth and when fatty acid biosynthesis is perturbed.

Alternatively, *L. pneumophila* may monitor the acyl chains attached to ACP to regulate its phenotypic switch. In support of this model, western analysis determined that when E phase *L. pneumophila* were treated with excess SCFAs or cerulenin, the profiles of the acyl-ACPs in the cell changed significantly (Chapter 3). By the proposed ACP-SpoT interaction, *L. pneumophila* may recognize when acyl-ACPs levels are sparse or when the ratio is altered. The design of this regulatory mechanism may enable the bacteria to swiftly synthesize ppGpp when perturbations in fatty acid biosynthesis occur. To analyze which *L. pneumophila* acyl-ACPs are depleted during different phases of growth and upon treatment with excess SCFAs and cerulenin, the acyl species could be separated by gel electrophoresis and then identified by mass spectrometry.

Implications of thesis

Naturally found in aquatic environments as a parasite of fresh water protozoa, *L. pneumophila* can also exploit similar metabolic and regulatory pathways present in the alveolar macrophages to cause the acute respiratory illness, Legionnaires' disease. Due to the ubiquitous nature of *Legionella* and the various ecological niches within which this bacterium can persist, *L. pneumophila* must possess mechanisms that enable swift adaptations to various environmental stresses. Through analysis of the LetA/LetS two-component system, I have determined that the complex architecture of the regulon likely confers flexibility to the organism when confronted by disparate conditions. Importantly, sequence data suggest that this phenomenon is not unique to *L. pneumophila*, but is probably applicable to other microbes. Therefore, I predict that the multi-step design of tripartite two-component systems equip bacteria with a way to customize their traits to meet the demands of the local environment. Moreover, my data challenges the model of most other two-component systems, which are thought to function as on/off switches to activate or repress their target genes. This conceptual bias affects the design of experiments to analyze how regulatory proteins operate, since typically only a snapshot

of the cell is obtained at any given point in time. The work I have presented demonstrates that, instead, many two-component systems may function as rheostats to fine-tune traits according to stresses incurred in the environment.

By screening hundreds of metabolites with phenotypic microarrays I have uncovered novel cues of *L. pneumophila* differentiation and virulence. Specifically, *L. pneumophila* monitors the fatty acid biosynthetic pathway; when fluctuations occur, the bacteria activate the stringent response to induce a panel of traits that promote survival. To my knowledge, this data is the first to suggest that a pathogen can regulate its virulence traits by monitoring fatty acid metabolism via the stringent response. Since many of the metabolic enzymes and pathways are conserved between microbes, I presume that other bacteria employ analogous strategies to coordinate an appropriate response.

Similar to work in *Bordetella*, I have determined that NA induces *L. pneumophila* PE genes and phenotypes. However, even though NA modulation of the BvgA/BvgS system has been well documented, the mode of action has remained elusive. By comparing the transcriptional profiles of both replicative and transmissive phase *L. pneumophila* to the genes that are controlled by NA, I have identified a cohort of genes that are specific for this phenotypic modulator. In particular, my data suggest that a putative membrane protein may be involved in NA transport and regulation. Additionally, NA activates nearly 45 *L. pneumophila* genes that lack an assigned function in publicly available databases. I expect that further analysis of the transcriptional data presented herein will unveil the mechanisms of NA regulation and the biological significance of NA modulation, both of which may be applicable to other bacterial pathogens.

In conclusion, my thesis work has exemplified how *Legionella* has evolved mechanisms to augment its versatility and fitness. Specifically, *L. pneumophila* can assess metabolic fluctuations and stresses in its environment, and then translate these

stimuli into a coordinated response that ultimately promotes self-preservation. Moreover, the elegant regulatory cascade that governs *L. pneumophila* differentiation enables the microbe to express a spectrum of traits that are ideal for its surroundings. Finally, I speculate that the variability in the genotypic and phenotypic repertoires that are displayed by *L. pneumophila* may generate cellular diversity within the population, which provides the bacterium with a selective advantage during the course of evolution.

APPENDICES

APPENDIX A

SPOT GOVERNS *LEGIONELLA PNEUMOPHILA* DIFFERENTIATION IN HOST MACROPHAGES

Summary

To transit between host cells, *Legionella pneumophila* converts from a replicative to a transmissive state. In broth, this transformation is coordinated by ppGpp. To determine its role in the intracellular life cycle of *L. pneumophila,* the two ppGpp synthetases, RelA and SpoT, were disrupted. Importantly, ppGpp synthesis was required for transmission, as *relA spoT* mutants were killed during the entry and exit periods of primary infections. RelA senses amino acid starvation and is dispensable in macrophages, as *relA* mutants failed to activate transmissive gene expression following serine hydroxamate treatment, yet spread efficiently in macrophage cultures. SpoT monitors fatty acid biosynthesis, since following cerulenin treatment, transmissive gene expression was normal in *relA* strains but abolished in *relA spoT* mutants. As in *E. coli*, the SpoT response to perturbations in fatty acid biosynthesis required SpoT-acyl-carrier protein interaction, as judged by the failure of the *spoT^{A413E}* allele to rescue transmissive trait expression of *relA spoT* bacteria. SpoT, but not RelA, was essential for transmission between host cells, since only induction of *spoT* restored intracellular replication of *relA spoT* mutants. More specifically, SpoT hydrolase activity is critical, as mutants lacking this function failed to convert from the transmissive to the replicative phase in macrophages. Thus, *L. pneumophila* requires SpoT to monitor fatty acid biosynthesis through SpoT-ACP interaction and to alternate between replication and transmission in macrophages.

Introduction

To cope with environmental fluctuations such as changes in temperature, osmolarity, and nutrient availability, bacteria modify their physiology. Specific metabolic pathways become activated or deactivated, gene expression is altered, and distinct behaviors emerge. To increase resilience and promote survival, some bacteria undergo morphological adaptations in response to deteriorating conditions. Accordingly, differentiation is often essential to resilience and versatility of the organism.

There are numerous examples of microbial differentiation in nature. During starvation, the soil dwelling bacteria *Myxococcus xanthus* transitions from a swarming state to an aggregative state and develops multicellular fruiting bodies (Zusman *et al.*, 2007). As a means to survive hostile environments, species of *Bacillus* and *Clostridium* form highly resilient endospores (Paredes *et al.*, 2005). The intracellular pathogen *Coxiella burnetti*, the causative agent of Q-fever, transitions between two distinct phases within macrophages: a highly stress-resistance small cell variant (SCV), and a replicative, more metabolically active, large cell variant (LCV) (Voth and Heinzen, 2007). Likewise, within host cells, *Chlamydia trachomatis* alternates between an infectious and metabolically inert, elementary body (EB) and a non-infectious, replicative reticulate body (RB) (Abdelrahman and Belland, 2005).

Similar to *C. burnettii* and *C. trachomatis*, the intracellular pathogen *Legionella pneumophila* also differentiates during its life cycle. *L. pneumophila* is ubiquitous in aquatic environments where it resides either in biofilms or within freshwater protozoa (Swanson and Hammer, 2000). Aerosolization of contaminated water can result in inhalation of the microbe by humans where it acts as an opportunistic pathogen of alveolar macrophages (Swanson and Hammer, 2000). To efficiently transit between host cells, *L. pneumophila* transforms itself from a replicative state into a transmissive state suited for prolonged viability in the environment and evasion of host cell defenses (Molofsky and Swanson, 2004; Swanson and Hammer, 2000). Upon phagocytosis,

174

transmissive *L. pneumophila* resist phagosome acidification and become sequestered within a protective, ER-derived vacuole (Joshi *et al.*, 2001). Favorable metabolic conditions within the vacuole prompt repression of transmissive genes and induction of genes required for protein synthesis and replication (Bruggemann *et al.*, 2006; Molofsky and Swanson, 2003; Sauer *et al.*, 2005). Following multiple rounds of cell division that presumably exhaust host cell nutrients, the starved bacteria differentiate back to the transmissive form (Molofsky and Swanson, 2004; Swanson and Hammer, 2000). Finally, transmissive bacteria escape the depleted host cell to invade a naive one, and the cycle is repeated (Molofsky and Swanson, 2004).

Many of the factors required for transmission have been elucidated through phenotypic analysis of exponential (E) and post-exponential (PE) phase broth-grown bacteria. PE phase, or transmissive, *L. pneumophila* are more infectious toward macrophages and amoeba than bacteria in the replicative, or E phase (Byrne and Swanson, 1998). Increased infectivity of transmissive bacteria has been attributed both to activation of Type IV secretion and to modifications of the bacterial surface that together inhibit phagosome-lysosome fusion (Fernandez-Moreira *et al.*, 2006). Flagellar expression and motility also promote infection by transmissive *L. pneumophila,* likely by enabling the bacterium more efficient access to host cells (Molofsky *et al.*, 2005).

As in broth, *L. pneumophila* cycles between replicative and transmissive phases in host cells. Microscopic examination of *flaA* expression and flagella revealed biphasic regulation in macrophages (Hammer and Swanson, 1999). Cytotoxicity and sodium sensitivity measurements of bacteria harvested from macrophages indicate intracellular *L. pneumophila* differentiate during infection (Byrne and Swanson, 1998). Recently, *in vivo* transcriptional profiling demonstrated that, as in broth, *L. pneumophila* exhibits biphasic gene expression patterns in amoebae, with later time points of primary infections matching the transmissive phase gene expression observed *in vitro* (Bruggemann *et al.*, 2006). Therefore, the transition between the E and the PE phase in broth cultures at least

partially mimics exit from the replicative phase and entry into the transmissive phase in host cells.

In broth cultures, the *L. pneumophila* E to PE phase transition is concomitant with accumulation of guanosine tetraphosphate, or ppGpp (Hammer and Swanson, 1999; Zusman *et al.*, 2002). The alarmone ppGpp acts as a general signal of bacterial starvation and stress (Magnusson *et al.*, 2005; Srivatsan and Wang, 2008). In many gram-negative species, ppGpp, in cooperation with the transcription factor DksA, interacts with secondary channel near the active site of RNA polymerase (RNAP) to control gene expression by altering RNAP affinity for specific promoters (Magnusson *et al.*, 2005; Srivatsan and Wang, 2008). The global transcriptional changes that ppGpp and DksA instruct are collectively referred to as the stringent response (Magnusson *et al.*, 2005; Srivatsan and Wang, 2008). During the stringent response, transcriptional deactivation of ribosomal RNA operons by ppGpp and DksA increases the availability of RNAP for ppGpp- and DksA-mediated activation of amino acid biosynthetic operons and genes required for stabilization of alternative sigma factors (Bougdour and Gottesman, 2007; Paul *et al.*, 2004; Paul *et al.*, 2005). Global transcriptional profiling of the stringent response in *Escherichia coli* has revealed that, in addition to direct regulation of ribosomal and amino acid biosynthetic operons, flagellar and chemotaxis related genes are also under stringent control, as are key enzymes involved in fatty acid biosynthesis (Durfee *et al.*, 2008; Traxler *et al.*, 2008). Thus, by modulating ppGpp levels, a variety of bacteria balance nutrient availability with their protein synthetic capacity and expression of metabolic pathways essential for stress survival.

Several pathogenic bacteria also exploit ppGpp for virulence gene expression and survival in host cells. For *L. pneumophila*, a rise in intracellular ppGpp levels coordinates a switch from a bacillus-shape to a more coccoid morphology, and the cells become motile, resistant to osmotic and heat stresses, and are more infectious (Hammer and Swanson, 1999). Uropathogenic *E. coli*, an organism that uses fimbriae to attach and

colonize the urinary tract, requires ppGpp for expression of FimB, a site-specific recombinase controlling type I fimbriae expression (Aberg *et al.*, 2006). *Salmonella*, a pathogen that cycles between extracellular and intracellular virulence gene programs, require ppGpp for invasion of intestinal epithelial cells, survival in murine macrophages *in vitro*, and colonization of BALB/c mice *in vivo* (Pizarro-Cerda and Tedin, 2004; Song *et al.*, 2004; Tompson *et al.*, 2006). Other pathogens, including *Mycobacterium tuberculosis*, *Listeria moncytogenes*, *Pseudomonas aeruginosa*, and *Campylocbacter jejuni*, also require ppGpp to regulate particular virulence mechanisms (Erickson *et al.*, 2004; Gaynor *et al.*, 2005; Primm *et al.*, 2000; Taylor *et al.*, 2002).

In gram-negative bacteria such as *E. coli* and *Salmonella* spp., the levels of ppGpp in the cell are regulated by the ppGpp synthetase RelA and the bifunctional synthetase/hydrolase SpoT (Magnusson *et al.*, 2005; Srivatsan and Wang, 2008). During amino acid starvation, uncharged tRNAs accumulate at the ribosome, triggering rapid accumulation of ppGpp by ribosome-bound RelA and, consequently, activation of the stringent response (Magnusson *et al.*, 2005; Srivatsan and Wang, 2008). SpoT hydrolyzes ppGpp during exponential growth, an activity that might be regulated through a direct interaction with the ribosome-associated bacterial G-protein CgtA (Jiang *et al.*, 2007; Raskin *et al.*, 2007). In this model, in the absence of metabolic stress, CgtA activation of SpoT hydrolase activity maintains a steady state level of ppGpp, thereby repressing the stringent response when metabolic conditions are favorable (Jiang *et al.*, 2007; Raskin *et al.*, 2007). Since SpoT hydrolase activity is required to prevent RelA-dependent ppGpp from accumulating unabatedly, *spoT* is an essential gene in the numerous bacteria that encode *relA*. However, since *relA* mutants are defective for RelA-dependent ppGpp production, *spoT* is not essential when the RelA synthetase has been disrupted; within this genetic context, SpoT function can be analyzed (Magnusson *et al.*, 2005; Srivatsan and Wang, 2008).

SpoT can also synthesize ppGpp. In particular, the enzyme elicits accumulation of the alarmone in response to a variety of stresses, including carbon source deprivation, phosphate starvation, iron starvation, and fatty acid biosynthesis inhibition (Magnusson *et al.*, 2005; Srivatsan and Wang, 2008). In *E. coli*, SpoT interacts with acyl-carrier protein (ACP), an enzyme critical for fatty acid biosynthesis (Battesti and Bouveret, 2006). Moreover, to respond to fatty acid biosynthesis inhibition, the SpoT-ACP interaction is required (Battesti and Bouveret, 2006). Site directed point mutations within the C-terminal TGS domain of SpoT not only disrupts interaction with ACP, but also alters the enzymatic balance of the enzyme such that synthesis is favored over hydrolysis (Battesti and Bouveret, 2006). Phosphate starvation also results in SpoT-dependent ppGpp accumulation that requires SpoT hydrolase activity, not synthetase activity (Bougdour and Gottesman, 2007; Spira and Yagil, 1998). It remains to be determined if all starvation conditions that elicit ppGpp accumulation alter the association of SpoT with ACP, or result from either an inhibition of ppGpp hydrolysis or an increase in synthesis.

The role of ppGpp in *L. pneumophila* pathogenesis was discovered when experimental induction of alarmone accumulation triggered exponentially growing bacteria to rapidly transition into the transmissive state (Hammer and Swanson, 1999). A rise in intracellular ppGpp levels caused cells to become motile, sodium sensitive, and more infectious and cytotoxic toward macrophages. Subsequent genetic studies demonstrated that *L. pneumophila* requires RelA both for ppGpp accumulation upon entry into stationary phase and for maximal expression of the primary flagellar subunit *flaA* (Zusman *et al.*, 2002). However, RelA was dispensable for *L. pneumophila* growth in *Acanthamobae castellanii* or HL-60-human derived macrophages (Abu-Zant *et al.*, 2006; Zusman *et al.*, 2002). *Legionella* also encode a SpoT homolog with putative ppGpp hydrolase and synthetase domains. Attempts to disrupt the *spoT* locus in both wild-type (WT) and *relA* mutant backgrounds were unsuccessful, leading to the conclusion that SpoT is essential to *L. pneumophila* (Zusman *et al.*, 2002).

For the present study, we undertook a comprehensive analysis of the contributions of RelA and SpoT to the *L. pneumophila* life cycle. We found distinct metabolic cues trigger SpoT and RelA activity and that, during the *L. pneumophila* life cycle in host macrophages, SpoT is critical for both the replicative to the transmissive phase transition and the transmissive to the replicative phase transition.

Experimental procedures

Bacterial strains, culture conditions and reagents. *L. pneumophila* strain Lp02 (*thyA hsdR rpsL*; MB110), a virulent thymine auxotroph derived from Philadelphia 1, was the parental strain for all the strains analyzed. *L. pneumophila* was cultured at 37°C in 5 ml aliquots of *N*- (2-acetamido)-2-aminoethanesulfonic acid (ACES; Sigma)-buffered yeast extract (AYE) broth with agitation or on ACES-buffered charcoal yeast extract (CYE), both supplemented with 100 µg/ml thymidine (AYET, CYET) when necessary. Bacteria obtained from colonies <5 days old were cultured in broth overnight, than subcultured into fresh AYET prior to experimentation. For all experiments, exponential (E) cultures were defined as having an optical density at 600 nm (OD_{600}) of 0.3 to 2.0 and post-exponential (PE) cultures as having an OD_{600} of 3.0 to 4.5. Where indicated, ampicillan (amp; Fisher) was added to a final concentration of 100 µg/ml, kanamycin (kan; Roche) to 10 µg/ml, gentamycin (gent; Fisher) to 10 µg/ml, chloramphenicol (cam; Roche) to 5 µg/ml, cerulenin (Cer; Sigma) to 0.5 µg/ml, serine hydroxamate (Sigma) to 1 mM, propionic acid to 10 mM, acetic acid to 10 mM, and isopropyl-beta-D-thiogalactopyranoside (IPTG) to the concentrations specified. To determine colony-forming units (CFU), serial dilutions of *L. pneumophila* were plated on CYET and incubated at 37°C for 4-5 days.

relA and relA spoT mutant strain construction. To construct a *relA* insertion mutant, we generated pGEM-*relA* by amplifying the *relA* locus (*lpg1457*) plus flanking sequence from Lp02 genomic DNA using the primers relA1 and relA2. The kanamycin resistance gene cassette from pUC4K and the gentamycin cassette from PUCGent were obtained from their respective plasmids by *Eco*RI digestion, and pGEM-*relA* was digested with *Sna*BI. The fragments containing the resistance cassettes were blunted with Klenow, gel extracted, and ligated into the blunted pGEM-*relA* plasmid, creating pGEM-*relA*::*kan* and pGEM-*relA*::*gent*. After verification by PCR and restriction enzyme digest, the insertion alleles were used to transform Lp02 by natural competence, and the resulting transformants were selected using the appropriate antibiotic (Stone and Kwaik, 1999). Recombination of the desired *relA* insertion alleles onto the Lp02 chromosome was confirmed by PCR, and the resulting *relA*::*kan* and *relA*::*gent* mutant *L. pneumophila* were designated MBXXX and MBXXX, respectively.

To construct the *relA spoT* double mutant, we generated pGEM-*spoT* by amplifying the *spoT* locus (*lpg2009*) plus flanking sequence from Lp02 genomic DNA using the primers spoT1 and spoT2. pGEM-*spoT* was digested with *Hin*dIII, which cuts at sites ~100-bp and ~590-bp 3' to the transcriptional start, releasing a ~490-bp fragment encoding a significant portion of the predicted hydrolase and synthetase coding regions at the N-terminus of SpoT. The linear fragment containing the *spoT* deletion was blunted, and a kanamycin cassette was ligated to the blunted fragment, generating pGEM-*spoT*::*kan*. After verification by PCR and restriction enzyme digest, the deletion/insertion alleles were used to transform *relA*::*gent* mutant *L. pneumophila* MBXXX by natural competence, and transformants were selected using the appropriate antibiotic (Stone and Kwaik, 1999). Recombination of the desired *spoT* deletion/insertion allele into the *relA*::*gent* mutant chromosome was confirmed by PCR. The resulting *relA*::*gent spoT*::*kan* double mutant *L. pneumophila* was designated MBXXX. MB355 contains the p*flaA*gfp plasmid that encodes thymidylate synthetase as

a selectable marker and a transcriptional fusion of the *flaA* promoter to *gfp* (Hammer and Swanson, 1999; Hammer *et al.*, 2002). MBXXX and MBXXX were transformed with the p*flaA*gfp reporter plasmid to create MBXXX and MBXXX, respectively.

Inducible relA and spoT expression. To generate strains in which expression of either *relA* or *spoT* could be induced, we cloned promoterless fragments of *relA* and *spoT* into pMMB206-Δmob, a plasmid containing a P$_{taclacUV5}$ IPTG inducible promoter and a chloramphenicol resistance cassette. To construct pGEM-*relA*i, the *relA* locus was amplified from Lp02 genomic DNA using the primers relAi1 and relAi2, each containing a *Sal*I restriction site. The fragment was excised from pGEM-*relA*i using *Sal*I and ligated into pMMB206-Δmob at the *Sal*I site within the MCS immediately 3' of the P$_{taclacUV5}$ promoter, generating p*relA*i. Insertion and orientation were confirmed by both PCR and restriction enzyme digest. p*relA*i was used to transform MBXXX, and transformants were selected on chloramphenicol, creating MBXXX for inducible *relA* expression. To construct pGEM-*spoT*i, the *spoT* locus was amplified from Lp02 genomic DNA using the primers spoTi1, which contains a *Sal*I restriction site, and spoTi2, which contains a *Hin*dIII site. pGEM-*spoT*i and pMMB206-Δmob were each digested with *Sal*I and *Hin*dIII and then ligated, generating p*spoT*i. Insertion and orientation of *spoT* in the MCS of pMMB206-Δmob was confirmed by PCR and restriction enzyme digest. p*spoT*i was used to transform MBXXX, generating MBXXX for inducible *spoT* expression.

Construction of spoT^{A413E} and spoT^{E319Q} inducible constructs. pGEM-*spoT* was used as a template for *spoT^{A413E}* and *spoT^{E319Q}* mutant allele construction. To generate site-directed mutations in *spoT*, Stratagene's QuickChange® II XL Site-Directed Mutagenesis Kit was used. To synthesize *spoT^{A413E}*, pGEM-*spoT* plasmid DNA was amplified with P*fuUltra* HF DNA polymerase (Stratagene) and the complementary primers spoTA413E1 and spoTA413E2. Parental DNA was digested with *Dpn*I, and DH5α transformants were

181

selected on ampicillin. To verify the G<u>CC</u> to G<u>AA</u> codon change, candidate plasmids were sequenced and then designated pGEM-$spoT^{A413E}$. pGEM-$spoT^{A413E}$ was digested with *Sal*I and *Hin*dIII, and the locus cloned into pMMB206-Δmob, as described for the WT *spoT* allele, generating p$spoT^{A413E}$. MBXXX was transformed with p$spoT^{A413E}$, and transformants were selected on chloramphenicol, generating MBXXX for inducible $spoT^{A413E}$ expression. Except for primer variations, construction of p$spoT^{E328Q}$ was carried out identically to p$spoT^{A413E}$. In this case, the primers spoTE328Q1 and spoTE328Q2 were used to generate pGEM-$spoT^{E328Q}$. The desired <u>GAG</u> to <u>CAG</u> codon change was verified by sequencing, and the $spoT^{E328Q}$ allele was then cloned into pMMB206-Δmob as described for $spoT^{A413E}$, generating p206-$spoT^{E328Q}$. MBXXX was transformed with p$spoT^{E328Q}$, and transformants were selected on chloramphenicol to generate MBXXX for inducible $spoT^{E328Q}$ expression.

Detection of ppGpp. Accumulation of the ppGpp in the PE phase and in response to amino acid starvation and fatty acid biosynthesis inhibition was detected by thin-layer chromatography (TLC) as described (Cashel, 1969, 1994; Hammer and Swanson, 1999). Briefly, to detect PE phase ppGpp production in WT and mutant *L. pneumophila*, 100 μCi/ml carrier-free [^{32}P]-phosphoric acid was added in late-E phase, and bacteria were cultured at 37°C on a roller drum to the PE phase, or approximately 6 h. To detect ppGpp accumulation following amino acid starvation and fatty acid biosynthesis inhibition, E phase cultures were diluted to an OD_{600} = 0.25 and labeled with approximately 100 μCi/ml of carrier-free [^{32}P]-phosphoric acid (ICN Pharmaceuticals) for 6 h, or two generation times, at 37°C on a roller drum. After incorporation of the radioactive label, cultures were supplemented with a carrier control, 1 mM serine hydroxamate, or 0.5 μg/ml cerulenin. Cultures were incubated for an additional 1.5 h at 37°C. To extract the nucleotides, 50 μl aliquots were removed from each culture, added to 13 M formic acid, and then incubated on ice for 15 min. Samples were subjected to

two freeze-thaw cycles and stored at -80°C until chromatographed. Formic acid extracts (35 µL in the case of the treated cultures and 25 µL in the case of the PE samples) were applied to a PEI-cellulose TLC plates (20 × 20; Sorbent) and developed with 1.5 M KH_2PO_4, pH 3.4 as described (Cashel, 1969, 1994; Hammer and Swanson, 1999). TLC plates were exposed to Kodak BioMax MR Film (18 × 24 cm) for 72 hours before development. To monitor growth in these experiments, OD_{600} were determined for non-radioactive cultures grown under identical conditions.

Fluorometry. To monitor expression of the flagellin promoter in WT and mutant cultures, *L. pneumophila* containing the reporter plasmid p*flaAgfp* were cultured in AYE media. Overnight cultures in mid-E phase OD_{600} = 1.0-1.75 were back diluted to early-E phase OD_{600} = 0.50-0.85 (T = 0). At the times indicated, the cell density of each culture was measured as OD_{600}. To analyze similar bacterial concentrations, aliquots were collected by centrifugation, and the cells were normalized to OD_{600} = 0.01 in 1 × PBS. An aliquot of each sample (200 µL) was transferred to black 96-well plates (Costar), and the relative fluorescence intensity was measured using a Synergy™ HT microplate reader and 485 nm excitation, 530 nm emission, sensitivity of 50. A similar protocol was used to monitor *flaA* promoter activity in cultures supplemented with 1 mM serine hydroxamate and 0.5 µg/ml cerulenin. Overnight cultures in mid-E phase OD_{600} of 1.0-1.75 were back diluted to early-E phase OD_{600} of 0.50-0.85 (T = 0), at which time WT and mutant bacteria were treated with either serine hydroxamate or cerulenin. *L. pneumophila* cultures supplemented with water or DMSO served as negative and vehicle controls, respectively. Optical density and relative fluorescence were measured as described above.

Sodium sensitivity. To calculate the percentage of *L. pneumophila* that were sensitive to sodium, PE bacteria or E cultures were plated onto CYET and CYET containing 100 mM

NaCl. After a 6-day incubation at 37°C, CFUs were enumerated, and the percentage of

sodium sensitive microbes calculated as described (Byrne and Swanson, 1998).

Macrophage cultures. Macrophages were isolated from femurs of female A/J mice

(Jackson Laboratory) and cultured in RPMI-1640 containing 10% heat-inactivated fetal

bovine serum (RPMI/FBS; Gibco BRL) as described previously (Swanson and Isberg,

1995). Following a 7-day incubation in L-cell supernatant-conditioned media,

macrophages were plated at either 5×10^4 per well for cytotoxicity, or 2.5×10^5 per well

for degradation assays, infectivity assays and intracellular growth curves.

Lysosomal degradation. The percentage of intracellular *L. pneumophila* that remain

intact after a 2 h macrophage infection was quantified by fluorescence microscopy

(Bachman and Swanson, 2001; Molofsky and Swanson, 2003). Briefly, macrophages

were plated at 2.5×10^5 onto coverslips in 24 well plates. Then, E or PE phase microbes

were added to macrophage monolayers at an MOI ~ 1. The cells were centrifuged at 400

$\times$ g for 10 min at 4°C and then incubated for 2 h at 37°C. Extracellular bacteria were

removed by washing the monolayers three times with RPMI/FBS, and the macrophages

were fixed, permeabilized and stained for *L. pneumophila* as described (Molofsky *et al.*,

2005).

Infectivity and intracellular growth. Infectivity is a gauge of the ability of *L.

pneumophila* to bind, enter, and survive inside macrophages during a 2 h incubation, as

previously described (Byrne and Swanson, 1998; Molofsky and Swanson, 2003). In brief,

macrophages were infected with strains at an MOI of ~1, with centrifugation at 400 x g

for 10 min. Cells were incubated for 2 h at 37°C, washed three times with fresh RPMI,

and lysed in a 1:1 solution of RPMI and saponin, then intracellular CFU were

enumerated. Results are expressed as the percentage of the inoculated CFU recovered

from lysed macrophages at 2 h post-infection. To gauge intracellular growth, the pooled macrophage supernatant and lysate were plated for CFU at various times post-infection, as described elsewhere (Molofsky and Swanson, 2003). Results for intracellular growth are expressed as either total CFU recovered or relative CFU. In the latter, CFU recovered at 24, 48 and 72 h are divided by the number of CFU at 2 h. Culturing conditions for WT and mutant *L. pneumophila* varied depending upon the experimental question addressed. For experiments assaying infectivity and intracellular survival of WT, *relA* and *relA spoT* bacteria lacking expression vectors, cultures were grown to E or PE phase prior to infection. To test the contribution of *relA* and *spoT* to the replicative to transmissive phase transition in broth, overnight cultures in mid-E phase OD_{600} = 1.0-1.75 were diluted to early-E phase OD_{600} = 0.50-0.85. Cultures were incubated for approximately 3 h at 37°C to an OD_{600} = 1.0-1.75; then, 200 µM IPTG was added and maintained until PE phase. To assess the role of *relA* and *spoT* in the transmissive to replicative phase transition within host cells, bacteria were cultured in broth with 200 µM IPTG to PE phase, and 200 µM IPTG was maintained throughout macrophage infection. A similar protocol was used to test the transmissive to replicative transition in bacteriological medium by plating bacteria that had been induced with 200 µM IPTG and cultured into PE phase onto CYET with 200 µM IPTG.

Cytotoxicity. To determine contact-dependent cytotoxicity of *L. pneumophila* following macrophage infection, bacteria were added to macrophage monolayers at the indicated MOI. After centrifugation at 400 × g for 10 min at 4°C (Molofsky *et al.*, 2005), the cells were incubated for 1 h at 37°C. For quantification of macrophage viability, RPMI/FBS containing 10% alamarBlue™ (Trek Diagnostic Systems) was added to the monolayers for 6-12 h, and the reduction of the colorimetric dye was measured spectrophoretically as described (Molofsky *et al.*, 2005). Protocols for culturing WT and mutant microbes varied depending upon the experimental question. To determine the effect *relA* and *spoT*

induction on cytotoxicity of *relA spoT* mutant bacteria, microbes were cultured with 200 µM IPTG to PE phase in broth as described above. To determine if expression of WT and mutant *spoT* was sufficient to rescue the cytotoxicity defect of *relA spoT* mutant bacteria in which fatty acid biosynthesis had been perturbed, overnight cultures in mid-E phase OD_{600} = 1.0-1.75 were back diluted to early-E phase OD_{600} = 0.45-0.60 and treated with either 25 or 50 µM IPTG for 1 h. After a 1 h incubation on a roller at 37°C, mutant cultures were split and either mock-treated or treated with propionic acid, acetic acid, or cerulenin. Cultures were incubated at 37°C for an additional 3 h prior to assaying cytotoxicity.

Results

In the absence of relA, spoT is not essential in L. pneumophila

To rigorously test the hypothesis that the stringent response controls *L. pneumophila* virulence expression, we created *relA* and *relA spoT* double mutant strains. In the stationary phase, *L. pneumophila* secretes pyomelanin, a molecule important for iron metabolism, in a *relA*-dependent manner (Chatfield and Cianciotto, 2007; Zusman *et al.*, 2002). Therefore, to verify that *relA* was disrupted, we assayed extracellular pigment production by stationary phase cultures. As expected, our *relA* insertional null mutant was completely defective for pigment production (data not shown).

As observed for other gram-negative bacteria, we and others were unable to generate single *spoT* null mutant strains of *L. pneumophila,* and attempts to construct a conditional *spoT* mutant were also unsuccessful (Zusman *et al.*, 2002). Therefore, to analyze the contribution of SpoT to the *L. pneumophila* life cycle, we constructed a *relA spoT* double mutant in which a significant portion of the putative, overlapping synthetase and hydrolase domains of SpoT were deleted and replaced by a gentamycin resistance cassette. The *relA spoT* double mutant cells exhibited a hyperfilamentous cellular

morphology (data not shown) reminiscent of that described for *relA spoT* mutants of *E. coli* (Traxler *et al.*, 2008; Xiao *et al.*, 1991). Therefore, in the absence of *relA*, *spoT* is not essential for *L. pneumophila* replication on rich bacteriological medium.

RelA and SpoT contribute to ppGpp accumulation and motility in the stationary phase

To assess the contribution of SpoT to *L. pneumophila* PE phase biology, we tested the ability of *relA* and *relA spoT* mutants to accumulate ppGpp in stationary phase. After radiolabeling the *L. pneumophila* guanosine nucleotide pools for 6 h (two doubling times), ppGpp levels were analyzed by thin-layer chromatography. WT *L. pneumophila* cultured to the PE phase accumulated a pool of ppGpp, much of which was dependent upon *relA* (Fig. A.1A). The *relA* mutants also accumulated a small but appreciable pool of ppGpp that was not observed in the *relA spoT* double mutant (Fig. A.1A). Thus, when *L. pneumophila* are cultured in rich broth, RelA synthetase activity accounts for the majority of ppGpp in the PE phase, whereas SpoT synthetase activity contributes modestly (Fig A.1A). *L. pneumophila* obtains carbon and energy from amino acids, not sugars (Tesh and Miller, 1981; Tesh *et al.*, 1983). Therefore, it is not surprising that, upon starvation in a rich medium composed of yeast extract, much of the ppGpp that accumulates is dependent upon RelA activity (Hammer and Swanson, 1999; Zusman *et al.*, 2002).

To test the biological consequence of the small amount of *spoT*-dependent ppGpp accumulating in PE phase and determine its contribution to *L. pneumophila* differentiation, we assayed *flaA* expression and motility, two hallmarks of stationary phase cells. The *relA* and *relA spoT* mutants were transformed with a plasmid containing a *flaAgfp* transcriptional fusion that enables promoter activity of *flaA*, the primary flagellar subunit of *L. pneumophila* to be analyzed by fluorometry (Fig. A.1B) (Hammer and Swanson, 1999). As expected, the *flaA* promoter was inactive during exponential (E) phase in WT, *relA* and *relA spoT* cultures (Hammer and Swanson, 1999). Upon entry

into the PE phase, both WT and *relA* mutant *L. pneumophila* activated the *flaA* promoter; however, in *relA* mutant cultures the *flaA* promoter activity was decreased relative to WT, consistent with a previous report (Zusman *et al.*, 2002). In contrast, *relA spoT* mutant cultures failed to activate *flaA* expression upon entry into PE, indicating that the residual *flaA* promoter activity observed in *relA* mutants is dependent upon SpoT (Fig. A.1B). Consistent with their *flaA* expression, the *relA* mutants also exhibited a 30-50% decrease in the fraction of motile bacteria per field relative to WT cultures, while *relA spoT* mutants failed to express motility at all PE phase time points analyzed (data not shown). Therefore, both RelA and SpoT contribute to *flaA* expression by PE *L. pneumophila*, and the small *spoT*-dependent ppGpp pool that accumulates in PE phase (Fig. A.1A) is nevertheless sufficient to activate *flaA* expression and motility by *L. pneumophila*.

The stringent response is required for PE phase survival

Upon entry into PE phase, *L. pneumophila* not only builds a flagellum and becomes motile, but the cells also change shape and surface properties, increase stores of energy rich polymers, and become resistant to environmental stresses (Fernandez-Moreira *et al.*, 2006; Molofsky and Swanson, 2004). To investigate the importance of the stringent response to survival in the the PE phase, we assessed the OD_{600} and CFU of WT, *relA* and *relA spoT* cultures over time (Fig. A.1C). Both parameters were similar for all strains between 2 and 30 h; however, by 44 h, or ~20 h after entry into stationary phase, *relA spoT* yielded higher OD_{600} values (~0.75-1.0 units) than WT and *relA*. When analyzed by microscopy at 44 h, the *relA spoT* cells appeared hyperfilamentous relative to WT and *relA*, which had adopted the more coccoid-like morphology that is characteristic of PE phase *L. pneumophila* (data not shown) (Molofsky and Swanson, 2004). In addition, by 44 h *relA spoT* cultures began to exhibit a loss in CFU relative to WT and *relA* (Fig. A.1C). This decrease in viability of *relA spoT* cells was even more

pronounced after 66 h. Therefore, as reported for other bacteria, including *C. jejuni* and *Helicobacter pylori* (Gaynor *et al.*, 2005; Mouery *et al.*, 2006), *L. pneumophila* requires the stringent response for differentiation and survival in stationary phase.

RelA-dependent ppGpp synthesis is required for flaA expression following amino acid starvation

To verify that, like *E. coli*, *L. pneumophila* relies on RelA to initiate the stringent response following amino acid starvation, we subjected WT and mutant cultures to treatment with serine hydroxamate. Since serine hydroxamate, an analog of the amino acid serine, inhibits the attachment of serine to transfer RNA, it has been used extensively in *E. coli* to characterize the mechanism by which RelA senses accumulation of uncharged tRNAs at the ribosome (Magnusson *et al.*, 2005; Tosa and Pizer, 1971). Unlike mock-treated cultures, WT cells subjected to serine hydroxamate treatment accumulated an appreciable pool of ppGpp (Fig. A.2A). In contrast, neither *relA* nor *relA spoT* mutant *L. pneumophila* responded to serine hydroxamate treatment. Thus, like *E. coli*, *L. pneumophila* relies on RelA to synthesize ppGpp following amino acid starvation.

To determine the physiological relevance of the ppGpp pool observed, we asked if the *relA*-dependent ppGpp that accumulated after serine hydroxamate treatment was sufficient to activate *flaA* expression. Indeed, the pattern of *flaA* expression in serine hydroxamate-treated cultures (Fig. A.2B, top panel) mimicked that observed for ppGpp production (Fig. A.2A). Whereas WT cultures activated *flaA* as early as 3 h post treatment, neither *relA* nor *relA spoT* treated with serine hydroxamate activated *flaA* throughout the time course analyzed (Fig. A.2B, top panel). Mock-treated cultures exhibited patterns of *flaA* activation similar to those observed upon entry into PE phase (Fig. A.1B). Serine hydroxamate treatment did lead to partial growth inhibition of all strains relative to mock-treated control samples (Fig. A.2B, bottom panel), an effect that occurred independently of ppGpp accumulation in the strain (Fig. A.2A). Together these

observations verify that in response to amino acid starvation, RelA synthesizes adequate ppGpp to activate *flaA* in *L. pneumophila*.

SpoT-dependent ppGpp accumulation leads to flaA activation following inhibition of fatty acid biosynthesis

For *E. coli*, it is known that RelA and SpoT respond to distinct starvation stimuli to trigger ppGpp accumulation. Whereas RelA responds to amino acid starvation, SpoT responds to carbon source deprivation, fatty acid biosynthesis inhibition, phosphate starvation, and iron starvation (Magnusson *et al.*, 2005). Therefore, we tested the hypothesis that *L. pneumophila* RelA and SpoT also respond to distinct metabolic cues. For this purpose we used the antibiotic cerulenin, a specific inhibitor of fatty acid biosynthesis in bacteria that acts on the 3-ketoacyl-[acyl carrier-protein (ACP)] synthases I and II, FabB and FabF (Seyfzadeh *et al.*, 1993). Appreciable amounts of ppGpp were detected in WT and *relA* cultures treated with cerulenin, whereas *relA spoT* mutant *L. pneumophila* failed to accumulate ppGpp under these conditions (Fig. A.2C). The response was specific to the antibiotic, since cultures receiving the DMSO vehicle did not generate detectable ppGpp.

To investigate the phenotypic consequences of the SpoT-dependent ppGpp pool, we assayed the ability of WT and mutant cultures to activate *flaA* following cerulenin treatment. As observed after the serine hydroxamate treatment, the pattern of *flaA* expression reflected the size of the ppGpp pool in each strain (Fig. A.2D, top panel). Cerulenin-treated WT and *relA* mutant *L. pneumophila* activated *flaA*, but *relA spoT* cells did not (Fig. A.2D, top panel). As observed for cultures treated with serine hydroxamate, cerulenin treatment also inhibited growth independently of ppGpp accumulation in the strain (Fig. A.2D, bottom panel). Cultures treated with DMSO were not inhibited for growth and activated fluorescence only upon entry into PE phase. Thus, with RelA and SpoT, *L. pneumophila* is equipped to differentiate in response to a diversity of starvation

190

signals, including amino acid starvation via RelA, and inhibition fatty acid biosynthesis using SpoT.

Amino acid substitution in SpoT renders the enzyme insensitive to fatty acids

In addition to responding to fatty acid biosynthesis inhibition (Fig. A.2), *L. pneumophila* that are exposed to excess short chain fatty acids (SCFA) also activate transmissive phenotypes in a SpoT-dependent manner (Chapter 3). Like cerulenin treatment, addition of either 10 mM acetic or propionic acid to E phase *L. pneumophila* triggers expression of several transmission traits, including lysosome evasion, motility, and cytotoxicity (Chapter 3). In *E. coli*, SpoT monitors and responds to perturbations in fatty acid metabolism through a specific interaction with ACP (Battesti and Bouveret, 2006). Accordingly, we tested the hypothesis that a SpoT-ACP interaction is essential for *L. pneumophila* to activate transmissive phenotypes in response to SCFA. To do so, we designed plasmids for the inducible expression of either WT *spoT* or *spoT*^{A413E}, an allele encoding an enzyme predicted to be defective for ACP interaction (Battesti and Bouveret, 2006). We then asked whether expression of either plasmid-borne *spoT* or *spoT*^{A413E} was sufficient to restore cytotoxicity to *relA spoT* bacteria (Fig. A.3A) exposed to SCFA.

WT or mutant *spoT* expression was first induced for 1 h with 25 μM IPTG before the cells were cultured for 3 h with 10 mM SCFA and 25 mM IPTG. When exposed to propionic acid, WT *spoT* restored *relA spoT* mutant cytotoxicity toward macrophages, but *spoT*^{A413E} did not (Fig. A.3A). Likewise, only WT *spoT* rescued *relA spoT* cytotoxicity after acetic acid or cerulenin addition (data not shown). The plasmid-encoded *spoT*^{A413E} allele was functional: When the IPTG concentration was doubled to 50 μM, *relA spoT* mutants carrying the *spoT*^{A413E} plasmid were even more cytotoxic than those harboring either WT *spoT* or the empty vector (Fig. A.3B). Furthermore, the enhanced cytotoxicity was independent of SCFA treatment. Thus, the *spoT*^{A413E} mutation

renders the enzyme insensitive to perturbations in fatty acid metabolism and also leads to increased ppGpp pools, presumably by disrupting the balance between ppGpp synthesis and hydrolysis.

The stringent response activates transmissive traits

L. pneumophila coordinates entry into stationary phase with expression of not only motility but also virulence-associated phenotypes like sodium sensitivity, cytotoxicity, and lysosome avoidance (Byrne and Swanson, 1998). Accordingly, to assess the contributions of RelA and SpoT to virulence trait expression in PE *L. pneumophila*, we assayed WT and mutant bacteria for sodium sensitivity and lysosome evasion. As predicted, *relA spoT* mutants remained sodium resistant even when cultured into PE phase (Fig. A.4A). PE phase *relA* mutant *L. pneumophila*, which accumulate low amounts of ppGpp, activate *flaA* and become motile (Fig. A.1), also become sensitive to sodium. Likewise, whereas PE WT and *relA* resisted phagosome-lysosome fusion and remained intact following macrophage phagocytosis, E phase WT and PE phase *relA spoT* were degraded (Fig. A.4B). Therefore, even the modest SpoT-dependent pool of ppGpp is sufficient to induce sodium-sensitivity and protect *L. pneumophila* from lysosomal degradation.

Induction either ppGpp synthetase is sufficient rescue relA spoT mutants in broth

Since *L. pneumophila* requires ppGpp for *flaA* expression, motility, sodium sensitivity and lysosome avoidance (Fig. A.1, and A.4) we predicted that, during PE phase starvation, induction of either synthetase would equip replicative *relA spoT* mutants to enter the transmissive phase. Indeed, IPTG induction of plasmid-borne *relA*, *spoT*, or $spoT^{A413E}$ suppressed both the flagellar and the cell-remodeling defect of *relA spoT* mutant bacteria, as judged by the motility of coccoid bacteria. In contrast, *relA spoT* bacteria carrying the vector alone remained amotile and elongated (data not shown).

When *relA*, *spoT* or *spoT*[A413E] was induced, *relA spoT L. pneumophila* killed more macrophages than either *relA spoT* mutant bacteria carrying vector alone or E phase WT (Fig. A.5A). Induction of *relA*, *spoT* and *spoT*[A413E] also increased the infectivity of *relA spoT* bacteria: When cultured with IPTG to the PE phase, *relA spoT* mutants harboring plasmids encoding either ppGpp synthetase were 10-25% more infectious than *relA spoT* mutants with empty vector (Fig. A.5B). Thus, expression of *relA*, *spoT* or *spoT*[A413E] was sufficient to trigger replicative phase *relA spoT* mutants to enter the transmissive phase. These results not only verify that the phenotypic defects of *relA spoT* mutants were not due to secondary site mutations or polar effects, but also indicate that, regardless of its source, ppGpp coordinates the replicative to transmissive phase transition in broth.

The stringent response is essential during macrophage infection

As in broth, *L. pneumophila* cycles between replicative and transmissive phases in host cells (Bruggemann *et al.*, 2006; Byrne and Swanson, 1998; Hammer and Swanson, 1999). Since ppGpp is essential for activation of the transmission phenotype *in vitro* (Fig. A.1A), we postulated that RelA and SpoT are also required for transmission between host cells.

As observed previously, *relA* was dispensable for *L. pneumophila* growth and survival in macrophages (Fig. A.6A) (Abu-Zant *et al.*, 2006; Zusman *et al.*, 2002). In contrast, *relA spoT* mutants infected with a decreased efficiency relative to PE phase WT, a phenotype similar to WT in the E phase (Fig. A.6A; 2 h time point). Those *relA spoT* and E phase WT bacteria that survived the initial attack moved on to replicate efficiently between 2 and 24 h. However, after 24 h, when E phase WT CFU had increased to values equivalent to PE phase WT, *relA spoT* mutants exhibited no further increase in CFU over the remainder of the period analyzed (Fig. A.4A).

Since 24 h corresponds to the period of flagellar expression and initiation of secondary infection (Byrne and Swanson, 1998), we postulated that *relA spoT* mutants

193

were defective for either escape from an exhausted host or entry into a naive one. To distinguish between these two hypotheses, we performed immunofluorescence microscopy. At 16 and 24 h, both WT and *relA spoT* bacteria occupied replication vacuoles (data not shown); however, between 24 and 36 h, a unique class of infected macrophages emerged in *relA spoT* cultures. Intact bacteria were no longer observed (data not shown); instead, degraded *L. pneumophila* particles were dispersed throughout the macrophage. In addition, there was scant evidence of secondary infection at time points between 24 and 48 h (data not shown). Thus, the majority of bacteria were apparently destroyed following the replicative growth period, prior to escape. In the rare macrophage that contained one or two bacteria at time points beyond 24 h, the *relA spoT* mutants were also degraded, likely due to their inability to avoid phagosome-lysosome fusion (data not shown). Therefore, the stringent response is required for *L. pneumophila* transmission between macrophages, and SpoT is a critical component of its developmental switch.

SpoT, not RelA is essential for transmission in macrophages

Based on the degradation of intracellular *relA spoT* mutants that we observed after 24 h (Fig. A.6A), we postulated that ppGpp must accumulate to equip *L. pneumophila* to escape from an exhausted host cell. To investigate the contributions of RelA and SpoT to transmission in macrophages, we tested whether induction of either *relA* or *spoT* was sufficient to rescue the intracellular *relA spoT* mutants.

The *relA spoT* mutant *L. pneumophila* were cultured in the absence of IPTG to the early PE phase and then added to macrophages. After ~16 h, IPTG was added to the cultures and maintained for the remainder of the infection. Like *relA spoT* harboring empty vector, double mutants in which *relA* had been induced exhibited an ~20 fold increase in CFU between 2 and 24 h, but no appreciable increase beyond 24 h (Fig. A.7A). In contrast, when *spoT* was induced, growth of the *relA spoT* mutants continued

beyond 24 h, and by 72 h, their yield was nearly equivalent to that of WT (Fig. A.7A). Thus, SpoT activity, but not RelA, was critical for *L. pneumophila* transmission in macrophages.

SpoT is required for the transmissive to replicative phase transition in host cells

Since induction of plasmid borne *relA* in the *relA spoT* mutant likely results in unrestrained ppGpp accumulation due to lack of SpoT hydrolase activity in this strain, cells cultured in the presence of IPTG are predicted be locked in the transmissive phase and so incapable of re-entering the replicative phase. Therefore, to address whether SpoT synthetase and/or hydrolase activity is critical for the life cycle of *L. pneumophila*, we tested whether induction of *relA*, *spoT* or *spoT*[A413E] equipped transmissive bacteria to differentiate into the replicative phase in both macrophages and on solid medium. Broth grown cultures of *relA spoT* bacteria carrying *relA*, *spoT*, or *spoT*[A413E] were induced with IPTG into PE phase to active transmission traits. Transmissive bacteria were either used to infect macrophages in the presence of IPTG (Fig. A.8A), or plated onto rich medium with or without IPTG (Fig. A.8B). During macrophage infection with the *relA spoT* strains, induction of WT *spoT* resulted in a pattern of intracellular growth identical to that of PE phase WT bacteria (Fig. A.8A). Interestingly, neither induction of *relA* nor *spoT*[A413E] equipped *relA spoT L. pneumophila* to replicate intracellularly (Fig. A.8A). Similar patterns were observed when transmissive bacteria were plated onto bacteriological medium with or without IPTG. Mutant *L. pneumophila* that expressed WT *spoT* and *relA spoT* bacteria carrying vector alone readily formed colonies on medium containing IPTG (Fig. A.8B, left panel). In contrast, consistent with their intracellular phenotype, *relA spoT* mutants harboring either *relA* or *spoT*[A413E] failed to replicate when IPTG was present in the medium (Fig. A.8B, left panel). Together, these results suggest that SpoT hydrolase activity is required for transmissive cells to re-enter replicative growth during infection and on bacteriological medium. Furthermore, these

195

data also indicate that the $spoT^{A413E}$ allele encodes an enzyme defective for ppGpp hydrolysis.

Discussion

To endure starvation and other stresses, many bacteria rely on the stringent response pathway to alter their transcriptional profiles and enhance their fitness. When nutrients become scarce, *L. pneumophila* generates ppGpp to coordinate the transition from a replicative to a transmissive form (Hammer and Swanson, 1999; Zusman *et al.*, 2002). Although *L. pneumophila* requires RelA to produce ppGpp upon entry into the PE phase in yeast extract broth, this enzyme is dispensable for replication in either amoeba or human macrophages (Figs. A.1A and A.7) (Abu-Zant *et al.*, 2006; Zusman *et al.*, 2002). Like several other microbes, *L. pneumophila* also encodes the bifunctional and essential enzyme SpoT, which either synthesizes or hydrolyzes ppGpp depending on the nutrient supply. We report here that the RelA and SpoT enzymes equip *L. pneumophila* to respond to distinct metabolic stresses, and that SpoT in particular is a critical regulator of the pathogen's life cycle in both broth and macrophages.

When *L. pneumophila* is cultured in broth, a large proportion of its ppGpp pool is generated by RelA (Fig. A.1A). The more minor contribution by SpoT can be observed as the residual ppGpp detected in *relA* mutants (Fig. A.1A), since only two ppGpp synthetases are apparent in the *L. pneumophila* genome, and no alarmone is detectable in *relA spoT* double mutant cells (Fig. A.1A). Like *E. coli* SpoT, the *L. pneumophila* enzyme may be a weak synthetase (Seyfzadeh *et al.*, 1993). Alternatively, the low levels of SpoT-dependent ppGpp observed may be a consequence of experimental conditions: Because its fastidious character precludes use of low-phosphate medium, *L. pneumophila* was cultured in a rich media that contains amino acids as the sole energy source, which not only reduces the efficiency of radiolabeling the nucleotide pools but also favors RelA-dependent ppGpp production. Nevertheless, the weak ppGpp signal generated by

SpoT is sufficient to induce not only the *flaA* promoter, but also motility, sodium sensitivity, and evasion of lysosomes (*relA* mutant; Figs. A.1B, A.4 and data not shown). Taken together, our phenotypic and biochemical analysis of WT, *relA,* and *relA spoT* bacteria establish that the stringent response alarmone ppGpp coordinates differentiation of replicating *L. pneumophila* to the transmissive form.

In addition to triggering its panel of transmission traits, ppGpp is also critical for *L. pneumophila* to survive the PE phase in broth cultures (Fig. A.1B and A.C). In *E. coli*, ppGpp-dependent control of fatty acid and phospholipid metabolism allows the bacterium to selectively modify its membranes during stress. For example, ppGpp inhibits fatty acid and phospholipid biosynthesis through repression of *plsB* (sn-glycerol-3-phosphate acyltransferase), resulting in accumulation of long-chain acyl-ACPs and cell shortening (Heath *et al.*, 1994). Indeed, the *E. coli* stringent response both activates and represses several genes in the fatty acid and phospholipid biosynthetic pathways, as judged by transcriptional profile analysis (Durfee *et al.*, 2008). Accordingly, we predict that the stringent response pathway induces synthesis of specific membrane constituents that are critical for *L. pneumophila* to survive prolonged periods of starvation.

As described previously (Abu-Zant *et al.*, 2006; Zusman *et al.*, 2002), the RelA enzyme itself is dispensable for *L. pneumophila* to survive phagocytosis by macrophages and also for the intracellular bacteria to replicate (Fig. A.6). On the other hand, the alarmone ppGpp is critical to induce the virulence factors that equip *L. pneumophila* to establish its protected intracellular niche, since mutants that lack both *relA* and *spoT* survive poorly within macrophages (Fig. A.6). The source of ppGpp is inconsequential, since expression of either RelA or SpoT largely bypasses the transmissive trait defects of *relA spoT* double mutant bacteria (Fig. A.5A). Once replication ensues, ppGpp is no longer required, since the few *relA spoT* mutant bacteria that do survive the initial infection replicate efficiently during the subsequent 24 h primary infection period (Fig. A.6).

Many species of bacteria initiate the stringent response when their nutrient supply wanes. In *E. coli*, RelA responds to amino acid limitation, whereas SpoT activates the stringent response pathway during all other types of stresses and starvation (Magnusson *et al.*, 2005). Similarly, amino acid depletion stimulates *L. pneumophila* to produce ppGpp and induce differentiation by a RelA-dependent pathway (Fig. A.2A and A.B). On the other hand, to respond to perturbations in fatty acid biosynthesis, *L. pneumophila* relies on SpoT (Fig. A.2C and A.D). Since this environmental microbe and opportunistic pathogen thrives within a variety of ecological niches, we predict that its dual stringent response enzymes equips *L. pneumophila* to coordinately induce transmission traits when confronted with one of a variety of stresses.

To activate the stringent response pathway following fatty acid starvation, *E. coli* depends on a regulatory interaction between SpoT and ACP, a component of the fatty acid biosynthesis pathway (Battesti and Bouveret, 2006). In particular, Battesti and Bouveret identified a single amino acid substitution in SpoT that abrogates a physical interaction with ACP and renders the mutant bacteria blind to fatty acid starvation (Battesti and Bouveret, 2006). *L. pneumophila* also utilizes an interaction between SpoT and ACP to respond to alterations in fatty acid biosynthesis, since the analogous *spoT*^{A404E} mutant bacteria fail to trigger cytotoxicity in response to excess short chain fatty acids (Fig. A.3A). By some mechanism, ACP appears to regulate SpoT enzyme activity to reduce ppGpp pools, as judged by three phenotypic assays. *L. pneumophila* treated to express the *spoT*^{A413E} allele strongly apparently contain excessive ppGpp, as the cells are more cytotoxic than WT PE bacteria (Fig. A.3B), and they survive yet fail to replicate when cultured either in macrophages or on rich medium (Fig. A.8 and data not shown). Based on the capacity of the analogous *E. coli spoT*^{A404E} mutant to adapt to histidine starvation, Battesti and Bouveret also deduced that excess ppGpp accumulates when the SpoT-ACP interaction is disrupted (Battesti and Bouveret, 2006). Accordingly, our working model holds that, during fatty acid biosynthesis, acylated species of ACP

interact with SpoT, promoting its hydrolase activity. Thus, to transition to the replicative phase, transmissive *L. pneumophila* require that acyl-ACP stimulate SpoT to degrade the ppGpp alarmone. When fatty acid biosyntheses is perturbed, free ACP activates the SpoT synthetase to generate ppGpp. Biochemical studies can now test the prediction that the SpoT^{A413E} protein is a weak synthetase whose activity cannot be stimulated by the non-acylated forms of ACP.

During the replication period in A/J mouse macrophages, WT *L. pneumophila* reside within an acidic lysosomal compartment (Sturgill-Koszycki and Swanson, 2000). Like WT *L. pneumophila*, *relA spoT* mutant bacteria slowly traffic to the lysosomal compartment (data not shown). However, at the end of the intracellular replication cycle, *L. pneumophila* that cannot produce ppGpp become degraded and scattered throughout the macrophage cytosol, as judged both by microscopy and a decline in CFU (Fig. A.6, data not shown). Therefore, the ppGpp produced by SpoT is essential for *L. pneumophila* to escape from the harsh lysosomal environment and to move to another phagocyte.

In contrast to the critical role of the ppGpp alarmone, a number of positive activator proteins of transmission traits that are critical during culture in amino acid-rich broth are nevertheless dispensable for *L. pneumophila* to spread from one macrophage to another. These regulatory proteins include the LetA/S two-component regulatory system, the LetE enhancer of transmission traits, and the FliA flagellar sigma factor (Bachman and Swanson, 2004a; Hammer *et al.*, 2002). Apparently, the ppGpp-dependent regulators that operate in macrophage vacuoles are either redundant or distinct from those identified as critical for inducing transmission traits during the PE phase in yeast extract broth. One hypothesis is that *L. pneumophila* requires ppGpp for transcriptional activation of its six alternative sigma factors (Cazalet *et al.*, 2004; Chien *et al.*, 2004). Alternatively, the sigma factor competition model holds that stress-induced sigma factor proteins require ppGpp to displace RpoD from RNA polymerase to activate their specific cohort of targets (Nystrom, 2004). However, mutations in these specialty sigma factors, including RpoE,

199

RpoN, or FliA, do not confer an intracellular defect (Jacobi *et al.*, 2004). One exception is RpoS, which exhibits replication defects in amoebae and in macrophages (Bachman and Swanson, 2001; Hales and Shuman, 1999). Therefore, unless the regulators are redundant, some other ppGpp-dependent positive activators must induce the transmission phenotype of intracellular *L. pneumophila*.

The precise stimuli that cue *L. pneumophila* differentiation *in vivo* also remain to be determined. Several intracellular pathogens, including *Agrobacterium tumefacians*, *Brucella abortus* and *Mycobaterium tuberculosis*, sense host membrane lipids and initiate defense mechanisms when deemed appropriate. Also, *L. pneumophila* requires phosphotidylcholine for both survival in host cells and cytotoxicity (Conover *et al.*, 2008). Accordingly, we postulate that the ability of SpoT to sense variations in fatty acid metabolism in broth also equips *L. pneumophila* to respond to fluctuations in lipids during its intracellular life cycle in macrophages and amoebae.
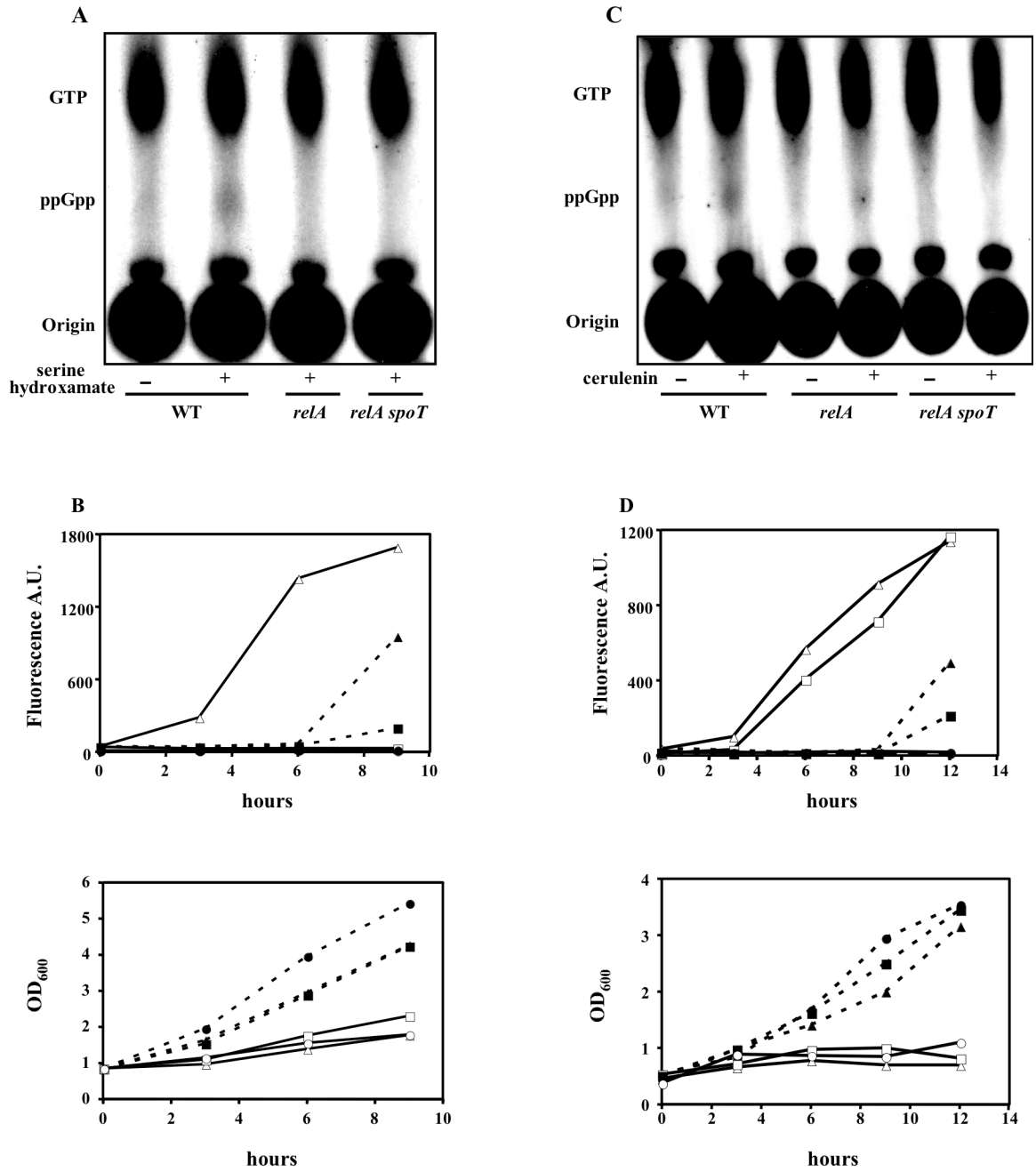
Figure A.1.
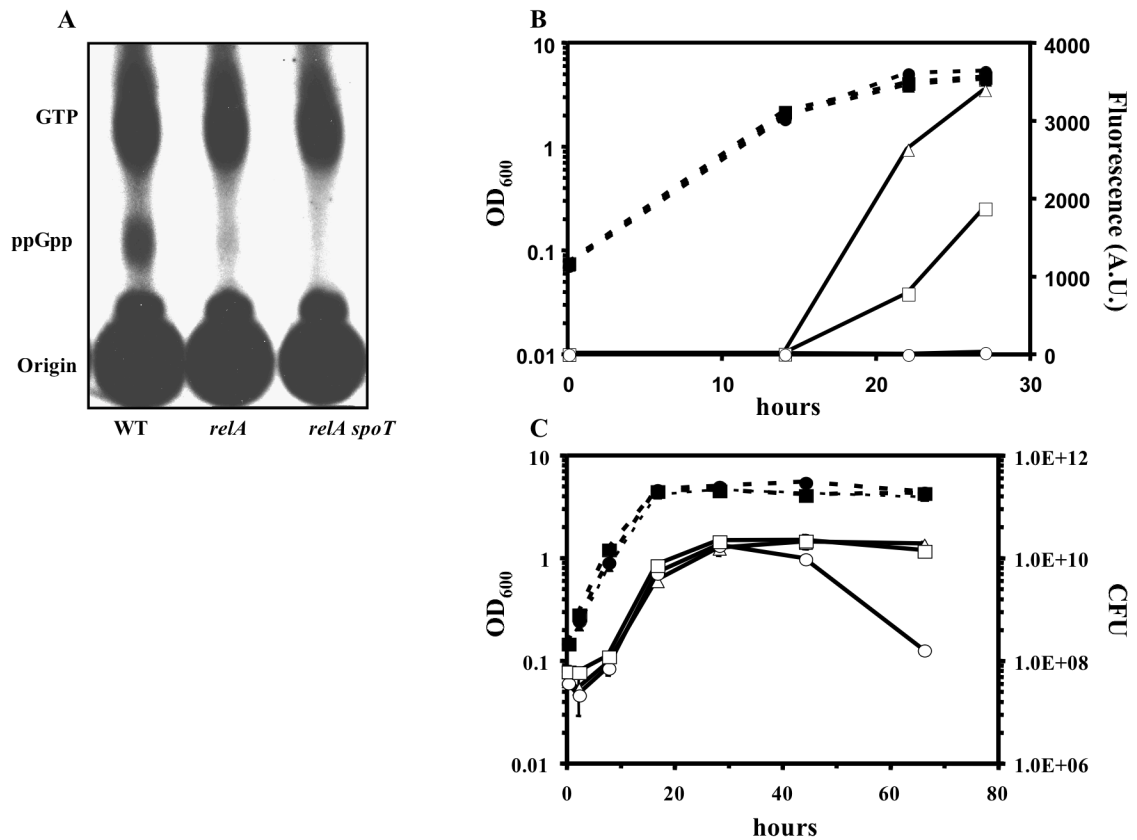
Figure A.1. RelA and SpoT contribute to ppGpp accumulation, motility and survival in PE phase.

(A) To evaluate ppGpp accumulation in the PE phase, mid-E phase AYET broth cultures of WT, *relA*, and *relA spoT* bacteria were incubated for 6 h with ^{32}P phosphoric acid (~two generation times), a period sufficient for the cells to enter the PE phase. At this time, cell extracts were prepared and nucleotides were separated by PEI-TLC. The autoradiogram shown represents one of two separate experiments. (B) To monitor *flaA* expression, WT (triangles), *relA* (squares) and *relA spoT* (circles) strains transformed with p*flaAgfp* were cultured in broth. At the times indicated, bacterial density was quantified by measuring OD_{600} (closed symbols, dashed lines), and GFP accumulation was quantified by fluorometry (open symbols, solid lines). Shown is a growth curve beginning in early-E phase that is representative of multiple cultures in >5 independent experiments. (C) To evaluate survival of PE phase stress, early-E phase cultures of WT (triangles), *relA* (squares), and *relA spoT* (circles) bacteria were diluted to an OD_{600} of 0.1. Then, bacterial density was quantified by measuring OD_{600} (closed symbols, dashed lines), and viability was assessed by enumerating CFU/ml on CYET (open symbols, solid lines). Shown are mean CFU ± SE from duplicate samples, and the data represent one of three independent experiments.

Figure A.2. *L. pneumophila* requires RelA and SpoT for ppGpp accumulation and *flaA* expression in response to distinct metabolic cues.
(A) To analyze ppGpp accumulation in response to amino acid starvation, early-E phase AYET broth cultures were labeled with ^{32}P phosphoric acid for two generations before addition of either 1 mM serine hydroxamate (+), or water (-). After an additional 1.5 h incubation period, cell extracts were prepared, and nucleotides were separated by PEI-TLC. The autoradiogram represents one of two independent experiments. (B) To quantify *flaA* expression in response to amino acid starvation, mid-E phase AYET cultures of WT (triangles), *relA* (squares), *relA spoT* (circles) strains harboring p*flaAgfp* were diluted to early-E phase before the addition of either 1 mM serine hydroxamate (open symbols, solid lines), or water (closed symbols, dashed lines). Then, cultures were sampled at 3 h intervals until WT and *relA* reference samples entered PE phase (OD$_{600}$, bottom panel) and exhibited *flaA* promoter activity fluorescence (9 h; top panel). These data represent one of three independent experiments.   (C)   To analyze ppGpp accumulation in response to inhibition of fatty acid biosynthesis, mid-E phase AYET cultures of WT (triangles), *relA* (squares), *relA spoT* (circles) were incubated for 1 h with cerulenin at 0.5 µg/ml (+) or DMSO (-). Then, cell extracts were prepared and analyzed by PEI-TLC.   Shown is one autoradiogram representing one of three independent experiments. (D) To quantify *flaA* expression in response to fatty acid biosynthesis inhibition, mid-E phase cultures of WT (triangles), *relA* (squares), or *relA spoT* (circles) bacteria were treated with cerulenin (open symbols, solid lines) or DMSO (closed symbols, dashed lines). Samples were collected at 3 h intervals to measure bacterial density (bottom panel) and fluorescence (top panel) until WT and *relA* reference cultures entered PE phase and exhibited fluorescence (12 h). The data depicted represent one of three independent experiments.
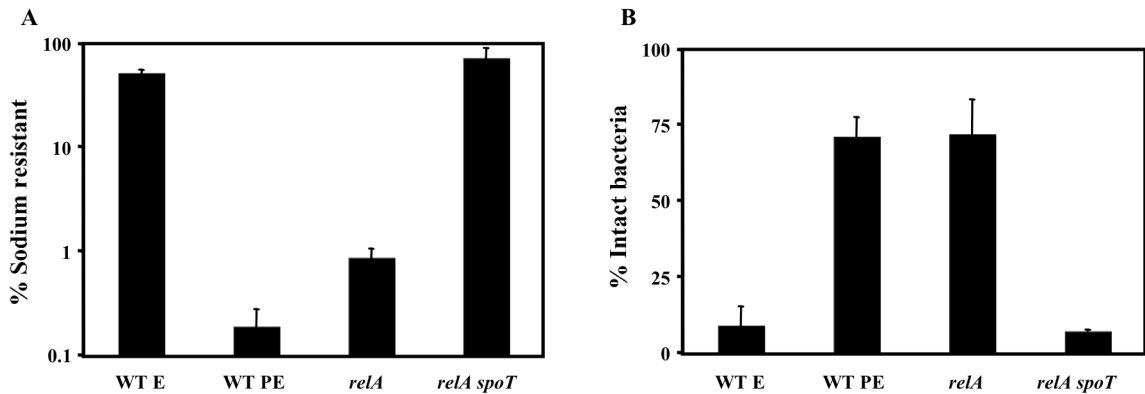
Figure A.2.

Figure A.3.
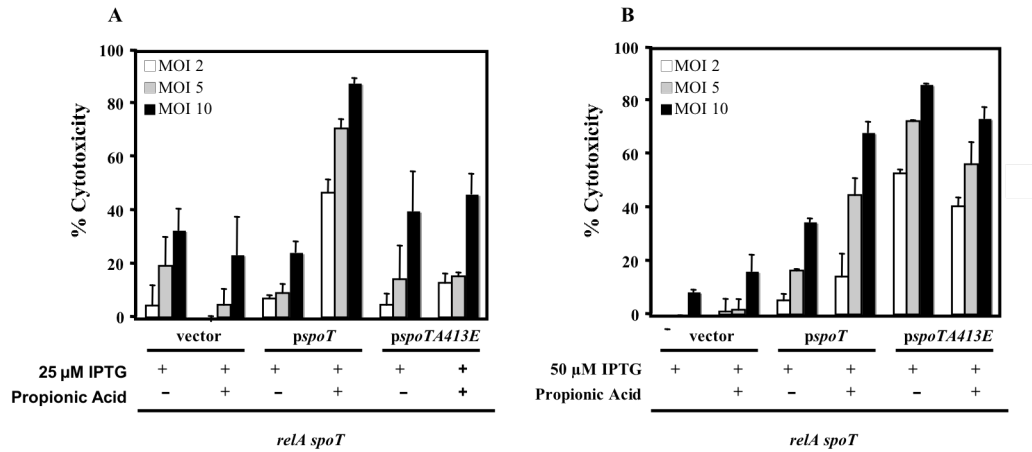
Figure A.3. SpoT mutation abrogates transmission gene expression following perturbations in fatty acid metabolism.

(A) E phase cells normalized to an OD_{600} of 0.5-0.6 were incubated with 25 μM IPTG for 1 h. Then, cultures were split and 10 mM propionic acid was added to one half, while the other half was mock-treated. After 3 h of incubation, triplicate wells of macrophages were infected at various multiplicities of infection (MOI) with treated or mock treated *relA spoT* mutant bacteria harboring vector backbone, p*spoT,* or p*spoT^A413E*. After 1 h incubation with the macrophages, cytotoxicity was measured as the ability of viable macrophages to reduce the calorimetric dye alamarBlue™. (B) As described in A, macrophages were infected with propionic acid-, or mock-treated *relA spoT* mutant bacteria harboring the plasmids shown. To induce high levels of protein, bacteria were incubated with 50 μM IPTG for 2 h, twice the amount and time used for A. Then, cultures were split and either treated with propionic acid or mock-treated. After 3 h of treatment, macrophages were infected in triplicate, and cytotoxicity was measured. The values plotted represent the mean ± standard error for triplicate samples determined in one of three similar experiments.
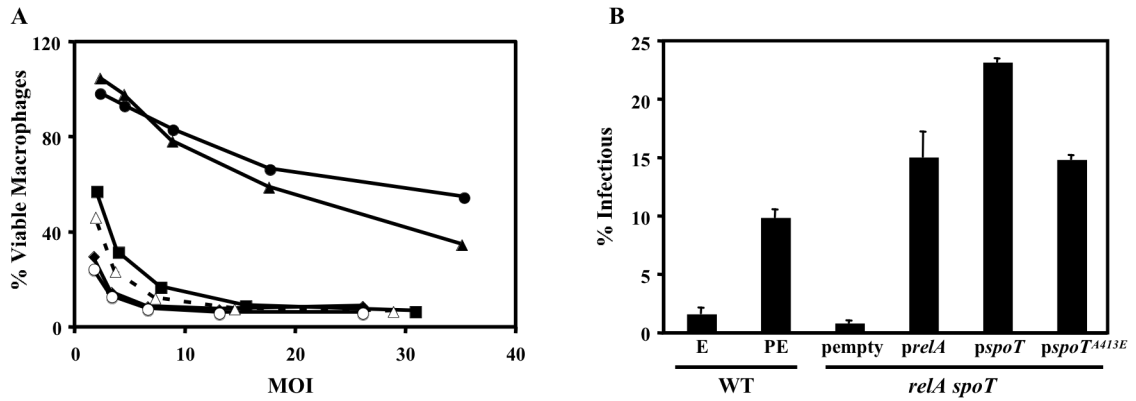
Figure A.4.

Figure A.4. The stringent response governs *L. pneumophila* transmission traits in broth.

(A) To quantify sodium resistance, E or PE phase cultures of the strains shown were plated on medium with or without 100 mM NaCl, then efficiency of colony formation was calculated as [(CFU on CYET + 100 mM NaCl)/(CFU on CYET)] x 100. Shown are mean percentages ± SE from duplicate samples, and the data represent one of three independent experiments. (B) The ability of bacteria to bind, enter, and survive ingestion by macrophages was quantified by fluorescence microscopy by scoring the percent of bacteria that were intact 2 h after infection. Infected macrophages were double-labeled with the DNA stain DAPI to visualize macrophage nuclei and intact bacteria and with *L. pneumophila*-specific antibody to visualize both intact and degraded *L. pneumophila*. Shown are mean percentages ± SE from duplicate samples, and the data represent one of three independent experiments.
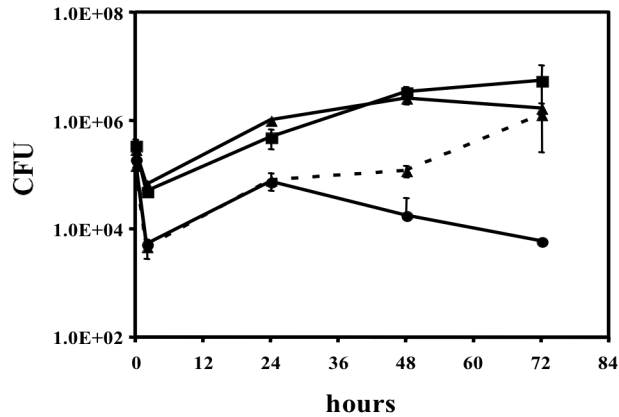
Figure A.5.

Figure A.5. Induction of either ppGpp synthetase rescues transmission trait expression of *relA spoT* mutants.

(A) To determine the contribution of RelA and SpoT to *L. pneumophila* cytotoxicity, *relA spoT* mutants transformed with vector (circles), p*relA* (squares), p*spoT* (diamonds), or p*spoT*^{A413E} (open circles) were cultured from mid-E phase to PE phase with 200 μM IPTG. Bacteria were added to triplicate wells of macrophages at the MOI shown. WT cells carrying vector and cultured to either E phase (triangles), or PE phase (dashed line, triangles) were added as controls. After 1 h incubation, cytotoxicity was measured. The values plotted represent the mean ± standard error for triplicate samples determined in one of three similar experiments. (B) Macrophages were infected at an MOI of ~1.0 for 2 h with either E or PE phase WT carrying vector, *relA spoT* mutants transformed with vector, p*relA*, p*spoT*, or p*spoT*^{A413E} cultured from mid-E phase to PE phase with 200 μM IPTG, as described above. Shown are mean percent of cell-associated CFU ± SE from duplicate wells in one of three independent experiments.
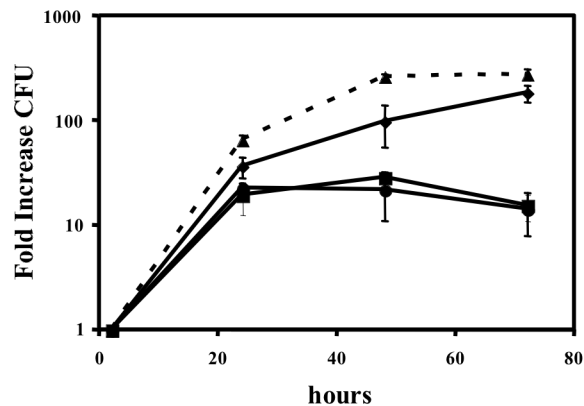
Figure A.6.

Figure A.6. The stringent response is essential for *L. pneumophila* transmission in macrophages.
Macrophages were infected at an MOI of ~1 with E phase WT (triangles, dashed line), PE phase WT (triangles, solid line), PE phase *relA* (squares) or PE phase *relA spoT* mutants (circles) for the periods shown, and then the number of viable bacteria per well was determined. Shown are mean CFU ± SE from duplicate samples in one of five independent experiments.
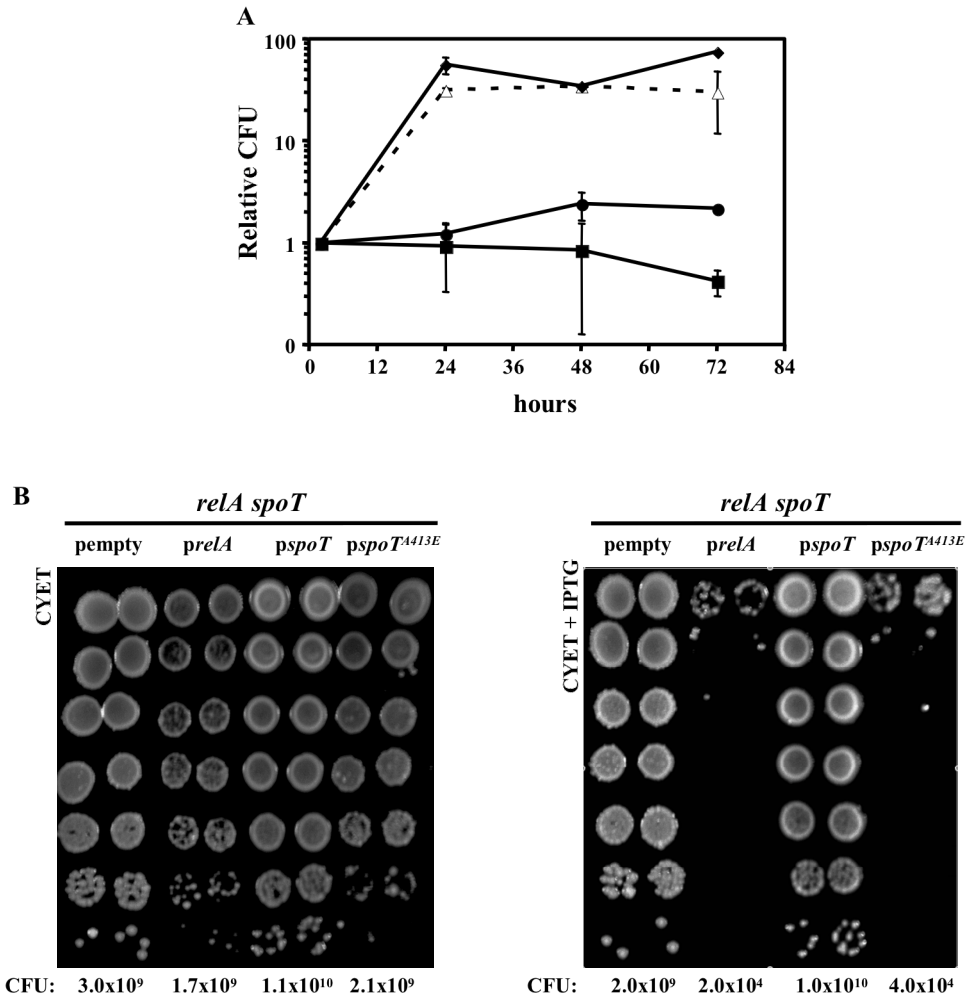

Figure A.7.

Figure A.7. SpoT, not RelA, is essential for *L. pneumophila* transmission in macrophages.
Macrophages were infected at an MOI ~ 1.0 with E phase WT (triangles, dashed line) and PE phase *relA spoT* harboring: vector (circles), *prelA* (squares) or *pspoT* (diamonds). At 16 h post infection, 200 µM IPTG was added to the wells and maintained throughout the remainder of experiment. Relative CFU was calculated by dividing the CFU values obtained at 24, 48 and 72 h by the 2 h value. Shown are mean fold increase in CFU ± SE from duplicate wells in one of three independent experiments.

Figure A.8.

Figure A.8. Transmissive *L. pneumophila* require SpoT to enter the replicative phase.
(A) To determine if SpoT hydrolase activity contributes to the transmissive to replicative phase transition within host cells, *relA spoT* mutant *L. pneumophila* carrying either p*relA* (squares), p*spoT* (diamonds) or p*spoT^{A413E}* (circles) were induced with 200 μM IPTG in mid-E phase, cultured into PE phase (4-5 h), and then used to infect macrophages at an MOI of ~1. During the 72 h infection, 200 μM IPTG was maintained. WT carrying empty vector cultured into PE phase (dashed line, open triangles) served as a positive control in this assay. Relative CFU was calculated as described above. Shown are mean fold increase in CFU ± SE from duplicate wells in one of three independent experiments.
(B) As in A, *relA spoT* mutant derivatives of *L. pneumophila* were cultured in mid-E phase to PE phase (4-5 h) in the presence of 200 μM IPTG. Then, to mimic the induction conditions used in the macrophage experiment, bacteria were plated onto CYET with or without 200 μM IPTG. Shown are images of CYET agar plates of one of three independent experiments.

APPENDIX B

EFFECT OF DECREASING COLUMN INNER DIAMETER AND THE USE OF OFF-LINE TWO-DIMENSIONAL CHROMATOGRAPHY ON METABOLIC DETECTION IN COMPLEX MIXTURES

Summary

Capillary liquid chromatography coupled with electrospray ionization to a quadropole ion trap mass spectrometer was explored as a method for the analysis of polar anionic compounds in complex metabolome mixtures. A ternary mobile phase gradient, consisting of aqueous acidic, aqueous neutral and organic phases in combination with an aqueous compatible reversed-phase stationary phase allowed metabolites with a wide range of polarities to be resolved and detected. Detection limits in the full scan mode for glycolysis and tricarboxylic acid cycle intermediates were from 0.9 to 36 fmol. Using this system, 111 ± 9 (n = 3) metabolites were detected in *Escherichia coli* lysate samples. Reducing column I.D. from 50 μm to 25 μm increased the number of metabolites detected to 156 ± 17 (n = 3). The improvement in number of metabolites detected was attributed to an increase in separation efficiency, an increase in sensitivity, and a decrease in adduct formation. Implementation of a second separation mode, strong anion exchange, to fractionate the sample prior to capillary RPLC increased the number of metabolites detected to 244 ± 21 (n = 3). This improvement was attributed to the increased peak capacity which decreased co-elution of molecules enabling more sensitive detection by mass spectrometry. This system was also applied to islets of Langerhans where more significant improvements in metabolite detection were observed. In islets, 391 ± 33 small molecules were detected using the two-dimensional separation. The

results demonstrate that column miniaturization and use of two-dimensional separations can yield a significant improvement in the coverage of the metabolome.

Introduction

Analysis of small molecule pools present in cells holds the promise of elucidating novel biochemical pathways, functions of genes, drug effects and mechanisms of pathophysiological states. Coupling of separation methods such as capillary electrophoresis (CE) (Edwards *et al.*, 2006; Soga *et al.*, 2002; Soga *et al.*, 2003), gas chromatography (GC) (Fiehn *et al.*, 2000; Jonsson *et al.*, 2004), reversed-phase liquid chromatography (RPLC) (Lu *et al.*, 2006; Tolstikov *et al.*, 2003), strong anion-exchange chromatography (SAX) (Mashego *et al.*, 2004) and hydrophilic interaction liquid chromatography (HILIC) (Lafaye *et al.*, 2005) with mass spectrometry (MS) has proven effective for detecting large numbers of metabolites in complex mixtures. Despite the resolving power of these methods, they generally only detect a fraction of the metabolites that are present. Several factors contribute to the difficulty of detecting all metabolites in a given sample. The many components demand high peak capacity of the separation to detect the complete metabolome. The huge variation of metabolite concentrations requires wide dynamic range of the measurement. Finally, the chemical heterogeneity of metabolites in terms of polarity, size, and charge suggest that not all components will be compatible with a single extraction and separation protocol. In this work, we examine how column miniaturization and use of two-dimensional (2D) separations impacts the coverage of the metabolome in complex mixtures by increasing peak capacity and sensitivity.

One approach to improving peak capacity is to improve efficiency by using smaller particles, as in ultra-high-pressure liquid chromatography (UHPLC). Application of UHPLC to metabolomic analysis has yielded impressive resolution of complex mixtures of metabolites (Wilson *et al.*, 2005). It is also well known that using 2D separations can

also improve peak capacity. While dual column GC-MS is becoming prevalent for analysis of some classes of metabolites (Mohler *et al.*, 2006; Welthagen *et al.*, 2005), 2D condensed-phase separations for metabolites has received less attention. In one example, a combination of conventional RPLC with a fast 2nd dimension of carbon-coated zirconia RPLC was used to analyze plant extracts and allowed detection of 100 small molecules in 25 min (Stoll *et al.*, 2006). An offline combination of LC with CE has been used to separate and detect 63 metabolite standards (Jia *et al.*, 2005). The use of absorbance detection likely limited both detection and identification of more metabolites in these cases. The relative lack of multi-dimensional analysis for metabolites is in contrast to proteomics where multi-dimensional separations have been widely developed and characterized (Opiteck *et al.*, 1997; Washburn *et al.*, 2001).

In this work, we examined the effect that 2D separations would have on the numbers of metabolites detected in complex mixtures from extracts of both prokaryotes and eukaryotes. Polar anions were selected as a group of compounds to target because they include energy metabolites, central to any organism, and their related products. Therefore, a combination of SAX and RPLC for the two-dimensions of separation was used.

In addition to exploring the effect of 2D separations, we also examined the utility of decreasing column inner diameter (I.D.) for improving the number of metabolites detected in a complex mixture. Column miniaturization improves separation efficiency (Kennedy and Jorgenson, 1989) and electrospray ionization efficiency (Schmidt *et al.*, 2003). Both of these effects are expected to aid in detection of more metabolites in a complex mixture. For these reasons, and because of the reduced sample consumption, capillary LC is commonly used in proteomics. In contrast, capillary LC has been relatively unexplored for metabolomic analysis (although, CE has seen some use for this application). This lack of application of capillary LC may be because most metabolomic studies have been directed towards samples that are relatively abundant, such as plants,

microbes, and bodily fluids, thus negating the need to analyze small quantities.

Nevertheless, miniaturization may be expected to improve sensitivity, and therefore the

number of compounds detected. Furthermore, use of miniaturized columns should also

enable analysis of more limited samples including specific mammalian tissues (Harwood

et al., 2006; Kennedy *et al.*, 1989; Wolters *et al.*, 2005; Woods *et al.*, 2005) such as

embryos, neurons, and islets of Langerhans, which are too small to analyze with currently

used methods.

Experimental procedures

Reagents and materials. All chemicals were purchased from Sigma-Aldrich (St Louis,

MO USA) unless otherwise noted. All solvents were purchased from Burdick and

Jackson (Muskegon, MI USA). Fused silica capillary was purchased from Polymicro

Technologies (Phoenix, AZ USA). Reversed phase chromatographic stationary phase

was purchased from Waters (Milford, MA USA). SAX chromatographic stationary

phase was donated by Dionex (Sunnyvale, CA USA). Eppendorf Safelock Biopur tubes

were purchased from Fisher Scientific (Fairland, NJ).

Capillary column fabrication. Capillary columns were prepared as previously described

(Haskins *et al.*, 2001). Briefly, macroporous photopolymerized frits were placed 5 cm

from the end of 50 cm long by 50 μm or 25 μm I.D. capillaries. Using a P-2000 laser

puller, tips were pulled 1 cm downstream of the frit, then etched for 30 seconds in 49%

HF (v/v) and rinsed to create a ~3 μm opening at the outlet of the column unless stated

otherwise. Capillaries were packed with 3 μm Atlantis C18 aqueous reversed phase

particles (Waters) using an acetone-slurry packing method (Kennedy and Jorgenson,

1989). All columns had 30 cm packed bed length and were subsequently cut to 35 cm total length.

For the SAX capillary columns, frits were formed by tapping 10 μm diameter borosilicate particles (Duke Scientific Palo Alto, CA USA) into the orifice of a 50 cm long by 250 μm I.D. capillary to a distance < 2 mm. The glass particles were then sintered in place with a flame (Kennedy and Jorgenson, 1989). SAX particles (CarboPac PA-100, 8.5 μm diameter) were slurry-packed at 2,000 psi, using 1 M NaCl as the solvent, to a bed length of 40 cm.

Chromatography conditions. The RPLC system utilized two flow-splitters, one before the injection valve and one after the injection valve, to reduce flow into the system and control flow during injection (Fig. B.1). To avoid extra-column band broadening from the use of a conventional six port injection valve onto capillary columns, samples were loaded off-line. In the injection procedure, flow was diverted from the column to splitter 1 using the injection valve. The column was uncoupled from the system and sample (9 nL for 50 μm I.D. and 2.5 nL for 25 μm I.D.) pumped onto the column using gas pressure applied to a sample reservoir. The column was then reconnected to the splitting tee and the injection valve actuated to initiate flow through the column. With this procedure, the HPLC pump (Model 626, Waters) was able to maintain a constant pressure and initiated flow immediately after the valve actuation. Despite multiple re-connections, no air bubbles were observed during the course of these experiments. Three mobile phases were used to form the reversed phase gradient. Mobile phase A was 20 mM formic acid pH 2.7, mobile phase B was 20 mM ammonium acetate pH 6.5, and mobile phase C was acetonitrile. All gradient transitions were linear, with the following profile (time: %A, %B, %C); initial time 0 min: 100%, 0%, 0%; hold 5 min.; 10 min: 0%, 100%, 0%; 18 min: 0%, 80%, 20%; 23 min: 0%, 65% 35%; 60 min: 0%, 25%, 75%; 65 min: 100%, 0%, 0%. The column was re-equilibrated for 30 min with mobile phase A following gradient

completion. Extended gradient consisted of 0 min: 100%, 0%, 0%; hold 5 min.; 10 min: 0%, 100%, 0%; 23 min: 0%, 80%, 20%; 34 min: 0%, 65% 35%; 60 min: 0%, 25%, 75%; 65 min: 100%, 0%, 0%.

The SAX chromatography system was operated in a conventional 6 port injection valve format. After injection of 10 μL of sample, a step gradient was used to elute anionic metabolites off the column. All gradient steps were 10 min in duration with mobile phase A: 5 mM ammonium formate pH 6.5 and mobile phase B: 700 mM ammonium formate (NH_4HCO_2) pH 6.5. Buffer was adjusted using ammonium hydroxide and formic acid as needed to reach the desired pH. The gradient profile was as follows (time: %A, %B): 0 min: 100%, 0%; 10 min: 86%, 14%; 20 min: 72%, 28%; 30 min: 58%, 42%; 40 min: 44%, 56%; 50 min: 30%, 70%; 60 min: 0%, 100%. Six fractions were collected from the capillary outlet in 10 min intervals. Fractions were then evaporated to dryness using a vacuum centrifuge and reconstituted to 10 μL with 10 mM formic acid for further analysis using RPLC-MS.

Mass spectrometry. Detection was accomplished using a LCQ Deca XP Plus quadrupole ion trap mass spectrometer (Thermo-Electron, San Jose, CA USA) operated in negative mode (spray voltage: -1.0 kV). Spectra were obtained in centroid mode with the mass spectrometer tuned for nucleotides (GTP) and the capillary temperature set to 150°C. Experiments were performed in full scan mode with the maximum injection time of 25 ms and the scan range between 50-1500 m/z. The capillary column was interfaced to the mass spectrometer using a nanospray interface (Thermo-Electron).

Sample preparation: E. coli. For cells cultured in minimal media, *E. coli* N99 was first grown in LB media on an orbital shaker overnight. The following morning, 25 μL of culture was added to 50 mL of minimal media (48 mM Na_2HPO_4, 22 mM KH_2PO_4, 8.6 mM NaCl, 18.8 mM NH_4Cl, 2.0 mM $MgSO_4$, 0.1 mM $CaCl_2$). Cells were grown on a

shaker at 37°C until OD_{600} = 1.5 (~20 h) when 15 mL of cultured *E. coli* was added to 35

mL of water at 4°C. Afterwards, the sample was spun and rinsed with cold water.

After a second rinse-resuspension, the *E. coli* suspension was centrifuged,

supernatant decanted and replaced with -20°C 500 μL of 50:50 methanol-water (v/v).

Cells were lysed using a sonic dismembrator (Fischer Scientific, model 60) set to power

of 9 W for 10 s. The lysate was then mixed 50:50 (v/v) with chloroform and set to

equilibrate on ice for 10 min. The final solvent composition was 25:25:50 (v/v/v)

methanol: water: chloroform. The aqueous portion was then removed and centrifuged at

4°C, 1200 g for 10 min. Supernatant was collected and vacuum centrifuged to near

dryness (< 5 μL), then reconstituted with mobile phase A to 100 μL for analysis.

Samples were stored at -80°C until use (< 1 week).

Sample preparation: Islets of Langerhans. Islets of Langerhans were isolated from CD-1

mice (20-30 g) as previously described (Edwards and Kennedy, 2005) with slight

modifications. Briefly, collagenase XI (0.5 mg/mL) was infused through the pancreatic

duct. Pancreas was then removed and incubated in 5 mL of collagenase XI (0.5 mg/mL)

at 37 ºC for 7 min. Islets were isolated by passing digested pancreas through a 100 μm

pore diameter nylon cell strainer (Fisher Scientific) with 10 mL of Krebs ringer buffer.

This procedure collected islets that were greater than 100 μm in diameter. Islets were

transferred to a Petri dish by inverting the filter, which was rinsed with 5 mL of buffer.

Islets were manually selected using a pipette and transferred to a Petri dish containing

cell culture media (10 mM glucose RPMI media 1640 with L-glutamine) supplemented

with 10% fetal bovine serum and 100 units/mL of penicillin and 100 μg/mL of

streptomycin. Islets were incubated in this media at 37ºC, 5% CO_2 for 2 to 7 days before

use.

A total of 50 islets were transferred from media to a rinse solution of 10 mM

glucose in water. Islets were rapidly removed in 15 μL of rinse solution, placed in a

Biopure tube and tapped down to deposit islets at the bottom of the tube. Rinse solution was then removed to ~ 5 μL and 10 μL of 50:50 MeOH-H$_2$O (v/v) at -20°C was added. Islets were triturated using a pipette until they appeared shredded as imaged through an inverted microscope. The process between rinse and ending trituration took ~45 sec. After islets were lysed, 15 μL of chloroform was added to the lysate and allowed to equilibrate on ice for 10 min. Sample was then treated as *E. coli* samples, with a post evaporation reconstitution volume of 15 μL.

Data processing. Peaks were discriminated from noise using MS Processor version 8.0 from Advanced Chemistry Development (Toronto, Canada). Detection of peaks, using a reconstructed ion chromatogram format, was performed using the following parameters: MCQ threshold = 0.85; smoothing window width = 3 scans; minimum full width at half maximum height = 3 scans; signal-to-noise = 5. Peaks were matched between runs when t_r < 3% RSD and Δm/z < 0.5. Statistical comparison was performed using a two-tailed student's t-test.

Results and discussion

Chromatography of metabolite standards

Our initial experiments focused on developing a capillary RPLC system for separation of polar metabolites. In order to ensure separation of a wide scope of small molecules, 24 metabolites from glycolysis and the tricarboxylic acid (TCA) cycle were targeted for separation and detection (see Table B.1 for compounds used). These analytes were chosen because they cover a broad range of charges and polarities, from polar glucose-6-phosphate to nonpolar FAD. A silica-based reversed-phase particle designed to be compatible with 100% aqueous mobile phases (Atlantis) was used to facilitate retention and separation of highly polar compounds.

216

Work with this stationary phase revealed that manipulation of mobile phase pH was critical in allowing separation of the different types of analytes present in glycolysis and the TCA cycle. With aqueous mobile phases at pH < 3.0, polar organic acids were well-retained and resolved but, phosphorylated nucleotides yielded poor peak shape and peak height (See supporting information Fig. B.S1 and B.S2). When the aqueous component of the mobile phase had pH > 6.5, the phosphorylated nucleotides were well resolved but, polar organic acids co-eluted near the column dead volume. Intermediate pH mobile phases (pH = 4.5) yielded poor resolution and peak shape for all classes of metabolite standards (data not shown). These data indicated that low pH mobile phase was necessary for separation of small organic acids while higher pH was required for separation of phosphorylated nucleotides. To resolve this problem, a gradient of formic acid pH 2.7 to ammonium formate pH 6.5 was used for the initial part of the separation followed by an increase in acetonitrile content to elute the less polar analytes. As seen in Fig. B.2, these conditions allowed separation of 23 of the 24 metabolite standards and were used for all further RPLC experiments.

For detection, negative mode ESI was used. Preliminary experiments revealed that negative mode ESI substantially decreased adduct formation and increased S/N when compared to positive mode ESI for these metabolites (data not shown). The use of capillary columns allowed for good sensitivity with lower detection limits of 0.3-12 fmol for glycolytic and TCA metabolite standards (see Table B.1). These detection limits are a two to three order of magnitude improvement over previous reports even though the prior work used SRM for detection instead of full-scan mode (Bajad *et al.*, 2006; Mashego *et al.*, 2004). For these measurements, only 9 nL of sample were consumed for the injection. Although the mass detection limit was considerably improved over previous results, the concentration detection limit was generally not improved over prior results. The use of full scan mode was chosen to facilitate an untargeted metabolomics approach, though this is likely the reason why cLODs were not improved over previous tandem MS

modes. The good mass detection limits suggest that this method may have utility for sample limited metabolomic analysis; although that application was not explored in this work.

E. coli metabolite detection

When this method was applied to extracts of *E. coli*, 157 features were detected in the LC-MS data. We were interested in determining the number of actual endogenous small molecules detected; therefore, data were analyzed to eliminate false peaks and multiple peaks for single compounds. Peaks due to Na^+ and formate adducts (as indicated by $+22$ and $+46$ m/z respectively and identical retention time to the base analyte), multiple charge states, and water loss, were eliminated from analyte count. Using the above criteria, a total of 111 ± 9 (n = 3) compounds were detected in the *E. coli* samples that were not present in background.

Using the average peak width for the compounds detected and the retention time window, a peak capacity of 110, based on unity resolution, was calculated for this separation. In calculating peak capacity, we determined the peak capacity separately for the two different gradients (a pH gradient and the organic phase gradient), because the peaks had different widths in these gradients, and added them together. Detection of more small molecules than indicated by the calculated peak capacity is due to the use of the mass spectrometer as the detector, which substantially increases the peak capacity.

To evaluate the effect of column dimension on detection of metabolites in *E. coli*, the capillary column I.D. was reduced from 50 μm to 25 μm. For these experiments, the gradient conditions and mobile phase velocity were kept the same but the volume injected was decreased by 4 in proportion to the column volume. The ESI tip I.D. was decreased from 3.0 to 1.5 μm and the volumetric flow rate from 104 to 25 nL/min. Decreasing the column I.D. is expected to improve separation efficiency primarily by decreasing the A term of the Van Deemter equation (Kennedy and Jorgenson, 1989).

218

Furthermore, the lower flow rate and smaller emitter tips may be expected to improve ionization efficiency and therefore sensitivity (Andren and Caprioli, 1995; Korner *et al.*, 1996). Both of these effects are seen in the comparison of the reconstructed ion chromatograms for m/z 662, chosen as a typical analyte, shown in Fig. B.3. On average, peak width decreased by 25 ± 14% (n = 4) while the signal increased by 88 ± 21% (n = 4) for decreasing the column I.D. by 2-fold. The signal increased even though 4-fold less sample was injected. The improvement in signal intensity cannot be solely attributed to improved peak shape as peak area was also increased (23% greater) in the 25 μm column.

An added benefit of the decrease in column I.D. was a decrease in adduct formation. As shown in Fig. B.3B and C, peaks 698 m/z and 720 m/z, adducts to 662 were reduced from ~40% of base height to ~20%. The increase in signal intensity discussed above can be in large part attributed to the reduced adduct formation and increased ionization efficiency (Schmidt *et al.*, 2003).

As summarized in Fig. B.4, the decrease in peak width associated with decreasing the column bore increased peak capacity from 114 to 168. The actual number of peaks detected in *E. coli* extracts increased in proportion to the peak capacity from 111 ± 9 to 156 ± 17 (n = 3). These results illustrate a multi-faceted improvement in decreasing column I.D. for complex metabolite detection. We also examined the effect of extending the gradient time from 11 to 24 min. This manipulation had a modest, but not statistically significant, improvement in peak capacity and number of metabolites detected (Fig. B.4).

Two-dimensional capillary chromatography

After establishing the peak capacity and number of components detected on the reversed phase column, the effect of pre-fractionation using a SAX column was evaluated. For this investigation, six fractions resulting from step gradients of 100 mM increments of ammonium formate were collected from the SAX column off-line and stored for a second separation on the reversed phase column. The SAX-RPLC-MS

method was applied to extracts of *E. coli* lysate. Fig. B.5B-G shows the base peak chromatogram of six SAX fractions injected onto a capillary RPLC column. The use of a 2D separation resulted in detection of 244 ± 21 compounds compared to 170 ± 14 (n = 3) for the single dimension RPLC with the same RPLC gradient. As the SAX eluent was dried and then reconstituted to the same volume as initially injected (Fig. B.5B-G), dilution effects of the first dimension should not be present. The peak capacity of the separation is estimated as 970 (6 SAX fractions $\times$ 161 peaks for RPLC).

Carryover, defined as detection of a given compound in more than 1 SAX fraction, was found for approximately 14% of the small molecules detected. The majority of the carryover was present between the first two fractions. This indicated that those compounds which were weakly retained on the SAX column were overloaded, whereas those compounds of higher affinity were well retained and preconcentrated in the 1st dimension.

In principle, the MS adds a significant resolving component making it unnecessary to use extremely high peak capacity separations; however, the above results illustrate that the improved separation resolution increased the coverage of the metabolome. At least part of this effect is due to signal enhancement associated with reducing the number of co-eluting components. Signal enhancement was quantified by comparing signal intensity from co-eluting compounds in the 1-D RPLC with those same compounds which were separated into different fractions by SAX and analyzed by RPLC. Seven sets of peaks were found to co-elute in the 1D analysis, which were resolved into different fractions by SAX. These peaks increased signal intensity on average by 47% ($\pm$ 29%). Presumably this improvement is due to reduction of competing ionization and other matrix effects.

Islet analysis

The majority of metabolomic analyses have involved plants and prokaryotes; however, metabolomic analysis of specific tissues is mammalian systems is emerging as an important application (Haskins *et al.*, 2001; Jensen *et al.*, 2006). We therefore also evaluated the effectiveness of these methods on islets of Langerhans. Islets are microorgans dispersed throughout the pancreas, which contain about 3000 cells each. Islets secrete insulin in a process driven by glucose metabolism. Metabolic disturbances of islets are a possible root cause of type 2 diabetes, therefore considerable benefit may emerge from metabolomic analysis of these cells. Only ~70 islets can be isolated from a single mouse and the smallest reasonable sample volume for extracting this amount of tissue is ~ 20 μL; therefore, minimizing the sample volume required for analysis is of interest. The use of capillary columns is well-suited for analysis of such samples.

Fig. B.6A shows the base peak chromatogram from a capillary RPLC-MS analysis of lysate from 50 islets in 15 μL. Average peak width for these samples (n = 3) was 8 s, which is ~ 2 s less than those found with *E. coli* samples. The decrease in average peak width was due to detecting a larger number of hydrophobic compounds, which tend to elute as narrower zones in this gradient. As a result of the decrease in peak width, the peak capacity calculated for the separation was increased to 240 from 161 for the *E. coli* sample (Fig. B.4). Using the criteria described above for the *E. coli* analysis for distinguishing peaks from compounds, an average of 191 ± 14 (n = 3) compounds were detected in the islet samples.

As with the *E. coli* samples, use of the 2D separation significantly increased the coverage of the metabolome (Fig. B.4 and B.6B-G). Whereas the single dimension RPLC yielded on average 191 small molecules, 2D-LC allowed for detection of 391 ± 33 peaks with a peak capacity of 1200. Fig. B.6 illustrates that the number of peaks detected decreased over the course of the step gradient, with the majority found in the first three

fractions. The limited number of compounds found in the last three steps suggests that metabolites with a high degree of charge are relatively rare in islets.

Interestingly, islets yielded significantly more metabolites than the *E. coli* (Fig. B.4) even though the islet samples were about 1% as concentrated on a per gram of tissue basis. Many of these metabolites were fairly large (m/z > 600) and non-polar (i.e., eluted during the organic phase of the gradient). The greater complexity of the metabolome is likely due to in part to the media in which the cells are cultured. Islets were incubated in media containing glucose, amino acids, vitamins and fetal bovine serum, which would allow for synthesis and uptake of more metabolites than the media containing only glucose as a fuel as was the case for *E. coli*. The differences in metabolites detected may also reflect inherent differences in the complexity of the metabolomes of the different tissue types. Because of the greater complexity of the islet metabolome, the use of 2D separation was even more important for increasing the number of detected metabolites in these samples than for the *E. coli* samples (compare increase in detected metabolites in Fig. B.4).

Our experiments have addressed the potential impact of column dimensions and multi-dimensionality on metabolite separations. Many other factors are important in determining the quality of metabolomic data including sample extraction, quantification, and peak identification. Recent data has suggested for example that the use of water rinses on bacteria samples, such as those used here, prior to extraction may result in disturbance of metabolite levels (Saghatelian *et al.*, 2004). Therefore, development of metabolomic methods for quantification will require consideration of those variables as well.

Conclusion

The work presented here demonstrates the utility of an aqueous-compatible stationary phase in combination with a ternary gradient to separate and detect metabolites

with a wide range of polarities and charge, including those in glycolysis and the TCA cycle. Reduction of column I.D. led to superior peak shape, reduction of adducts, and higher signal intensity. The use of multiple dimensions improved peak capacity as expected. Combined, these effects more than doubled the number of metabolites detected from a complex metabolomic samples as summarized in Fig. B.4. A comparison of the number of metabolites in the *E. coli* and islet samples reveals detection of approximately 60% more in the islets. Furthermore, the islet samples had more high molecular weight molecules. These differences may reflect either an inherently more complex metabolome or effects of incubation media or both. Regardless, these results illustrate the potential for high sensitivity and high resolution for metabolomic analysis by multi-dimensional separations on capillary columns.
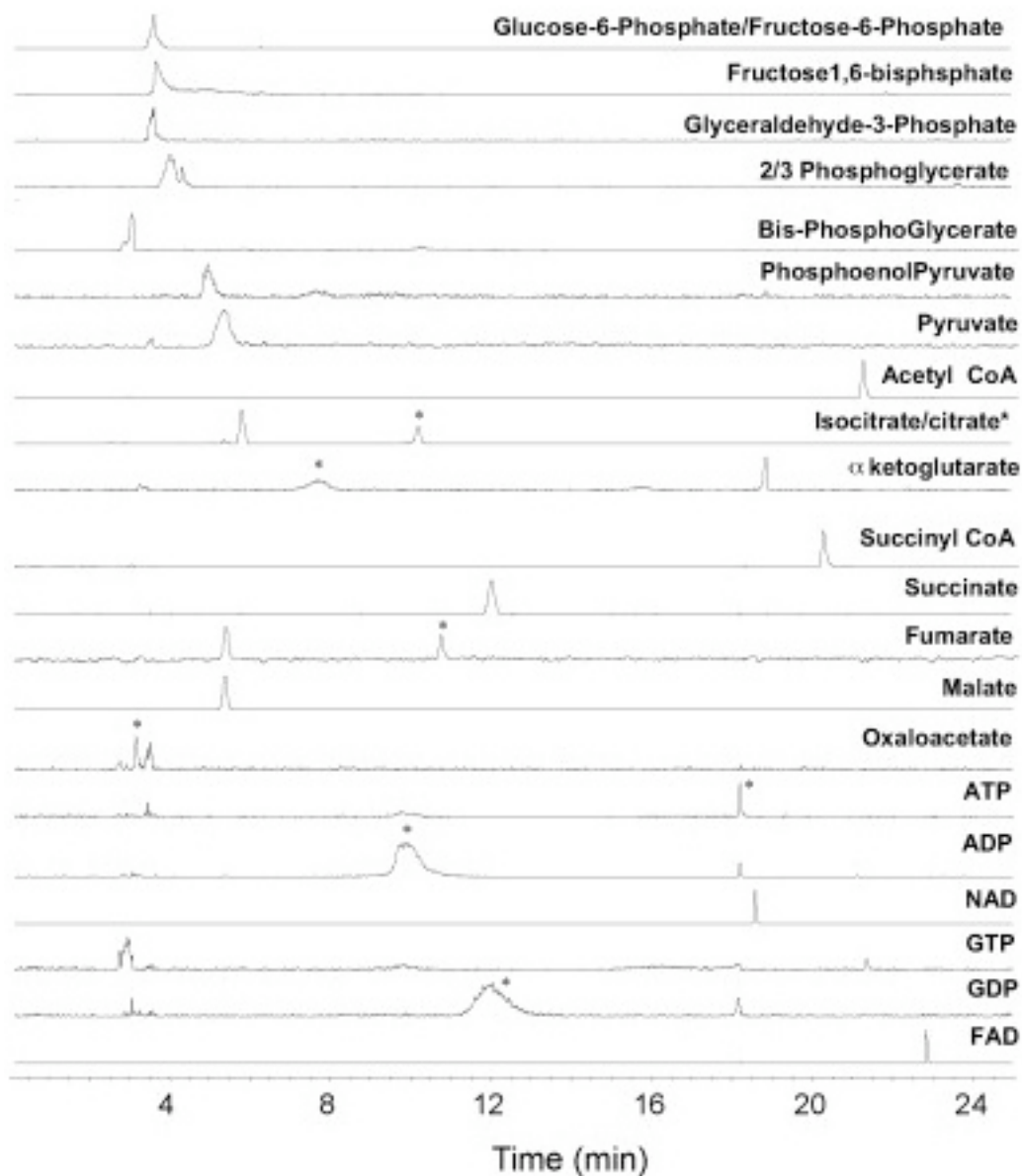
Figure B.1.
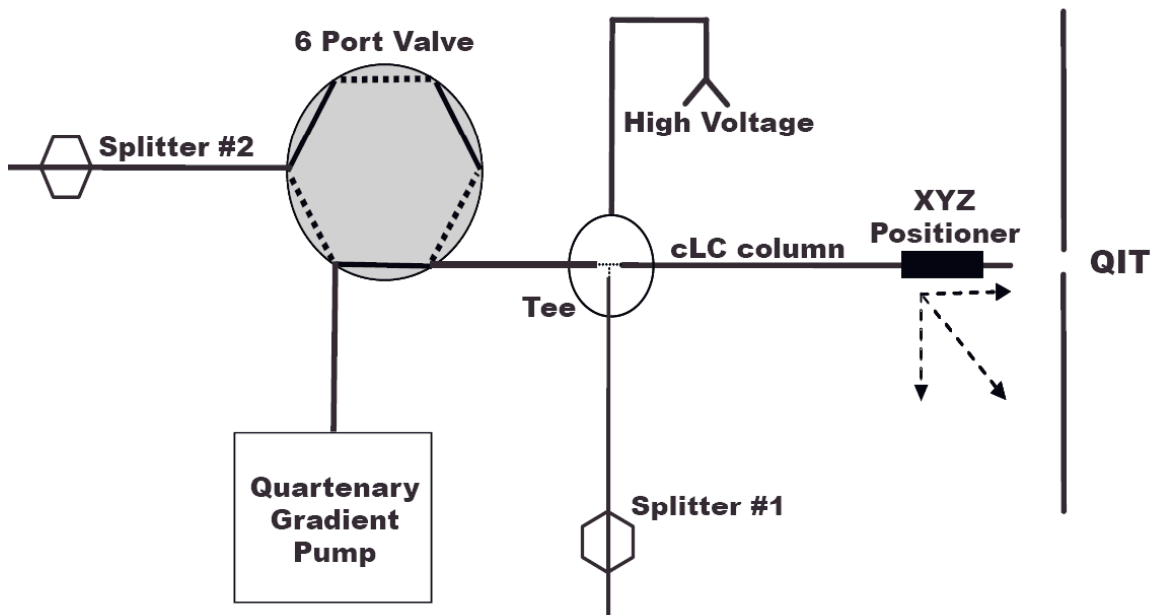
Figure B.1. Block diagram of capillary LC system illustrating splitters and voltage application.
For sample loading, the 6 port valve is set in "load" position (flow path represented by dashed line), the column is removed from the tee, sample loaded onto column using gas pressure sample reservoir (500 psi) and then reconnected to tee. The valve is actuated to inject position (solid lines) and gradient initiated. With this configuration, the pump is maintained at near constant pressure during the entire experiment.
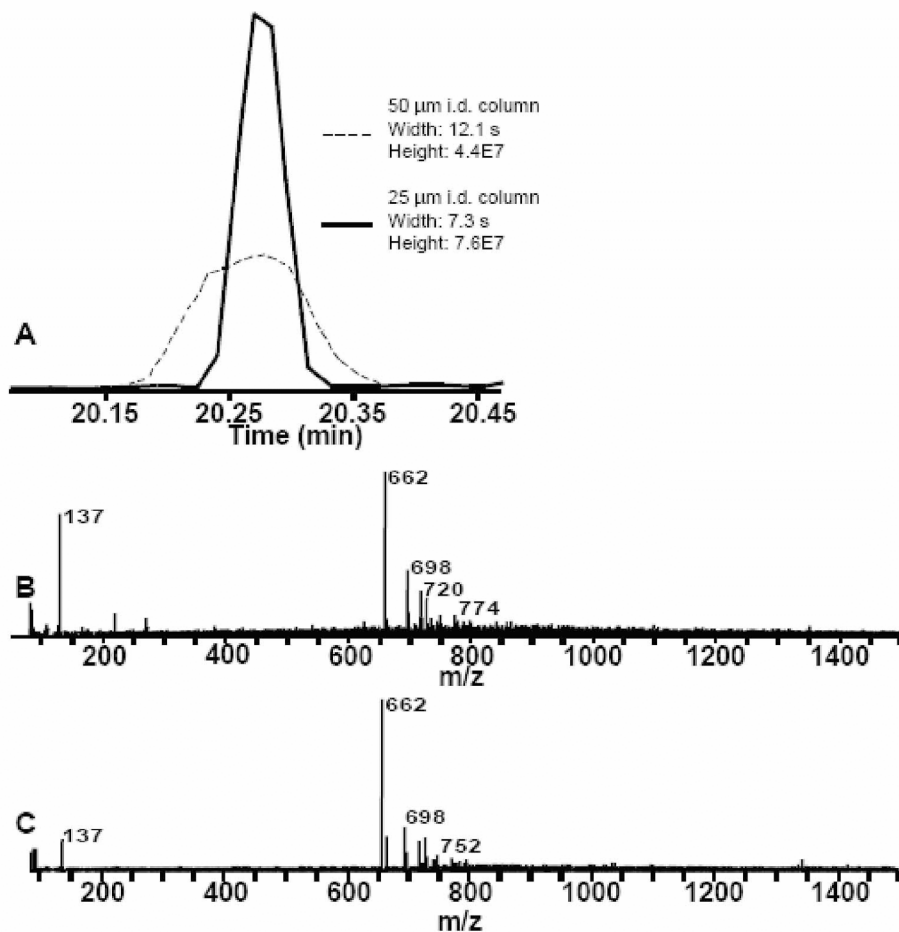
Figure B.2.

Figure B.2. Reconstructed ion chromatogram illustrating resolution of 23 of 24 metabolite standards using ternary gradient of formic acid, ammonium formate and acetonitrile.
Standards were mixed together before analysis. The LC column used was 30 cm long × 50 μm I.D. packed with Atlantis dC-18 3 μm particles and equipped with an integrated nanospray tip with 3 μm diameter. Gradient is given in the experimental section. Flow velocity was 100 nl/min. * indicate peak for the analyte when multiple peaks are detected.

Figure B.3.

Figure B.3. Effect of decreasing column I.D. on peak signal and mass spectrum.
(A) Reconstructed ion chromatogram of 662 m/z from 50 μm I.D. and 25 μm I.D. column. (B) Average mass spectrum over width of 662 m/z peak from 50 μm I.D. column. (C) Average mass spectrum over width of 662 m/z peak from 25 μm I.D. column. Comparison of B and C illustrates fewer adducts to the 662 m/z peak and a 73% increase in signal intensity.
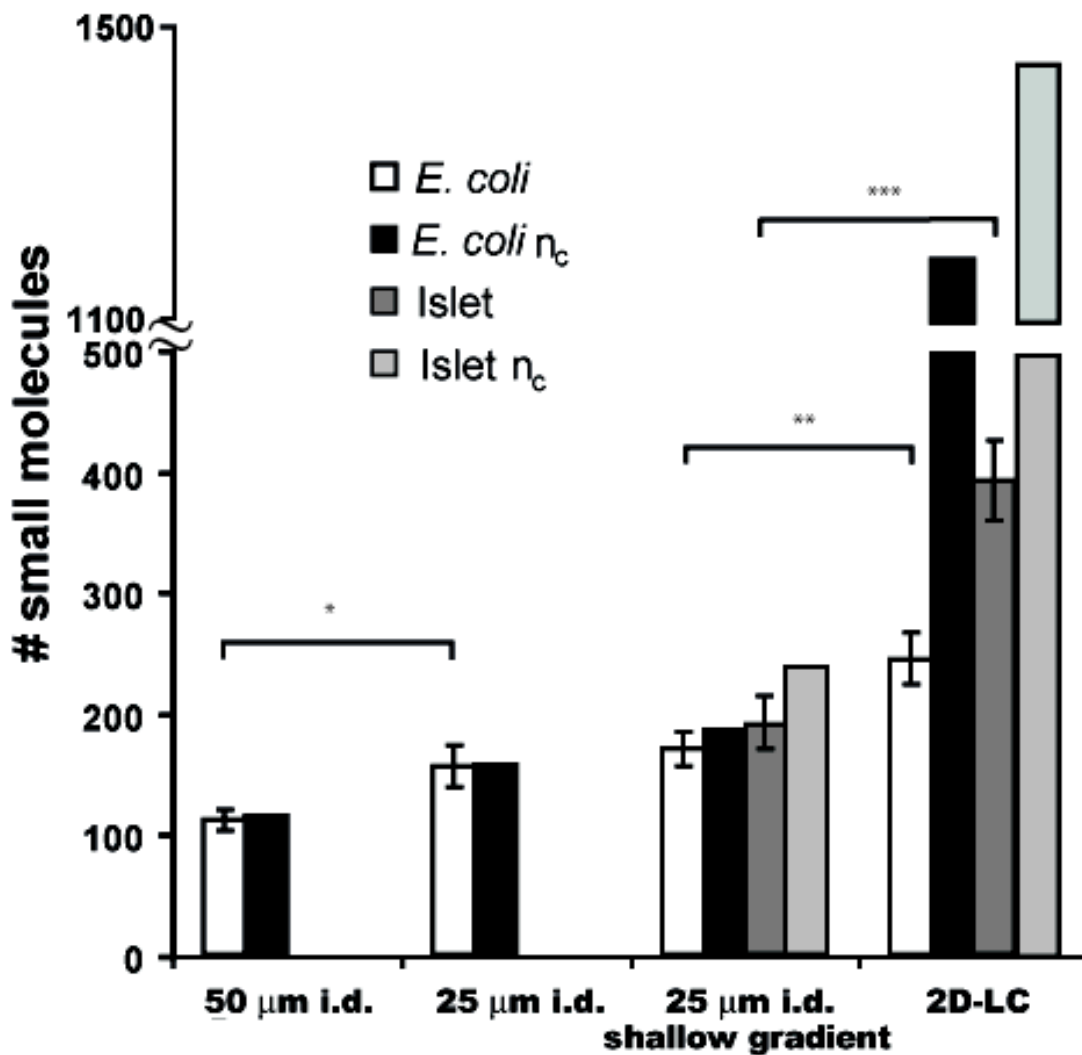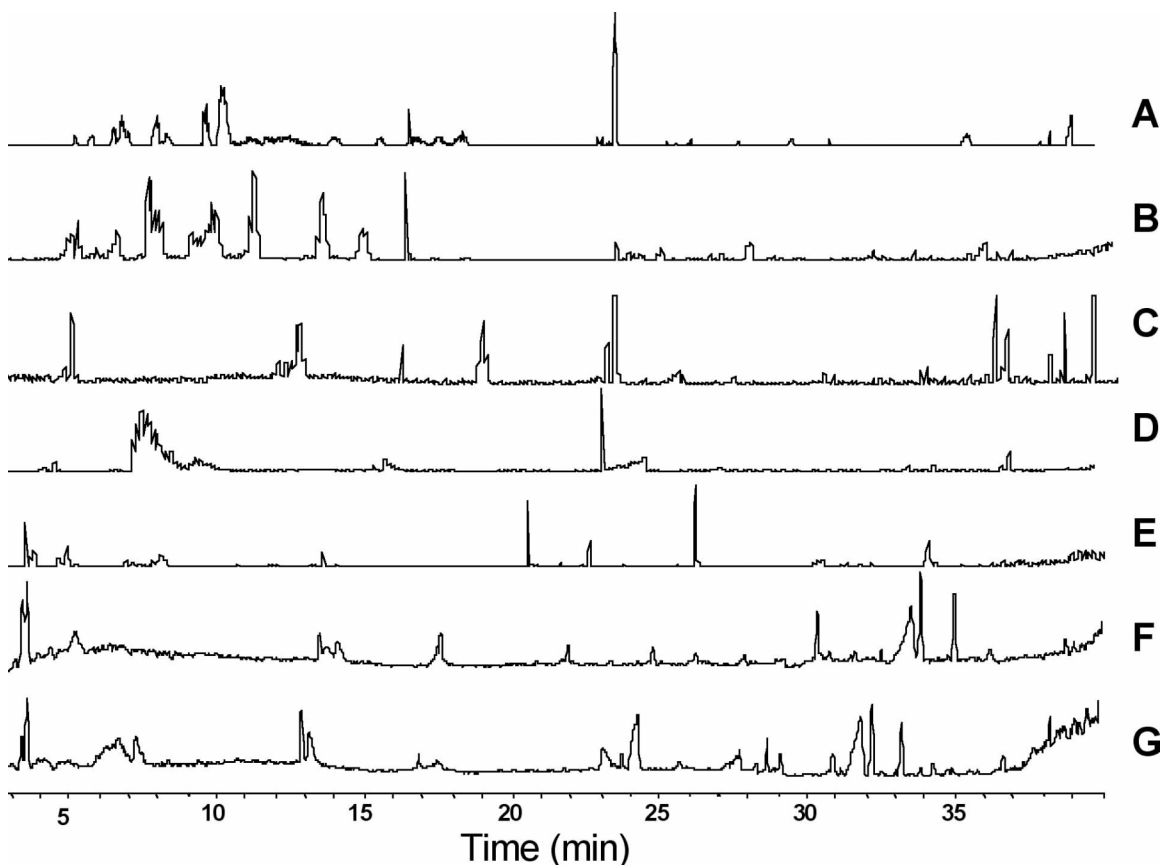
Figure B.4.

Figure B.4. Effect of chromatographic changes on the peak capacity and number of small molecules detected in complex mixtures.
Error bars represent 1 standard deviation. Statistical significance between samples is as follows: * $p < 0.05$; ** $p < 0.01$; *** $p < 0.005$.

Figure B.5.

Figure B.5. Base peak chromatograms from 1D and 2D separation of small molecules from *E. coli*.
RPLC was performed using 30 cm × 25 μm I.D. column. 2D was performed by off-line fraction collection in 10 min step intervals from SAX capillary column. [Brackets] indicate the average number of small molecules detected. (A) 1-D RPLC-MS [170]. (B-G) 2-D SAX-RPLC. (B) 5 mM NH_4HCO_2 fraction [79]. (C) 100 mM NH_4HCO_2 fraction [46]. (D) 200 mM NH_4HCO_2 fraction [45]. (E) 300 mM NH_4HCO_2 fraction [38]. (F) 400 mM NH_4HCO_2 fraction [19]. (G) 500 mM NH_4HCO_2 fraction [16].

Figure B.6.
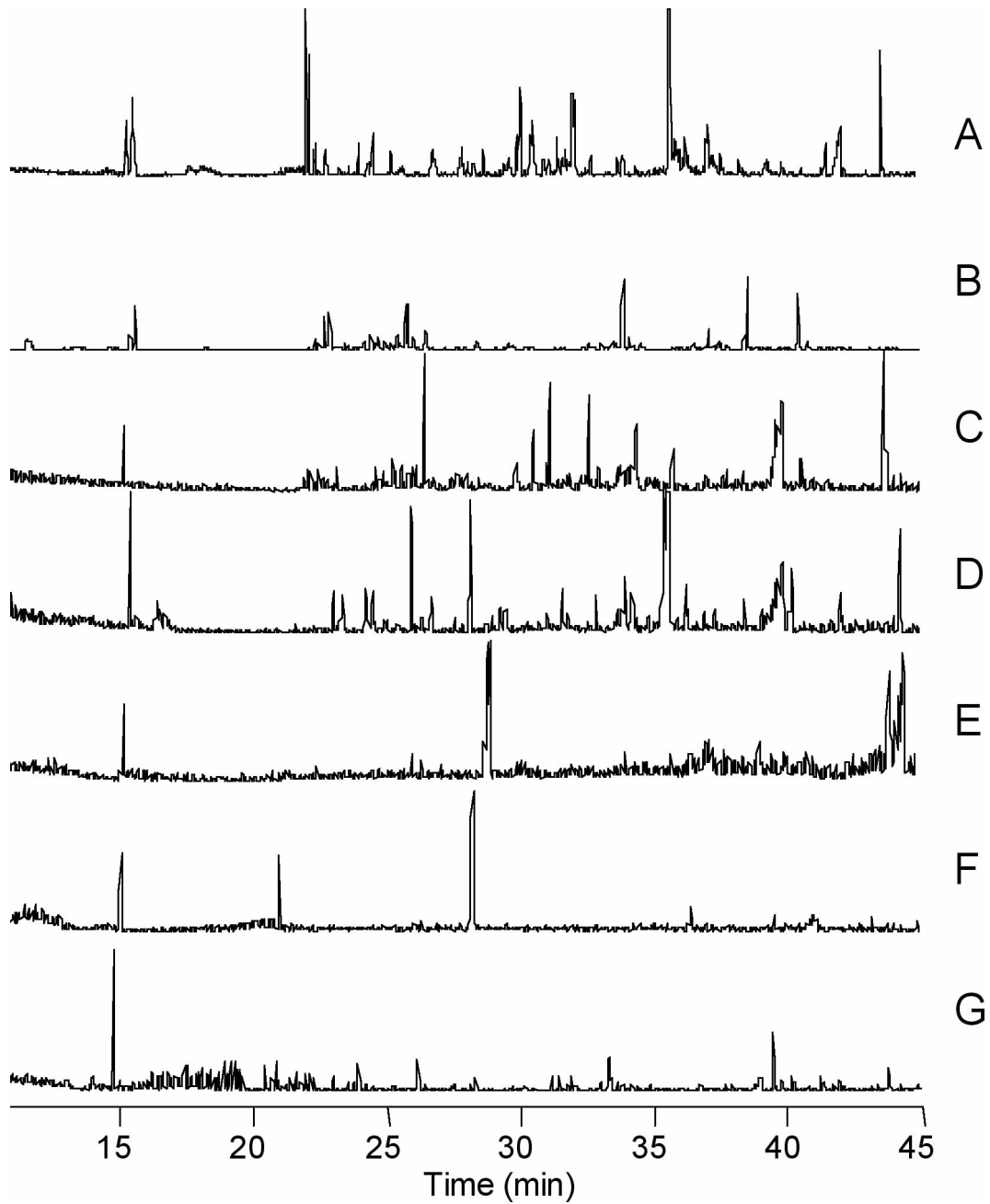
Figure B.6. Base peak chromatograms from 1D and 2D separation of small molecules from 50 islets of Langerhans.
Experiment performed as in Figure B.5. [Brackets] indicate the average number of small molecules detected. (A) 1-D RPLC-MS [191]. (B-G) 2-D SAX-RPLC. (B) 5 mM NH_4HCO_2 fraction [155]. (C) 100 mM NH_4HCO_2 fraction [70]. (D) 200 mM NH_4HCO_2 fraction [73]. (E) 300 mM NH_4HCO_2 fraction [41]. (F) 400 mM NH_4HCO_2 fraction [36]. (G) 500 mM NH_4HCO_2 fraction [18].

Table B.1.

Metabolite	% RSD	LLOD (fmol)	LLOD (μM)
G6P/F6P	24	4	0.5
F1,6P	18	6	0.6
Glyceraldehyde-3-Phosphate	16	30	4
2/3 Phospho-glycerate	26	30	4
Bis-phospho-glycerate	17	7	0.8
Phosphoenol Pyruvate	11	20	3
Pyruvate	33	20	2
Acetyl CoA	25	2	0.2
Citrate	31	10	1
Isocitrate	30	7	0.8
α–Ketoglutarate	18	10	1
Succinyl CoA	30	4	0.4
Succinate	10	9	1
Fumarate	27	10	2
Malate	19	3	0.3
Oxaloacetate	24	20	2
ATP	6	5	0.6
ADP	10	4	0.4
NAD	17	1	0.1
GTP	19	5	0.6
GDP	34	4	0.4
FAD	32	2	0.2

Table B.1. Figures of merit for metabolite standards.
% RSDs were analyzed based on peak height for 5 μM n = 3. Lower limits of detection were calculated as the concentration that would give a S/N of 3 based on the average S/N ratio of peaks at sample concentrations of 5 μM, n = 3. Detection limits were determined using gradient separation conditions similar to those used in Figure B.2.

Figure B.S1.
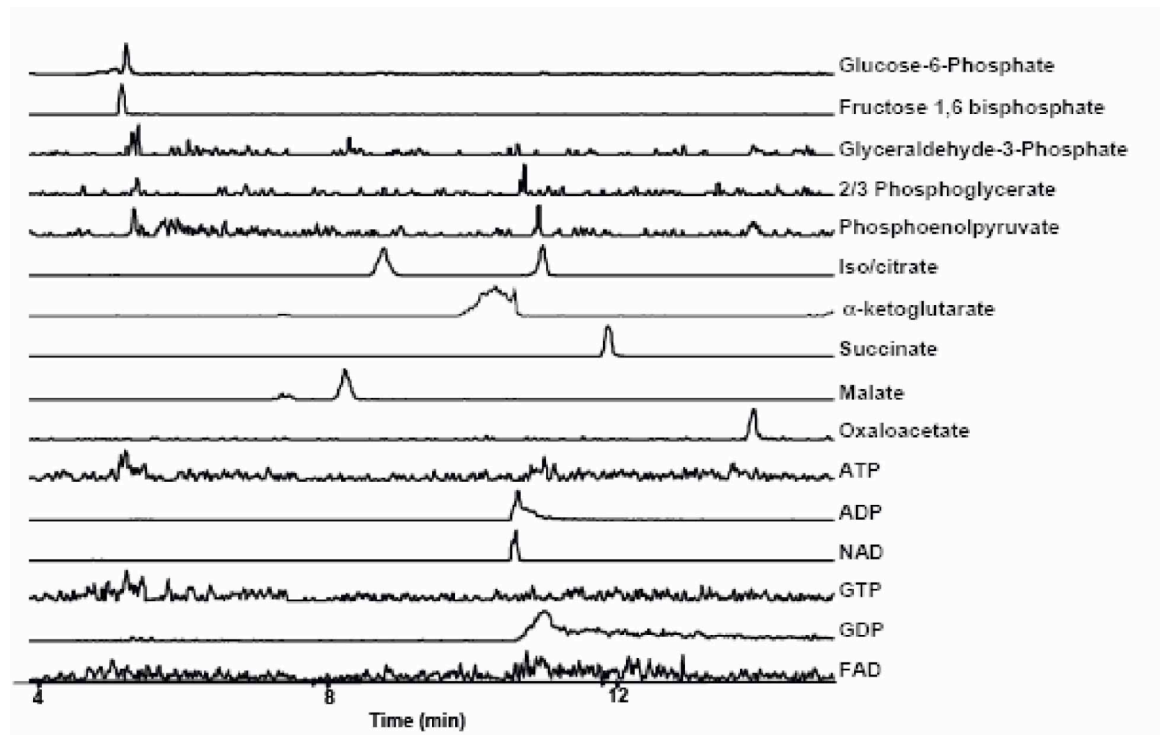
Figure B.S1. Separation of metabolite standards under acidic (pH 2.7) conditions with ACN.
Gradient was 0-20% ACN over 20 min. Metabolite concentrations were 10 μM each.
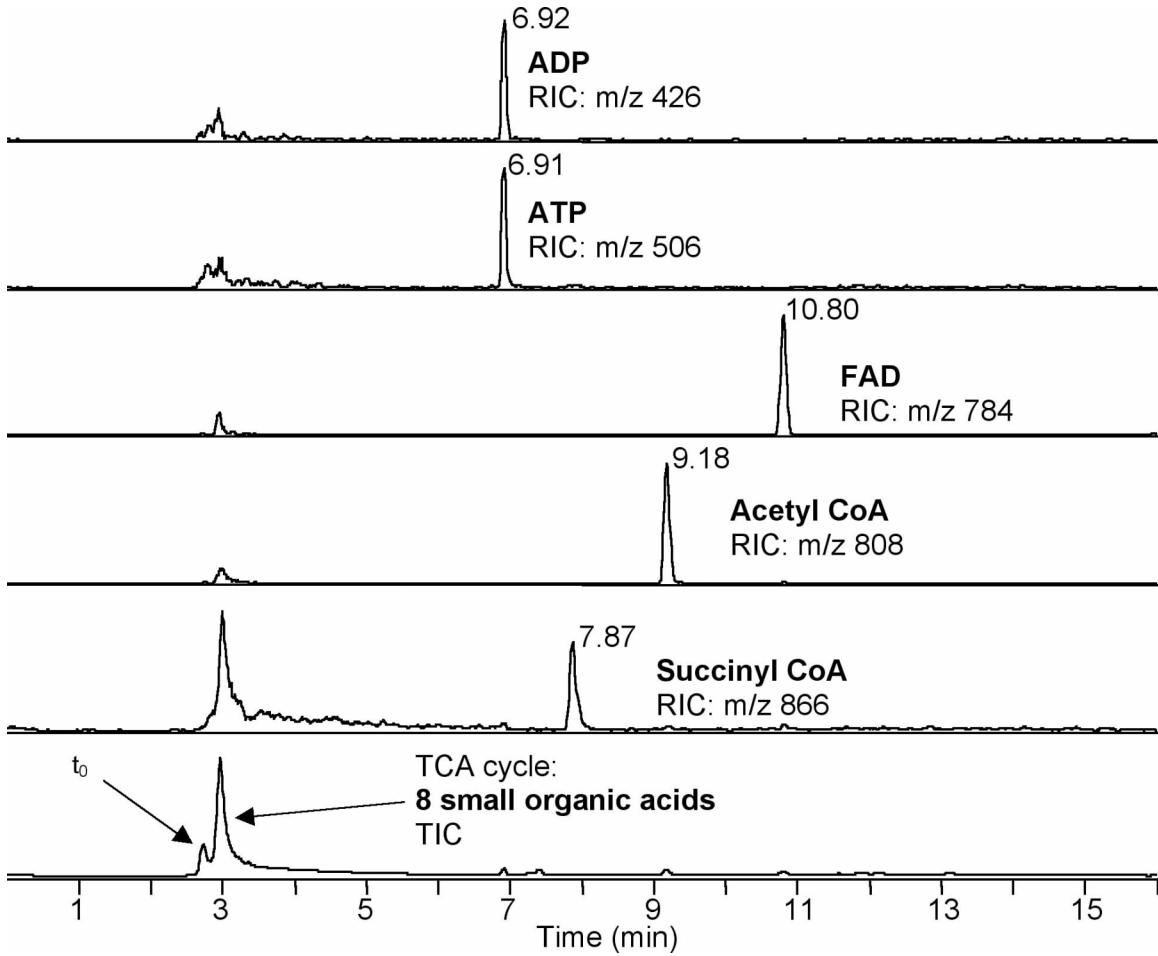
Figure B.S2.

Figure B.S2. Separation of metabolite standards under neutral (pH 6.5) conditions with ACN gradient.
Gradient was 0-20% ACN over 20 min. Top 5 traces are reconstructed ion chromatograms (RIC) for mass of each compound indicated. Bottom trace is total ion chromatogram (TIC). Metabolite concentrations were 10 μM each.

BIBLIOGRAPHY

BIBLIOGRAPHY

Abdelrahman, Y.M., and Belland, R.J. (2005) The Chlamydial developmental cycle. *FEMS Microbiol. Rev.* **29**: 949-959.

Aberg, A., Shingler, V., and Balsalobre, C. (2006) (p)ppGpp regulates type 1 fimbriation of *Escherichia coli* by modulating the expression of site-specific recombinase FimB. *Mol. Microbiol.* **60**: 1520-1533.

Abu-Zant, A., Asare, R., Graham, J.E., and Abu Kwaik, Y. (2006) Role for RpoS but not RelA of *Legionella pneumophila* in modulation of phagosome biogenesis and adaptation to the phagosomal environment. *Infect. Immun.* **74**: 3021-3026.

Alli, O.A.T., Gao, L.-Y., Pedersen, L.L., Zink, S., Radulic, M., Doric, M., and Abu Kwaik, Y. (2000) Temporal pore formation-mediated egress from macrophages and alveolar epithelial cells by *Legionella pneumophila*. *Infect. Immun.* **68**: 6431-6440.

Andren, P.E., and Caprioli, R.M. (1995) *In vivo* metabolism of substance-P in rat striatum utilizing microdialysis liquid-chromatography micro-electrospray mass-spectrometry. *J. Mass. Spectrom.* **30**: 817-824.

Appleby, J.L., Parkinson, J.S., and Bourret, R.B. (1996) Signal transduction via the multi-step phosphorelay: not necessarily the road less traveled. *Cell* **86**: 845-848.

Archuleta, R.J., Hoppes, P.Y., and Primm, T.P. (2005) *Mycobacterium avium* enters a state of metabolic dormancy in response to starvation. *Tuberculosis* **85**: 147-158.

Bachman, M.A., and Swanson, M.S. (2001) RpoS co-operates with other factors to induce *Legionella pneumophila* virulence in the stationary phase. *Mol. Microbiol.* **40**: 1201-1214.

Bachman, M.A., and Swanson, M.S. (2004a) The LetE protein enhances expression of multiple LetA/LetS-dependent transmission traits by *Legionella pneumophila*. *Infect. Immun.* **72**: 3284-3293.

Bachman, M.A., and Swanson, M.S. (2004b) Genetic evidence that *Legionella pneumophila* RpoS modulates expression of the transmission phenotype in both the exponential phase and the stationary phase. *Infect. Immun.* **72**: 2468-2476.

Bajad, S.U., Lu, W., Kimball, E.H., Yuan, J., Peterson, C., and Rabinowitz, J.D. (2006) Separation and quantitation of water soluble cellular metabolites by hydrophilic interaction chromatography-tandem mass spectrometry. *J. Chromatogr. A* **1125**: 76-88.

Barker, J., Lambert, P.A., and Brown, R.W. (1993) Influence of intra-amoebic and other growth conditions on the surface properties of *Legionella pneumophila*. *Infect. Immun.* **61**: 3503-3510.

Battesti, A., and Bouveret, E. (2006) Acyl carrier protein/SpoT interaction, the switch linking SpoT-dependent stress response to fatty acid metabolism. *Mol. Microbiol.* **62**: 1048-1063.

Belyi, Y., Tabakova, I., Stahl, M., and Aktories, K. (2008) Lgt: a family of cytotoxic glucosyltransferases produced by *Legionella pneumophila*. *J. Bacteriol.* **190**: 3026-2025.

Berger, K.H., and Isberg, R.R. (1993) Two distinct defects in intracellular growth complemented by a single genetic locus in *Legionella pneumophila*. *Mol. Microbiol.* **7**: 7-19.

Berger, K.H., Merriam, J.J., and Isberg, R.R. (1994) Altered intracellular targeting properties associated with mutations in the *Legionella pneumophila dotA* gene. *Mol. Microbiol.* **14**: 809-822.

Bijlsma, J.J.E., and Groisman, E.A. (2003) Making informed decisions: regulatory interactions between two-component systems. *Trends Microbiol.* **11**: 359-366.

Blander, G., and Guarente, L. (2004) The Sir2 family of protein deacetylases. *Annu. Rev. Biochem.* **73**: 417-435.

Boon, E.M., and Marletta, M.A. (2005) Ligand specificity of H-NOX domains: from sGC to bacterial NO sensors. *J. Inorg. Biochem.* **99**: 892-902.

Boucher, P.E., Menozzi, F.D., and Locht, C. (1994) The modular architecture of bacterial response regulators: insights into the activation mechanism of the BvgA transactivator of *Bordetella pertussis*. *J. Mol. Biol.* **241**: 363-377.

Bougdour, A., and Gottesman, S. (2007) ppGpp regulation of RpoS degradation via anti-adaptor protein IraP. *Proc. Natl. Acad. Sci. USA* **104**: 12896-12901.

Brassinga, A.K., Hiltz, M.F., Sisson, G.R., Morash, M.G., Hill, N., Garduno, E., Edelstein, P.H., Garduno, R.A., and Hoffman, P.S. (2003) A 65-kilobase pathogenicity island is unique to Philadelphia-1 strains of *Legionella pneumophila*. *J. Bacteriol.* **185**: 4630-4637.

Bruggemann, H., Hagman, A., Jules, M., Sismeiro, O., Dillies, M.A., Gouyette, C., Kunst, F., Steinert, M., Heuner, K., Coppee, J.Y., and Buchrieser, C. (2006) Virulence strategies for infecting phagocytes deduced from the *in vivo* transcriptional program of *Legionella pneumophila*. *Cell. Microbiol.* **8**: 1228-1240.

Buttke, T.M., and Ingram, L.O. (1978) Inhibition of unsaturated fatty acid synthesis in *Escherichia coli* by the antibiotic cerulenin. *Biochemistry* **17**: 5282-5286.

Byrne, B., and Swanson, M.S. (1998) Expression of *Legionella pneumophila* virulence traits in response to growth conditions. *Infect. Immun.* **66**: 3029-3034.

Calva, E., and Oropeza, R. (2006) Two-component signal transduction systems, environmental signals, and virulence. *Microb. Ecol.* **51**: 166-176.

Cashel, M. (1969) The control of ribonucleic acid synthesis in *Escherichia coli*. *J. Biol. Chem.* **244**: 3133-3141.

Cashel, M. (1994) Detection of (p)ppGpp accumulation patterns in *Escherichia coli* mutants. *In K.W. Adolph (ed.) Methods in Molecular Genetics, vol. 3. Molecular Microbiology Techniques, part A. Academic Press, New York.*

Cazalet, C., Rusniok, C., Bruggemann, H., Zidane, N., Magnier, A., Ma, L., Tichit, M., Jarraud, S., Bouchier, C., Vandenesch, F., Kunst, F., Etienne, J., Glaser, P., and Buchrieser, C. (2004) Evidence in the *Legionella pneumophila* genome for exploitation of host cell functions and high genome plasticity. *Nat. Genet.* **36**: 1165-1173.

Chatfield, C.H., and Cianciotto, N.P. (2007) The secreted pyomelanin pigment of *Legionella pneumophila* confers ferric reductase activity. *Infect. Immun.* **75**: 4062-4070.

Chatterji, D., and Kumar Ojha, A. (2001) Revisiting the stringent response, ppGpp and starvation signaling. *Curr. Opin. Microbiol.* **4**: 160-165.

Chien, M., Morozova, I., Shi, S., Sheng, H., Chen, J., Gomez, S.M., Asamani, G., Hill, K., Nuara, J., Feder, M., Rineer, J., Greenberg, J.J., Steshenko, V., Park, S.H., Zhao, B., Teplitskaya, E., Edwards, J.R., Pampou, S., Georghiou, A., Chou, I.C., Iannuccilli, W., Ulz, M.E., Kim, D.H., Geringer-Sameth, A., Goldsberry, C., Morozov, P., Fischer, S.G., Segal, G., Qu, X., Rzhetsky, A., Zhang, P., Cayanis, E., De Jong, P.J., Ju, J., Kalachikov, S., Shuman, H.A., and Russo, J.J. (2004) The genomic sequence of the accidental pathogen *Legionella pneumophila*. *Science* **305**: 1966-1968.

Cirillo, J.D., Cirillo, S.L., Yan, L., Bermudez, L.E., Falkow, S., and Tompkins, L.S. (1999) Intracellular growth in *Acanthamoeba castellanii* affects monocyte entry mechanisms and enhances virulence of *Legionella pneumophila*. *Infect. Immun.* **67**: 4427-4434.

Conover, G.M., Martinez-Morales, F., Heidtman, M.I., Luo, Z.Q., Tang, M., Chen, C., Geiger, O., and Isberg, R.R. (2008) Phosphatidylcholine synthesis is required for optimal function of *Legionella pneumophila* virulence determinants. *Cell. Microbiol.* **10**: 514-528.

Cook, G.A., King, M.T., and Veech, R.L. (1978) Ketogenesis and malonyl coenzyme A content of isolated rat hepatocytes. *J. Biol. Chem.* **253**: 2529-2531.

Cotter, P.A., and Miller, J.F. (1997) A mutation in the *Bordetella bronchiseptica bvgS* gene results in reduced virulence and increased resistance to starvation, and identifies a new class of Bvg-regulated antigens. *Mol. Microbiol.* **24**: 671-685.

Cotter, P.A., and DiRita, V.J. (2000) Bacterial virulence gene regulation: an evolutionary perspective. *Annu. Rev. Microbiol.* **54**: 519-565.

Cotter, P.A., and Jones, A.M. (2003) Phosphorelay control of virulence gene expression in *Bordetella*. *Trends Microbiol.* **11**: 367-373.

Cummings, C.A., Bootsma, H.J., Relman, D.A., and Miller, J.F. (2006) Species- and strain-specific control of a complex, flexible regulon by *Bordetella* BvgAS. *J. Bacteriol.* **188**: 1775-1785.

Debroy, S., Aragon, V., Kurtz, S., and Cianciotto, N.P. (2006) *Legionella pneumophila* Mip, a surface-exposed peptidylproline *cis-trans*-isomerase, promotes the presence of phospholipase C-like activity in culture supernatants. *Infect. Immun.* **74**: 5152-5160.

Delmar, P., Robin, S., and Daudin, J.J. (2005) VarMixt: efficient variance modelling for the differential analysis of replicated gene expression data. *Bioinformatics* **21**: 502-508.

DiRusso, C.C., and Nystrom, T. (1998) The fats of *Escherichia coli* during infancy and old age: regulation by global regulators, alarmones and lipid intermediates. *Mol. Microbiol.* **27**: 1-8.

Domergue, R., Castano, I., De Las Penas, A., Zupancic, M., Lockatell, V., Hebel, J.R., Johnson, D., and Cormack, B.P. (2005) Nicotinic acid limitation regulates silencing of *Candida* adhesins during UTI. *Science* **308**: 866-870.

Drysdale, G.R., and Lardy, H.A. (1953) Fatty acid oxidation by a soluble enzyme system from mitochondria. *J. Biol. Chem.* **202**: 119-136.

Durfee, T., Hansen, A.M., Zhi, H., Blattner, F.R., and Jin, D.J. (2008) Transcription profiling of the stringent response in *Escherichia coli*. *J. Bacteriol.* **190**: 1084-1096.

Edwards, J.L., and Kennedy, R.T. (2005) Metabolomic analysis of eukaryotic tissue and prokaryotes using negative mode MALDI time-of-flight mass spectrometry. *Anal. Chem.* **77**: 2201-2209.

Edwards, J.L., Chisolm, C.N., Shackman, J.G., and Kennedy, R.T. (2006) Negative mode sheathless capillary electrophoresis electrospray ionization-mass spectrometry for metabolite analysis of prokaryotes. *J. Chromatogr. A* **1106**: 80-88.

Edwards, R.L., and Swanson, M.S. (2006) Regulation of the *L. pneumophila* life cycle. In *Legionella pneumophila: Pathogenesis and Immunity*. Hoffman, P., Klein, T. and Friedman, H. (eds): Springer Publishing Corp., pp. 95-111.

Eguchi, Y., Oshima, T., Mori, H., Aono, R., Yamamoto, K., Ishihama, A., and Utsumi, R. (2003) Transcriptional regulation of drug efflux genes by EvgAS, a two-component system in *Escherichia coli*. *Microbiology* **149**: 2819-2828.

Erickson, D.L., Lines, J.L., Pesci, E.C., Venturi, V., and Storey, D.G. (2004) *Pseudomonas aeruginosa relA* contributes to virulence in *Drosophila melanogaster*. *Infect. Immun.* **72**: 5638-5645.

Faulkner, G., and Garduno, R.A. (2002) Ultrastructural analysis of differentiation in *Legionella pneumophila*. *J. Bacteriol.* **184**: 7025-7041.

Fernandez-Moreira, E., Helbig, J.H., and Swanson, M.S. (2006) Membrane vesicles shed by *Legionella pneumophila* inhibit fusion of phagosomes with lysosomes. *Infect. Immun.* **74**: 3285-3295.

Fettes, P.S., Forsbach-Birk, V., Lynch, D., and Marre, R. (2001) Overexpresssion of a *Legionella pneumophila* homologue of the *E. coli* regulator *csrA* affects cell size, flagellation and pigmentation. *Int. J. Med. Microbiol.* **291**: 353-360.

Fiehn, O., Kopka, J., Dormann, P., Altmann, T., Trethewey, R.N., and Willmitzer, L. (2000) Metabolite profiling for plant functional genomics. *Nat. Biotechnol.* **18**: 1157-1161.

Fields, B.S., Benson, R.F., and Besser, R.E. (2002) *Legionella* and Legionnaires' Disease: 25 Years of Investigation. *Clin. Microbiol. Rev.* **15**: 506-526.

Flieger, A., Gong, S., Faigle, M., Mayer, H.A., Kehrer, U., MuBotter, J., Bartmann, P., and Neumeister, B. (2000) Phospholipase A secreted by *Legionella pneumophila* destroys alveolar surfactant phospholipids. *FEMS Microbiol. Lett.* **188**: 129-133.

Forsbach-Birk, V., McNealy, T., Shi, C., Lynch, D., and Marre, R. (2004) Reduced expression of the global regulator protein CsrA in *Legionella pneumophila* affects virulence-associated regulators and growth in *Acanthamoeba castellanii*. *Int. J. Med. Microbiol.* **294**: 15-25.

Gal-Mor, O., Zusman, T., and Segal, G. (2002) Analysis of DNA regulatory elements required for expression of the *Legionella pneumophila icm* and *dot* virulence genes. *J. Bacteriol.* **184**: 3823-3833.

Gal-Mor, O., and Segal, G. (2003a) Identification of CpxR as a positive regulator of *icm* and *dot* virulence genes of *Legionella pneumophila*. *J. Bacteriol.* **185**: 4908-4919.

Gal-Mor, O., and Segal, G. (2003b) The *Legionella pneumophila* GacA homolog (LetA) is involved in the regulation of *icm* virulence genes and is required for intracellular multiplication in *Acanthamoeba castellanii*. *Microb. Pathog.* **34**: 187-194.

Galka, F., Wai, S.N., Kusch, H., Engelmann, S., Hecker, M., Schmeck, B., Hippenstiel, S., Uhlin, B.E., and Steinert, M. (2008) Proteomic characterization of the whole secretome of *Legionella pneumophila* and functional analysis of outer membrane vesicles. *Infect. Immun.* **76**: 1825-1836.

Garduno, R.A., Garduno, E., Hiltz, M., and Hoffman, P.S. (2002) Intracellular growth of *Legionella pneumophila* gives rise to a differentiated form dissimilar to stationary-phase forms. *Infect. Immun.* **70**: 6273-6283.

Gaynor, E.C., Wells, D.H., MacKichan, J.K., and Falkow, S. (2005) The *Campylobacter jejuni* stringent response controls specific stress survival and virulence-associated phenotypes. *Mol. Microbiol.* **56**: 8-27.

Godfrey, H.P., Bugrysheva, J.V., and Cabello, F.C. (2002) The role of the stringent response in the pathogenesis of bacterial infections. *Trends Microbiol.* **10**: 349-351.

Gong, L., Takayama, K., and Kjelleberg, S. (2002) Role of spoT-dependent ppGpp accumulation in the survival of light-exposed starved bacteria. *Microbiology* **148**: 559-570.

Gottesman, S. (2004) The small RNA regulators of *Escherichia coli*: roles and mechanisms. *Annu. Rev. Microbiol.* **58**: 303-328.

Grabner, R., and Meerbach, W. (1991) Phagocytosis of surfactant by alveolar macrophages *in vitro*. *Am. J. Physiol.* **261**: L472-477.

Greub, G., and Raoult, D. (2003) Morphology of *Legionella pneumophila* according to their location within *Hartmanella vermiformis*. *Res. Microbiol.* **154**: 619-621.

Hales, L.M., and Shuman, H.A. (1999) The *Legionella pneumophila rpoS* gene is required for growth within *Acanthamoeba castellanii*. *J. Bacteriol.* **181**: 4879-4889.

239

Hammer, B.K., and Swanson, M.S. (1999) Co-ordination of *Legionella pneumophila* virulence with entry into stationary phase by ppGpp. *Mol. Microbiol.* **33**: 721-731.

Hammer, B.K., Tateda, E.S., and Swanson, M.S. (2002) A two-component regulator induces the transmission phenotype of stationary-phase *Legionella pneumophila*. *Mol. Microbiol.* **44**: 107-118.

Han, Y.W., Uhl, M.A., Han, S.J., and Shi, W. (1999) Expression of *bvgAS* of *Bordetella pertussis* represses flagellar biosynthesis of *Escherichia coli*. *Arch. Microbiol.* **171**: 127-130.

Harb, O.S., and Abu Kwaik, Y. (2000) Characterization of a macrophage-specific infectivity locus (*milA*) of *Legionella pneumophila*. *Infect. Immun.* **68**: 368-376.

Harwood, M.M., Christians, E.S., Fazal, M.A., and Dovichi, N.J. (2006) Single-cell protein analysis of a single mouse embryo by two-dimensional capillary electrophoresis. *J. Chromatogr. A* **1130**: 190-194.

Haskins, W.E., Wang, Z., Watson, C.J., Rostand, R.R., Witowski, S.R., Powell, D.H., and Kennedy, R.T. (2001) Capillary LC-MS2 at the attomole level for monitoring and discovering endogenous peptides in microdialysis samples collected *in vivo*. *Anal. Chem.* **73**: 5005-5014.

Heath, R.J., Jackowski, S., and Rock, C.O. (1994) Guanosine tetraphosphate inhibition of fatty acid and phospholipid synthesis in *Escherichia coli* is relieved by overexpression of glycerol-3-phosphate acyltransferase (*plsB*). *J. Biol. Chem.* **269**: 26584-26590.

Heath, R.J., and Rock, C.O. (1995) Regulation of malonyl-CoA metabolism by acyl-acyl carrier protein and beta-ketoacyl-acyl carrier protein synthases in *Escherichia coli* *J. Biol. Chem.* **270**: 15531-15538.

Heeb, S., and Haas, D. (2001) Regulatory roles of the GacS/GacA two-component system in plant-associated and other gram-negative bacteria. *Mol. Plant Microbe Interact.* **14**: 1351-1363.

Heinzen, R.A., Hackstadt, T., and Samuel, J.E. (1999) Developmental biology of *Coxiella burnetii*. *Trends Microbiol.* **7**: 149-154.

Heuner, K., Hacker, J., and Brand, B.C. (1997) The alternative sigma factor σ^{28} of *Legionella pneumophila* restores flagellation and motility to an *Escherichia coli* *fliA* mutant. *J. Bacteriol.* **179**: 17-23.

Heuner, K., Dietrich, C., Skriwan, C., Steinert, M., and Hacker, J. (2002) Influence of the alternative σ^{28} factor on virulence and flagellum expression of *Legionella pneumophila*. *Infect. Immun.* **70**: 1604-1608.

Heuner, K., and Steinert, M. (2003) The flagellum of *Legionella pneumophila* and its link to the expression of the virulent phenotype. *Int. J. Med. Microbiol.* **293**: 133-143.

Hood, M.A., Guckert, J.B., White, D.C., and Deck, F. (1986) Effect of nutrient deprivation on lipid, carbohydrate, DNA, RNA, and protein levels in *Vibrio cholerae*. *Appl. Environ. Microbiol.* **52**: 788-793.

Horwitz, M.A., and Silverstein, S.C. (1980) Legionnaires' disease bacterium (*Legionella pneumophila*) multiplies intracellularly in human monocytes. *J. Clin. Invest.* **66**: 441-450.

Jackowski, S., and Rock, C.O. (1983) Ratio of active to inactive forms of acyl carrier protein in *Escherichia coli*. *J. Biol. Chem.* **258**: 15186-15191.

Jacobi, S., Schade, R., and Heuner, K. (2004) Characterization of the alternative sigma factor σ^{54} and the transcriptional regulator FleQ of *Legionella pneumophila*, which are both involved in the regulation cascade of flagellar gene expression. *J. Bacteriol.* **186**: 2540-2547.

Jensen, M.V., Joseph, J.W., Ilkayeva, O., Burgess, S., Lu, D., Ronnebaum, S.M., Odegaard, M., Becker, T.C., Sherry, A.D., and Newgard, C.B. (2006) Compensatory responses to pyruvate carboxylase suppression in islet β-cells. Preservation of glucose-stimulated insulin secretion. *J. Biol. Chem.* **281**: 22342-22351.

Jia, L., Tanaka, N., and Terabe, S. (2005) Two-dimensional separation system of coupling capillary liquid chromatography to capillary electrophoresis for analysis of *Escherichia coli* metabolites. *Electrophoresis* **26**: 3468-3478.

Jiang, M., Sullivan, S.M., Wout, P.K., and Maddock, J.R. (2007) G-protein control of the ribosome-associated stress response protein SpoT. *J. Bacteriol.* **189**: 6140-6147.

Jones, A.M., Boucher, P.E., Williams, C.L., Stibitz, S., and Cotter, P.A. (2005) Role of BvgA phosphorylation and DNA binding affinity in control of Bvg-mediated phenotypic phase transition in *Bordetella pertussis*. *Mol. Microbiol.* **58**: 700-713.

Jonsson, P., Gullberg, J., Nordstrom, A., Kusano, M., Kowalczyk, M., Sjostrom, M., and Moritz, T. (2004) A strategy for identifying differences in large series of metabolomic samples analyzed by GC/MS. *Anal. Chem.* **76**: 1738-1745.

Joshi, A.D., Sturgill-Koszycki, S., and Swanson, M.S. (2001) Evidence that Dot-dependent and -independent factors isolate the *Legionella pneumophila* phagosome from the endocytic network in mouse macrophages. *Cell. Microbiol.* **3**: 99-114.

Kennedy, R.T., and Jorgenson, J.W. (1989) Preparation and evaluation of packed capillary liquid-chromatography columns with inner diameters from 20 to 50 µM. *Anal. Chem.* **61**: 1128-1135.

Kennedy, R.T., Oates, M.D., Cooper, B.R., Nickerson, B., and Jorgenson, J.W. (1989) Microcolumn separations and the analysis of single cells. *Science* **246**: 57-63.

Korner, R., Wilm, M., Morand, K., Schubert, M., and Mann, M. (1996) Nano electrospray combined with a quadrupole ion trap for the analysis of peptides and protein digests. *J. Am. Soc. Mass. Spectrom.* **7**: 150-156.

Kulkarni, P.R., Cui, X., Williams, J.W., Stevens, A.M., and Kulkarni, R.V. (2006) Prediction of CsrA-regulating small RNAs in bacteria and their experimental verification in *Vibrio fischeri*. *Nucleic Acids Res.* **34**: 3361-3369.

Kyte, J., and Doolittle, R.F. (1982) A simple method for displaying the hydropathic character of a protein. *J. Mol. Biol.* **157**: 105-132.

Lacey, B.W. (1960) Antigenic modulation of *Bordetella pertussis*. *J. Hyg., Camb.* **58**: 57-93.

Lafaye, A., Labarre, J., Tabet, J.C., Ezan, E., and Junot, C. (2005) Liquid chromatography-mass spectrometry and ^{15}N metabolic labeling for quantitative metabolic profiling. *Anal. Chem.* **77**: 2026-2033.

Lapouge, K., Schubert, M., Allain, F.H.-T., and Haas, D. (2008) Gac/Rsm signal transduction pathway of γ-proteobacteria: from RNA recognition to regulation of social behavior. *Mol. Microbiol.* **67**: 241-253.

Lawhon, S.D., Maurer, R., Suyemoto, M., and Altier, C. (2002) Intestinal short-chain fatty acids alter *Salmonella typhimurium* invasion gene expression and virulence through BarA/SirA. *Mol. Microbiol.* **46**: 1451-1464.

Lebeau, I., Lammertyn, E., De Buck, E., Maes, L., Geukens, N., Van Mellaert, L., Arckens, L., Anne, J., and Clerens, S. (2005) First proteomic analysis of *Legionella pneumophila* based on its developing genome sequence. *Res. Microbiol.* **156**: 119-129.

Leonardo, M.R., Dailly, Y., and Clark, D.P. (1996) Role of NAD in regulating the *adhE* gene of *Escherichia coli*. *J. Bacteriol.* **178**: 6013-6018.

Lu, W., Kimball, E., and Rabinowitz, J.D. (2006) A high-performance liquid chromatography-tandem mass spectrometry method for quantitation of nitrogen-containing intracellular metabolites. *J. Am. Soc. Mass. Spectrom.* **17**: 37-50.

Lucchetti-Miganeh, C., Burrowes, E., Baysse, C., and Ermel, G. (2008) The post-transcriptional regulator CsrA plays a central role in the adaptation of bacterial pathogens to different stages of infectiopn in animal hosts. *Microbiology* **154**: 16-29.

Lynch, D., Fieser, N., Gloggler, K., Forsbach-Birk, V., and Marre, R. (2003) The response regulator LetA regulates the stationary-phase stress response in *Legionella pneumophila* and is required for efficient infection of *Acanthamoeba castellanii. FEMS Microbiol. Lett.* **219**: 241-248.

Magnuson, K., Jackowski, S., Rock, C.O., and Cronan, J.E., Jr. (1993) Regulation of fatty acid biosynthesis in *Escherichia coli. Microbiol. Rev.* **57**: 522-542.

Magnusson, L.U., Farewell, A., and Nystrom, T. (2005) ppGpp: a global regulator in *Escherichia coli. Trends Microbiol.* **13**: 236-242.

Majdalani, N., Vanderpool, C.K., and Gottesman, S. (2005) Bacterial small RNA regulators. *Crit. Rev. Biochem. Mol. Biol.* **40**: 93-113.

Marchler-Bauer, A., Anderson, J.B., Cherukuri, P.F., DeWeese-Scott, C., Geer, L.Y., Gwadz, M., He, S., Hurwitz, D.I., Jackson, J.D., Ke, Z., Lanczycki, C.J., Liebert, C.A., Liu, C., Lu, F., Marchler, G.H., Mullokandov, M., Shoemaker, B.A., Simonyan, V., Song, J.S., Thiessen, P.A., Yamashita, R.A., Yin, J.J., Zhang, D., and Bryant, S.H. (2005) CDD: a Conserved Domain Database for protein classification. *Nucleic Acids Res.* **33**: D192-196.

Mashego, M.R., Wu, L., Van Dam, J.C., Ras, C., Vinke, J.L., Van Winden, W.A., Van Gulik, W.M., and Heijnen, J.J. (2004) MIRACLE: mass isotopomer ratio analysis of U-^{13}C-labeled extracts. A new method for accurate quantification of changes in concentrations of intracellular metabolites. *Biotechnol. Bioeng.* **85**: 620-628.

Masuda, N., and Church, G.M. (2002) *Escherichia coli* gene expression responsive to levels of the response regulator EvgA. *J. Bacteriol.* **184**: 6225-6234.

Masuda, N., and Church, G.M. (2003) Regulatory network of acid resistance genes in *Escherichia coli. Mol. Microbiol.* **48**: 699-712.

McCleary, W.R., Stock, J.B., and Ninfa, A.J. (1993) Is acetyl phosphate a global signal in *Escherichia coli*? *J. Bacteriol.* **175**: 2793-2798.

McCune, S.A., and Harris, R.A. (1979) Mechanism responsible for 5-(tetradecyloxy)-2-furoic acid inhibition of hepatic lipogenesis. *J. Biol. Chem.* **254**: 10095-10101.

McDade, J.E., Shepard, C.C., Fraser, D.W., Tsai, T.R., Redus, M.A., and Dowdle, W.R. (1977) Legionnaires' disease: isolation of a bacterium and demonstration of its role in other respiratory diseases. *N. Engl. J. Med.* **297**: 1197-1203.

McNealy, T.L., Forsbach-Birk, V., Shi, C., and Marre, R. (2005) The Hfq homolog in *Legionella pneumophila* demonstrates regulation by LetA and RpoS and interacts with the global regulator CsrA. *J. Bacteriol.* **187**: 1527-1532.

McPheat, W.L., Wardlaw, A.C., and Novotny, P. (1983) Modulation of *Bordetella pertussis* by nicotinic acid. *Infect. Immun.* **41**: 516-522.

Miller, J.F., Roy, C.R., and Falkow, S. (1989) Analysis of *Bordetella pertussis* virulence gene regulation by use of transcriptional fusions in *Escherichia coli*. *J. Bacteriol.* **171**: 6345-6348.

Milohanic, E., Glaser, P., Coppee, J.Y., Frangeul, L., Vega, Y., Vazquez-Boland, J.A., Kunst, F., Cossart, P., and Buchrieser, C. (2003) Transcriptome analysis of *Listeria monocytogenes* identifies three groups of genes differently regulated by PrfA. *Mol. Microbiol.* **47**: 1613-1625.

Mintz, C.S., Chen, J., and Shuman, H. (1988) Isolation and characterization of auxotrophic mutants of *Legionella pneumophila* that fail to multiply in human monocytes. *Infect. Immun.* **56**: 1449-1455.

Mohler, R.E., Dombek, K.M., Hoggard, J.C., Young, E.T., and Synovec, R.E. (2006) Comprehensive two-dimensional gas chromatography time-of-flight mass spectrometry analysis of metabolites in fermenting and respiring yeast cells. *Anal. Chem.* **78**: 2700-2709.

Molofsky, A.B., and Swanson, M.S. (2003) *Legionella pneumophila* CsrA is a pivotal repressor of transmission traits and activator of replication. *Mol. Microbiol.* **50**: 445-461.

Molofsky, A.B., and Swanson, M.S. (2004) Differentiate to thrive: lessons from the *Legionella pneumophila* life cycle. *Mol. Microbiol.* **53**: 29-40.

Molofsky, A.B., Shetron-Rama, L.M., and Swanson, M.S. (2005) Components of the *Legionella pneumophila* flagellar regulon contribute to multiple virulence traits, including lysosome avoidance and macrophage death. *Infect. Immun.* **73**: 5720-5734.

Molofsky, A.B., Byrne, B.G., Whitfield, N.N., Madigan, C.A., Fuse, E.T., Tateda, K., and Swanson, M.S. (2006) Cytosolic recognition of flagellin by mouse macrophages restricts *Legionella pneumophila* infection. *J. Exp. Med.* **203**: 1093-1104.

Mouery, K., Rader, B.A., Gaynor, E.C., and Guillemin, K. (2006) The stringent response is required for *Helicobacter pylori* survival of stationary phase, exposure to acid and aerobic shock. *J. Bacteriol.* **188**: 5494-5500.

Nishino, K., and Yamaguchi, A. (2001) Overexpression of the response regulator *evgA* of the two-component signal transduction system modulates multidrug resistance conferred by multidrug resistance transporters. *J. Bacteriol.* **183**: 1455-1458.

Nishino, K., Inazumi, Y., and Yamaguchi, A. (2003) Global analysis of genes regulated by EvgA of the two-component regulatory system in *Escherichia coli*. *J. Bacteriol.* **185**: 2667-2672.

Notredame, C., Higgins, D.G., and Heringa, J. (2000) T-Coffee: A novel method for fast and accurate multiple sequence alignment. *J. Mol. Biol.* **302**: 205-217.

Nystrom, T. (2004) Growth versus maintenance: a trade-off dictated by RNA polymerase availability and sigma factor competition? *Mol. Microbiol.* **54**: 855-862.

Opiteck, G.J., Lewis, K.C., Jorgenson, J.W., and Anderegg, R.J. (1997) Comprehensive on-line LC/LC/MS of proteins. *Anal. Chem.* **69**: 1518-1524.

Oyston, P.C.F., Sjostedt, A., and Titball, R.W. (2004) Tularaemia: bioterrorism defense renews interest in *Francisella tularensis*. *Nat. Rev. Microbiol.* **2**: 967-978.

Panek, E., Cook, G.A., and Cornell, N.W. (1977) Inhibition by 5-(tetradecyloxy)-2-furoic acid of fatty acid and cholesterol synthesis in isolated rat hepatocytes. *Lipids* **12**: 814-818.

Pao, S.S., Paulsen, I.T., and Saier, M.H., Jr. (1998) Major Facilitator Superfamily. *Micro. Mol. Biol. Rev.* **62**: 1-34.

Paredes, C.J., Alsaker, K.V., and Papoutsakis, E.T. (2005) A comparative genomic view of clostridial sporulation and physiology. *Nat. Rev. Microbiol.* **3**: 969-978.

Paul, B.J., Ross, W., Gaal, T., and Gourse, R.L. (2004) rRNA transcription in *Escherichia coli*. *Annu. Rev. Genet.* **38**: 749-770.

Paul, B.J., Berkmen, M.B., and Gourse, R.L. (2005) DksA potentiates direct activation of amino acid promoters by ppGpp. *Proc. Natl. Acad. Sci. USA* **102**: 7823-7828.

Pearson, W.R., Wood, T., Zhang, Z., and Miller, W. (1997) Comparison of DNA sequences with protein sequences. *Genomics* **46**: 24-36.

Perraud, A., Weiss, V., and Gross, R. (1999) Signalling pathways in two-component phosphorelay systems. *Trends Microbiol.* **7**: 115-120.

Pizarro-Cerda, J., and Tedin, K. (2004) The bacterial signal molecule, ppGpp, regulates *Salmonella* virulence gene expression. *Mol. Microbiol.* **52**: 1827-1844.

Pizer, E.S., Thupari, J., Han, W.F., Pinn, M.L., Chrest, F.J., Frehywot, G.L., Townsend, C.A., and Kuhajda, F.P. (2000) Malonyl-coenzyme-A is a potential mediator of cytotoxicity induced by fatty-acid synthase inhibition in human breast cancer cells and xenografts. *Cancer Res.* **60**: 213-218.

Post-Beittenmiller, D., Jaworski, J.G., and Ohlrogge, J.B. (1991) *In vivo* pools of free and acylated acyl carrier proteins in spinach. *J. Biol. Chem.* **266**: 1858-1865.

Primm, T.P., Andersen, S.J., Mizrahi, V., Avarbock, D., Rubin, H., and Barry, C.E., 3rd (2000) The stringent response of *Mycobacterium tuberculosis* is required for long-term survival. *J. Bacteriol.* **182**: 4889-4898.

Purevdorj-Gage, B., Costerton, W.J., and Stoodley, P. (2005) Phenotypic differentiation and seeding dispersal in non-mucoid and mucoid *Pseudomonas aeruginosa* biofilms. *Microbiol.* **151**: 1569-1576.

Rankin, S., Li, Z., and Isberg, R.R. (2002) Macrophage-induced genes of *Legionella pneumophila*: protection from reactive intermediates and solute imbalance during intracellular growth. *Infect. Immun.* **70**: 3637-3648.

Raskin, D.M., Judson, N., and Mekalanos, J.J. (2007) Regulation of the stringent response is the essential function of the conserved bacterial G protein CgtA in *Vibrio cholerae. Proc. Natl. Acad. Sci. USA* **104**: 4636-4641.

Reiner, A., Yekutieli, D., and Benjamini, Y. (2003) Identifying differentially expressed genes using false discovery rate controlling procedures. *Bioinformatics* **19**: 368-375.

Ren, T., Zamboni, D.S., Roy, C.R., Dietrich, W.F., and Vance, R.E. (2006) Flagellin-deficient *Legionella* mutants evade caspase-1- and Naip5-mediated macrophage immunity. *PLoS Pathog.* **2**: e18.

Richardson, D.J., and Watmough, N.J. (1999) Inorganic nitrogen metabolism in bacteria. *Curr. Opin. Chem. Biol.* **3**: 207-219.

Ristroph, J.D., Hedlund, K.W., and Gowda, S. (1981) Chemically defined medium for *Legionella pneumophila* growth. *J. Clin. Microbiol.* **13**: 115-119.

Rock, C.O., and Cronan, J.E., Jr. (1981) Acyl carrier protein from *Escherichia coli*. *Methods Enzymol.* **71**: 341-351.

Romeo, T. (1998) Global regulation by the small RNA-binding protein CsrA and the non-coding RNA molecule CsrB. *Mol. Microbiol.* **29**: 1321-1330.

Rowbotham, T.J. (1986) Current views on the relationships between amoebae, legionellae and man. *Isr. J. Med. Sci.* **22**: 678-689.

Roy, C.R., Berger, K.H., and Isberg, R.R. (1998) *Legionella pneumophila* DotA protein is required for early phagosome trafficking decisions that occur within minutes of bacterial uptake. *Mol. Microbiol.* **28**: 663-674.

Sadosky, A.B., Wiater, L.A., and Shuman, H.A. (1993) Identification of *Legionella pneumophila* genes required for growth within and killing of human macrophages. *Infect. Immun.* **61**: 5361-5373.

Saghatelian, A., Trauger, S.A., Want, E.J., Hawkins, E.G., Siuzdak, G., and Cravatt, B.F. (2004) Assignment of endogenous substrates to enzymes by global metabolite profiling. *Biochemistry* **43**: 14332-14339.

Samuel, J.E., Kiss, K., and Varghees, S. (2003) Molecular pathogenesis of *Coxiella burnetii* in a genomics era. *Ann. N.Y. Acad. Sci.* **990**: 653-663.

Sauer, J.D., Bachman, M.A., and Swanson, M.S. (2005) The phagosomal transporter A couples threonine acquisition to differentiation and replication of *Legionella pneumophila* in macrophages. *Proc. Natl. Acad. Sci. USA* **102**: 9924-9929.

Schmidt, A., Karas, M., and Dulcks, J. (2003) Effect of different solution flow rates on analyte ion signals in nano-ESI MS, or: When does ESI turn into nano-ESI? *J. Am. Soc. Mass. Spectrom.* **14**: 492-500.

Schneider, D.R., and Parker, C.D. (1982) Effect of pyridines on phenotypic properties of *Bordetella pertussis*. *Infect. Immun.* **38**: 548-553.

Schujman, G.E., Altabe, S., and de Mendoza, D. (2008) A malonyl-CoA-dependent switch in the bacterial response to a dysfunction of lipid metabolism. *Mol. Microbiol.* **68**: 987-996.

Segal, G., Purchell, M., and Shuman, H.A. (1998) Host cell killing and bacterial conjugation require overlapping sets of genes within a 22-kb region of the *Legionella pneumophila* genome. *Proc. Natl. Acad. Sci. USA* **95**: 1669-1674.

Segal, G., Feldman, M., and Zusman, T. (2005) The Icm/Dot type-IV secretion systems of *Legionella pneumophila* and *Coxiella burnetii*. *FEMS Microbiol. Rev.* **29**: 65-81.

Sexton, J.A., and Vogel, J.P. (2002) Type IVB secretion by intracellular pathogens. *Traffic* **3**: 178-185.

Seyfzadeh, M., Keener, J., and Nomura, M. (1993) spoT-dependent accumulation of guanosine tetraphosphate in response to fatty acid starvation in *Escherichia coli*. *Proc. Natl. Acad. Sci. USA* **90**: 11004-11008.

Soga, T., Ueno, Y., Naraoka, H., Ohashi, Y., Tomita, M., and Nishioka, T. (2002) Simultaneous determination of anionic intermediates for *Bacillus subtilis* metabolic pathways by capillary electrophoresis electrospray ionization mass spectrometry. *Anal. Chem.* **74**: 2233-2239.

Soga, T., Ohashi, Y., Ueno, Y., Naraoka, H., Tomita, M., and Nishioka, T. (2003) Quantitative metabolome analysis using capillary electrophoresis mass spectrometry. *J. Proteome Res.* **2**: 488-494.

Song, M., Kim, H.J., Kim, E.Y., Shin, M., Lee, H.C., Hong, Y., Rhee, J.H., Yoon, H., Ryu, S., Lim, S., and Choy, H.E. (2004) ppGpp-dependent stationary phase induction of genes on *Salmonella* pathogenicity island 1. *J. Biol. Chem.* **279**: 34183-34190.

Spira, B., and Yagil, E. (1998) The relationship between ppGpp and the PHO regulon in *Escherichia coli*. *Mol. Gen. Genet.* **257**: 469-477.

Srivatsan, A., and Wang, J.D. (2008) Control of bacterial transcription, translation and replication by (p)ppGpp. *Curr. Opin. Microbiol.* **11**: 100-105.

Starai, V.J., Celic, I., Cole, R.N., Boeke, J.D., and Escalante-Semerena, J.C. (2002) Sir2-dependent activation of acetyl-CoA synthetase by deacetylation of active lysine. *Science* **298**: 2390-2392.

Starai, V.J., Takahashi, H., Boeke, J.D., and Escalante-Semerena, J.C. (2004) A link between transcription and intermediary metabolism: a role for Sir2 in the control of acetyl-coenzyme A synthetase. *Curr. Opin. Microbiol.* **7**: 115-119.

Steinert, M., Heuner, K., Buchrieser, C., Albert-Weissenberger, C., and Glockner, G. (2007) *Legionella* pathogenicity: genome structure, regulatory networks and the host cell response. *Int. J. Med. Microbiol.* **297**: 577-587.

Stockbauer, K.E., Fuchslocher, B., Miller, J.F., and Cotter, P.A. (2001) Identification and characterization of BipA, a *Bordetella* Bvg-intermediate phase protein. *Mol. Microbiol.* **39**: 65-78.

Stoll, D.R., Cohen, J.D., and Carr, P.W. (2006) Fast, comprehensive online two-dimensional high performance liquid chromatography through the use of high temperature ultra-fast gradient elution reversed-phase liquid chromatography. *J. Chromatogr. A* **1122**: 123-137.

Stone, B.J., and Abu Kwaik, Y. (1999) Natural competence for DNA transformation by *Legionella pneumophila* and its association with expression of type IV pili. *J. Bacteriol.* **181**: 1395-1402.

Sturgill-Koszycki, S., and Swanson, M.S. (2000) *Legionella pneumophila* replication vacuoles mature into acidic, endocytic organelles. *J. Exp. Med.* **192**: 1261-1272.

Suzuki, K., Wang, X., Weilbacher, T., Pernestig, A.-K., Melefors, O., and Georgellis, D. (2002) Regulatory circuitry of the CsrA/CsrB and BarA/UvrY systems of *Escherichia coli*. *J. Bacteriol.* **184**: 5130-5140.

Swanson, M.S., and Isberg, R.R. (1995) Association of *Legionella pneumophila* with the macrophage endoplasmic reticulum. *Infect. Immun.* **63**: 3609-3620.

Swanson, M.S., and Isberg, R.R. (1996) Identification of *Legionella pneumophila* mutants that have aberrant intracellular fates. *Infect. Immun.* **64**: 2585-2594.

Swanson, M.S., and Hammer, B.K. (2000) *Legionella pneumophila* pathogesesis: a fateful journey from amoebae to macrophages. *Annu. Rev. Microbiol.* **54**: 567-613.

Taylor, C.M., Beresford, M., Epton, H.A., Sigee, D.C., Shama, G., Andrew, P.W., and Roberts, I.S. (2002) *Listeria monocytogenes relA* and *hpt* mutants are impaired in surface-attached growth and virulence. *J. Bacteriol.* **184**: 621-628.

Tesh, M.J., and Miller, R.D. (1981) Amino acid requirements for *Legionella pneumophila* growth. *J. Clin. Microbiol.* **13**: 865-869.

Tesh, M.J., Morse, S.A., and Miller, R.D. (1983) Intermediary metabolism in *Legionella pneumophila*: utilization of amino acids and other compounds as energy sources. *J. Bacteriol.* **154**: 1104-1109.

Tiaden, A., Spirig, T., Weber, S.S., Bruggemann, H., Bosshard, R., Buchrieser, C., and Hilbi, H. (2007) The *Legionella pneumophila* response regulator LqsR promotes host cell interactions as an element of the virulence regulatory network controlled by RpoS and LetA. *Cell. Microbiol.* **9**: 2903-2920.

Tolstikov, V.V., Lommen, A., Nakanishi, K., Tanaka, N., and Fiehn, O. (2003) Monolithic silica-based capillary reversed-phase liquid chromatography/electrospray mass spectrometry for plant metabolomics. *Anal. Chem.* **75**: 6737-6740.

Tompson, A., Rolfe, M.D., Lucchini, S., Schwerk, P., Hinton, J.C., and Tedin, K. (2006) The bacterial signal molecule, ppGpp, mediates the environmental regulation of both the invasion and intracellular virulence gene programs of *Salmonella*. *J. Biol. Chem.* **281**: 30112-30121.

Tosa, T., and Pizer, L.I. (1971) Biochemical basis for the antimetabolite action of L-serine hydroxamate. *J. Bacteriol.* **106**: 972-982.

Traxler, M.F., Summers, S.M., Nguyen, H.T., Zacharia, V.M., Hightower, G.A., Smith, J.T., and Conway, T. (2008) The global, ppGpp-mediated stringent response to amino acid starvation in *Escherichia coli*. *Mol. Microbiol.* **68**: 1128-1148.

Uhl, M.A., and Miller, J.F. (1994) Autophosphorylation and phosphotransfer in the *Bordetella pertussis* BvgAS signal transduction cascade. *Proc. Natl. Acad. Sci. USA* **91**: 1163-1167.

Uhl, M.A., and Miller, J.F. (1996a) Integration of multiple domains in a two-component sensor protein: the *Bordetella pertussis* BvgAS phosphorelay. *EMBO J.* **15**: 1028-1036.

Uhl, M.A., and Miller, J.F. (1996b) A new type of phosphodonor in two-component signal transduction systems: the *Bordetella pertussis* BvgAS phosphorelay. *EMBO J.* **15**: 1028-1036.

Uhl, M.A., and Miller, J.F. (1996c) Central role of the BvgS receiver as a phosphorylated intermediate in a complex two-component phosphorelay. *J. Biol. Chem.* **271**: 33176-33180.

Ulrich, A.K., de Mendoza, D., Garwin, J.L., and Cronan, J.E., Jr. (1983) Genetic and biochemical analyses of *Escherichia coli* mutants altered in the temperature-dependent regulation of membrane lipid composition. *J. Bacteriol.* **154**: 221-230.

Utsumi, R., Katayama, S., Taniguchi, M., Horie, T., Ikeda, M., Igaki, S., Nakagawa, H., Miwa, A., Tanabe, H., and Noda, M. (1994) Newly identified genes involved in the signal transduction of *Escherichia coli* K-12. *Gene* **140**: 73-77.

Vance, D., Goldberg, I., Mitsuhashi, I., Bloch, K., Omura, S., and Nomura, S. (1972) Inhibition of fatty acid synthetases by the antibiotic cerulenin. *Biochem. Biophys. Res. Commun.* **48**: 649-656.

Vogel, J.P., Roy, C., and Isberg, R.R. (1996) Use of salt to isolate *Legionella pneumophila* mutants unable to replicate in macrophages. *Ann. N.Y. Acad. Sci.* **797**: 271-272.

Vogel, J.P., H. L. Andrews, S. K. Wong, R. R. Isberg. (1998) Conjugative transfer by the virulence system of *Legionella pneumophila*. *Science* **279**: 873-876.

Voth, D.E., and Heinzen, R.A. (2007) Lounging in a lysosome: the intracellular lifestyle of *Coxiella burnetii*. *Cell. Microbiol.* **9**: 829-840.

Warren, W.J., and Miller, R.D. (1979) Growth of Legionnaires disease bacterium (*Legionella pneumophila*) in chemically defined medium. *J. Clin. Microbiol.* **10**: 50-55.

Washburn, M.P., Wolters, D., and Yates, J.R., 3rd (2001) Large-scale analysis of the yeast proteome by multidimensional protein identification technology. *Nat. Biotechnol.* **19**: 242-247.

Watarai, M., Andrews, H.L., and Isberg, R.R. (2001a) Formation of a fibrous structure on the surface of *Legionella pneumophila* associated with exposure of DotH and DotO proteins after intracellular growth. *Mol. Microbiol.* **39**: 313-329.

Watarai, M., Derre, I., Kirby, J., Growney, J.D., Dietrich, W.F., and Isberg, R.R. (2001b) *Legionella pneumophila* is internalized by a macropinocytotic uptake pathway controlled by the Dot/Icm system and the mouse Lgn1 locus. *J. Exp. Med.* **194**: 1081-1096.

Weissman, K.J. (2004) Polyketide biosynthesis: understanding and exploiting modularity. *Philos. Transact. A Math. Phys. Eng. Sci.* **362**: 2671-2690.

Welthagen, W., Shellie, R.A., Spranger, J., Ristow, M., Zimmermann, R., and Fiehn, O. (2005) Comprehensive two-dimensional gas chromatography-time-of-flight mass spectrometry (GC x GC-TOF) for high resolution metabolomics: biomarker discovery on spleen tissue extracts of obese NZO compared to lean C57BL/6 mice. *Metabolomics* **1**: 65-73.

Wiater, L.A., Sadosky, A.B., and Shuman, H. (1994) Mutagenesis of *Legionella pneumophila* using Tn903dII*lacZ*: identification of a growth-phase-regulated pigmentation gene. *Mol. Microbiol.* **11**: 641-653.

Wieland, H., Faigle, M., Lang, F., Northoff, H., and Neumeister, B. (2002) Regulation of the *Legionella mip*-promotor during infection of human monocytes. *FEMS Microbiol. Lett.* **212**: 127-132.

Wieland, H., Ullrich, S., Lang, F., and Neumeister, B. (2005) Intracellular multiplication of *Legionella pneumophila* depends on host cell amino acid transporter SLC1A5. *Mol. Microbiol.* **55**: 1528-1537.

Williams, C.L., Boucher, P.E., Stibitz, S., and Cotter, P.A. (2005) BvgA functions as both an activator and a repressor to control Bvgi phase expression of *bipA* in *Bordetella pertussis*. *Mol. Microbiol.* **56**: 175-188.

Wilson, I.D., Nicholson, J.K., Castro-Perez, J., Granger, J.H., Johnson, K.A., Smith, B.W., and Plumb, R.S. (2005) High resolution "ultra performance" liquid chromatography coupled to oa-TOF mass spectrometry as a tool for differential metabolic pathway profiling in functional genomic studies. *J. Proteome. Res.* **4**: 591-598.

Wintermeyer, E., Flügel, M., Ott, M., Steinert, M., Rdest, U., Mann, K., and Hacker, J. (1994) Sequence determination and mutational analysis of the *lly* locus of *Legionella pneumophila*. *Infect. Immun.* **62**: 1109-1117.

Wolfe, A.J. (2005) The acetate switch. *Micro. Mol. Biol. Rev.* **69**: 12-50.

Wolters, A.M., Jayawickrama, D.A., and Sweedler, J.V. (2005) Comparative analysis of a neurotoxin from *Calliostoma canaliculatum* by on-line capillary isotachophoresis/^{1}H NMR and diffusion ^{1}H NMR. *J. Nat. Prod.* **68**: 162-167.

Woods, L.A., Powell, P.R., Paxon, T.L., and Ewing, A.G. (2005) Analysis of mammalian cell cytoplasm with electrophoresis in nanometer inner diameter capillaries. *Electroanalysis* **17**: 1192-1197.

Xiao, H., Kalman, M., Ikehara, K., Zemel, S., Glaser, G., and Cashel, M. (1991) Residual guanosine 3', 5'-bispyrophosphate synthetic activity of *relA* null mutants can be eliminated by *spoT* null mutations. *J. Biol. Chem.* **266**: 5980-5990.

Yang, Y.H., Dudoit, S., Luu, P., Lin, D.M., Peng, V., Ngai, J., and Speed, T.P. (2002) Normalization for cDNA microarray data: a robust composite method addressing single and multiple slide systematic variation. *Nucleic Acids Res.* **30**: e15.

Zusman, D.R., Scott, A.E., Yang, Z., and Kirby, J.R. (2007) Chemosensory pathways, motility and development in *Myxococcus xanthus*. *Nat. Rev. Microbiol.* **5**: 862-872.

Zusman, T., Gal-Mor, O., and Segal, G. (2002) Characterization of a *Legionella pneumophila relA* insertion mutant and toles of RelA and RpoS in virulence gene expression. *J. Bacteriol.* **184**: 67-75.